Expression studies on PPAR in pancreatic neuroendocrine tumours

Hanson, Matthew Richard

Expression Studies on PPARγ in Pancreatic Neuroendocrine Tumours

Thesis submitted as requirement for MD (Res)

Matthew Richard Hanson 2010

Barts and the London School of medicine

Queen Mary, University of London

Abstract

Pancreatic NETs occur with an annual incidence of around 5 per 1,000,000 population per year, with survival rates of between 30 – 97% at 5 years depending on the tumour subtype. The PPARs (peroxisomal proliferator-activated receptors) are members of the nuclear receptor superfamily that includes receptors for thyroid, steroid and retinoid hormones. PPARγ protein is also thought to be expressed in human pancreatic islet cells and has been shown to be a negative regulator of islet β cell mass both in vivo and in vitro. Its emerging function in controlling cell proliferation, differentiation and apoptosis, both in vivo and in vitro, has suggested a putative role as a tumour suppressor gene.

I postulated that PPARγ is expressed in pancreatic neuroendocrine tumours and that agonism with a thiazolidinedione will cause an anti-proliferative effect. Three different types of tissue/cells were available to me: frozen human pancreatic neuroendocrine tumours following surgical resection, paraffin-embedded samples held in the histopathology archives, and human neuroendocrine tumour cell lines CM, BON and QGP1 (insulinoma, carcinoid and somatostatinoma respectively).

PPARγ RNA was shown to be present in the majority of frozen surgical samples. Immunohistochemistry for PPARγ protein on the paraffin-embedded samples, however, revealed a lack of positive staining. These samples were then subjected to further immunohistochemistry for detection of other potentially important proteins involved with cellular proliferation including p27, phospho-p27, JAB1, PTEN and phospho-AKT. In the tumour cell models, PPARγ RNA and protein was present in both BON and QGP1. Proliferation studies following treatment doses of PPARγ agonist

rosiglitazone show a significant anti-proliferative effect. Recovery of cells was shown following removal of treatment. However, inhibition of the effect was not achieved with the use of PPARγ antagonists raising the possibility that the anti-proliferative effects of thiazolidinediones may be independent of PPARγ.

Contents

Figures

Tables

Declaration

The work presented herein is the independent work of the author, unless otherwise stated, with guidance from Marta Korbonits and Ashley Grossman.

Mr M R Hanson 2010

Acknowledgements

I would like to thank everyone that has helped me during the course of this project from Mr Satya Bhattacharya and Mr Robert Hutchins who helped set the project up, to the members of the laboratory, including Drs Madalina Musat, Blerina Kola and Sarah Bonner who played significant roles in teaching me the laboratory skills required.

During the course of this MD I required the specialist help and a considerable amount of time from Dr Salvadore Diaz-Cano who was invaluable with the setting up, optimisation and interpretation of the immunohistochemistry section of this work. Following his departure, I am grateful for the help given by Dr Eivind Carlsen for further quality assurance and work done on Ki-67 index.

The work on cell cultures could not have been done without the generosity of Professor Nicolas Lemoine and the technical assistance of Dr Gabriele Capurso, based at Cancer Research UK, in providing the cell lines and the basic information on media and conditions required for healthy populations.

Finally, completion of this project could not have happened without the continued support, guidance and patience of my wife Philippa and my supervisors, Professors Marta Korbonits and Ashley Grossman: my sincerest thanks.

Abbreviations

ACTH	adrenocorticotropic hormone
AP	activator protein
BSA	bovine serum albumin
cAMP	cyclic adenosine monophosphate
CDK	cyclin dependent kinase
CDKI	cyclin dependent kinase inhibitors
CGH	comparative genomic hybridization
DMEM	dulbecco’s modified eagle’s medium
DMSO	dimethyl sulphoxide
DNA	deoxyribonucleic acid
DNase	deoxyribonuclease
ECL	enterochromaffin-like cell
EDTA	ethylene-diamine-tetra-acetic acid
ERK	extracellular signal-regulated kinase
FCS	foetal calf serum
GAPDH	glyceraldehyde 3 phosphate dehydrogenase
GEP	gastroenteropancreatic
GHRH	growth hormone releasing hormone
HRP	horseradish peroxidase
JAB 1	jun activation domain-binding protein 1
JNK	c-jun N-terminal kinase
LOH	loss of heterozygosity
MAPK	mitogen activated protein kinase

MEN	multiple endocrine neoplasia
MMP 2	matrix metallopeptidase 2
mRNA	messenger ribonucleic acid
mTOR	mammalian target of rapamycin
MLPA	multiplex ligation-dependent probe amplification
NET	neuro endocrine tumour
NSE	neuron specific enolase
PBS	phosphate buffered saline
PCR	polymerase chain reaction
PI 3K	phosphatidylinositol-3 kinase
PPAR	peroxisome proliferator-activated receptor
PSEN	papillary and solid epithelial neoplasm
PTEN	phosphatase and tensin homologue
PVDF	polyvinylidene difluoride
Rb	retinoblastoma
RNA	ribonucleic acid
RNase	ribonuclease
RT	reverse transcriptase
RXR	retinoid X receptor
SEM	standard error of the mean
SNP	single nucleotide polymorphisms
TZD	thiazolidinedione
UV	ultraviolet
VHL	von Hippel-Lindau disease

CHAPTER 1

INTRODUCTION

1.1 Tumours of the neuroendocrine system

Neuroendocrine cells may either co-localise within glands (for example the pituitary, parathyroid, and adrenal medulla), or may be found scattered amongst other non-endocrine cells throughout the body making up the diffuse neuroendocrine system. Initially thought to derive from a common origin within the neural crest, it appears that neuroendocrine cells have diverse embryological origins and acquire similar properties during cell differentiation (Duerr et al 2007, Andrews et al 1998). Tumours arising from neuroendocrine cells, neuroendocrine tumours (NETs) thus comprise a heterogeneous group of disorders that have defied easy classification. The majority of NETs associated with the diffuse neuroendocrine system arise from the gastro-enteropancreatic (GEP) system, although up to 30% may develop in the bronchopulmonary system, with occasional tumours arising within tissues including the urogenital system, thyroid and thymus (Modlin et al 2003, Rindi et al 1998). The annual incidence of these tumours is around 5 per 1,000,000 per year and is thought to have increased in recent years – probably reflecting both greater awareness and improved diagnostic modalities. Predicted frequencies from autopsy series suggest that they remain under-diagnosed (Gustaffson et al 2008).

The term “carcinoid” has in the past been widely applied to NETs in general, but was first coined by Oberndorfer (Karzinoide Tumoren des Dünndarmes. Frankfurter Zeitschrift für Pathologie, 1907, 1: 426-429) to describe “cancer like” tumours with apparently low malignant potential identified in the small bowel (Modlin et al 2004). The classical symptoms of “carcinoid syndrome” include flushing, hypotension, wheezing and diarrhoea, and may be related, at least in part, to serotonin released from tumours derived from the EC (Kultchitsky) cells of the gastrointestinal tract or bronchi, although vasoative substances are also involved.

Early categorisation divided neuroendocrine tumours according to the embryological site of origin. Thus foregut tumours included those arising from the lung, stomach, duodenum and upper jejunum and pancreas, midgut tumours comprising lower jejunum, ileum, appendix and caecum, and hindgut tumours describing those found within the colon and rectum. However, this classification failed to take into account the diversity of neuroendocrine cell types from which these tumours arise, a distinction that is more relevant to the syndromes encountered clinically than the embryological site of tumour origin (reviewed by Kloppel 2004). To add further complexity, eponymous terms such as Zollinger-Ellison syndrome and Verner-Morrison syndrome are still frequently used in the context of NETs, as are descriptive terms such as Watery Diarrhoea Hypokalaemia Achlorhydra (WDHA) syndrome.

A recent classification system introduced by the World Health Organisation has attempted to clarify the nomenclature applied to GEP-NETs, although it is not relevant to tumours arising elsewhere. The term carcinoid has been replaced (to a large extent) by the term neuroendocrine tumour. Such tumours are described histologically as either a well differentiated tumour (confined to mucosa/submucosa, non-angio-invasive), a well differentiated carcinoma, (with invasion of the lamina propria or identifiable metastases) or a poorly differentiated carcinoma with high malignant potential. There is also a mixed-exocrine-endocrine carcinoma. Tumours may then be further subclassified according to their anatomical site of origin and secretory profile (Kloppel 2007).

Pancreatic NETs have survival rates of between 30 – 97% 5 year survival depending on the tumour subtype (Modlin et al 2003). 50–60% of pancreatic NETs are hormonally active, with the remainder being hormonally silent. The numbers of hormonally silent

pancreatic NETs diagnosed has risen over recent years, probably as a result of improved imaging rather than a true increase in incidence. Functioning tumours are associated with the secretion of a large variety of hormones including insulin (insulinoma), glucagon (glucagonoma), gastrin (gastrinoma), and vasoactive intestinal peptide (VIPoma). They may rarely secrete adrenocorticotropic hormone (ACTH), or growth hormone. A single tumour may be associated with the secretion of more than one hormone (Belchetz et al 1973). Pancreatic NETs are usually solitary (but may be multiple in familial disease) and well-demarcated, measuring between 1 – 4 cm in diameter. Although insulinomas are usually histologically benign (the clinical consequences of uncontrolled insulin release may however be catastrophic), the remainder of the pancreatic NETs frequently show malignant features. Evidence of microangioinvasion, high mitotic rate and a size greater than 2 cm give cause for concern (Kloppel 2007). Interestingly, the organ of origin of NETs appears to play a part in the clinical progression of disease – for example pancreatic gastrinomas are in general more aggressive that those arising in the duodenum (Modlin et al 2005).

1.2 Pancreatic development and cellular differentiation

The pancreas is an organ containing two distinct populations of cells, the exocrine cells that secrete enzymes into the digestive tract and the endocrine cells that secrete hormones into the bloodstream. During early embyrogenesis (28 days in the human) the ventral and dorsal buds of the early pancreas develop as evaginations of the embryonal foregut. Arising opposite each other, the ventral bud moves round to form the posterior part of the pancreatic head and uncinate process while the remainder of the organ develops from the dorsal bud (reviewed Peters et al 2000). The longstanding hypothesis that pancreatic exocrine and endocrine cells are derived from different cell pools (gut endoderm and neural crest respectively) has been refuted with a number of cell lineage

experiments and molecular studies. Pancreatic NETs are likely to originate from cells of the primitive gut endoderm that ultimately give rise to all the cell types of the mature pancreas - the ductal cells, acinar cells and endocrine cells.

The exocrine pancreas is a lobulated, branched, acinar gland. The acini are pyramidal in shape with basal nuclei, regular arrays of rough endoplasmic reticulum, a prominent golgi complex and numerous secretory granules containing the digestive enzymes, of which there are at least 22 including proteases, lipases, amylases and nucleases. Often, these are precursors which are activated within the gut following secretion. Control of secrtetion is by hormonal stimulation including secretin, cholecystokinin and gastrin. Neural stimulus is also involved.

The endocrine cells are mainly grouped into Islets of Langerhans, which are compact spherical clusters of cells embedded within the exocrine pancreas. They form by aggregation of polyclonal endocrine cells. This seems to occur when they start to express cell adhesion molecules such as N-CAM and cadherins. There are four principal types of endocrine cell. The β cells secrete insulin and also Islet Amyloid Polypeptide (IAPP) or amylin. These are the most common cells in the islets. The α cells secrete glucagon, the δ cells secrete somatostatin and the PP cells secrete pancreatic polypeptide. A proportion of the adult islet cells make peptide YY in addition to their principal product. Ghrelin, an endogenous ligand of the growth hormone secretagogue receptor (GHS-R) is also thought to be expressed by the endocrine pancreas. Wierup et al. (2002) identified ghrelin secreting cells (upto 10% of all endocrine cells) in the fetus from mid gestation to post natally. In the adult the cells were few and seen at the periphery of the islets, exocrine tissue, ducts and ganglia. They were not co-expressed and therefore a new islet cell type was proposed. Controversy has surrounded this issue,

Volante et al (2002), again confirmed the presence of ghrelin in the islets but it was confined to the β cell population. Date et al (2002) on the other hand confirmed ghrelin to be present at the periphery of the islets in humans and rats but only co-expressed with glucagon suggesting localisation in the α cells. Furthermore, Prado et al (2004) identified that mice lacking Nkx2.2, a homeodomain protein known to be essential for β cell differentiation, have normal sized islets but the resulting cells produce ghrelin. They postulated that insulin and ghrelin cells share a common progenitor and that the lack of β cell stimulus leads to preferential ghrelin cell differentiation.

In the developing pancreatic buds, the endocrine cells start to differentiate before the exocrine cells and co-expression of different hormones by the same cell is possible at early stages. In humans, the first identifiable endocrine cells develop at around the 7th week of gestation and are found scattered amongst ductal cells. These cells express somatostatin and pancreatic polypeptide (PP). This is followed by the development of glucagon-producing cells, then insulin-producing cells. The embryonal pancreas also appears able to express gastrin, gastrin inhibitory peptide, serotonin, catecholamines and prostaglandins, expression of which is lost in the adult pancreas. This pattern of hormone expression is different to that seen in mice, where the first hormone expressed is insulin, then somatostatin and PP. Interestingly, mouse studies have suggested that cells of the foregut, not destined to form the pancreas, are also able initially to express pancreatic hormones including insulin, glucagon, PP, and somatostatin in chronological order. It may be that this expression of endocrine hormones heralds the development of neuroendocrine cells of the bowel and confirms that they have the potential to express a variety of endocrine hormones (reviewed Peters et al 2000).

By the twelfth week of human embryogenesis, small groups of endocrine cells begin to bud out from pancreatic ducts and become vascularised. These are the precursors to islets recognised in the adult pancreas. They loose contact with the ducts by about weeks 17-20 at which point total islet cell tissue has increased to 8-13% of total pancreatic mass. The foetal pancreas also contains a large number of cell aggregates which decreases with gestation but can still be present in the adult pancreas and maybe associated with ductules. This accumulation is concomitant with the expression of certain transcription factors including the neural cell adhesion molecules (N-CAM) and cadherins. The majority of endocrine cells are contained within such islets, although a few β cells remain scattered amongst the ductal cells of the pancreas (reviewed by Peters et al 2000). In rodents there is segregation of cell types within the islets so that β cells lie in the centre and the other types at the periphery. In humans, this segregation does occur but it is less pronounced. All the types of islet cells also express a number of gene products characteristic of neuroendocrine cells such as neuron-specific enolase.

It has been shown that in the developing pancreatic diverticula, exocrine and endocrine cells originate from epithelial cells with features of ductal cells (Pictet and Rutter, 1972). This suggests that the ductal cells harbour the stem cell compartment from which acinar or islet cells originate. The phenotype of this pancreatic stem cell is yet to be fully defined but various studies have suggested possible markers such as tyrosine hydroxylase (Teitelman et al, 1993), glucose transporter (GLUT-2) (Pang et al, 1994), cytokeratins (Bouwens et al, 1994), and PDX-1 (Jonsson et al, 1994). Regarding endocrine differentiation, Upchurch et al. (1994) found cells of all 4 main endocrine cell types to co–express peptide YY at the early stages and thus suggested a common peptide YY producing progenitor cell for all the endocrine cell types.

The differentiation of islet cells from pluripotent ductal cells appears to be dependent upon the influence of mesenchymal factors that induce the expression of transcription factors such as pancreas duodenum homeobox 1 (PDX1) and islet1 (ISL1) within the embryonic pluripotent cell (Peters 2000). PDX1 also known as IPF-1 is a transcription factor important in regulating the expression of insulin and somatostatin that is initially expressed throughout the embryonic pancreas and duodenum. Mouse knock-out models suggest that PDX1 is important in the initial organ commitment of the pancreas while the differentiation of cells into pancreatic endocrine cells is reliant upon the subsequent expression of pax genes. Indeed, PDX1 probably has one of the most critical roles in early pancreatic development because when it is removed from mice by targeted mutagenesis, the embryos completely lack a pancreas (Jonsson et al 1994). In later life this gene is thought to be expressed only in the β cells and acts as a transcription factor for insulin. Other transcription factors expressed in the early pancreas, as well as in other parts of the body, are prox-1 (Oliver et al 1993), Tlx-1 (Raju et al 1993) and pax6 (Turque et al 1994) which all belong to the homeobox gene group. The whole early rudiment of the pancreas also expresses the enzyme L-amino acid decarboxylase (AADC), which becomes confined to the islet cells postnatally (Teitelman et al 1987).

Epithelial- mesenchyme interactions have been thought to be important for some time. In the absence of mesenchyme it is thought that isolated pancreatic epithelium is unable to differentiate into exocrine or endocrine tissue. This role was further defined by Kim et al, 1997, who reported that removing the notochord (representing early mesenchymal tissue) from the endoderm essentially stops pancreatic development, thus suggesting that signals from the mesenchyme are essential for the differentiation of the primitive gut endoderm into pancreatic cells.

ISL1 is also important in the initial organ commitment of the pancreas and the differentiation of islet cells (Peters et al 2000). ISL1 is expressed in all classes of islet cells in the adult. It is also expressed in the mesenchymal cells that surround the dorsal but not the ventral evagination of the gut endoderm. Ahlgren et al (1997) analysed acinar and islet cell differentiation in the developing pancreas in mice deficient in ISL1 to define its role. They found that dorsal pancreatic mesochyme did not form in the ISL1 mutants and that there is an associated failure of exocrine cell differentiation in the dorsal but not the ventral pancreas. There was also a complete lack of differentiated islet cells. In vitro, the provision of mesochyme derived from the wild type resulted in exocrine but not endocrine cell differentiation. They argued that ISL1 by virtue of its requirement for dorsal mesenchyme formation is necessary for the formation of the dorsal exocrine pancreas. ISL1 expression in pancreatic epithelial cells was also shown to be required for the differentiation of islet cells. It would appear that the development of the pancreas is controlled by sequential activities of distinct classes of transcription factors. PDX1 specifies the early pancreatic epithelium, permitting its proliferation and differentiation. Other factors, such as neuroD/BETA2 which are expressed in pancreatic endocrine cells, may also act upstream of ISL1 in the islet cell differentiation sequence.

Growth factors are important in the induction of endocrine cell growth and functional differentiation. Insulin-like growth factor (IGF-1 and IGF-2) may exert diverse effects including mitogenic effects, insulin like action, stmulation of chemotaxis and induction of cell differentiation. IGF-1 binds to the IGF receptor, a tyrosine kinase which has considerable similarity to the insulin receptor (Ullrich et al, 1990). IGF-1 and -2 plus IGF binding proteins have been shown to be present and have developmental patterns which vary during early pancreatic life (Hogg et al, 1994).

Transforming Growth Factor (TGF) α exerts its effects through binding to the Epidermal Growth Factor (EGF) receptor. It has been identified that when the pancreatic duct is ligated, TGF-α protein levels in the cells of tubular complexes and ducts is elevated as remodelling of the pancreatic parenchyma occurs. As its expression co-incides with increased duct cell proliferation and the formation of new β-cells, it has been postulated that it is involved in islet cell neogenesis (Wang et al, 1997).Transforming Growth Factor (TGF) β_{1-3} has been shown to be present in islet, acinar and ductal cells in the human pancreas (Hogan et al, 1994). Transgenic mice which are TGF-β type 2 receptor negative have aberrant ducts and ductal cells suggesting TGF-β has an inhibitory growth effect on these cells (Bottinger et al, 1997). TGF-β may also induce the regression of the acinar compartment of the developing pancreas and promote endocrine tissue development (Sanvito et al, 1994).

Other growth factors that have been implicated include Hepatocyte Growth Factor (HGF), levels of which increase during proliferation induced by partial pancreatectomy (Bonner-Weir et al, 1997), Nerve Growth Factor (NGF), whose high affinity receptor Trk-A is seen in islet cells and ductal cells during late fetal life of the rat but only β-islet cells in the adult (Kanaka Gantenbein et al, 1995), Betacellulin, an EGF family member which converts pancreatic acinar cells into insulin secreting cells (Mashima et al, 1996), Vascular Endothelial Growth Factor (VEGF) which stimulates the proliferation of ductal but not endocrine cells in vitro (Rooman et al, 1997) and Gastrin which is expressed at the mRNA and protein level during the period of cellular differentiation into ductal, acinar or endocrine cells but which disappears rapidly from the pancreas in the post natal period (Pictet et al, 1972).

1.3 Diagnosis of GEP neuroendocrine tumours

NETs may cause symptoms simply by virtue of their physical presence, for example luminal obstruction, or as a consequence of hormones released from the tumour cells. Tumours not associated with hormone release are termed “silent” or “non-functioning” while the early symptoms associated with hormonally-active NETs are often non-specific and frequently defy early recognition.

1.3.1 Serum and immunohistochemical markers

Secretory tumours may be detected through a combination of clinical symptoms and specific hormone measurements. NETs of the pancreas may be associated with the secretion of a variety of biologically active hormones including pancreatic polypeptide, insulin, glucagon, gastrin, vasoactive intestinal peptide (VIP) and rarely ACTH or growth hormone. Some tumours may be associated with the secretion of more than one hormone. The predominant hormone produced, for example insulin (insulinoma), glucagon (glucagonoma) or VIP (VIPoma) characterises the tumour. The most frequently encountered secretory NET is the insulinoma, perhaps reflecting the distinct clinical consequences of fasting hypoglycaemia that can quickly impact on quality of life. Diagnosis relies upon the demonstration of confirmed hypoglycaemia in conjunction with inappropriately raised insulin (and C-peptide) levels and the exclusion of exogenous drug ingestion. Such tumours tend to be benign, but may be multiple when occurring in the context of familial disease such as MEN1 (see below). Raised fasting peptide levels specific to the other tumour types can aid diagnosis, although such tests, in particular fasting gastrin levels, may be complicated by concomitant disease or medications reducing its sensitivity (in particular proton pump inhibitors). Fluctuating hormone secretion and unusual symptoms may also complicate diagnosis. Tumours may be multifunctional, secreting more than one hormone (frequently PP in addition to

another hormone), although not all will be associated with clinical consequences. Non insulinoma NETs of the pancreas often show malignant behaviour and have frequently metastasised at the time of diagnosis (Modlin et al 2008, Kloppel et al 2007).

Serum chromogranin A levels are raised in 60-80% NETS and may be used as a general marker of both functioning and non-functioning neuroendocrine tumours (reviewed by Modlin et al 2008). However, they are non-specific markers, being positive tumour markers in other malignancies, and levels may also be raised in renal failure, or with enterochromaffin-like (ECL) cell hyperplasia seen in atrophic gastritis and with proton pump inhibitor therapy (Modlin et al 2008, Gustaffson et al 2008). Chromogranin B is more specific to insulinomas (Kaltsas et al 2004). Other general markers of NETs include neuron specific enolase (NSE) which may be raised in other pancreatic malignancies, chorionic gonadotrophin and pancreatic polypeptide, which is raised in up to 80% pancreatic NETs (Modlin et al 2008, Kloppel 2007). None, however, can reliably diagnose all pancreatic NETs and are thus suboptimal as tumour markers.

Some immunohistochemical markers can be used to aid tissue diagnosis of presumed NETs. Cells of the diffuse neuroendocrine system may be identified by the expression of both endocrine and neuronal features. Production of neurotransmitter, neuromodulators or neuropeptides from small clear vesicles (40-80nm diameter), the presence of dense core secretory granules that release hormones by exocytosis (>80nm diameter), and the absence of axons, identify such cells histologically. In addition, the expression of molecular markers including chromogranin A (large granule associated), synaptophysin (small granule associated) and NSE can be used to confirm neuroendocrine cell origin. The majority of NETs express somatostatin receptors, and confirmation of this can also aid diagnosis of such tumours (Modlin et al 2008).

Although a high mitotic rate, nuclear atypia and few secretory granules may identify poorly differentiated, highly malignant neuroendocrine tumours, there are few histological clues as to predicting malignant behaviour in well-differentiated tumours (Kloppel 2004, 2007). The proliferation marker Ki-67 may be used to assess the rate of cell proliferation and thus suggest malignant potential (Modlin et al 2008), but an improved understanding of the biology of these tumours is required to aid diagnosis and prognostic predictions.

1.3.2 Imaging

Several imaging modalities are employed in localising pancreatic NETs and associated metastases, although the primary tumour may never be found. Imaging techniques may identify tumours by physical presence alone or by functionality. Imaging is important not only in initial tumour localisation and staging, but also in treatment planning and assessing response to therapy.

Standard transabdominal ultrasound alone offers limited value in the management of pancreatic NETs, although endoscopic ultrasound and intraoperative ultrasound techniques have proven valuable in the assessment of disease – particularly in cases such as MEN1 where pancreatic lesions may be small and multiple. Endoscopic ultrasound has been developing over the past decade as an alternate form of imaging for diagnosis and localisation of tumours, with the added benefit of guided biopsies. It has been seen to be sensitive in up to 93% of proven pancreatic neuroendocrine tumours (Anderson et al. 2000), but is heavily operator-dependent. Multidetector CT scanning and MRI offer complementary aspects to the identification of mass lesions, the presence of metastases and subsequent response to treatment. MRI provides a good assessment of liver metastases but may also localise lesions not found on CT images (Rockall et al

2007). A review of MRI in the detection of pancreatic neuroendocrine tumours identified the fat saturated T1 weighted spin echo sequence as the most useful in the detection of these tumours (Owen et al 2001). Newer CT scanning techniques allow the detection of smaller pancreatic NETs, and sensitivities of up to 100% may be achieved when this imaging technique is used in conjunction with other modalities such as MRI and endoscopic ultrasound of the pancreas.

Functional imaging of NETs provides a further means by which the physical presence of disease may be detected, but may also identify suitable candidates for targeted treatment in the form of labelled radionuclide therapy. Neuroendocrine cells are characterised by their ability to take up and concentrate amine precursors and to produce amines or peptides; they may also express peptide hormone receptors on the cell surface which together make functional imaging of these tumours possible. Somatostatin receptors (types 1-5) are widely expressed on neuroendocrine cells. This may be targeted in pancreatic NETs using radiolabelled somatostatin analogues, typically indium-labelled octreotide. The sensitivity of this technique in localising lesions may be further improved by its combination with CT. MIBG, a catecholamine analogue, may be useful in the detection of some carcinoid tumours, which have been reported to take up and concentrate MIBG, in addition to paragangliomas and phaeochromocytomas. Its use is, however, limited in pancreatic NETs (Kaltsas et al 2004). Positron Emission Tomography (PET) scanning again utilises the ability of NET cells to take up and concentrate substances that may then be identified if they have been labelled, in this case by positron emitting radionuclides. Uptake of fluorodeoxyglucose (FDG, a glucose analogue), L-hydroxyphenylalanine (L-DOPA) and 5 hydroxy-L-tryptophan (5HTP) have all been used in imaging NETs with variable success. FDG-PET uptake is not specific to NETs but is used widely in the diagnosis of oncological

disease processes. It is mainly helpful in detecting poorly differentiated lesions with a high proliferative rate. L-DOPA-PET has proven successful in detecting carcinoid type tumours, phaeochromocytomas and possibly medullary carcinoma of the thyroid, but has limited value in other subtypes of NET. Initial results using HTP-PET are promising but require further evaluation (Sundin 2007), and both of these require a cyclotron nearby as the isotopes have very short half-lives. As an alternative, more invasive procedures may be of value in difficult cases, for example, the direct injection of calcium gluconate into the arteries supplying the pancreas can stimulate insulin release and aid the diagnosis of insulinomas (Kaltsas et al 2004).

1.4 Treatment

1.4.1 Surgery

Surgical management of pancreatic NETs depends on the primary diagnosis. Insulinomas are usually small and rarely metastatic. Thus, they may be surgically enucleated with good results. The exceptions are those associated with MEN1 that may be multiple and where identification of the principle secretory lesion should be attempted preoperatively. Insulinomas are frequently palpable at the time of surgery but the use of intraoperative ultrasound can complement this in identifying lesions. Malignant insulinomas are associated with multiple distal metastases and poor prognosis. The management of the other pancreatic NETs includes surgical resection and lymph node clearance, since the malignant potential of these tumours is high. Limited resection of hepatic metastases may also be attempted (Ackerstrom et al 2007).

1.4.2 Hepatic embolisation

Hepatic metastases may be managed with surgical resection where disease is limited. Localised hepatic embolisation either with or without additional chemotherapeutic

agents provides an alternative method. Since hepatic metastases receive most of their blood supply via the hepatic artery, while the liver itself receives part of its blood supply from the portal vein, occlusion of the branch of the hepatic artery feeding the tumour is a viable therapeutic option. Cells are thought to be more sensitive to chemotherapeutic agents when ischaemic, thus a local injection of chemotherapy may be used in addition (Toumpanakis et al 2007).

1.4.3 Somatostatin analogues

The majority of neuroendocrine tumours express somatostatin receptors and this can be used therapeutically. Somatostatin reduces hormone secretion from the anterior pituitary, gastrointestinal tract and pancreas. In general, NETs express a high density of such receptors, but the receptor subtype expressed can vary between tumours and within the same tumour. Somatostatin analogues including both short-acting and the long-acting formulations have been successful in reducing the clinical burden associated with tumour hypersecretion syndromes, although tumour regression has not been a common result of therapy. Although somatostatin therapies could be used for all tumour subtypes, in general better symptom control is achieved in gastrinomas with proton pump inhibitors, and using diazoxide to manage insulinomas. Some stabilisation of tumour progression may be achieved using somatostatin analogues, but ultimately the effect of therapy wanes over time with tachyphylaxis. Interferon therapy may be associated with a reduction in tumour growth, but the side effect profile is more significant than that seen with somatostatin analogues (Plockinger et al 2007).

1.4.4 Radiolabelled somatostatin analogues

Tumour expression of somatostatin receptors has been exploited for the delivery of radiolabelled somatostatin analogues directly to the tumour bulk. Indium, yttrium, and

lutetium are the main radionuclides available for such therapy, and their effects vary according to the emitted particles that vary in terms of tissue penetration. Yttrium, a β-emitter, has the most far reaching range which has benefits in terms of tumour management, but increases the risk of damage to other organs such as the kidneys (Forrer et al 2007).

1.4.5 Chemotherapy

The use of systemic chemotherapy on the management of NETs remains under evaluation. As slow growing malignancies they tend to respond poorly to such regimes. Streptozocin-based chemotherapy including either fluoruoracil or doxorubicin has been used in metastatic pancreatic NETs, although the optimal time to offer such therapies remains unclear. A combination of cisplatin and etoposide can be used in poorly differentiated NETs (Toumpanakis 2007).

1.5 Models of tumour formation

Disruption of the process of cell differentiation may result in malignant transformation of a cell. Abnormal cell cycle progression and tumour formation can be consequent on inappropriate gene expression (oncogenes) or a failure of tumour suppresser gene activity that would normally prevent uncontrolled progression through the cell cycle. Mutation of a single dominant oncogene can result in uncontrolled cell growth; however, recessive oncogenes are also recognised, where functional deletion of two copies of the same gene is required for tumour formation. Spontaneous mutations affecting both genes in the somatic cell would be relatively unusual, and thus sporadic forms of such tumours are rare. However, if a single autosomal recessive mutation in an oncogene is inherited at the germ cell level and a second gene deletion or mutation

occurs within the somatic daughter cell, tumour formation will result. This is the basis for Knudson's "two-hit hypothesis" where a silent genetic fault is unveiled by a second deletion. Thus a recessive genotype becomes a dominant phenotype, where the second genetic "hit" is inevitable given the vast number of cells expressed in the target tissue. Such genetic abnormalities can be identified using loss of heterozygosity studies that confirm heterozygosity for a certain gene in non-tumour tissue (typically leucocytes) that is lost in tumour tissue (LOH). Genetic gain or loss may also be detected by comparative genomic hybridization (CGH) a technique that may be used to complement LOH studies or other more recent developments such as multiplex ligation-dependent probe amplification (MLPA) or single nucleotide polymorphisms (SNP) analysis.

Genes may also be silenced through epigentic phenomena such as abnormal methylation patterns that would not be detected by LOH or CGH methods. DNA methylation, important in X chromosome inactivation and parental gene imprinting, is the transfer of a methyl group to the cytosine of a cytosine-guanine (CpG) nucleotide. CpG nucleotides tend to cluster as "islands" particularly at gene promoter regions, reflecting their role in control of gene expression.

The process by which cells replicate DNA and divide is a tightly regulated cycle requiring input and facilitation from a variety of mitogens and growth factors. Activation mutations of oncogenes or loss of tumour suppressor genes may be implicated in many models of tumorigenesis, but so far none appear to be sufficient in explaining pancreatic NET formation. Studying inherited conditions in which NETs commonly occur has facilitated analysis of important molecular events in the differentiation of neuroendocrine cells. Familial diseases such as multiple endocrine neoplasia 1 (MEN1) and Von Hippel-Lindau disease (VHL) are typified by the

occurrence of neuroendocrine tumours within the context of complex disease that may also include the presence of other non-endocrine malignancies.

MEN1 is an autosomal dominant disorder typified by the formation of multiple endocrine tumours affecting the parathyroids, anterior pituitary, and endocrine pancreas. The MEN1 gene is located on chromosome 11q13 and its gene product menin probably has functions in both genome stability and transcriptional control. Up to 600 mutations have been identified in the MEN1 gene, including nonsense mutations, deletions or insertions, and splice variants. Although only 20% of sporadic foregut NETs (including pancreatic NETs) harbour an identifiable mutation in the MEN1 gene, up to 60% of sporadic pancreatic NETs exhibit LOH at chromosome 11, suggesting the presence of alternative genetic mutations at that locus (reviewed by Leotlela 2003, Duerr 2007).

VHL disease is associated with pancreatic NETs occurring in conjunction with renal cell carcinomas, retinal/cerebellar haemangioblastomas and phaeochromocytomas. The VHL gene, located on chromosome 3p25-26 encodes a tumour suppresser gene important in hypoxia-induced cell proliferation and angiogenesis. Although the majority of VHL-associated pancreatic NETs exhibit LOH in the VHL gene, studies including both sporadic and VHL-associated pancreatic NETs suggest that a critical genetic defect may lie proximal to the VHL gene locus on chromosome 3, independently contributing to the development of such tumours (Lott 2002). Indeed, up to 30% of sporadic pancreatic NETs show LOH on chromosome 3p, an area that encodes many important genes including VHL, Retinoic acid receptor b (RARb), peroxisomal proliferator-activated receptor (PPAR), RASSF1A (see below) and p51 (a member of the p53 tumour suppresser family). Interestingly, no mutations in the VHL gene were identified

within this group of tumours, suggesting that its role is limited in explaining the pathogenesis of pancreatic NETs (Chung 1997, Zicusoka 2005).

Pancreatic NETs are frequently associated with chromosomal changes, and these seem distinct from those identified as important in gastrointestinal NETs. Different chromosomal losses or gains may themselves be identified at distinct stages of disease, and may also predict tumour behaviour. Genetic aberrations may have a cumulative effect, some being important in early cell hyperplasia and dysplasia, others playing a role in the loss of cell differentiation and metastases (Baracat et al 2004). Pancreatic NETs may be either oligoclonal or monoclonal in origin, suggesting that more than one mechanism may result in tumour formation in a single individual (Katona et al 2006). Genomic gains have been identified on 4p, 4q, 7p, 7q, 9q, 12q, 14q, 17pq, 18q and 20q, while genomic losses have been identified on 1p, 3p, 6q, 10p, 11p, 11q, X and Yq. Efforts to identify specific genetic aberrations predictive of tumour behaviour have failed, although loss of 11q and gain of 7q appear most consistently to associate with pancreatic NETs, while malignancy may be predicted by gains on chromosomes 4, 7, 14 and X or losses on 3, 21 and 6 (Zicusoka et al 2005).

Non-functioning pancreatic NETs are associated with more genomic alterations, as compared to functioning tumours, in particular losses of 3p and MEN1 (reviewed Duerr 2007). The pattern of allelic loss may also predict the type of pancreatic NET, functioning tumours associating with LOH of chromosomes 3, 11, 16 and 22, while non-functioning pancreatic NETs associate with LOH of 6 and 11 (reviewed by Rigaud et al 2001). LOH of chromosome 1 has been identified in one third of pancreatic NETs and appears to predict hepatic metastases (Ebrahimi et al 1999). Similarly, LOH studies have shown that chromosome 3q may play a critical role in the development of a more

malignant pancreatic NET phenotype (Guo et al 2002). CGH studies have identified loss of chromosome 6q in 100% of malignant insulinomas, possibly reflecting genetic influences specific to β-cell neoplasia. High expression of neuroendocrine secretory pepetide 55 (NESP55), a chromogranin gene product of chromosome 20, may be used to distinguish pancreatic NETS from gastric carcinoid tumours, a potentially useful tool in the evolution of metastatic disease of unknown origin (reviewed by Zicusoka 2005).

1.6 Pancreatic neuroendocrine tumours and the cell cycle

Several cell cycle regulators have been studied in the context of pancreatic NETs. The cyclin D proteins are critical in permitting a cell to advance through the cycle of DNA replication and division, and are of interest in many tumour models. Cyclin D1 allows progression through G1 and into the S phase of DNA synthesis by activating cyclin dependent kinases (CDK). These phosphorylate retinoblastoma protein (Rb - see below), thereby reducing its anti-proliferative effect (reviewed Musat et al 2004). The cyclin D1 gene (CCND1) is one of the most frequently amplified genes in human tumours and is associated with increased cyclin D1 protein expression (reviewed Hibberts et al 1999). Increased nuclear expression of cyclin D1 has been shown in 50% pancreatic NETs as compared to non-neoplastic islet cell tissue, and is found regardless of tumour type or malignancy. This would suggest that it is an important factor early in development of the disease, and relevant to all tumours irrespective of the cell of origin (Chung et al 2000).

Activation of the p53/MAPK and Akt/protein kinase B pathways have also been identified in pancreatic NETS, and may also influence progression through the cell cycle through increased cyclin D levels (reviewed Zicusoka et al 2006). Frequent activation of the p38/MAPK and Akt pathways but down regulation of the ERK

pathway in cyclin D1 over-expressing pancreatic neuroendocrine tumours has been reported (Guo et al, 2003). Hypermethylation of RASSF1A, a tumour suppresser that induces cell cycle arrest by interaction with cyclin D, has been identified in a subset of pancreatic NETs (Duerr 2007).

Rb is a tumour suppressor gene that prevents progression of the cell cycle from G1 through to the S phase of DNA replication. Phosphorylation of Rb by cyclin D1 and its associated kinases (CDKs) reduces the ability of Rb to prevent progression through the cell cycle. Although p53 and Rb deficient mouse models show a propensity towards developing neuroendocrine tumours, including pancreatic malignancies (Harvey 1995), there has not been conclusive evidence to implicate Rb in the pathogenesis of human pancreatic NETs to a date (Chung 1997).

The cell cycle is regulated at various stages by the combined actions of cyclins, CDKs, and cyclin dependent kinase inhibitors (CDKIs). There are two main groups of CDKIs, the INK4 group comprising $p15^{INK4B}$, $p16^{INK4A}$, $p18^{INK4C}$, $p19^{INK4D}$, and the CIP/KIP group comprising $p21^{CIP1}$, $p27^{KIP1}$ and $p57^{KIP2}$. The CDKI p27 maintains cells in a quiescent state by binding to and inactivating cyclin/CDK complexes to prevent entry into S phase (reviewed Musat et al 2004) and is negatively correlated to Ki-67 in pancreatic NETs, suggesting that it may reduce the proliferative rate in such tumours (reviewed Zicusoka et al 2006). Down regulation of p27 has also been identified in MEN1 knock-out mice that develop β cell hyperplasia within a phenotype that resembles MEN1 (reviewed by Duerr 2007). In mice lacking p27, created by gene targeting in embryonic stem cells, an increase in body size is noted with substantial increases in thymus, pituitary, adrenal and gonadal organ size, suggesting an important role for p27 in a variety of endocrine tissues (Nakayama et al, 1996). Reduced

expression of p27 has been associated with poor prognosis in most human cancers, including pancreatic adenocarcinoma (Lu et al 1999).

Regulation of p27 within the cell is thought to occur at two levels, the rate of protein synthesis and, probably more importantly, the rate of protein degradation, in particular by the ubiquitin/proteasome pathway. Several studies have indicated that that phosphorylation of p27 is an important primary trigger for p27 degradation and is cell cycle-dependent, peaking in late G1 phase (Sheaff et al 1997, Vlach et al 1997, Montagnoli et al 1999). It appears that phosphorylation-mediated p27 degradation facilitates transition from G1 into S phase and thus enhanced phosphorylation has been implicated in over-proliferation of cells and many cancers.

Jun activation domain-binding protein 1 (JAB1), an activator protein (AP-1) coactivator implicated in p27 degradation and transportation, is over-expressed in various tumours and correlates with low p27 expression. JAB1 interacts with p27 shuttling it from the nucleus to the cytoplasm; it has been shown that JAB1 binds directly to the C-terminal part of p27 in the nucleus and over-expression of JAB1 causes translocation of p27 into the cytoplasm (Tomoda et al, 1999). An inverse relationship in expression levels of p27 and JAB1 has been reported in various cancer tissues, including ovarian (Sui et al, 2001), invasive breast carcinoma and their adjacent normal breast tissue (Kouvaraki et al, 2003) and anaplastic large cell lymphoma (Rassidakis et al, 2003). High expression of JAB1 has also been shown in medullary cell carcinomas with a concomitant reduction in p27 expression (Ito et al 2005). Increased JAB1 expression was seen in pancreatic carcinoma samples and forced expression of JAB1 in pancreatic cell lines was associated with decreased p27 expression (Kouvaraki et al, 2006).

The protein Ki-67 was originally defined by the prototype monoclonal antibody Ki-67 generated by immunising mice with nuclei of a Hodgkin lymphoma cell line (Gerdes et al 1983). The name is derived from the city of origin (Kiel) and the number of the original clone in the 96-well plate. When the antigen was found to be a protein, it was found that there was no homology to any known polypeptide. The function therefore remained indistinct and the name was kept. It has been well documented over the years that Ki-67 is associated with cell proliferation, being present during all active phases of the cell cycle but being absent in quiescent or resting cells in G_0 (Gerdes et al, 1984). Ki-67 labelling index in neuroendocrine tumours of the pancreas have been shown to be independent predictors of survival in two separate studies showing reduced survival with values of >4% (Perret et al, 1998) and >5% (Pelosi et al, 1996).

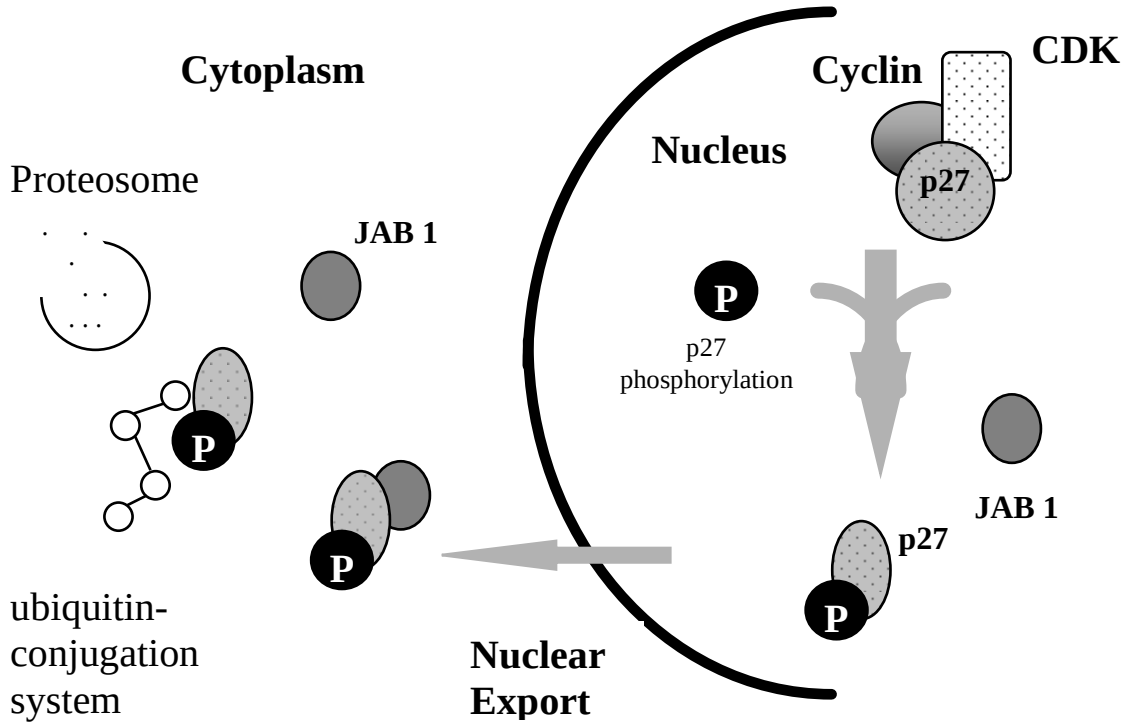

Figure 1.1 Diagram showing the mechanism of p27 degradation within the cytoplasm following phosphorylation and nuclear export by JAB

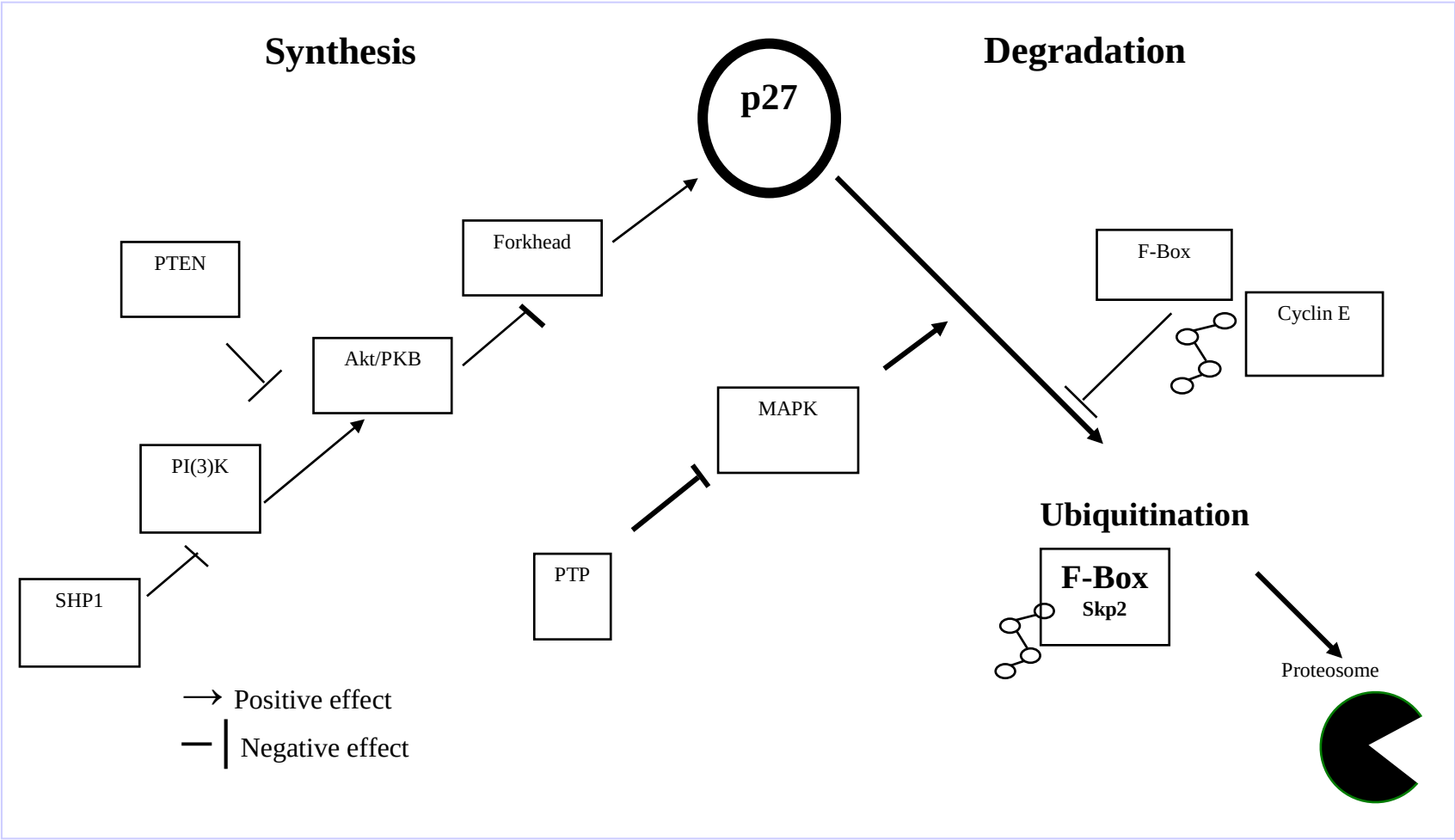

Figure 1.2 Diagram showing some of the pathways that influence p27 synthesis and degradation

1.7 The peroxisomal proliferator-activated receptor

The PPARs (peroxisomal proliferator-activated receptors) are members of the nuclear receptor superfamily that includes receptors for thyroid, steroid and retinoid hormones. They were first identified in rodents following the observation that certain chemicals (peroxisome proliferators) could augment the size and number of hepatic and renal cell peroxisomes, thereby increasing their capacity for fatty acid metabolism (reviewed in Kliewer 1994). Natural ligands include long-chain polyunsaturated fatty acids, metabolites of the arachidonic and lipoxygenase pathways, oxidised low-density lipoproteins and prostaglandins. The major synthetic ligands of PPARs are the anti-diabetic agents, thiazolidinediones, and non-steroidal anti-inflammatory agents including indomethacin and ibuprofen (reviewed in Wang et al 2006).

Consistent with other members of the nuclear hormone receptors the PPARs comprise an N-terminal ligand-independent transcriptional activation domain (AF1), a central DNA-binding domain, and a C-terminal ligand binding and ligand dependent transcriptional activation domain (AF2). Ligand binding results in a conformational change, releasing corepressors and recruiting coactivators to allow gene transcription (reviewed Knouff et al 2004). The PPARs form heterodimers with members of the retinoid X receptor (RXR) superfamily to initiate transcription of target genes (Thompson 2007). Preformed PPAR/RXR heterodimers interact with corepressor proteins such as retinoblastoma (Rb) in the basal state, which may then be released following ligand binding and consequent conformational change (reviewed Knouff et al 2004). PPARs may also influence gene transcription independently of ligand binding, probably through phosphorylation of the AF1 domain by kinases; for example alterations in PPARγ phosphorylation by ERK- and JNK- MAPK can affect both ligand dependent and ligand independent effects on gene transcription (Burns et al 2007).

Three main isoforms have been identified, PPARα, PPARγ and PPARβ/δ. All have a similar structure but are coded for by different genes, on chromosomes 22, 3 and 6 respectively (reviewed in Theocaris 2004). The PPARs are widely expressed throughout many tissues. PPARα, the first PPAR to be identified, is expressed in tissues with high oxidative capacity including cardiomyocytes, hepatocytes, enterocytes and the renal proximal tubule. PPARβ/δ, the least studied of the PPAR family, is expressed almost ubiquitously (Burns et al 2007). PPARγ, intensively investigated for its role in lipid metabolism, is expressed in adipose tissue as well as intestine, liver, prostate, colon, pneumocytes and cells of the immune system including T and B cells, natural killer cells, dendritic cells and macrophages (Theocaris et al 2004, Wang et al 2006). PPARγ protein is also highly expressed in human pancreatic islet cells including the α, β and δ cell subtypes (Dubois 2000) and has been shown to be a negative regulator of islet β cell mass both in vivo and in vitro (Rosen 2003). Four isoforms of PPARγ (PPARγ1-4) have been identified thus far and are generated by alternate splicing of a single gene, located on chromosome 3, band 3p25 (Beamer et al 1997, Wang et al 2006). The majority of biological actions of PPARγ are mediated by the widely expressed PPARγ1. PPARγ2 expression is limited to adipose tissue; the protein product comprises 30 additional amino-acids in comparison to PPARγ1, with a consequent increase in ligand-independent activation. PPARγ3 and 4 are identical in terms of protein product to PPARγ1, but PPARγ3 expression is restricted to macrophages, adipose tissue and colon, while the tissue distribution of PPARγ4 remains unclear (reviewed Knouff et al 2004).

PPARγ has been implicated not only in adipocyte differentiation and insulin sensitivity, but also in atherosclerosis and inflammation. Its emerging function in controlling cell proliferation, differentiation and apoptosis, both in vivo and in vitro, has suggested a

putative role as a tumour suppresser gene, although an anti-tumour effect is not universal (Muellar et al 2000, Yang et al 2005, Wang et al 2006). In particular, there have been concerns that the TZD agents may predispose to colonic neoplasia in an in vivo mouse model (Yang et al 2005). PPARγ is highly expressed in a variety of solid malignancies including prostate, breast, colon and gastric carcinoma, and may be associated with pancreatic adenocarcinoma, with a possible prognostic value in identifying the more malignant cases (Kristiansen 2006). PPARγ has been shown to induce terminal differentiation in a variety of cancer models, including the upregulation of markers of cell differentiation carcinoembryonic antigen, E-cadherin and alkaline phosphatase in pancreatic cell lines (reviewed Wang et al 2006). One study has shown differential anti-tumour effects of TZDs in breast cancer cell lines, rosiglitazone being associated with reduced cell proliferation and promotion of cell differentiation while the agent KR-62980 only induced a reduction in cell proliferation. Thus, the effects of each single TZD should not be regarded as indicative of the potential action of the whole group (Kim et al 2006).

Interestingly, LOH studies of human pancreatic neuroendocrine tumours have indicated allelic loss at the chromosomal site corresponding to 3p25 in up to 30% patients, also with a possible predictive role of outcome in advanced disease (Chung et al 1997). Despite this, no mutation affecting the PPARγ gene was identified in a series of 23 pancreatic neuroendocrine tumours (including insulinomas, gastrinomas, glucagonomas and non-functioning tumours). This may suggest that either epigentic phenomena occur to affect gene function (for example hypermethylation) or that an alternative candidate gene exists at the chromosomal locus (Costa-Guda 2005).

PPARγ agonists have been associated with an up-regulation of CDKIs including p18, p21 and p27. These inhibitors are critical in preventing phosphorylation and inactivation of Rb. Rb in the unphosphorylated form exists as a "gatekeeper" preventing uncontrolled progression through the cell cycle from G1 to S. Upregulation of p21 and p27 with associated cell cycle arrest in G1 has been described in pancreatic tumour cell lines following treatment with glitazones (Motamura et al 2000, Kawa 2002). PPARγ agonists have also been shown to reduce activation of CDKs in a variety of tumour cell lines including the pancreas by reducing the expression of cyclin D1, an important activator of CDKs (Toyota et al 2002).

PPARγ agonists have also been implicated in attenuating Ras (a commonly altered oncogene in human malignancy)-dependent phosphatidylinositol 3-kinase (PI3K) activity (Bos et al 1989). Growth factor signalling via tyrosine kinase receptors leads to up-regulation of Akt via phosphorylation and activation of PI3K. PPARγ has been associated with up-regulation of the PI3K inhibitor Phophatase and tensin homologue (PTEN), a lipid phosphatase that is critical in controlling cell cycle arrest and apoptosis.

PTEN is a tumour suppressor gene which encodes a multifunctional phosphatase which is expressed almost ubiquitously and regulates the cell cycle, apoptosis and possibly cell adhesion. It is linked to cell cycle control through the retinoblastoma gene (Paramio et al, 1999) and promotes cell death. Deletions and mutations to PTEN occur in a range of cancers including breast (Perren et al, 1999), endometrial (Mutter et al, 2000), brain and prostate (Li et al, 1997). PTEN is thought to negatively control the PI3K-Akt pathway by dephosphorylating the 3 position of phosphoinositide. A mutation in the PTEN gene on arm 10q that causes loss of the protein's function result in excessive proliferation of cells, resulting in hamartomatous growths in a syndrome called Cowdens disease.

Loss of PTEN has been implicated in the development of metaplasia in pancreatic ductal cells, which may herald the early genesis of pancreatic adenocarcinoma (Stanger et al 2006). Akt over expression has been shown in pancreatic adenocarcinoma cells, with associated loss of PTEN expression (Schleiman 2003, Altomare 2002). Putative PPARγ response elements have been identified within the promoter region of the PTEN gene, and a dose-dependent upregulation of PTEN protein expression has been confirmed following treatment of macrophages with rosiglitazone. This increase in PTEN was associated with a down regulation of PI3K activity (Patel et al 2001). PTEN expression has been shown to be raised in pancreatic cancer cells following treatment with the TZD rosiglitazone. Levels of phosphorylated Akt decreased as PTEN levels increased, indicating inhibition of PI3K. Antagonism of rosiglitazone by GW966 abolished these effects (Farrow et al, 2003).

Malignant progression of cancers relies upon breakdown of the extracellular matrix by proteinases allowing access of cells to lymphatics, the blood stream and invasion of local tissues. This process depends upon proteases such as the serine proteinase urokinase type plasminogen activator (uPA) and its receptor, which may be upregulated in a variety of malignancies including pancreatic cancer. Glitazones are known to reduce uPA activity and to increase levels of plasminogen activator inhibitor (PAI) in pancreatic cell lines (Sawai 2006).

Altered function of PPARγ may be associated with tumorigenesis. Sporadic loss of function mutations of PPARγ have been identified in human colonic cancer (Sarraf et al 1999), as have dominant negative splice variants of the gene product (Sabatino et al 2005). A dominant negative fusion protein combining the thyroid transcription factor

PAX-8 and PPARγ has also been identified in a subset of thyroid follicular carcinomas (Kroll et al 2000). However, screening of 159 samples of various human tumours including breast, colon, lung, prostate and haematological malignancies failed to identify mutations of PPARγ suggesting that these are rare events in malignancy (Ikezoe 2001).

An increased understanding of the molecular basis of pancreatic NETs is critical to explaining the diverse biological behaviour of this group of tumours. At present, diagnosis can be complicated and prediction of malignancy impossible making therapeutic decisions and monitoring of disease progress difficult. Modulation of cancer outcomes using nuclear hormone receptors has also gained interest recently through the use of retinoic acid in the treatment of a variety of malignancies including leukaemia, melanoma and cervical cancer (reviewed by Wang 2006).

1.8 Human Pancreatic Neuroendocrine Cell Lines

There are a large number of human pancreatic adenocarcinoma cell lines available commercially e.g., AsPC-1, BxPC-3, CAPAN-1, CAPAN-2, FA6, MIA PaCa-2, JF305 and PANC-1, amongst others. These have allowed a significant amount of research work to be performed on pancreatic adenocarcinoma, the processes involved and potential treatment models. Pancreatic endocrine cell lines are less common. Animal insulinoma cell lines such as Ins-1, RINm5F and HIT have been available for some time and have been used extensively to study the physiology and pathophysiology of the mechanisms involved in glucose homeostasis.

Human pancreatic neuroendocrine tumour cell lines are rare, and at the time of study the cell lines CM, BON and QGP1 represented the only tumour cell lines held in culture

and described in the literature. The CM cell line is a human pancreatic insulinoma cell line that was established from peritoneal ascites of a patient affected by a primary pancreatic insulinoma (Gueli, et al 1987). It grows spontaneously in vitro as an adherent semiconfluent monolayer. The CM line has been studied mainly for its antigenic properties with the purpose of establishing an in vitro model to investigate the immune mechanisms leading to β-cell destruction in IDDM (Cavallo et al. 1996). Studies on early-passaged cells provided evidence that insulin and C peptide were detectable in the supernatants of CM cell culture (Cavallo et al. 1992). Baroni et al (1999) showed that CM cells from an early passage express specific β-cell genes in response to glucose stimulation. In particular the insulin and glucose transporter (GLUT 1 And GLUT 2) genes are expressed. In insulin dependent diabetes, it has been postulated that β cells are subject to cytokine mediated cytotoxicty. Cavallo et al. (1996) showed that CM cells are subject to TNF-α mediated toxicity and that glutathione has a dose dependent protective effect. CM remains one of the very few human β-cell lines in existence due to the difficulties in obtaining and culturing them for long periods.

The BON cell line was established from a lymph node metastasis of a human pancreatic carcinoid tumour and was first described by Parekh et al (1994). The operative specimen of a peripancreatic lymph node was obtained in 1986 from a 28 year old man who presented with obstructive jaundice and diarrhoea from a metastatic carcinoid tumour of the pancreas. The node was washed and minced and tumour fragments were placed in cell medium. All fibroblasts were removed and the resulting cells frozen at passage 5. Evers et al. (1994) showed that BON cells contain serotonin, chromogranin A, neurotensin and pancreastatin and have a predictable pattern of growth. They possess receptors for gastrin, somatostatin and acetylcholine. They also showed that BON

tumours could be sensitive to a somatostatin analogue and INF-α. Both BON and CM cell lines were used in an investigation of the effects of gefitinib, an inhibitor of epidermal growth factor receptor-sensitive tyrosine kinase (Hopfner et al, 2003), which showed significant growth inhibition, increased apoptosis and cell cycle arrest.

The cell line QGP1 represents a human pancreatic somatostatinoma that was isolated and cultured by Kaku et al in 1980. QGP1 cells grow as a confluent monolayer of epithelioid cells. They express carcinoembryonic antigen (CEA). Iguchi et al, (1990) showed that they secrete somatostatin in keeping with a somatostatinoma. Implanting QGP1 cells into nude mice caused a tumour consisting of islet cells which secreted CEA and somatostatin. Doihara et al. (2009) showed that QGP1 cells expressed enterochromaffin cell markers such as tryptophan hydroxylase, chromogranin A, synaptophysin, ATP-dependent vesicular mono-amine transporter 1 (VMAT1), metabotrophic glutamate receptor 4 (mGluR4), β adrenergic receptor, muscarinic 4 acetylcholine receptor (ACM4), substance P, serotonin transporter (SERT) and guanylin. They also identified expression of transient receptor potential ankyrin1 channel (TRPA1) and showed that agonists of these channels increase intracellular calcium and release of 5-HT. Both BON and QGP1 cell lines were used in a study looking at the potential anti-proliferative effect of interferon alpha (Detjen et al, 2000). It found that interferon alpha directly inhibited growth by delaying progression through the S phase and into G2/M. More recently QGP1 and BON cell lines have been used to investigate the role of the PI3K/AKT/mTOR pathway during cell adhesion. Src kinase inhibitors reduced the activation of the mTOR pathway during QGP1 cell adhesion (Di Florio et al. 2008)

1.9 Aims

The aim of this project was identify the expression characteristics of PPARγ in human pancreatic neuroendocrine tumours in three different types of samples: resected freshly frozen specimens, archived paraffin-embedded specimens and cell cultures. Secondly, if PPARγ is present, I aim to explore whether proliferation is altered by the administration of an agonist at this receptor.

Additional aims include:

An examination of p27 and phospho-p27 expression

An examination of JAB1, p-Akt, and PTEN proteins implicated in p27 function

An examination of somatostatin receptor expression in cell cultures.

CHAPTER 2

MATERIALS AND METHODS

2.1 Laboratory consumables

Pipette tips, plastic and glassware were purchased and used as according to normal laboratory protocol. Solutions were autoclaved where appropriate. Heat labile solutions (e.g. foetal calf serum, FCS) were filtered through 0.22μm syringe filters prior to use. Standard tissue culture techniques were followed to maintain sterility.

2.2 Human tissue samples

2.2.1 Homogenization

Frozen tissue samples held at -80^{0}C were retrieved and placed in liquid nitrogen whilst waiting cutting to give a sample size of up to 30mg. Homogenization was performed mechanically using a mounted Sigma-Aldrich Ultra Turrax 8 devise. Care was taken to decontaminate and clean the blades, including immersion in hydrogen peroxide for 30 minutes prior to usage and thorough washings between samples with 1 x 100% ethanol and 2 x RNase free water.

2.2.2 RNA extraction

Promega SV Total RNA Isolation System

RNA isolation requires four essential steps: effective disruption of cells of tissue, denaturisation of nucleoprotein complexes, inactivation of endogenous ribonuclease (RNase) activity and removal of contaminating DNA and proteins. The technique allows the homogenisation of tissue within a buffered solution containing guanidine thiocyanate and β-mercaptoethanol to inactivate the ribonucleases present in cell extracts. Addition of dilution buffer and heating to 70^{0}C allows selective precipitation of cellular proteins to occur whilst the RNA remains in solution. The debris was removed with centrifugation and the RNA is precipitated out of solution by ethanol and

bound to silica glass fibres found in a manufactured ‘spin basket’. Contaminating DNA is then digested by the direct application of RNase-free DNase. Further washing steps help to improve the purity of the RNA. The RNA product is then eluted from the basket by the addition of nuclease free water.

2.2.3 Spectrophotometry

Quality and concentration of RNA can be estimated by the measurement of absorbance of light at wavelengths of 260nm and 280nm.

Following adequate calibration of the spectrophotometer, 5µl of prepared RNA solution is added to 495µl of TE (TRIS-EDTA buffer) and the absorbance at 260nm and 280nm were documented. Care was taken to prevent contamination between samples.

The yield of total RNA obtained is determined by the absorbance at 260nm where 1 absorbance unit equals 40µg of single stranded RNA/ml. The quality or purity can be estimated by the ratio of absorbance 260nm/280nm where pure RNA will exhibit a ratio of 2.0. Acceptable ratios are between 1.8 and 2.1.

2.2.4 RNA gel

Integrity of purified RNA can be estimated by agarose gel electrophoresis. The ratio of 28S to 18S eukaryotic ribosomal RNAs should be approximately 2:1 by ethidium bromide staining, indicating that no gross degradation of RNA has occurred. With degradation the ratio is reversed as 28S characteristically degrades into an 18S-like species.

2.2.5 Preparation of Agarose Gel for RNA electrophoresis

Stock TAE (x50)

242 g Tris base dissolved in approximately 750 ml deionized water.

Add 57.1 ml glacial acid and 100 ml of 0.5 M EDTA (pH 8.0).

Adjust the solution to a final volume of 1l

Working Solution of TAE (x1)

The working solution of 1x TAE buffer is made by simply diluting the stock solution by 50x in deionized water.

Final solute concentrations are 40 mM Tris acetate and 1 mM EDTA.

Gel

1% Agarose gel for RNA

0.5g agarose added to 50 ml 1x TAE (Tris-acetate-EDTA) buffer and heated in microwave for 2 minutes.

Add 1µl ethidium bromide (carcinogen)

Place combs and allow gel to set prior to transfer to running chamber and loading of sample.

Load 2µl RNA solution plus 8µl water plus 2µl loading dye and run at 150 Volts for 30 minutes.

Visualizing the RNA

The gel is placed on the transilluminator (UV light of wavelength 254 nm). Ethidium bromide is a fluorescent dye that intercalates between the bases of DNA and RNA. Photos taken as required.

Example of RNA gel showing 18S and 28S bands

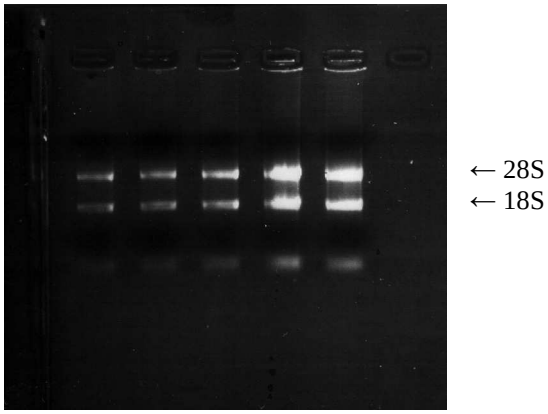

2.2.6 Reverse Transcription and production of cDNA

Applied Biosystems (ABI) TaqMan standard protocols. This produces 50µl of cDNA from 1µl of totalRNA.

Following calculation of the concentration of RNA by spectrophotometry, the volume for 1µg of RNA is pipetted and made upto 19.25µl inTE in a 0.2ml microtube.

A mastermix was prepared with the following constituents:

5µl	10x RT Buffer
11µl	25mM $MgCl_2$
10µl	deoxyNTPs (10nM)
2.5µl	Random Hexamers 50µM
1µl	Rnase Inhibitor (20U/µl)
1.25µl	Multiscribe RT enzyme (50U/µl)
Total 30.75µl	

The 30.75µl is added to the RNA solution to make a total solution of 50µl which was gently mixed. The mixed solution was then placed in the GeneAmp 970 thermal cycler programmed with the settings below.

25°C	10mins	1cycle
48°C	30mins	1cycle
95°C	5mins	1 cycle

Subsequent cDNA was frozen immediately at -20°C.

2.2.7 Polymerase Chain Reaction (PCR) for GAPDH

The standard Polymerase Chain Reaction (PCR) amplifies genes of interest, determined by the choice of primers introduced to the PCR mixture. Following a DNA denaturing step, these primer sequences bind to the template DNA allowing amplification of the subsequent DNA sequence with a DNA polymerase in the presence of excess dNTPs.

Primers used were standard laboratory primers.

GAPDH Genebank M33197

Primers

SHORT

GAPDH F	5' CCATGGAGAAGGCTGGGG
GAPDH R	5' CAAAGTTGTCATGGATGACC

LONG

GAPDH Long F	5' GAGTCAACGGATTTGGTCGT
GAPDH Long R	5' GGTGCTCCAGGGGTCTTACT

Product =486bp

Promega PCR protocol

Primers, dNTP and DNA polymerase were kept on ice during working time. A 'mastermix' of the components below was made up and added to 2.5µl of cDNA

H_2O	16.875µl
x10 Taq buffer	2.5µl
25mM $MgCl_2$	1.5µl
20mM dNTP	0.25µl
0.5 µmol S primer	0.625µl
0.5 µmol AS primer	0.625µl
Taq enzyme	0.125µl
Total	22.5µl

Samples were mixed thoroughly and 3 drops of mineral oil were added to the surface. Samples were then placed in the thermal cycler and run with the program below:

Stage 1	95^{o}C	5mins	1 cycle	Denaturing
Stage 2	94^{o}C	1mins		
	55^{o}C	1mins	26 cycles	Annealing
	72^{o}C	1mins		Extension
Stage 3	72^{o}C	10mins	1 cycle	Poly A tail

2.2.8 DNA gel

To assess the adequacy of the PCR products, samples were run on a 2% agarose gel with ethidium bromide, as described for the RNA gel above. 10µl of PCR product was mixed with 2µl loading dye. PhiX 174 HinF I digest (Promega G1751) molecular size markers were run alongside PCR products in each gel. Positive and negative controls

were used as appropriate. Electrophoresis was performed for 30-45 minutes at 150V depending on the size of gel. Bands were visualised by ethidium bromide fluorescence using a UV transilluminator and photographs taken.

2.2.9 PPARγ PCR

Tissue samples were assessed to identify the presence of PPARγ by standard Quiagen PCR protocols with conditions optimised within the laboratory by previous experimental work (Dr C Merulli).

Primers (Sigma-Genosys)

PPARγ sense	5’ TCTCTCCGTAATGGAAGACC
PPARγ antisense	5’ GCATTATGAGACATCCCCAC

Product = 474bp

A mastermix of the following components was made up and added to 2.5µl of cDNA.

H_20	13.5µl
Qiagen x10 buffer	2.5µl
Q solution	5µl
dNTP	0.25µl
0.4 µmol PPARgamma S	0.5µl
0.4 µmol PPARgamma AS	0.5µl
Q hotstart Taq	0.25µl
Total	22.5µl

Samples were mixed thoroughly and 3 drops of mineral oil were added to the surface. Samples were then placed in the thermal cycler and run with the program below:

Stage 1	95^{o}C	15mins	1 cycle
Stage 2	94^{o}C	1mins	
	55^{o}C	1mins	40 cycles
	72^{o}C	1mins	
Stage 3	72^{o}C	10mins	1 cycle

DNA gels were run on ethidium bromide agarose gels as previously described and visualised by UV transillumination.

2.3 Immunohistochemistry

2.3.1 Immunohistochemistry Objectives

Two objectives were set for this work. Firstly, the location and quantification of the strength of staining in each tissue type (insulinoma, gastrinoma, islet and exocrine pancreas). Secondly, a comparison of the tissues against each other, using total positive counts for both nuclear and cytoplasmic compartments, was determined.

In particular, interest was focused on differences between insulinoma and normal islets, which were considered its control. Although the number of gastrinomas was small (n=3) it was felt worthwhile to see if there were any significant differences between these and the insulinomas. Exocrine pancreas was included to highlight differences between the endocrine and exocrine pancreas.

2.3.2 Case selection

A trust wide search for pancreatic neuroendocrine tumours through histopathology records, endocrine department records and surgeons logbooks was performed. All paraffin embedded sections available were retrieved and closely inspected for suitability of usage.

Representative slides of each case were stained with haematoxylin and eosin and all were reviewed for suitability of study with consultant histopathologist Dr Diaz-Cano. Where possible, tumour, normal exocrine pancreatic tissue and islets were identified on each slide and marked to allow standardisation of slide assessment. The first and last

slides prepared from each block were checked to ensure that all contained the same components.

When multiple samples were present for a case, all underwent immunohistochemistry and were counted individually. The resulting counts were then combined to give an average result for that case.

2.3.3 Optimisation of Antibodies

With the exception of Ki-67, which has previously been widely used within the laboratory, all antibodies underwent optimisation studies. Starting points were guided by manufacturer advice and standard laboratory protocols with help from consultant histopathologist Dr S Diaz-Cano. Variations in antibody dilution and incubation times, blocking times, and staining times for DAB and Gills Haematoxylin were explored to identify optimal conditions of all antibodies.

2.3.4 Summary of antibodies

	DILUTION
PPARγ (E-8): c-7273 Santa Cruz Biotechnology	1:50
p27 (SX53G8) Gift from Dr X Lu, (Ludwig Institute for Cancer Research, St Marys Hospital, London.)	1:300
Phospho-p27 (71-7700) Zymed laboratories Inc.	1:250
JAB 1 (37-1400) Zymed laboratories Inc.	1:250
Phospho-Akt (Ser473) Cell Signaling Technology.	1:100
PTEN (NCL-PTEN) Novocastra Laboratories Ltd.	1:100
Ki-67 (NCL-Ki67-MM1) Novocastra Laboratories Ltd	1:200

2.3.5 Control Samples

For all immunohistochemistry experiments positive and negative controls were run simultaneously. Tonsil sections were used as positive controls for all antibodies with the exception of PPARγ, where skin samples containing sebaceous glands were found to be effective. Photographic examples of positive controls for each antibody are shown in the results section. Negative controls were constantly included where the primary antibody was excluded.

2.3.6 Supervision of Counting

Counting cells can be open to variability due to the subjective nature of interpretation of staining. We hoped that by separating the strength of staining out into strong, medium and weak would help highlight those which may be may difficult to classify. With little previous personal experience, it was felt imperative that expert instruction with the techniques of immunohistochemistry, cell counting and interpretation of results was gained. This was kindly provided by Dr S Diaz-Cano (Royal London Hospital). Subsequent review of all the slides and an estimation of Ki-67 index were performed by Dr E Carlson (St Bartholomew's Hospital). External quality control was therefore gained by 2 separate sources but it is accepted that no internal control studies were performed to confirm reliability and repeatability of my own counting on different days.

2.3.7 Vectastain Universal Elite ABC (kit code pk-6200)

All immunohistochemistry methods were based on the standard ABC method, the standard laboratory protocol being highlighted below.

Procedure

1. The following controls should be used.
2. Positive control section for each primary antibody used.
3. Negative control section [omitting primary antibody]
4. Dewax sections in xylene.
5. Dehydrate sections in alcohol.
6. Place sections in endogenous peroxidase block for 15 minutes.
7. Wash sections in tap water for 2 minutes.
8. If antigen retrieval is required, go to the appropriate procedure.
9. Transfer to tap water and wash for 2 minutes.
10. Soak sections in a trough of TBS for 3 minutes.
11. Wipe around the sections and apply the PAP pen.
12. Apply normal horse Serum for 3 minutes.
13. (Add 1 drop (50µl) of yellow labelled bottle to 5ml of antibody dilutant)
14. Tip off the horse serum.
15. Apply primary antibody at the appropriate dilution in antibody dilutant for 40 minutes.
16. Apply only antibody dilutant to the negative control section.
17. Wash off the antibody with TBS x 2 and flick slide to remove excess.
18. Apply the universal biotinylated secondary antibody (from the kit) for 20 minutes.

19. (Add 2 drops (100µl) of normal horse serum (yellow label) to 5ml of TBS, then add 2 drops (100µl) of biotinylated secondary antibody (blue labelled bottle). Vortex solution.)
20. Make up the Avidin Complex Solution. This must stand for 30 minutes before use.
21. (Add 2 drops (100µl) of Reagent A (grey label A) to 5ml of TBS, then add 2 drops (100µl) of Reagent B (grey label B). Vortex solution. Leave to stand.
22. Wash off the antibody with TBS x 2 and flick slide to remove excess.
23. Apply the avidin complex solution for 20 minutes.
24. Wash off with TBS x 2 and flick slide to remove excess.
25. Apply DAB solution for 3 – 5 minutes.
26. Wash in running tap water for 5 minutes.
27. Counterstain in Gills Haematoxylin for 60 seconds.
28. Wash in water bath for 2 mins (Blue)
29. Dip in acid-alcohol x 2 (Differentiate)
30. Wash in water again (Blue)
31. Dehydrate and clear (2 mins each in alcohol, alcohol, xylene, xylene)
32. Mount.

2.3.8 Antigen Retrieval

Antigen retrieval was performed using a microwave technique. Slides were placed in citrate buffer during treatment before continuing with step 7 above.

Microwave Buffers

Citrate buffer stock

Citric acid	7.56g
Trisodium citrate	47.56g
Distilled water	2000ml
Stored at 4°C	

Citrate buffer working solution

Citrate buffer stock	100ml
Distilled water	900ml
1M Sodium hydroxide	to bring pH to 6.0

2.3.9 Preparation of Immunohistochemistry Reagents

Antibody Dilutant

Sodium chloride	4.1g
Tris	0.3g
Bovine albumin	0.2g
Sodium azide	0.2g
1M Hydrochloric acid	2ml
Casein	50µl
Distilled water	500ml
0.1M Sodium hydroxide	to bring pH to 7.6
Stored at 4ºC	

Endogenous Peroxidase Block

100 vol. Hydrogen peroxide	3ml
Methanol	97ml

0·05M Tris Buffered Saline (TBS) pH7·6

Sodium Chloride	8.76g
Tris	6.06g
1M Hydrochloric acid	36ml
Distilled water	800ml
1M HCl	to bring pH to 7.6
Made up to 1 litre with distilled water	

2.3.10 Cell counting

Counting was performed using a grid overlying a 40x powered magnified field of view and reviewed on a computer screen. For each case and antibody, approximately 500 cells (approx 100 cells per high power field x 5) were counted for insulinoma, gastrinoma, islet and exocrine pancreas. Each was assessed for both nuclear and cytoplasmic staining. Staining was described as strong, moderate, weak or negative.

The total number of cells counted in each group (insulinoma, gastrinoma, islet or exocrine) was tabulated in Microsoft excel spreadsheets and calculation of a percentage and standard error of the mean for each strength of staining was performed. To allow for easier comparison between groups, it was felt that a single value for positive staining would be helpful. Due to the nature of counting in immunohistochemistry it was debated whether the positive count should be calculated by adding all stained cells (strong, moderate and weak) together or by adding the strong and moderately stained cells together, excluding the weakly stained cells as inconclusive. Both methods were used for all data: I found that the outcome was similar in nearly every case. For all results, the data shown uses positive count equal to strong + moderate + weak staining.

On occasion and where appropriate, data using positive count equal to strong plus moderate staining has been additionally used to illustrate patterns. This is highlighted in the text.

2.4 Cell culture work

2.4.1 Cell lines

All 3 cell lines were generously donated by Professor Nicolas Lemoine (Institute of Cancer, Barts and The London, Queen Mary's School of Medicine and Dentistry).

CM - Human insulinoma cell line isolated from ascites

QGP1 - Human pancreatic somatostatinoma

BON - Human pancreatic carcinoid

2.4.2 Culture media and conditions

CM - RPMI 1640 with L-glutamine (Gibco 21875)

QGP1 - RPMI 1640 with L-glutamine (Gibco 21875)

BON - DMEM high glucose (Gibco41966)

To all media, 10% foetal bovine serum (Gibco 10106) was added along with penicillin/streptomycin antibiotics (Gibco 15140) and fungizone (Gibco 15290). Cells were incubated in T-75 flasks with culture medium at 37ºC with 95% air, 5% CO_2. Media was freshened every two to three days by discarding old media and adding 10-15mls new culture medium, warmed to 37ºC. Cells were passaged once they reached 60-80% confluence. Medium was removed and the cells washed with 5ml warm (37ºC) PBS. 1ml trypsin/EDTA was added per flask and the cells incubated for approximately 5 minutes until all had detached from the flask. Trypsin activity was terminated by the addition of 5ml culture medium and the suspension mixed by gentle trituration.

Cells were counted using a Trypan Blue method, whereby dead cells stain deep blue while live cells remain translucent, since viable cells do not take up dye. 25µl of 0.4%

trypan blue (Sigma) was added to 75µl PBS. The addition of 100µl cell suspension gave a final concentration of 0.05% trypan blue. The suspension was mixed by gentle pipetting and 100µcl transferred to a haemocytometer. Cells falling within the boundaries of two squares were counted and the mean total for one square (volume $0.1mm^3$) was used to calculate the concentration of cells per ml of original suspension:

Cells/ml = average cell count x 2 (dilution factor) x 10000

Approximately 2 million cells were plated per fresh T-75 flask and 10-15ml culture medium added. Flasks were returned to the incubator.

2.4.3 Cell freezing

Medium was removed and the cells washed with 5ml warm (37ºC) PBS. 1ml trypsin/EDTA was added per flask and the cells incubated for approximately 5 minutes until all had detached from the flask. Trypsin activity was terminated by the addition of 5ml culture medium followed by gentle titration. Cells were centrifuged at 1000 rpm for 5 minutes then medium discarded. Cells were washed in PBS, centrifuged as before, and the pellet resuspended in cell freezing medium (90% fetal calf serum, 10% DMSO).

Cells were transferred to a cryotube and placed on ice for 20 minutes, then at -20ºC for approximately 2 hours, transferred to -70ºC for a further 2 hours prior to storage in liquid nitrogen.

2.4.4 RNA extraction

Cells were trypsinised, harvested, washed and counted prior to RNA extraction. Extraction was performed using standard Promega SV Total RNA Isolation System

protocols for lysis of cultured cells. A maximum of 5 x 10^6 cells were washed and centrifuged prior to addition of lysis buffer. Vigorous vortexing and passage through a 20 gauge needle aided DNA shearing prior to the addition of dilution buffer and preparation for RNA purification by centrifugation.

2.4.5 RNA spectrophotometry and electrophoresis

Quality of RNA was assessed by spectrophotometry and agarose gel electrophoresis as previously described for every RNA extraction.

2.4.6 Reverse transcription

Extracted RNA from cell lines were subject to reverse transcription using ABI standard protocols as described previously.

PCR for GAPDH

cDNA recovered following reverse transcription, underwent conventional PCR for GAPDH using Promega standard protocols as described previously. Electrophoresis on ethidium bromide agarose gel was performed for identification of products

2.4.7 Expression of PPARγ

Expression of PPARγ in each of the cell lines was assessed by conventional PCR using Quiagen kit and protocols as described previously. Products were run on ethidium bromide agarose gel for identification.

Primers (Sigma-Genosys)	Product = 474bp
PPARγ sense	5’ TCTCTCCGTAATGGAAGACC
PPARγ antisense	5’ GCATTATGAGACATCCCCAC

2.4.8 Expression of Somatostatin Receptors (SSTR1-5)

Widespread expression of somatostatin receptors in endocrine tissues and tumours led us to investigate the expression of SSTR's 1-5 in our cell lines. Previously extracted samples from all three cell lines were subject to conventional PCR using Promega materials and protocols as described earlier.

Thermal cycling conditions were:

Stage 1	95^{o}C	5 minutes	
Stage 2	94^{o}C	1 minute	
	60^{o}C	1 minute	35 cycles
	72^{o}C	1 minute	
Stage 3	72^{o}C	10 minutes	

SSTR Primers

SSTR1:	5'-GCTACGTGCTCATCATTGCTA-3'	
	5'-GGACTCCAGGTTCTCAGGTTG-3'	product 401 bp
SSTR2:	5'-TTGGTACACAGGGTTCATCAT-3'	
	5'-GTCTCCGTGGTCTCATTCAGC-3'	product 459 bp
SSTR3:	5'-CTGGGTAACTCGCTGGTCAT-3'	
	5'-CAGGCAGAATATGCTGGTGC-3',	product 225 bp
SSTR4:	5'-AACGGAGGCGCTCAGAGAAGAAGA-3'	
	5'-AGGCGAGGTGAGGGAGGGTAAAAT-3'	product 451 bp
SSTR5:	5'-TCATCTGCCTGTGCTACCTG-3'	
	5'-GGAGAGGATGACCACGAAGA-3'	product 233 bp

Products were subject to ethidium bromide agarose gel electrophoresis for identification of products. Photographs are shown in the Results section.

2.4.9 PPARγ Protein Expression

Untreated cells from all cell line cultures were subjected to protein extraction, performed using cytobuster reagent (Novagen 71009). Cytobuster is a formulation of detergents optimised for extraction of soluble proteins from mammalian cells. All protein extraction procedures were performed under strict laboratory protocols within the cell culture hood

Procedure

The below reagents were added together

- 3ml Cytobuster Protein Extraction Reagent
- 30µl Phosphatase Inhibitor 1 (Sigma P-2850)
- 30µl Phosphatase Inhibitor 2 (Sigma P-5726)

Spent media was removed from the cell wells and cells were washed briefly with ice cold PBS. PBS was removed. Then, 250µl of the above solution was added to each cell well to coat the wells and left in place for 5 minutes. After 5 minutes the wells were scraped and the resulting suspension was pipetted into a separate eppendorf tube. The suspension was then centrifuged at 13000 rpm for 5 minutes at $4^{o}C$ and the supernatant removed to a separate tube prior to protein assay or freezing.

2.4.10 Protein Assay Protocol

Initial assays were performed with Bradford reagents which is in general use in the laboratory. However, it became apparent that cytobuster is not compatible with Bradford reagents, and a different method of protein assay was applied – BCA Protein Assay Kit (Pierce 23225).

The BCA assay relies upon the formation of a copper (II) – protein complex under alkaline conditions, followed by reduction of the copper (II) to copper (I) which is associated with a colour change that can be measured. The amount of reduction is proportional to the amount of protein present. Generation of a BSA (Bovine serum albumin) standard curve allows for quantification of protein samples.

To allow direct comparison with the protein samples, BSA was diluted in Cytobuster. A known concentration of BSA, 1mg/ml, was made by dilution of 0.01g BSA in 10ml total volume made up of 8mls sterile water and 2mls Cytobuster. From this 1mg/ml solution further dilutions achieved concentrations of BSA ranging between 0 – 1mg/ml for generation of a standard curve. 25µl of each known BSA dilution or diluted sample was placed in triplicate into wells of a 96 well plate. 200µl of BCA/Copper mix was added to each well. Samples were left at 37˚C for 30 minutes and the colour change read on a Wallac “Victor” 1420 Multilabel Counter. An example standard BSA curve is shown in figure 2.1. The regression co-efficient was calculated to assess the suitability of the standard curve generated.

From this standard curve, concentrations of each protein sample can be estimated from their measured absorption at 595nm. Samples were then normalised for protein content, to the sample with the least amount of protein, prior to loading into SDS-PAGE gel.

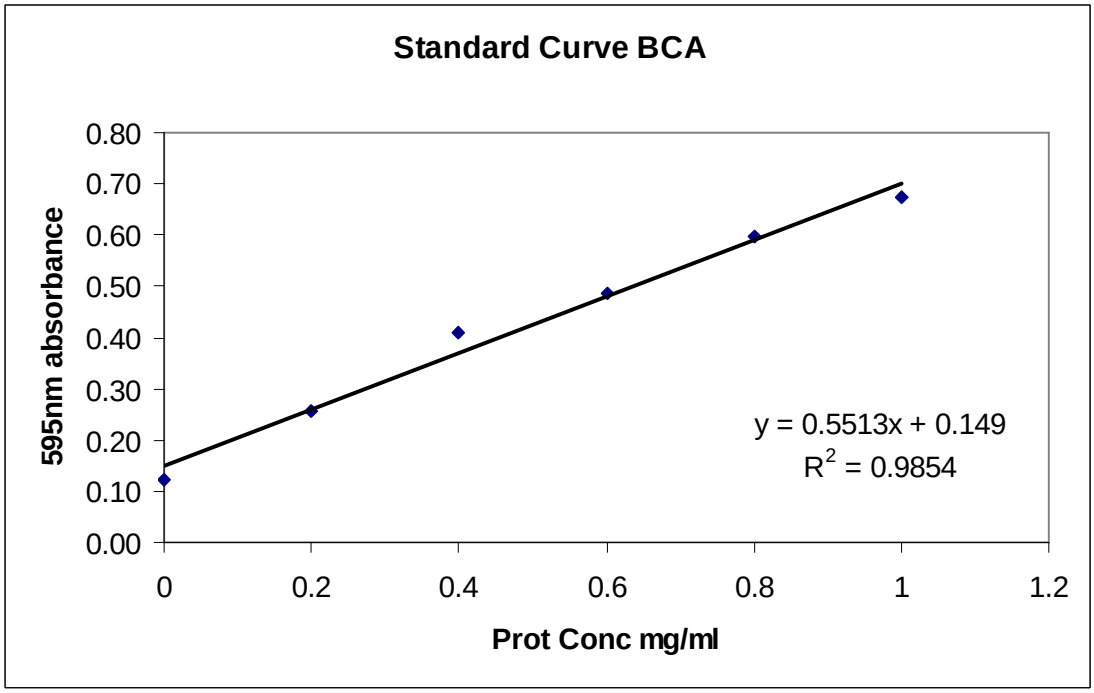

Figure 2.1 Example of a protein standard curve using BCA reagents.

2.5 Western Blotting Protocol

2.5.1 Materials Required

- Tris base (Tris hydroxymethyl methylamine) (VWR; 103156X)
- Tris acid (Tris hydroxymethyl aminoethane hydrochloride) (Sigma T-3253)
- Glycine (Sigma; G7126)
- SDS (sodium dodecyl sulfate) (Sigma; L-4509)
- Methanol (VWR; 101586B)
- Sodium chloride (NaCl) (Sigma)
- Hydrochloric acid (HCl) (Sigma)
- Tween-20 (polyoxyethylene (20) sorbitan monolaurate) (VWR; 66368-B)
- 2-mercaptoethanol (Sigma M-3148)
- Skimmed (no fat) milk powder; Tesco
- SDS-PAGE Ready Gels 10% Tris/HCl 10 wells (Bio-Rad; 161-1155)
- Kaleidoscope Protein Marker (Bio-Rad; 161-0324)
- Electrophoresis Tank (Bio-Rad; 165-3126)
- Transfer Kit (Bio-Rad)

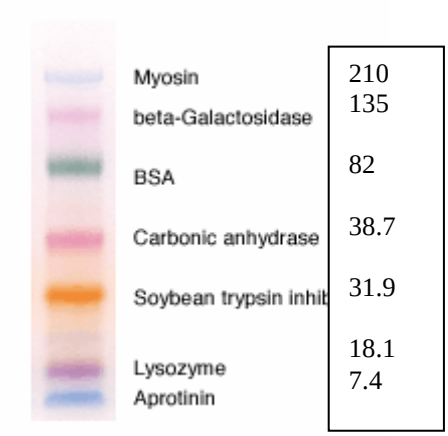

  2 pieces of sponge cut to size of gel

  4 pieces of blotting paper (Biorad; 170-3932)

  Transfer cassette and tank (Bio-Rad; 170-390)

- Detection Reagent ECL Plus Western Blotting System (Amersham; RPN2132)
- PVDF (polyvinylidene difluoride) Membrane (Amersham; RPN303F)

- Kodak Scientific Imaging Film X-OMAT (VWR no. 165-1579)
- Antibodies: primary and secondary
- Saran Wrap (VWR)
- Aluchef foil (VWR; 236401001)

2.5.2 Buffers and Reagents

SDS Loading Buffer

1.514g Tris base (125mM), 4g SDS (4% w/v), 16 ml Glycerol (20% w/v), 0.02g Bromophenol Blue (0.002% w/v)

Dissolve Tris base in 100 ml of ddH_2O and adjust pH to 6.8. Then add the remaining reagents and store at 4^0C.

Running Buffer

30.25g Tris base, 144.13g Glycine, 10g SDS.

Make up to 1 litre with ddH_20, gives 10X Tris/Glycine/SDS

Use 1 in 10 (i.e. 100 ml in 1000 ml ddH_2O)

Transfer Buffer

3.04g Tris base, 14.14g Glycine, 800 ml ddH_2O, 200 ml Methanol

Dissolve Tris and glycine in H_2O. Add methanol, total 1000 ml. Stir well with magnetic stirrer. Store at 4^0C.

Washing Buffer 1X TBS-Tween

10X TBS (Tris-buffered saline):

To prepare 1 litre of 10X TBS: 24.2g Tris base, 80g NaCl, Adjust pH to 7.6 with HCl (use at 1X).

To make 1XTBS-Tween (wash buffer): 1X TBS, 0.1% Tween (i.e. 500 µl Tween to 500 ml 1X TBS).

Blocking Buffer

2.5g Skimmed (no fat) milk, 50 ml 1X TBS-Tween

Gives 5% milk solution.

Stripping Buffer

0.985g Tris hydrochloride, 2g SDS, 781 µl 2-mercaptoethanol

Add 100 ml ddH_20 to SDS and Tris, then add 2-mercaptoethanol.

2.5.3 Antibodies

Anti-PPARγ(E-8): c-7273 Santa Cruz Biotechnology

A mouse monoclonal IgG antibody raised against a peptide mapping to the carboxy terminus of PPARγ of human origin. Used at a dilution of 1:50 at 4^oC overnight

Secondary antibody: Goat anti-mouse 1:10000

Anti-PPARγ(Calbiochem 516555)

A rabbit polyclonal antibody raised to a peptide found in mouse PPARγ2. Used at a dilution of 1:2000 for 90 minutes at room temperature

Secondary antibody: Goat anti-rabbit 1:10000

β-actin (Cell Signalling Technology)

Affinity purified rabbit polyclonal antibody raised against a synthetic peptide corresponding to the amino terminal of human β actin. Used at a dilution of 1:5000 at 4^{o}C overnight

Secondary antibody: Goat anti-mouse 1:10000

2.5.4 Method

Protein samples were normalised to the samples with the lowest protein concentration. The volumes required for each sample were calculated and aliquoted into 0.5ml tubes. Kaleidoscopic marker was also pipetted at this time. Equal volumes of SDS loading buffer were added to the samples and to the marker. Samples were heated for 5 minutes at 95^{0}C on thermal cycle to denature proteins and moved to ice immediately afterwards.

SDS-PAGE Electrophoresis Preparation

Following denaturing, a 10% Tris-HCl gel was inserted into a gel chamber which was placed into an electrophoresis tank ensuring that the chamber is balanced correctly. The tank was filled with 1x Running Buffer. The samples were then dispensed into the wells and run gel at 100V for 1 hour or until the samples reach the wire at the bottom of the gel chamber.

Electroblotting Protein to PVDF Membrane

A piece of polyvinylidene difluoride membrane (PVDF) (Amersham Biosciences) was soaked in methanol for 10 seconds then water for 5 minutes prior to use, to activate. Gel and membrane were compressed between blotting paper and sponges soaked in transfer buffer and proteins electro-transferred for 45 minutes at 90V.

The PVDF membrane was then washed twice in 1x TBS-Tween for 10 minutes. The blocking buffer was prepared and 30 mls was added to the membrane for 90 minutes at room temperature on a roller to block non specific protein binding sites. Blocking buffer was then removed and 5ml blocking buffer with primary antibody at the correct dilution added overnight at 4^{o}C (or otherwise specified).

Following 3 washes of 10 minutes with 15ml 1x TBS-Tween buffer the peroxidase conjugated (HRP) secondary antibody was added, at an appropriate dilution in 5ml blocking buffer. This was left for a further 90 minutes on a roller and then washed once more as above.

Detection of Proteins

Protein bands were visualised using a chemiluminescence detection system. Two different kits where used.

ECL Plus Western Blotting Detection Reagents Kit (Amersham Biosciences)

This system is based on the enzymatic generation of an acridium ester and numerous luminescent intermediates, the emissions of which can be detected on X-ray film. The kit was used in accordance with the manufacturer's recommendations.

In brief, 2ml of ECL Solution A was mixed with 25µl of ECL solution B and added to the membrane, the tube was wrapped with foil to shield it from light and it was mixed on a roller for 5 minutes to develop. The membrane was then wrapped in Saran Wrap and placed in a developing cassette. A sheet of X-OMAT x-ray film was placed over the membrane for varying exposure times and developed on a Compact X4 (Xograph Imaging Systems).

LumiGLO (Cell Signaling Technology 7003)

This is a luminol-based system. In the presence of hydrogen peroxide, horseradish peroxidase converts luminol to an excited intermediate which emits light on its return to ground state. 0.5ml of Reagent A and 0.5ml of reagent B were added to 9ml of water. This was then added to the membrane for 1 minute and then the membrane was prepared for x-ray in the same fashion as above.

Stripping PVDF Membrane and Reprobing

The membrane can be stripped of antibodies to allow further reprobing with different antibodies. This was done by washing twice on a roller with 10-15 ml TBS-Tween for 5 minutes each. Then 50 ml of Stripping Buffer was added and left for 30 minutes in a waterbath set to 50^0C. A further two washes on a roller with 10-15 ml TBS-Tween for 5 minutes each was performed and the membrane either stored (in TBS-Tween at 4°C) or re-probed.

β-actin

To confirm equal sample loading, the PVDF membrane was stripped and reprobed with a β-actin primary antibody at a dilution of 1:5000 at 4^oC overnight following the same procedures as above.

2.6 Cell proliferation studies

To assess whether cellular proliferation could be affected by interaction with PPARγ agonists, a series of experiments were set up to assess a cell lines proliferation with varying concentrations of treatments applied. The PPARγ agonist rosiglitazone (GlaxoSmithKline, UK) was chosen as the PPARγ agonist and stock solutions were made up by dissolving in dimethylsuphoxide (DMSO) to give a stock concentration of 10^{-2}M. Subsequent dilutions were done using H_2O. Cellular proliferation was assessed by thymidine incorporation. An example of the protocol used is detailed below.

2.6.1 Method

1. Culture cells until confluent according to standard protocol.

2. Harvest cells and centrifuge to give a pellet of cells. Re-suspend in normal culture medium of known volume.

3. Count cells using haemocytometer.

4. Pipette out the correct volume of cell suspension to each well to the required density e.g. 50,000 cells/well and add normal media up to a volume of 500-1000 μl.

5. Place cells into incubator for 24 hours to allow adhesion.

6. Make up treatment solutions e.g. rosiglitazone at 10^{-3}, 10^{-4}, 10-5, 10^{-6}, 10^{-8} concentrations. Note that these will be diluted by a factor of 10 when added to the wells containing media giving treatment concentrations of 10^{-4}, 10^{-5}, 10^{-6}, 10^{-7} and 10^{-9}.

7. Remove normal media from wells and replace with 900µl of serum free media (plus antibiotics), and add 100µl of the treatment solutions to each well to give final volume of 1ml containing the required concentration treatment.

(Note: BON cells did not survive well in serum starved media, instead, DMEM media with 2% (charcoal stripped) fetal calf serum was used.)

Example – 24 well plate

	1	2	3	4	5	6
1	Media Only	Rosiglit (10^{-4}M)	Rosiglit (10^{-5}M)	Rosiglit (10^{-6}M)	Rosiglit (10^{-7}M)	Rosiglit (10^{-9}M)
2	Media Only	Rosiglit (10^{-4}M)	Rosiglit (10^{-5}M)	Rosiglit (10^{-6}M)	Rosiglit (10^{-7}M)	Rosiglit (10^{-9}M)
3	Media Only	Rosiglit (10^{-4}M)	Rosiglit (10^{-5}M)	Rosiglit (10^{-6}M)	Rosiglit (10^{-7}M)	Rosiglit (10^{-9}M)
4	Media Only	Rosiglit (10^{-4}M)	Rosiglit (10^{-5}M)	Rosiglit (10^{-6}M)	Rosiglit (10^{-7}M)	Rosiglit (10^{-9}M)

8. Incubate the plate at 37°C in a humidified, 5% CO_2 atmosphere for 48 hours.

9. Six hours prior to the end of the experiment, add 2µCi (curie) of [3H]-thymidine (Amersham) to each well (i.e. add 50µl [3H]-thymidine to 2.5ml culture media and then add 100µl of this to each well).

10. At 24 hours, aspirate the media from the wells and briefly wash with 1ml ice-cold PBS.

11. Add 1ml of scintillant (Amersham) to each well and incubate the plate for 5 minutes.

12. Collect the fluid from each well into separate labelled scintillation vials and vortex thoroughly.

13. Incorporation of thymidine, in units of counts per minute (CPM), can then be measured using a scintillation counter.

Charcoal Stripping

50mls	fetal calf serum (FCS)
2g	charcoal

Left on rollers overnight at $4^{o}C$

Optimisation of Treatment Duration

Experimental plates were set up as described and treatments were left on for variable durations i.e. 24, 48 72 and 96 hours. Tritiated thymidine was added to the wells 6 hours prior to the completion of the experimental period. Scintillation counting was then performed and raw data collated on an excel file. Outcomes for the three cell lines are shown the results section. In all three cell lines, it was felt that treatment duration of 48 hours gave the best results.

2.6.2 Combined proliferation studies

All cell lines, CM, BON and QGP1, were then subjected to repeated experimentation and the results collated to give combined proliferation studies for treatment with rosiglitazone at concentrations of $10^{-4}M$, $10^{-5}M$, $10^{-6}M$, $10^{-7}M$ and $10^{-9}M$. Average counts for each group were calculated along with the standard error of the mean. Statistical significance was assessed by non-parametric Kruskal-Wallis test, followed by Conover-Inman if significance was achieved.

2.6.3 Proliferation studies with DMSO

Rosiglitazone was supplied in concentrated form and dissolved in dimethylsuphoxide (DMSO). Subsequent dilutions to treatment dose levels in H_2O reduced the effective concentration of DMSO in the wells during the treatment periods. This means that at higher concentrations of rosiglitazone there will also be higher concentrations of DMSO present. We felt that a toxic effect of DMSO on the cells should be excluded.

Proliferation studies were set up in exactly the same way except that rosiglitazone was not added. Instead equivalent 'treatments' containing H_2O and DMSO at the same concentration was added. This 'treatment' was left for 48 hours and subject to thymidine incorporation and scintillation counting in exactly the same way as previously performed. Again, repeated experiments were performed and results were combined prior to statistical analysis and graphical representation.

2.6.4 Rosiglitazone versus DMSO treatments in QGP1 cells

At the highest concentration of DMSO it appeared that there may be a toxic effect on the QGP1 cell line. A single experiment was performed where two plates were set up to allow direct comparison of the effects seen by rosiglitazone and DMSO. On one plate QGP1 cells were treated with varying rosiglitazone concentrations, as per previous experiments. On the second plate cells were treated with equivalent concentrations of DMSO. The results were subject to the same analysis and results are shown in the results section.

2.6.5 Recovery studies

As with all treatments, the effects seen may simply be due to a toxic effect which is undesirable if it leads ultimately to cell death. Recovery of cells following removal of treatment was therefore felt to be important. To assess this, experiments were set up at

the same time and date and from the same harvest of cell cultures to minimise error between groups.

- First set was treated with rosiglitazone for 48 hrs and harvested
- Second set was treated with rosiglitazone for 48 hrs then washed and left in normal media for a further 48 hours prior to harvesting.
- Third set was treated with rosiglitazone for 96 hrs and harvested at the same time as set 2.

The first set is essentially a control to make sure that we see the expected effects of rosiglitazone treatment. The second set is the experimental group. The third set is another control group to identify that there is a continued effect of rosiglitazone treatment and that the cells do not spontaneously recover or escape from treatment effects.

2.6.6 Antagonist studies

To complete the PPARγ cell proliferation experiments we decided to try and prevent the effect of rosiglitazone by blocking the PPARγ receptors irreversibly, thereby attempting to prove that the effects seen are mediated by the PPARγ.

A PPARγ antagonist was purchased from Calbiochem (Calbiochem-Novabiochem Corp., La Jolla, CA, USA) identified as T0070907 antagonist (2-Chloro-5-nitro-N-(4-pyridyl)benzamide)

T0070907 is a potent, specific, irreversible, and high-affinity antagonist of PPARγ with a K_i of 1nM. It also displays >800-fold greater selectivity for PPARγ over PPARα and PPARδ (K_i = 0.85μM and 1.8μM, respectively).

A second anatagonist was obtained through a colleague (Dr D B Bailey, St Bartholomews Hospital) identified as GW9662 antagonist (2-Chloro-5-nitro-N-phenyl-benzamide) (Sigma, St Louis, Missouri, USA).

GW9662 is an irreversible PPARγ antagonist. GW9662 binds PPARγ with IC50 in nanomolar range, and is 10- and 600-fold less potent in binding PPARα and PPARδ, respectively.

For both antagonists, a 1μM concentration was used. Plating was performed with a control group (no antagonist), antagonist on its own, plus cells treated with rosiglitazone at 10^{-4}M, 10^{-5}M and 10^{-6}M concentrations. Cells were pre-treated with the antagonist for 90 minutes prior to the addition of rosiglitazone. Incorporation of thymidine, harvesting and assessment of proliferation were performed as for previous experiments.

2.6.7 Direct comparison studies

So far all antagonist experiments had been run without a comparative rosiglitazone treated group. It was felt that if the antagonist was having any effect then there should be a significant difference seen when cells treated with rosiglitazone are compared directly with cells treated with antagonist and rosiglitazone. Thus direct comparison studies were performed. Cells were plated in two lines. Following cell adhesion, one line was treated with rosiglitazone at a concentration of 10^{-4}M, the second line being treated with rosiglitazone at a concentration of 10^{-4}M plus 1μM antagonist. This was repeated for rosiglitazone concentrations of 10^{-5}M and 10^{-6}M.

Repeated experiments were performed for QGP1 and BON cell lines at the above concentrations for 48 hours and subject to the same thymidine incorporation, harvesting and scintillation counting.

2.7 Statistical analysis

Statistical analysis was performed with StatsDirect software package. Data for immunohistochemistry and cell culture groups was not normally distributed as assessed by Shapiro-Wilk testing. The majority of comparisons were performed using Kruskal-Wallis analysis of variance test. If $P<0.05$ subgroup analysis was performed using the Conover-Inman test. Alternatively, Mann-Whitney test was performed to compare 2 groups following subgroup analysis by Ki-67 index. When appropriate, graphs have been generated to help present the data.

CHAPTER 3

RESULTS I

Human Frozen Tissue Samples

3.1 Human tissue Samples

A selection of pancreatic neuroendocrine tumours was held in the -80^{o}C freezer within the Academic Department of Endocrinology at St Bartholomew's Hospital. Ethical consent for collection and experimentation had been gained prior to the commencement of this project by Professor A. Grossman through the North East London Research Ethics Committee (Ref. P/02/069). Details of the diagnosis and histopathology were held on database.

SAMPLE	SEX	AGE	DATE OF SURGERY	DIAGNOSIS
1	F	42	1997	Gastrinoma
2A	F	26	1997	MEN-Insulinoma 1
2B	F	26	1997	MEN-Insulinoma 2
2C	F	26	1997	MEN-Insulinoma 3
3A	M	57	1995	Insulinoma
3B	M	57	1995	Lymph node met
4	F	44	1994	Gastrinoma
5	M	51	1998	MEN-Insulinoma
6A	M	34	1998	Normal pancreas
6B	M	34	1998	Insulinoma
7	F	67	2001	Gastrinoma
8	F	61	2001	Insulinoma

Table 1 Tumour bank samples and clinical details

3.1.1 RNA Extraction.

Work done on tissue samples:

Example – Sample 2C

3 X Homogenisation and RNA extraction (Promega SV Total RNA Isolation System)

3 X Spectrophotometry

2 X RNA gels

GAPDH PCR 4 X SHORT (repeated at 26 and 35 cycles)

1 X LONG

1 X PPARγ PCR

SAMPLE 2B 2C 3B 4 8

Figure 3.1 Example of a typical RNA gel result

3.1.2 GAPDH PCR

SAMPLE H_2O SM 2A 2B 2C 3B 4 8 6A

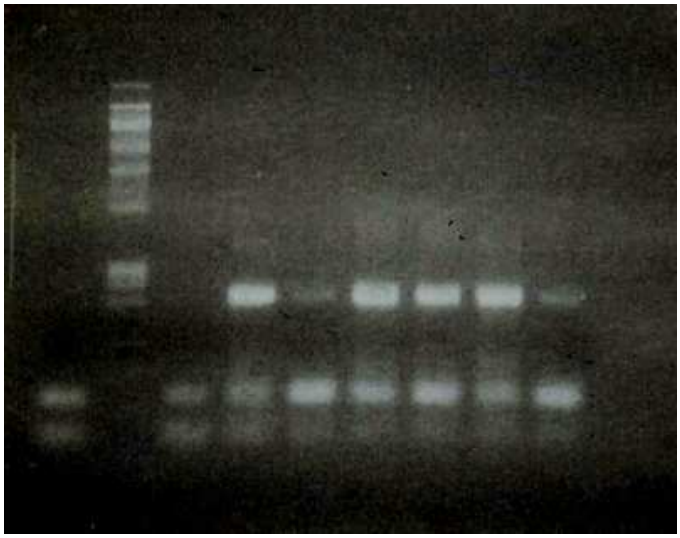

← **SHORT GAPDH**

← **PRIMER DIMERS**

Figure 3.2 Example of short GAPDH results

SAMPLE SM 2A 2B 2C 3B 4 8 6A H_2O

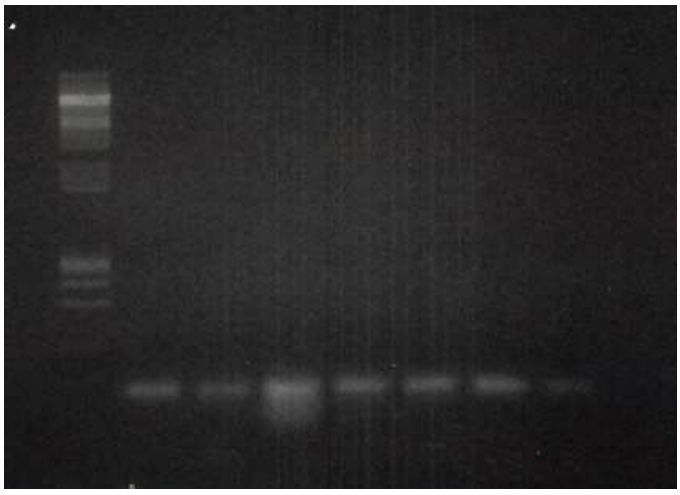

← **PRIMER DIMERS**

Figure 3.3 Example of long GAPDH results

SM = SIZE MARKER PROMEGA ϕX174 HAE III

SAMPLE	260/280 RATIO	RNA GEL	SHORT GAPDH	LONG GAPDH
1	2.1	No bands	Present-weak	Absent
2A	2.1	No bands	Present-weak	Absent
2B	2.3	Good bands	Present-good	Absent
2C	1.9	No bands	Present-weak	Absent
3A	1.6	No bands	Present-weak	Absent
3B	1.9	No bands	Present-good	Absent
4	2.1	No bands	Present-good	Absent
5	3.0	No bands	Present-good	Absent
6A	2.0	No bands	Absent	Absent
6B	2.1	No bands	Present-good	Present-good
7	3.1	Good bands	Present-good	Present-weak
8	2.3	Good bands	Present-good	Absent

Table 2 Summary of best results obtained for human tissue samples

3.1.3 PPARγ EXPRESSION

We wanted to look at PPARγ expression in fresh tumour samples at the RNA level and subjected the extracted RNA to Qiagen PCR, using the primers described.

SAMPLE	TUMOUR	PPARγ EXPRESSION
1	Gastrinoma	Absent
2A	Insulinoma	Absent
2B	Insulinoma	Present - good
2C	Insulinoma	Absent
3A	Insulinoma	Absent
3B	Lymph node met	Present – good
4	Gastrinoma	Present – good
5	Insulinoma	Present – weak
6A	Normal pancreas	Absent
6B	Insulinoma	Absent
7	Gastrinoma	Present – good
8	Insulinoma	Present - good

Table 3 Summary of PPARγ expression in human tumour samples

RNA extraction from previously frozen tissue samples was hampered by issues with the quality and quantity of samples available. Despite multiple procedures, reliable high quality RNA was not re-producible. PPARγ PCR was performed on all samples of RNA extracted. Although few conclusions can be made, given the limitations, PPARγ expression was seen in 6 out of the 8 patient samples. PPARγ expression was seen in 4 out of 5 insulinomas (1 insulinoma LN metastasis), and 2 out of 3 gastrinomas. For

those samples that had better RNA quality results, there is a more favourable outcome in terms of PPARγ expression.

PPARγ PCR products - examples

SAMPLES SM 2B 2C 3B 4 8 6A +VE H_2O

← PPARγ

Figure 3.4 DNA gel showing PCR products for PPARγ

SAMPLES SM 7 6B 1 3A 5 +VE H_2O

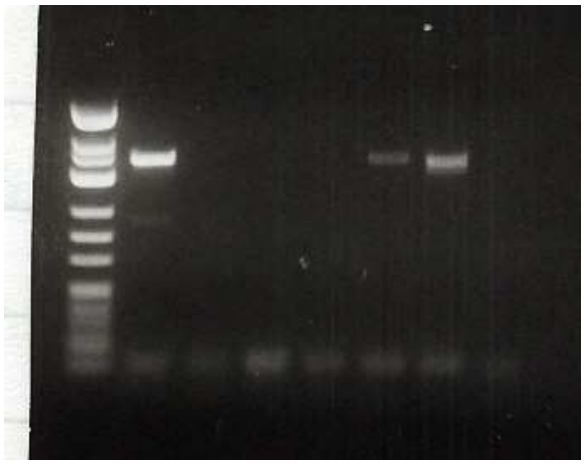

← PPARγ

Figure 3.5 DNA gel showing PCR products for PPARγ

SM = SIZE MARKER PROMEGA ϕX174 Hinf I

+VE = POSITIVE CONTROL (ADRENAL TUMOUR TISSUE)

RESULTS II

Immunohistochemistry

3.2.1 Immunohistochemistry

A trust-wide search for pancreatic neuroendocrine tumours through histopathology records, endocrine department records and surgeons logbooks revealed a total of 44 potential subjects going back over 20 years.

In total 25 cases were identified as having good quality specimens that could be used. In several cases there was more than 1 specimen available for the same patient – these were annotated A, B or C as seen in table 4.

Of the 25 cases, further information is noted to allow better understanding of the results:

1 patient only had tissue from a lymph node metastasis of a gastrinoma (Case 24). This was included as a gastrinoma in the tumour results series.

2 cases were removed from the 25 before final analysis.

Case 16 - equivocal diagnosis being undecided between an endocrine tumour and a papillary and solid epithelial neoplasm (PSEN).

Case 21 - identified as a lymph node metastasis of the gastrinoma in case 22.

Insufficient islets were available in cases 3, 19, 22 and 24.

Insufficient exocrine pancreas was seen in cases 4, 22 and 24.

Treated in this way the results could be generated in a standard format for all antibodies tested. In total, therefore, there are 20 insulinomas and 3 gastrinomas in the tumour series, 19 results for the islet series and 20 results for the exocrine series. These numbers are the same for all antibodies.

For all immunohistochemistry graphical illustrations therefore:-

Insulinomas	n=20
Gastrinomas	n=3
Islets	n=19
Exocrine	n=20

3.2.2 Cell counting

As described in the methods section, counting was performed using a grid system overlying a magnified field of view viewed on a computer screen. For each case and antibody, approximately 500 cells were counted for insulinoma, gastrinoma, islet and exocrine pancreas. Each was assessed for both nuclear and cytoplasmic staining. Staining was described as strong, moderate, weak or negative.

Table 4 Cases identified as suitable for immunohistochemistry

ID	SEX	AGE	DIAGNOSIS
1	M	24	INSULINOMA
2A/B	M	24	INSULINOMA
3A/B	F	69	INSULINOMA
4	F	58	GASTRINOMA
5	F	41	INSULINOMA
6	M	65	INSULINOMA
7	M	27	INSULINOMA
8	M	54	INSULINOMA
9	F	71	INSULINOMA
10	F	26	INSULINOMA
11	M	42	INSULINOMA
12	M	51	INSULINOMA
13	F	58	INSULINOMA
14A/B	F	39	INSULINOMA
15A/B	F	51	INSULINOMA
16	F	29	ENDO/PSEN
17	F	61	INSULINOMA
18A/B	M	21	INSULINOMA
19A/B	F	61	INSULINOMA
20	M	78	INSULINOMA
21	M	35	GASTRINOMA LN
22A/B/C	M	35	GASTRINOMA
23	F	55	INSULINOMA
24A/B	M	69	GASTRINOMA LN
25	M	37	INSULINOMA

3.2.3 PPARγ Immunohistochemistry

A mouse monoclonal IgG antibody to PPARγ was obtained from Santa Cruz Biotechnology. The antibody is raised against a peptide mapping to the carboxy terminus of PPARγ of human origin. Optimisation of the antibody was performed on normal skin samples which acted as the positive control. A dilution of 1:50 was identified as the optimal dilution. Very good staining of the control was observed (Figure 3.6)

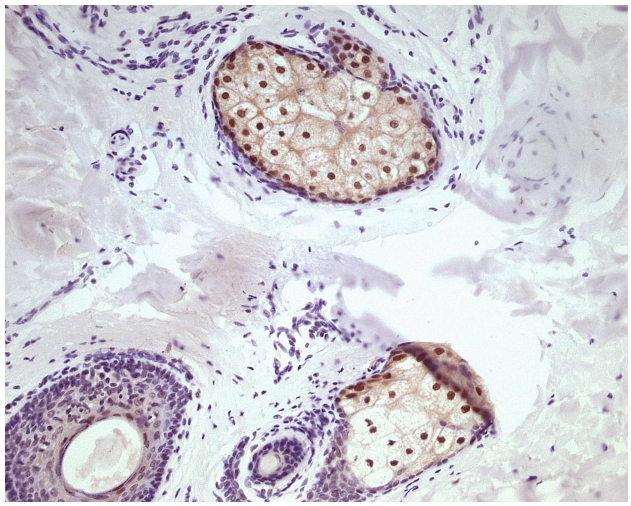

Figure 3.6 PPARγ positive control – skin sample with prominent sebaceous glands. The sebaceous glands can be seen staining strongly positive (red/brown colour).

From the results tables in the Appendix, it can be seen that only limited PPARγ staining was identified in any of the series for tumour, islet or exocrine, despite good positive control staining. All samples underwent repeat immunohistochemistry with similar results. Examples of staining seen are shown in the figures.

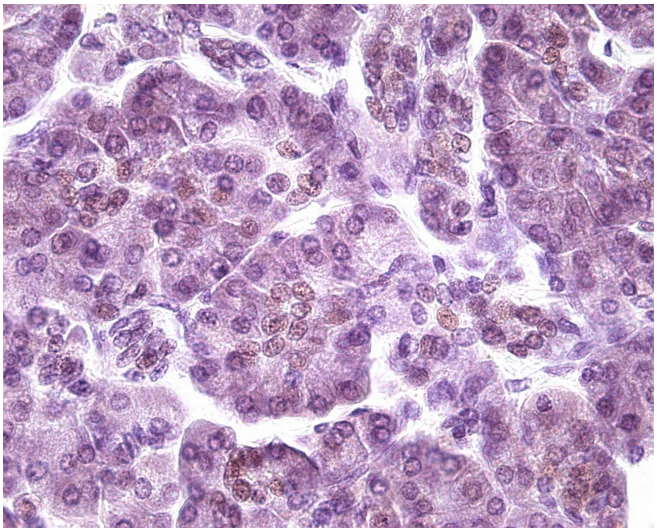

Figure 3.7 Only weak nuclear PPARγstaining can be seen here in sample 2

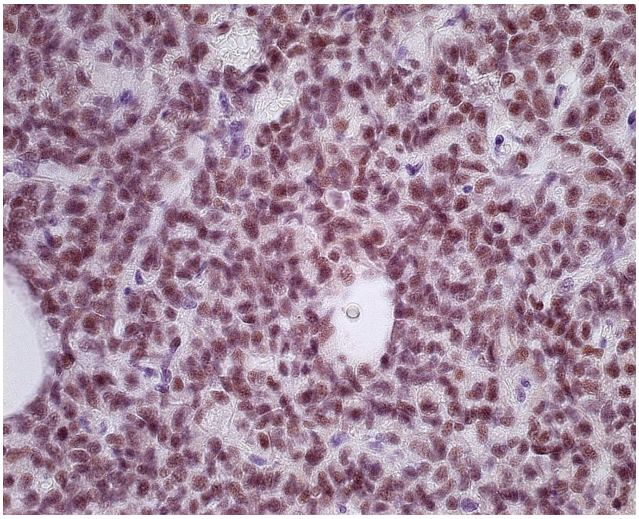

Figure 3.8 Stronger nuclear PPARγstaining can be seen in sample 15

It is clear that there is little evidence to suggest the nuclear or cytoplasmic presence of PPARγ within insulinoma, gastrinoma, islets or exocrine tissue in our samples.

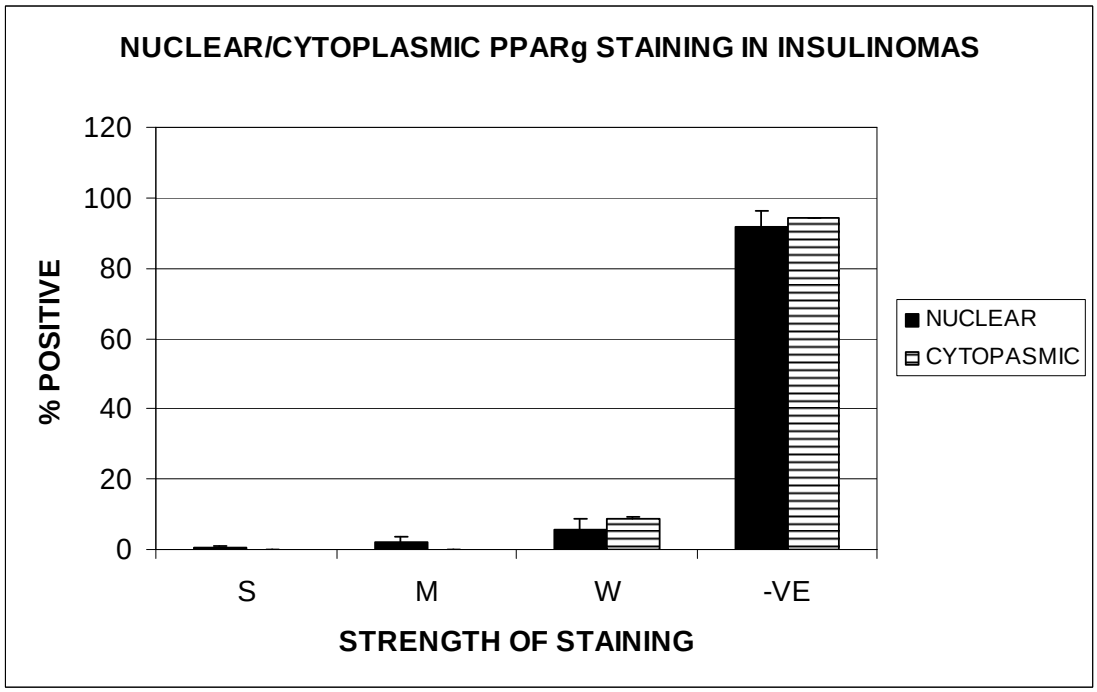

Figure 3.9 Graph showing the location and strength of PPARγstaining in insulinoma samples (S=strong, M=moderate, W=weak, -VE=negative)

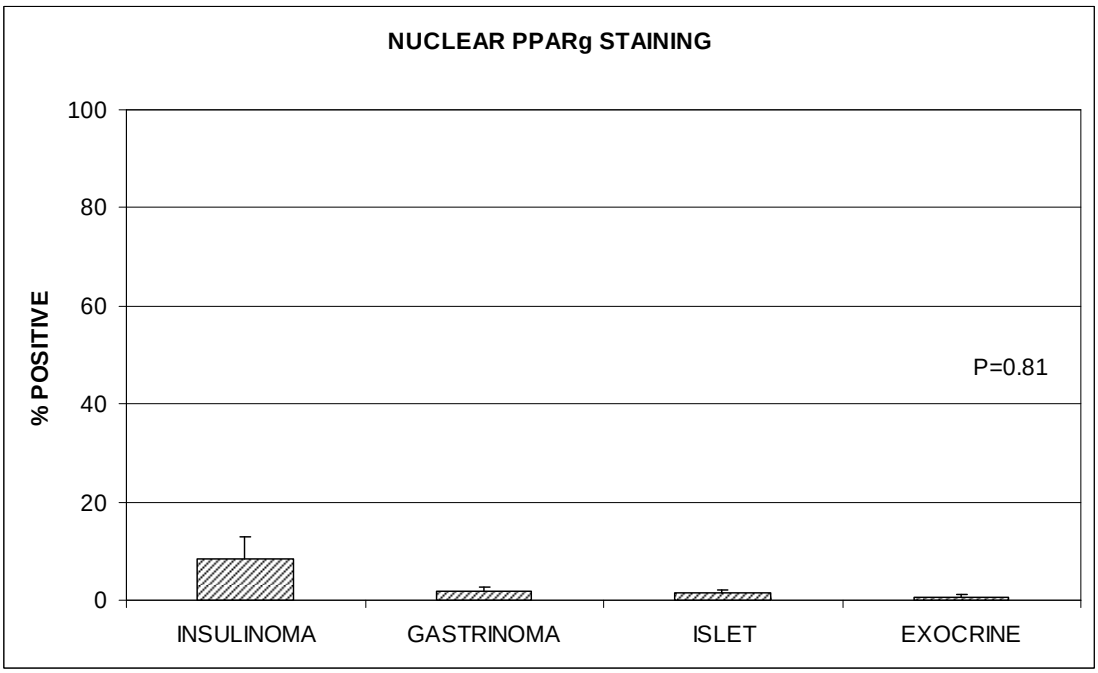

Figure 3.10 Graph representing total positive nuclear PPARγstaining in each group. Non parametric Kruskal-Wallis testing revealed no statistical difference.

3.2.4 p27 Immunohistochemistry

p27 is an inhibitor of both cyclin E-Cdk2 and cyclin A-Cdk2, two CDK complexes involved in the regulation of the G1/S transition. p27 has been found to be expressed at high levels in quiescent cells, playing an important role in maintaining cells in G0 through the inhibition of CDKs.

p27 was stained for using anti-p27 antibody from clone SX53G8 (gift from Dr X Lu, Barts and the London). After optimisation the antibody was used at a dilution of 1:300 with very good staining seen with tonsil sections acting as positive control.

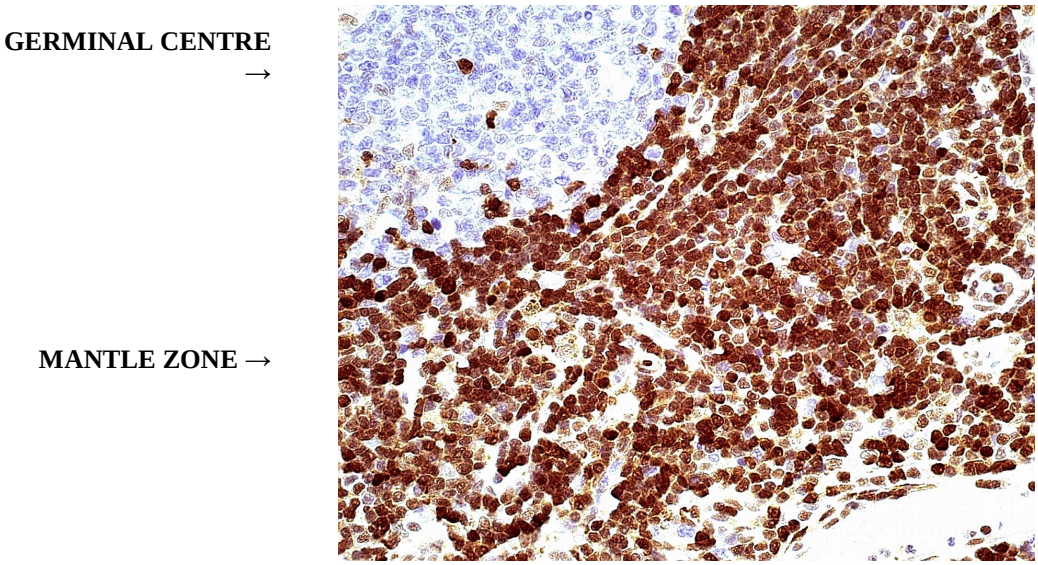

Figure 3.11 p27 positive control (tonsil) showing strong nuclear positive staining in the mantle zone

In the human tonsil there are multiple follicles which have both a germinal centre (consisting of predominantly proliferating T-lymphocytes) and a mantle zone (consisting of predominantly quiescent B-lymphocytes). In this control slide we see a predominantly unstained germinal centre (blue/purple) and a heavily stained (red/brown) mantle zone. For p27 this is an expected finding as cells with higher proliferation rates would be expected to show less nuclear p27.

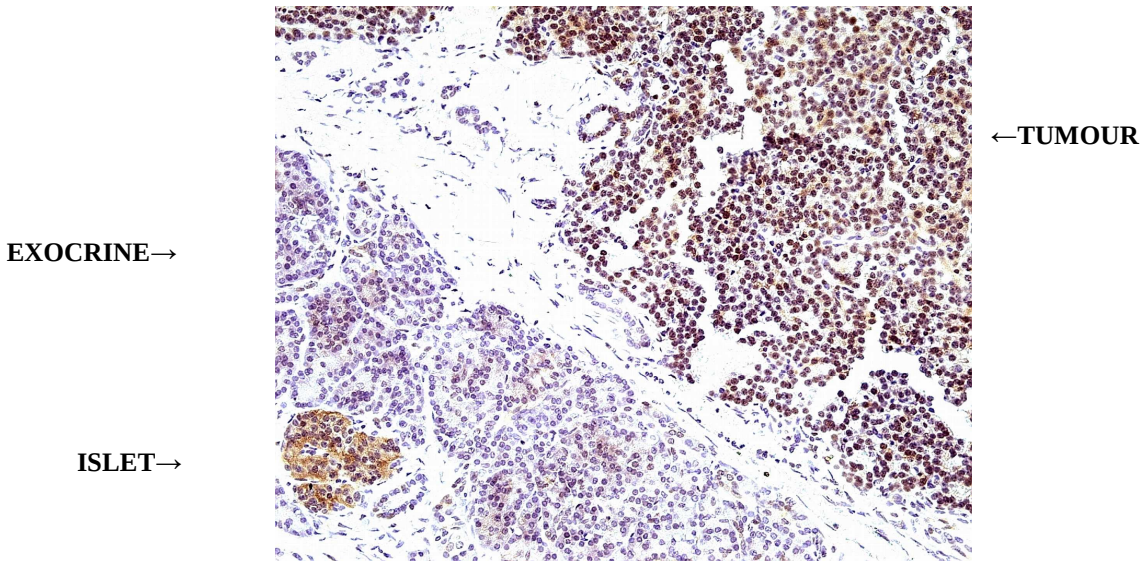

Figure 3.12 A lower powered slide of sample 6 showing islet, exocrine and tumour portions and the differences seen in staining

At lower magnification, the differences often seen in the staining patterns of tumour, exocrine tissue and islets can be seen on the same slide.

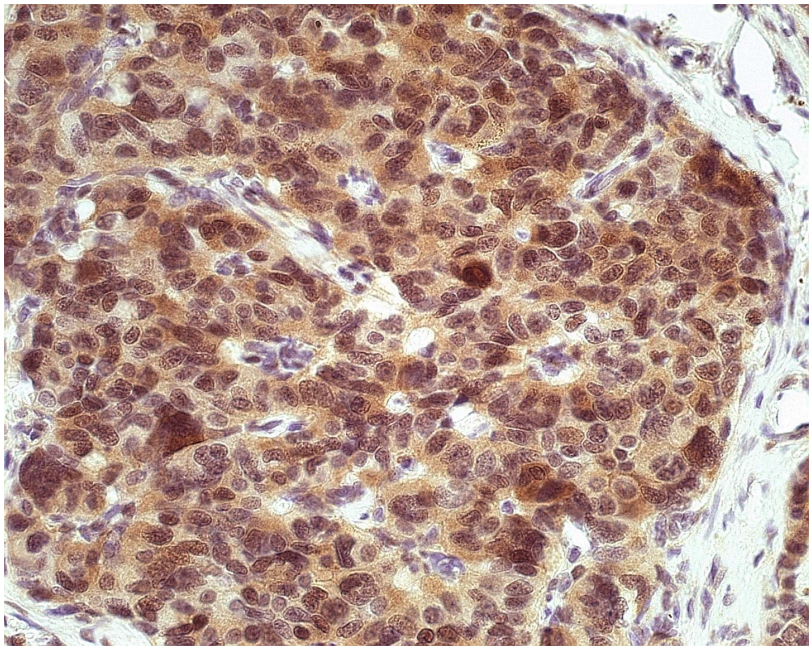

Figure 3.13 p27 staining of the insulinoma portion of sample 6, showing both nuclear and cytoplasmic staining

3.2.5 p27 Staining in insulinoma, gastrinoma, islet and exocrine pancreas

It can be seen from figures 3.14 – 3.17, that p27 is expressed in all the tissues in both the nuclear and cytoplasmic compartments. With the exception of exocrine pancreas, p27 expression shows a broad distribution of strong, moderate and weak staining. It also appears that p27 is expressed slightly higher in the cytoplasm than the nucleus of all three endocrine tissues.

In the insulinoma group no significant difference was seen between the nuclear and cytoplasmic localisation of p27 with positive nuclear staining seen in 68.7 +/- 6.81% and cytoplasmic staining seen in 74.6 +/- 5.6% (figure 3.18)

A significant difference is, however, seen in the case of gastrinoma (figure 3.19) and islets (figure 3.20). Nuclear staining in gastrinoma is 77.3 +/- 13.2% whereas cytoplasmic staining is 94 +/- 0.4% ($p<0.05$). Similarly, in islets, positive nuclear staining is 65.5 +/- 8.3% and cytoplasmic staining is 92.6 +/- 1.8% ($p<0.001$)

In exocrine tissue there is substantially less p27 expression with a trend towards higher nuclear localisation (figure 3.21). Positive nuclear staining was seen in 26.9 +/- 2.1% and cytoplasmic staining in 18.7 +/- 4.3% ($p=0.07$)

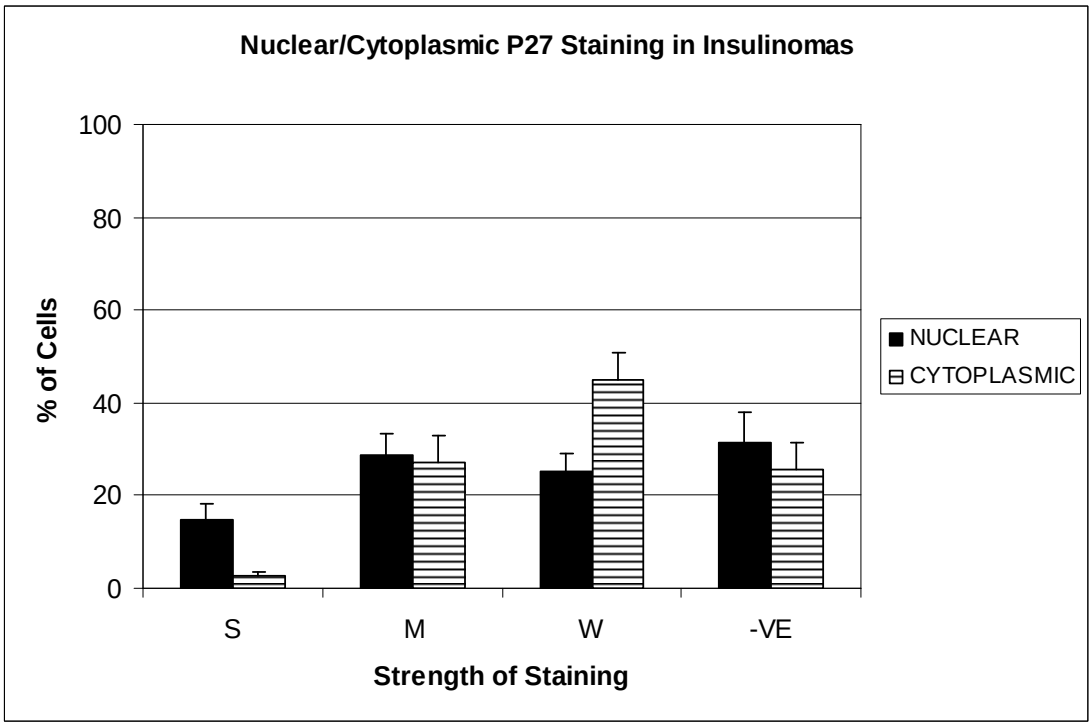

Figure 3.14 Graph showing the location and strength of p27 staining in insulinoma samples (S=strong, M=moderate, W=weak, -VE=negative)

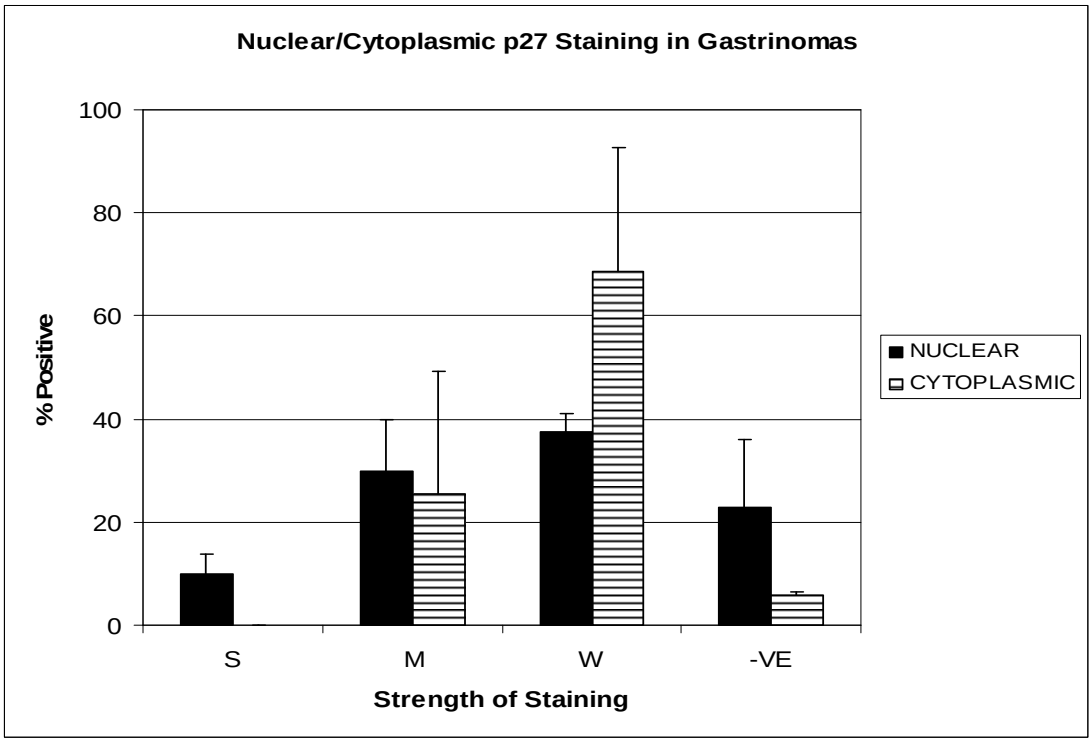

Figure 3.15 Graph showing the location and strength of p27 staining in gastrinoma samples (S=strong, M=moderate, W=weak, -VE=negative)

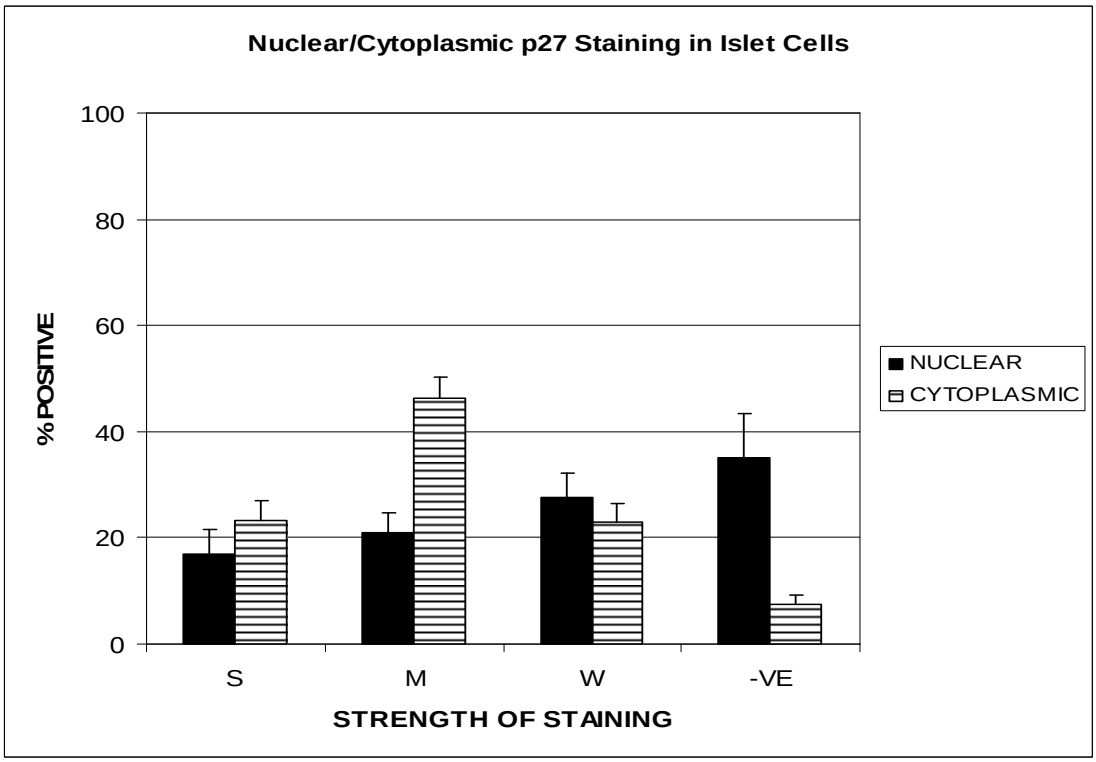

Figure 3.16 Graph showing the location and strength of p27 staining in islet samples (S=strong, M=moderate, W=weak, -VE=negative)

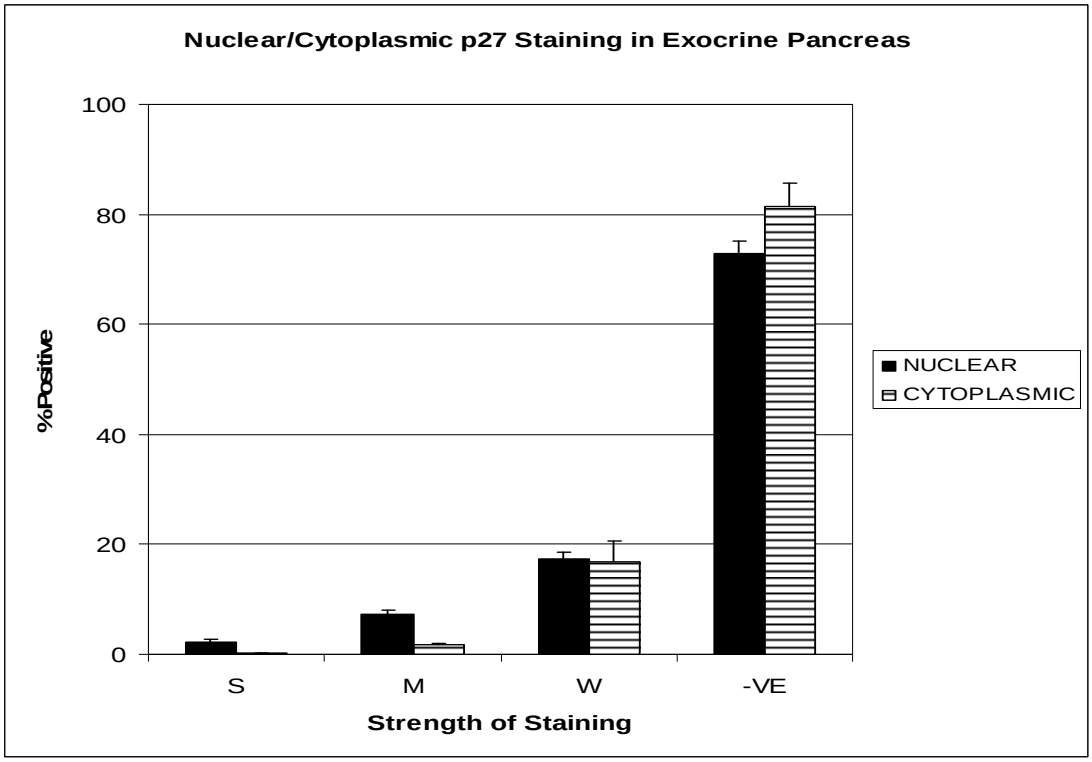

Figure 3.17 Graph showing the location and strength of p27 staining in exocrine samples (S=strong, M=moderate, W=weak, -VE=negative)

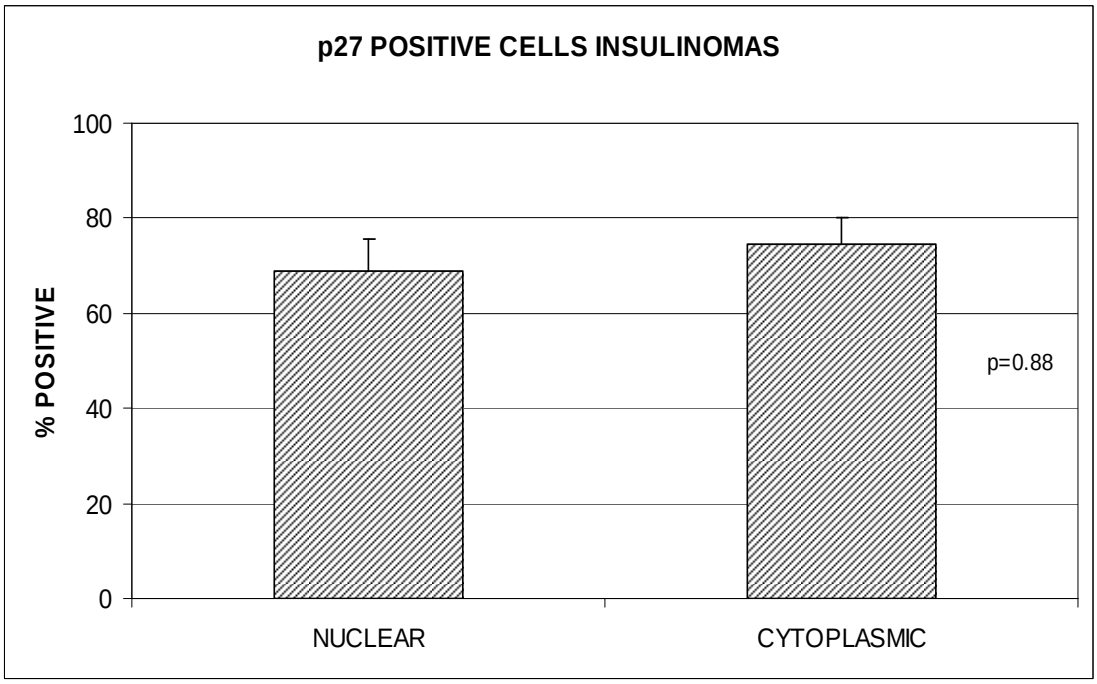

Figure 3.18 Graph showing the total positive (S+M+W) p27 nuclear and cytoplasmic staining in insulinoma samples.

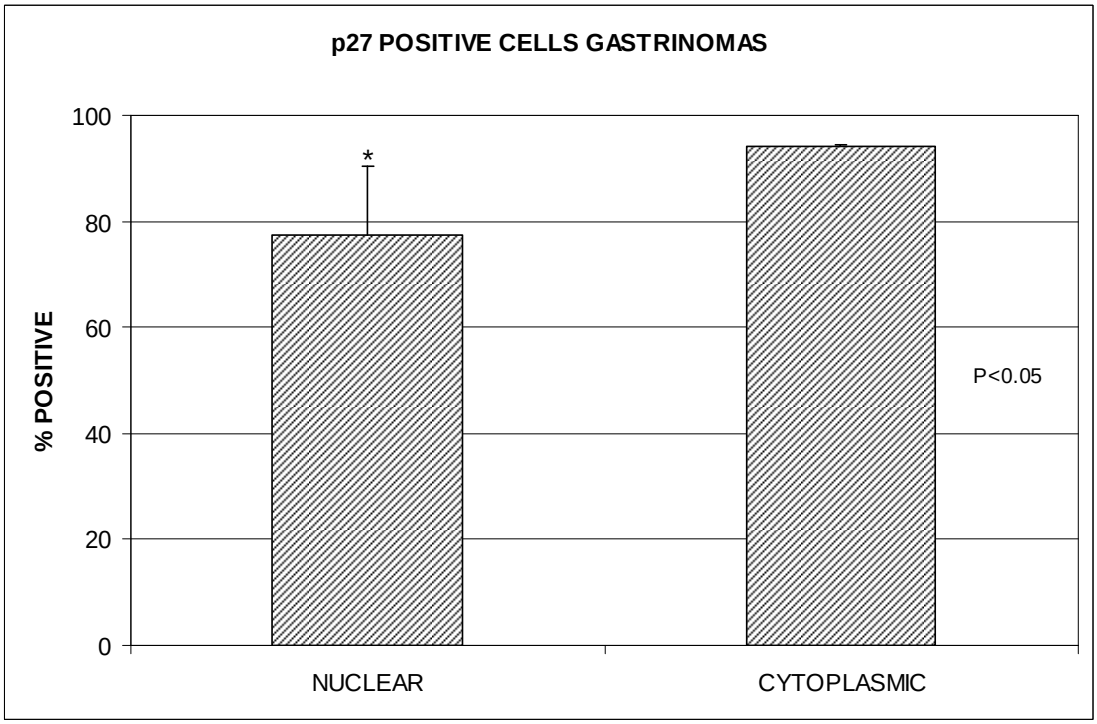

Figure 3.19 Graph showing the total positive (S+M+W) p27 nuclear and cytoplasmic staining in gastrinoma samples.

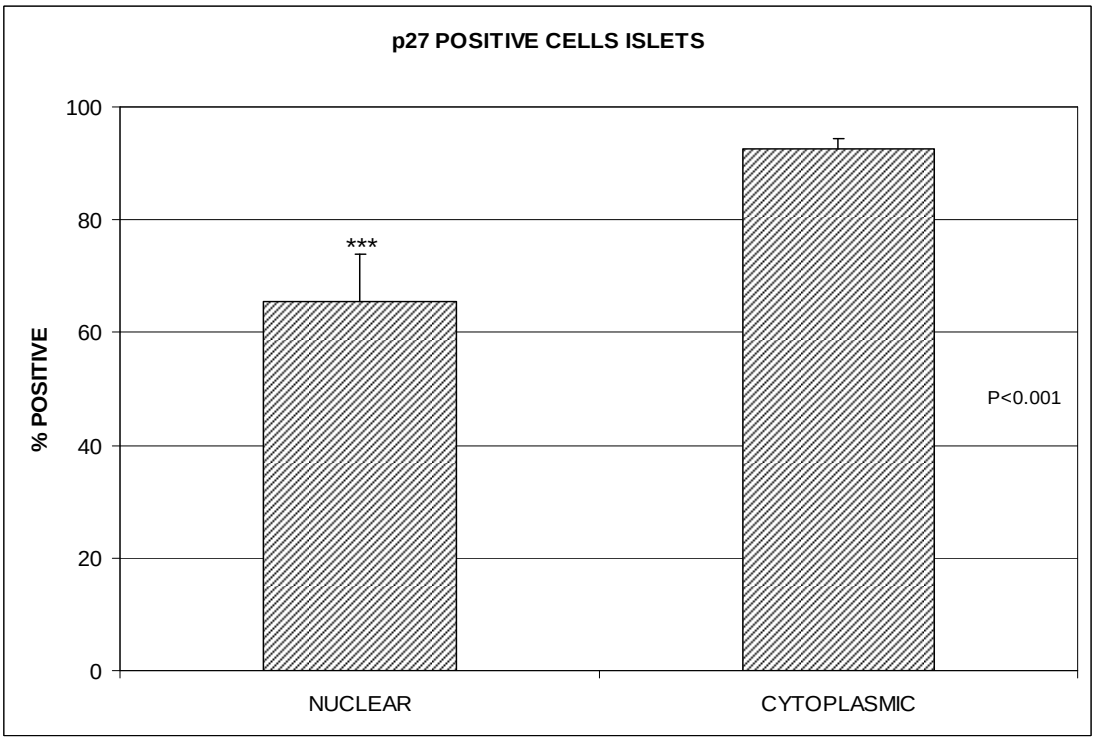

Figure 3.20 Graph showing the total positive (S+M+W) p27 nuclear and cytoplasmic staining in islet samples.

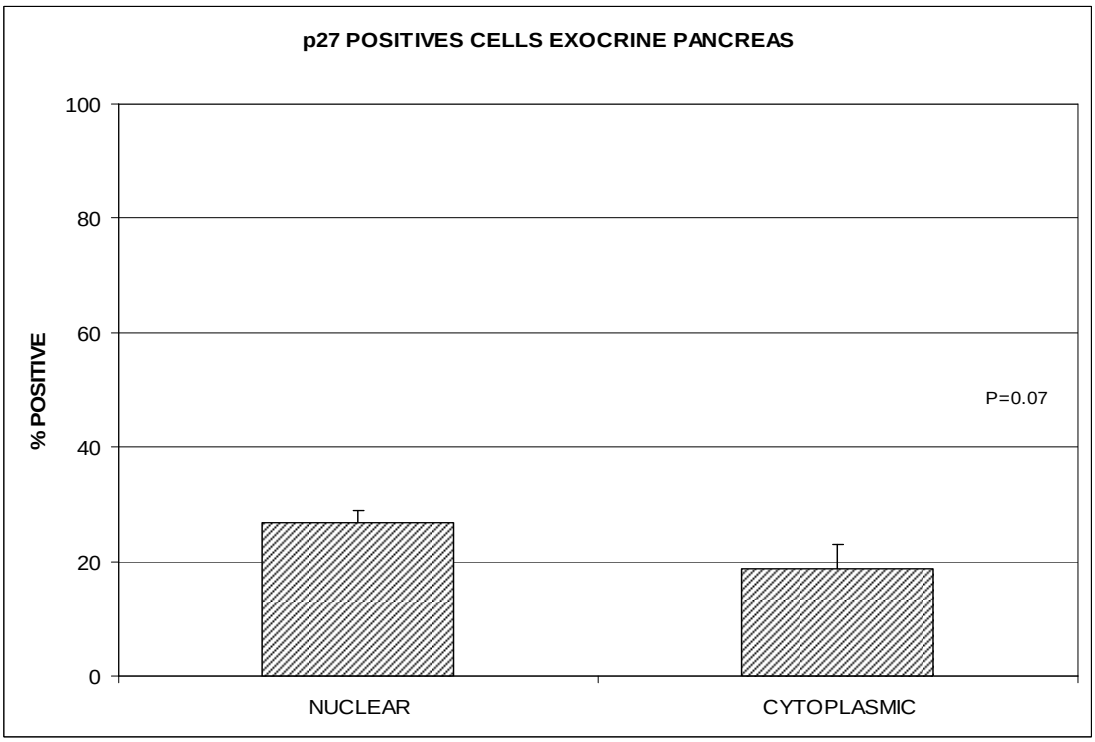

Figure 3.21 Graph showing the total positive (S+M+W) p27 nuclear and cytoplasmic staining in exocrine samples.

3.2.6 Comparison of p27 Nuclear Staining

Comparing nuclear p27 reveals the similarities in the pattern of staining in insulinoma, gastrinoma and islets. This is in contrast to the pattern of exocrine pancreas staining suggesting a significant difference in nuclear p27 expression of exocrine pancreatic tissue compared to endocrine tissues.

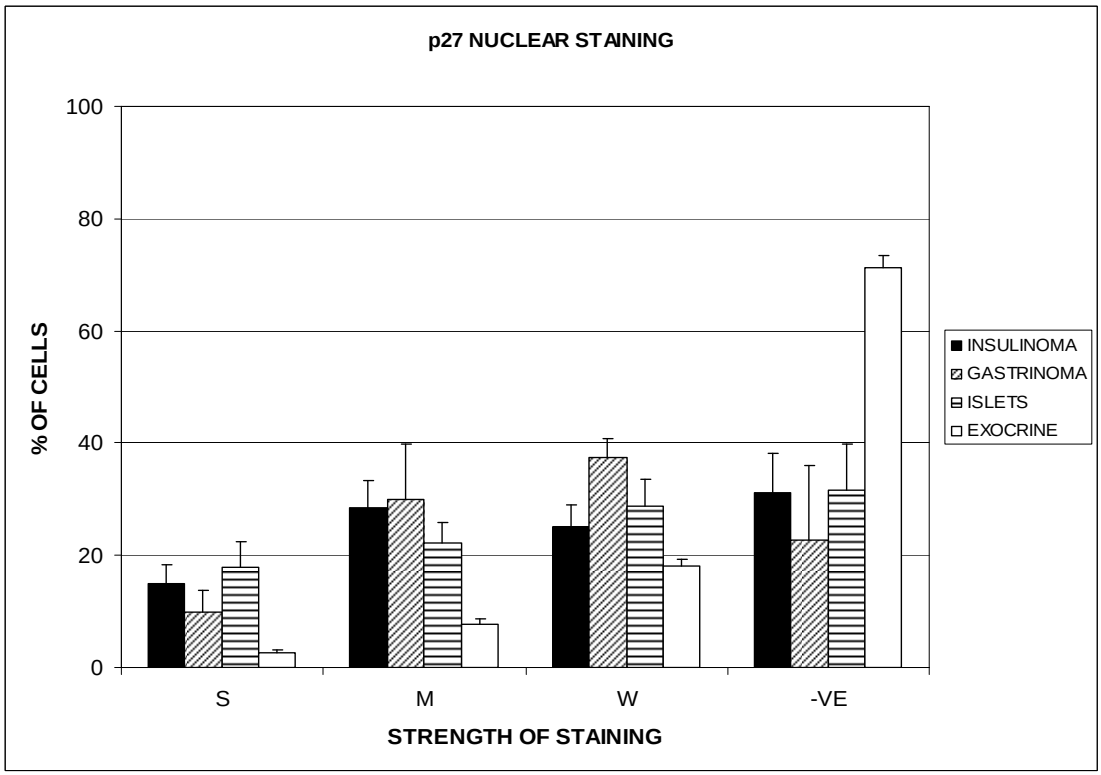

Figure 3.22 Graph comparing the relative strength of p27 nuclear staining for all tissue types

Comparing total positive counts confirms that there is no significant difference in the nuclear expression of p27 in insulinoma compared to islets, nor compared to gastrinoma. All three, however, are significantly different compared to exocrine pancreas (figure 3.23).

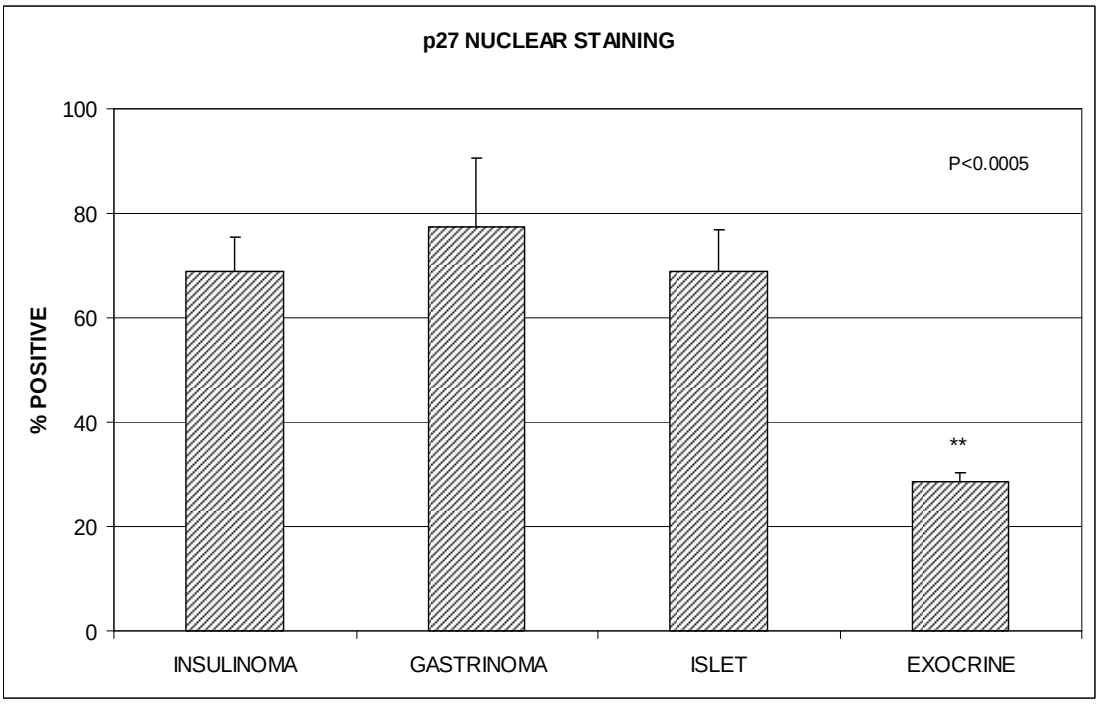

Figure 3.23 Graph comparing total positive p27 nuclear staining for all tissue types

Kruskal-Wallis P = 0.0005

Kruskal-Wallis: all pairwise comparisons (Conover-Inman)

INSULINOMA and EXOCRINE P < 0.0001

GASTRINOMA and EXOCRINE P = 0.0097

ISLET and EXOCRINE P = 0.0005

3.2.7 Comparison of p27 Cytoplasmic Staining

Trends in the pattern of cytoplasmic staining are less clear when looking at the strength of staining. The small numbers of gastrinomas with varying counts leading to large error.

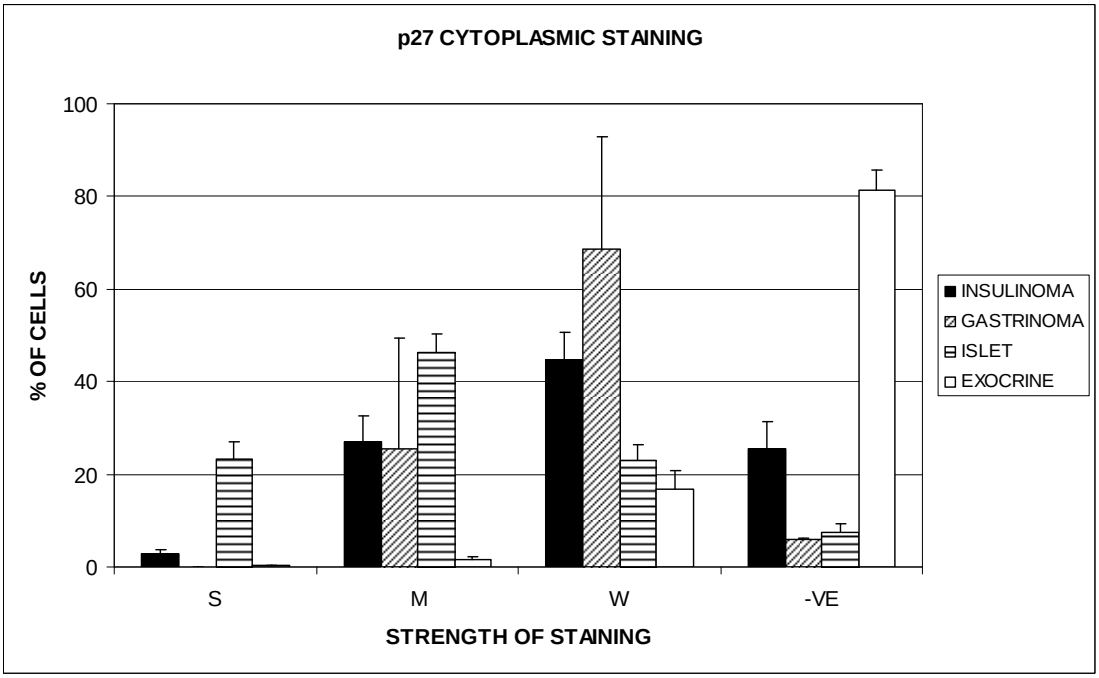

Figure 3.24 Graph comparing the relative strength of p27 cytoplasmic staining for all tissue types

On comparing the total positive counts (figure 3.25), there is a significant difference between insulinoma (74.6 +/- 5.6%) and islets (92.6 +/- 1.8%). Gastrinoma show a very similar level of positive staining to islets (94.1 +/- 0.4%), again, with a significant difference compared to insulinoma. Exocrine pancreas has significantly less p27 staining (18.7 +/- 4.3%) compared to insulinoma, gastrinoma or islets.

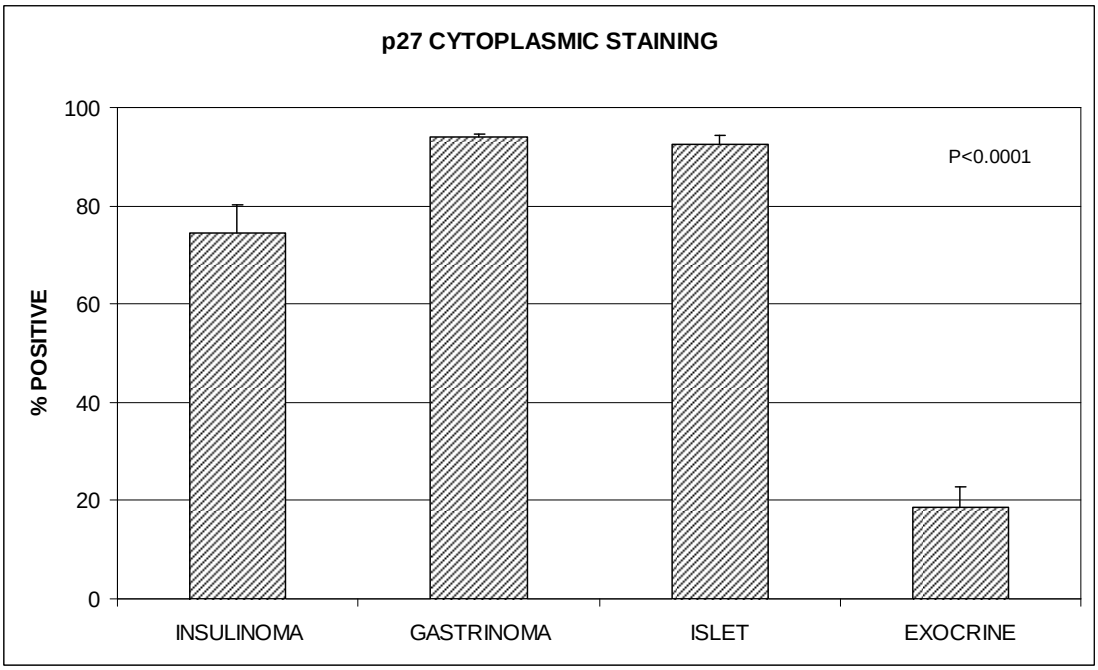

Figure 3.25 Graph comparing total positive p27 cytoplasmic staining for all tissue types

Kruskal-Wallis test P < 0.0001

Kruskal-Wallis: all pairwise comparisons (Conover-Inman)

INSULINOMA and GASTRINOMA	P = 0.0054
INSULINOMA and ISLET	P < 0.0001
INSULINOMA and EXOCRINE	P < 0.0001
GASTRINOMA and EXOCRINE	P < 0.0001
ISLET and EXOCRINE	P < 0.0001

These differences are enhanced when weak staining is excluded when calculating a value for positive staining. Clearly, the significant difference between insulinoma and gastrinoma has disappeared but there is a strengthening of the finding that insulinoma and islets are significantly different.

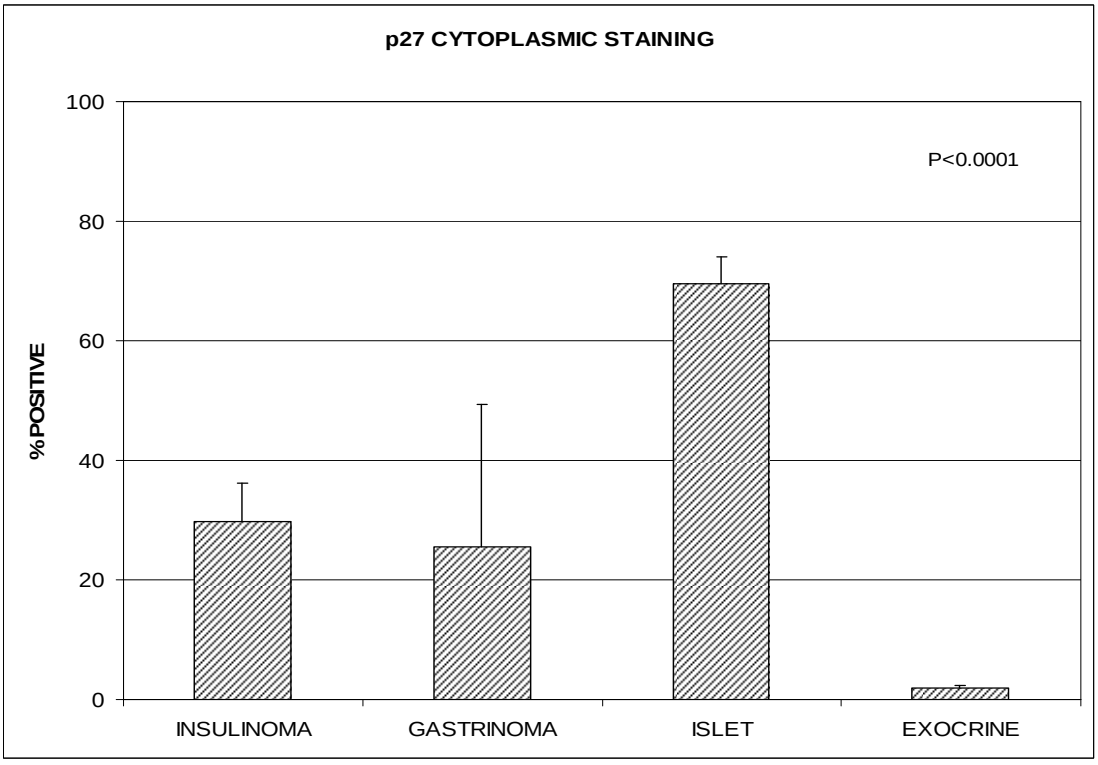

Figure 3.26 Graph comparing p27 positive staining (where positive = strong +moderate staining) for all tissue types.

Kruskal-Wallis test P < 0.0001

Kruskal-Wallis: all pairwise comparisons (Conover-Inman)

INSULINOMA and ISLET	P < 0.0001
INSULINOMA and EXOCRINE	P < 0.0001
GASTRINOMA and ISLET	P = 0.0005
ISLET and EXOCRINE	P < 0.0001

3.2.8 Phospho-p27 immunohistochemistry

p27 plays an important role in maintaining cells in G0 through the inhibition of CDKs. When cells re-enter the cell cycle, p27 protein levels but not mRNA levels decrease, this is thought to be due to an increase in p27 ubiquitin-mediated degradation. Phosphorylation of p27 on threonine 187 is thought to be an important step for the widespread ubiquitination of p27.

Slides were treated with an anti-phospho-p27 antibody obtained from Zymed laboratories. It is a polyclonal IgG antibody purified from rabbit antiserum. It detects threonine 187-phospholylated p27 peptide derived from the C-terminus of the human p27 protein. It does not cross react with non-phosphorylated p27 or related CDK inhibitor proteins. Optimisation led to an antibody dilution of 1:250 giving good staining as can be seen in the tonsil positive control section below.

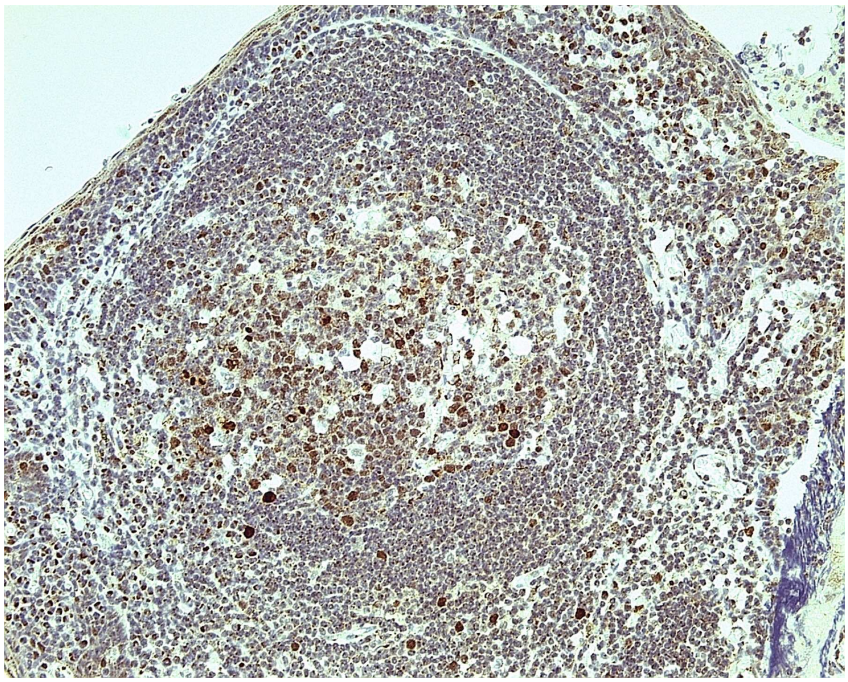

Figure 3.27 Positive control for phospho-p27 (tonsil). Stronger staining can be identified in the central germinal centre compared to the slide for p27

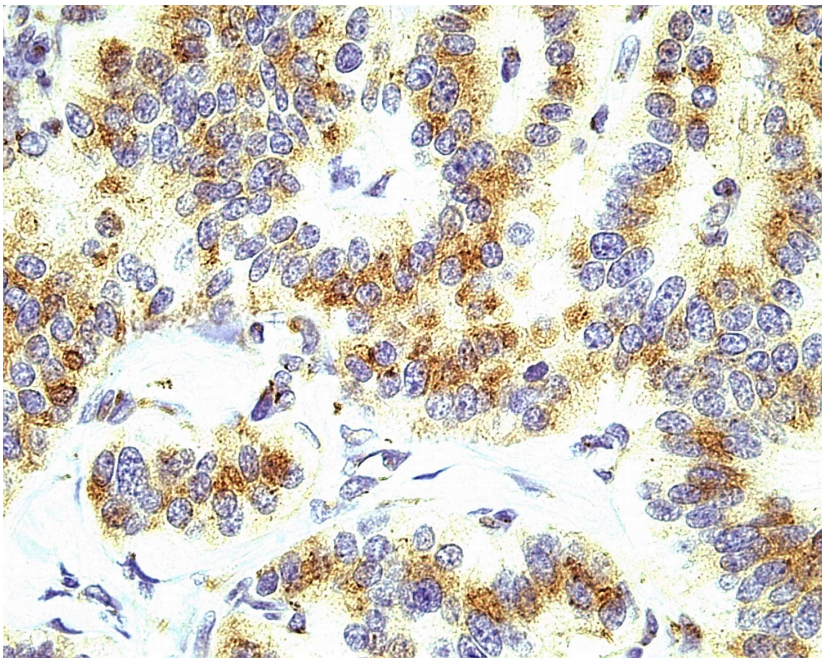

Figure 3.28 Positive phospho-p27 cytoplasmic staining seen in tumour sample 20

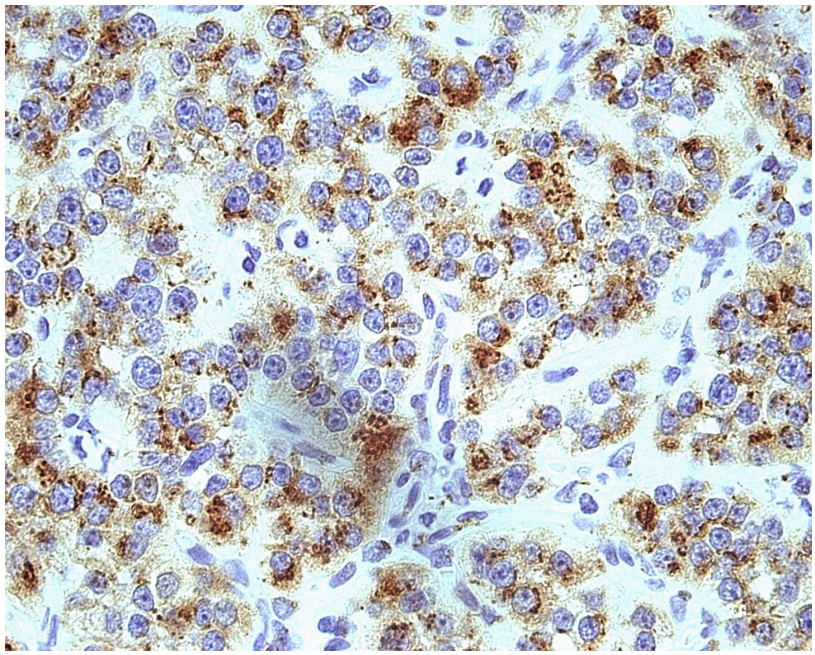

Figure 3.29 Positive phospho-p27 cytoplasmic staining seen in islet sample 20

3.2.9 Phospho-p27 staining in insulinoma, gastrinoma, islet and exocrine pancreas

Looking at the pattern of staining, the vast majority of phospho-p27 staining is seen in the cytoplasm of all tissue types (figures 3.30 – 3.33).

In insulinomas (figure 3.34), positive nuclear phospho-p27 staining was seen in only 1.5 +/- 0.8% compared to cytoplasmic staining of 78.9 +/- 6.2% ($p<0.001$). With gastrinomas (figure 3.35), nuclear staining was 6.8 +/- 4.3% compared to cytoplasmic staining of 86.2 +/- 11.6% ($p<0.05$). Similarly, islets (figure 3.36) show nuclear staining in only 3.6 +/- 2.1% but cytoplasmic staining in 87.4 +/- 4.2% ($p<0.001$).

Exocrine tissue had the highest positive nuclear count of 7.9 +/- 4.5% and the lowest cytoplasmic count of 41.5 +/- 4.5% (figure 3.37), but this is still a significant difference ($p<0.001$) in favour of cytoplasmic localisation of phospho-p27.

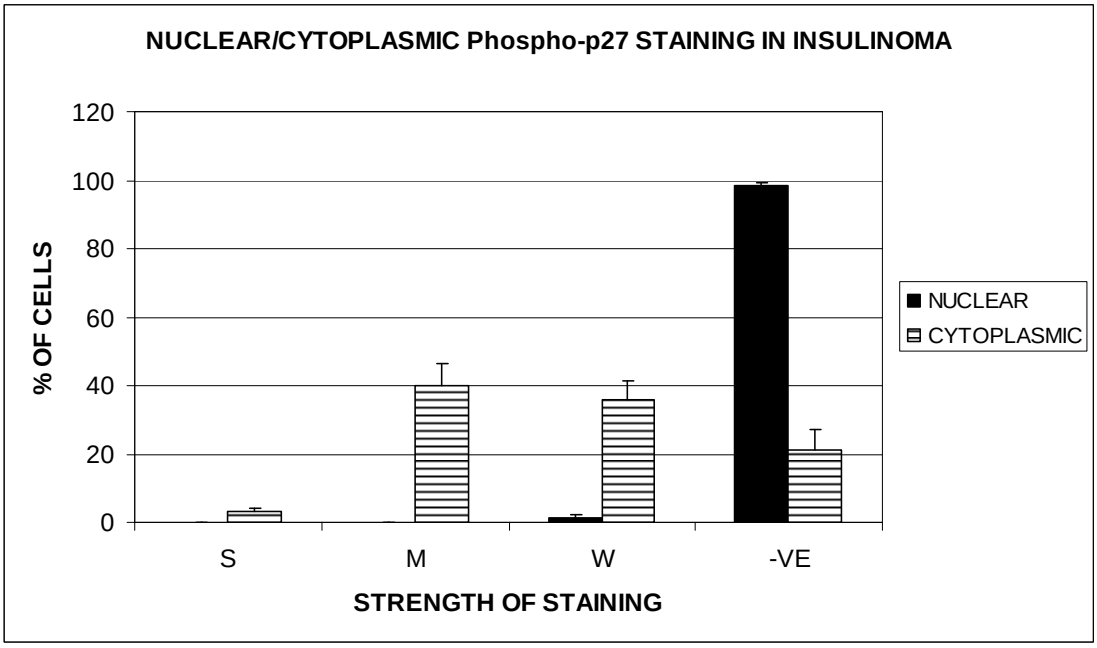

Figure 3.30 Graph showing the location and strength of phospho-p27 staining in insulinoma samples (S=strong, M=moderate, W=weak, -VE=negative)

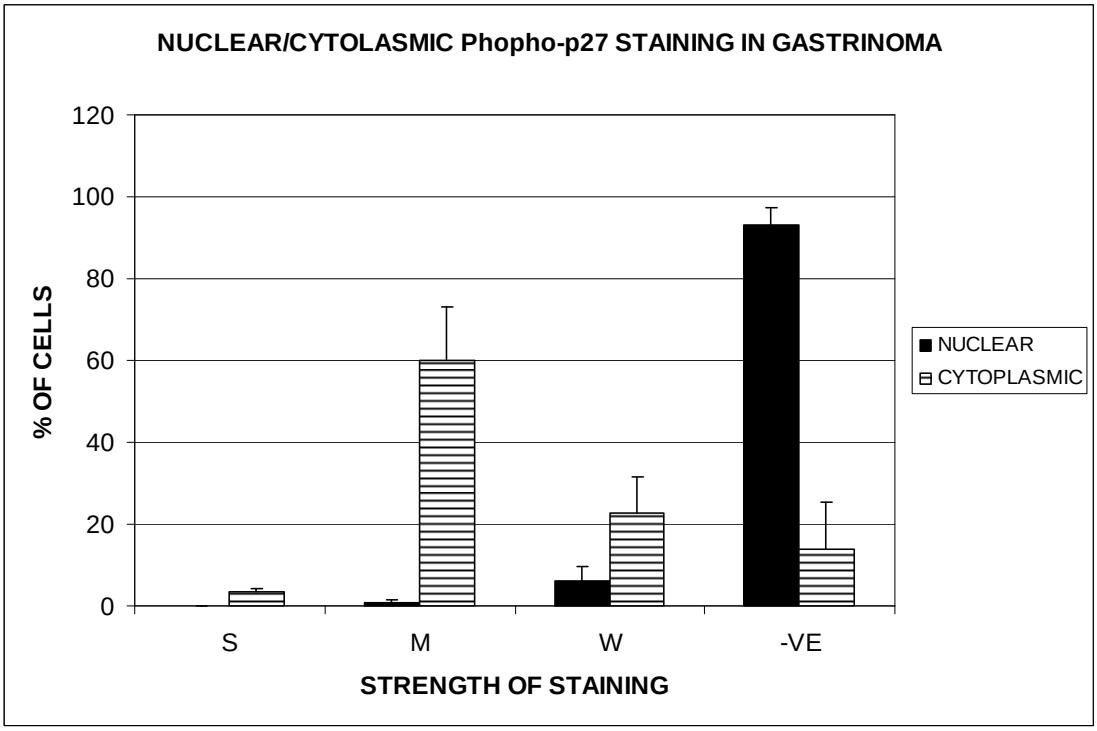

Figure 3.31 Graph showing the location and strength of phospho-p27 staining in gastrinoma samples (S=strong, M=moderate, W=weak, -VE=negative)

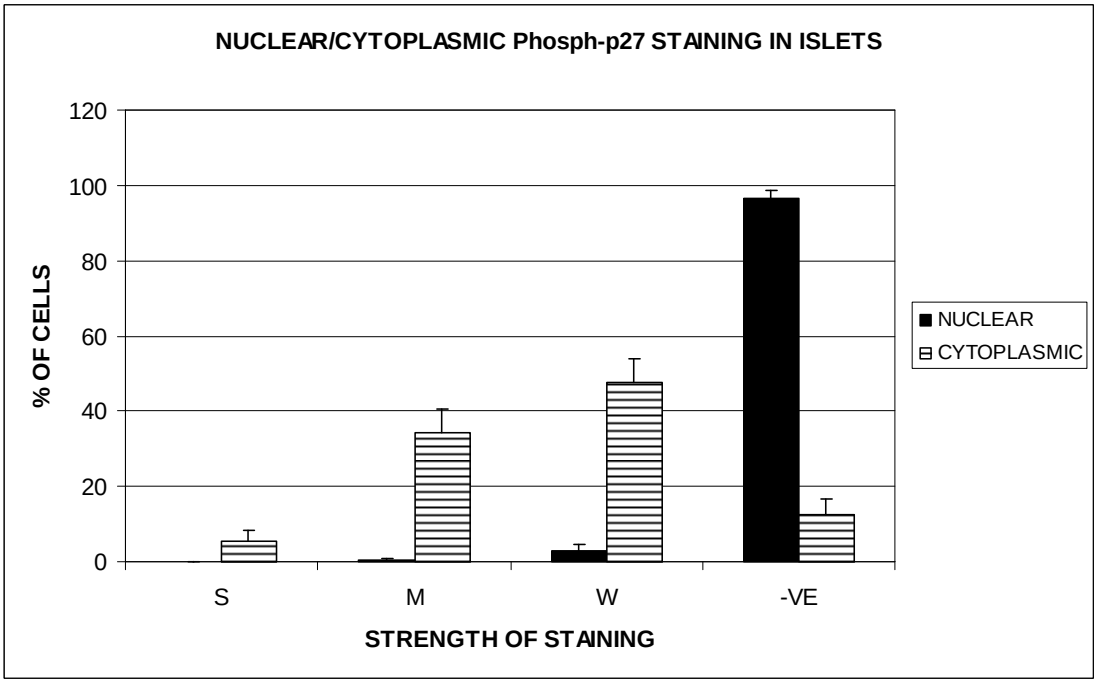

Figure 3.32 Graph showing the location and strength of phospho-p27 staining in islet samples (S=strong, M=moderate, W=weak, -VE=negative)

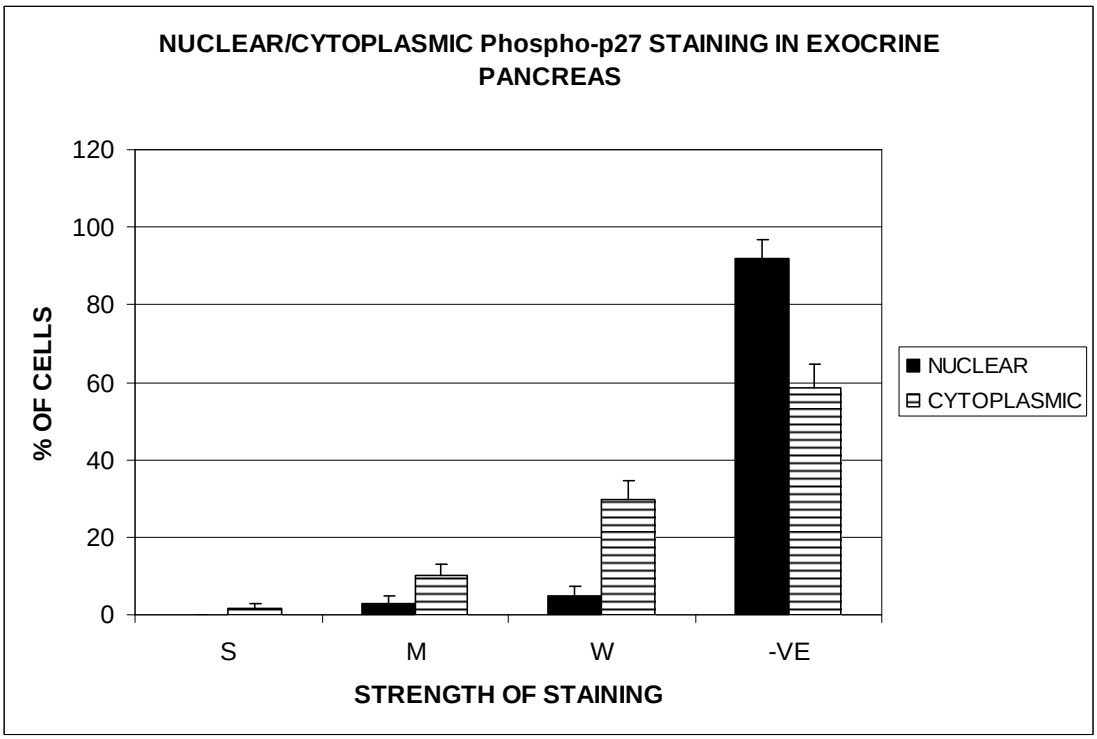

Figure 3.33 Graph showing the location and strength of phospho-p27 staining in exocrine samples (S=strong, M=moderate, W=weak, -VE=negative)

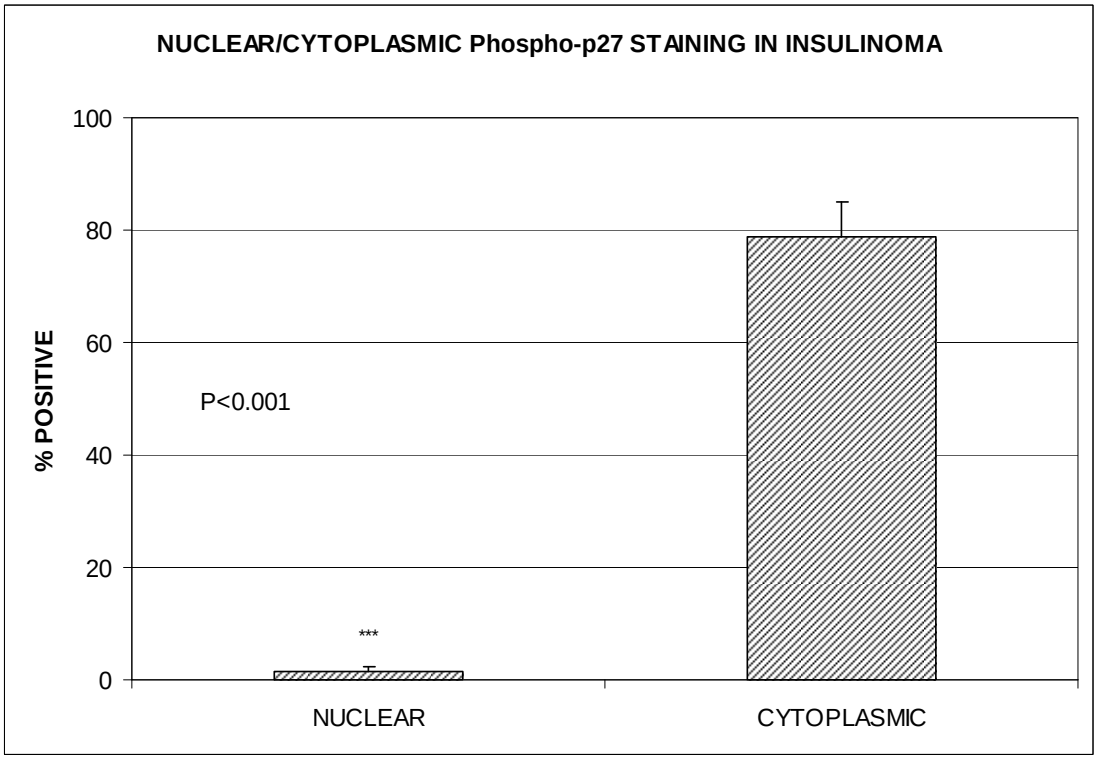

Figure 3.34 Graph showing the total positive (S+M+W) phospho-p27 nuclear and cytoplasmic staining in insulinoma samples.

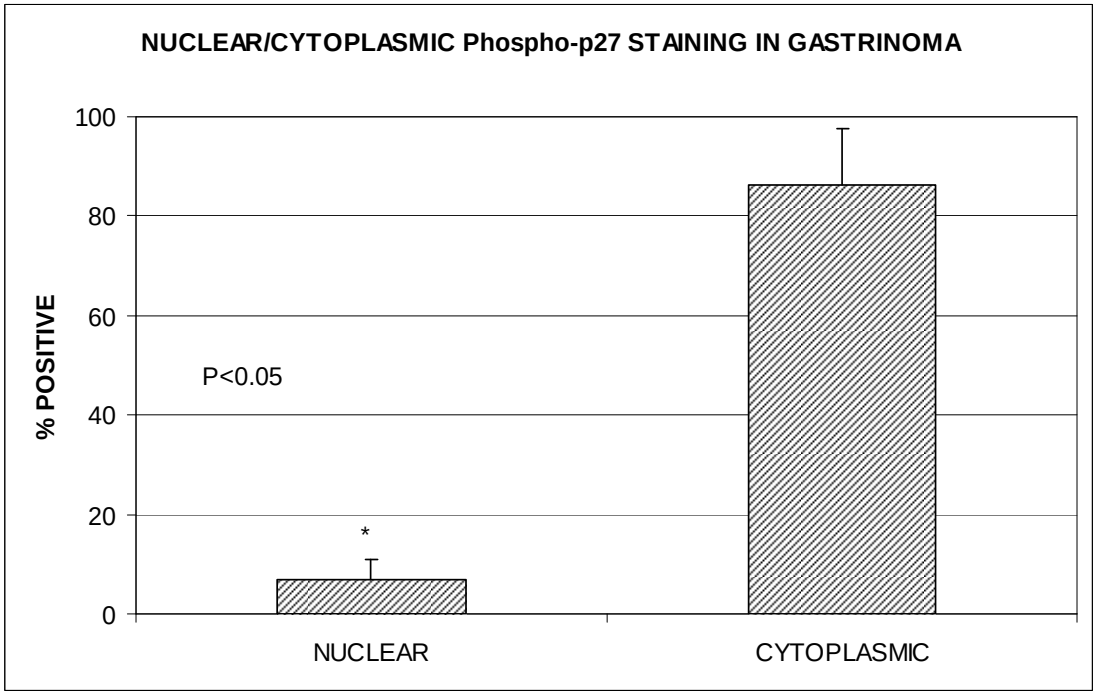

Figure 3.35 Graph showing the total positive (S+M+W) phospho-p27 nuclear and cytoplasmic staining in gastrinoma samples.

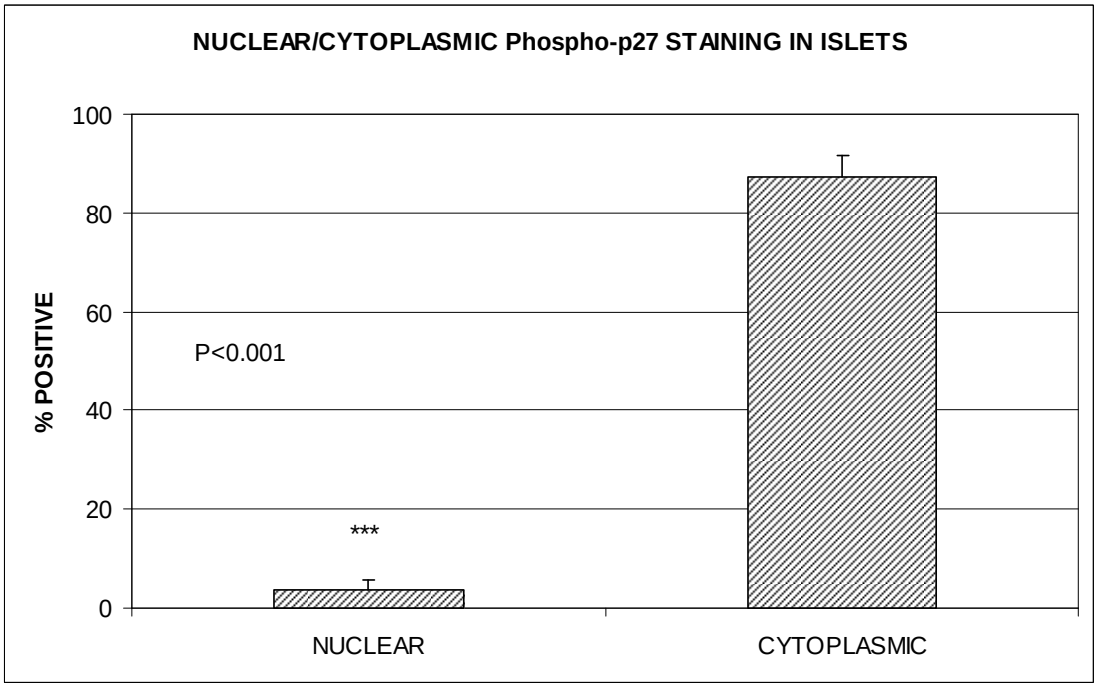

Figure 3.36 Graph showing the total positive (S+M+W) phospho-p27 nuclear and cytoplasmic staining in islet samples.

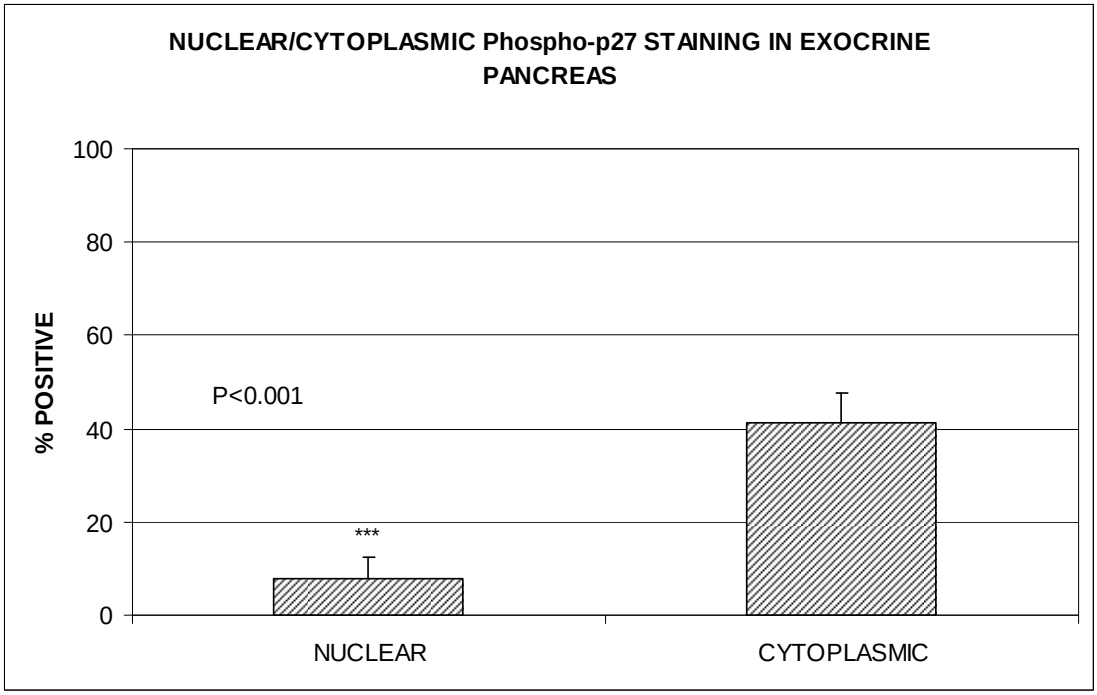

Figure 3.37 Graph showing the total positive (S+M+W) phospho-p27 nuclear and cytoplasmic staining in exocrine samples.

3.2.10 Comparison of phospho-p27 Nuclear Staining

In all tissues there was little phospho-p27 nuclear staining seen, as indicated by figure 3.38. Unsurprisingly, there is no significant difference between any of the tissue types.

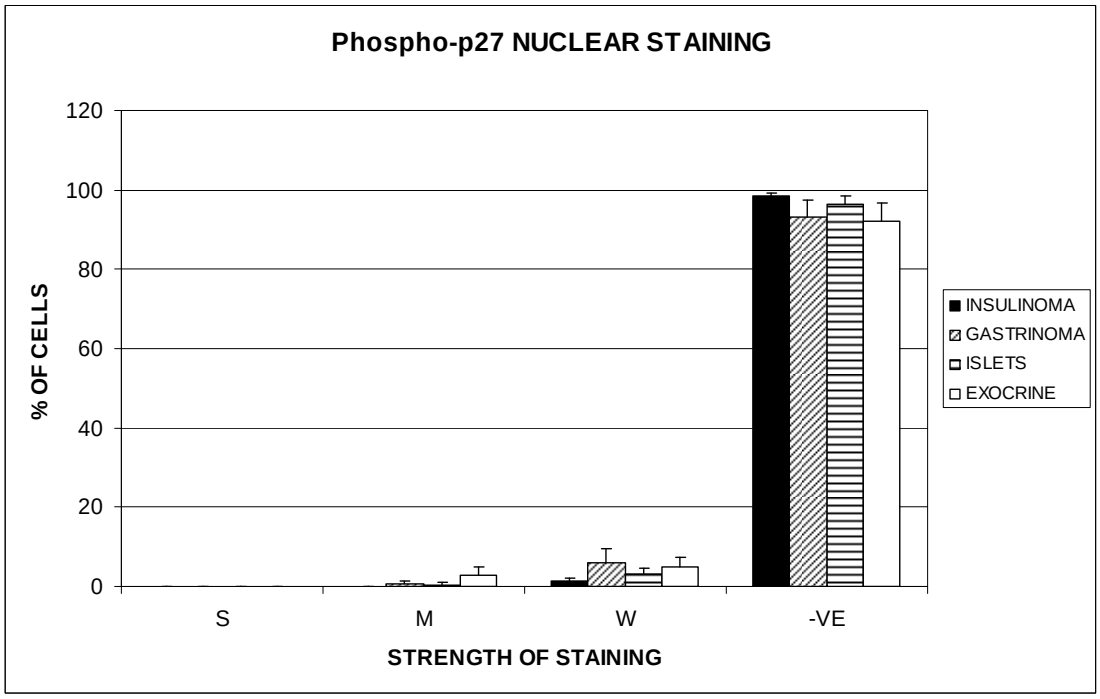

Figure 3.38 Graph comparing the relative strength of phospho-p27 nuclear staining for all tissue types

3.2.11 Comparison of phospho-p27 Cytoplasmic Staining

The pattern of phospho-p27 cytoplasmic staining was predominantly moderate to weak with only a few staining strongly positive (figure 3.39).

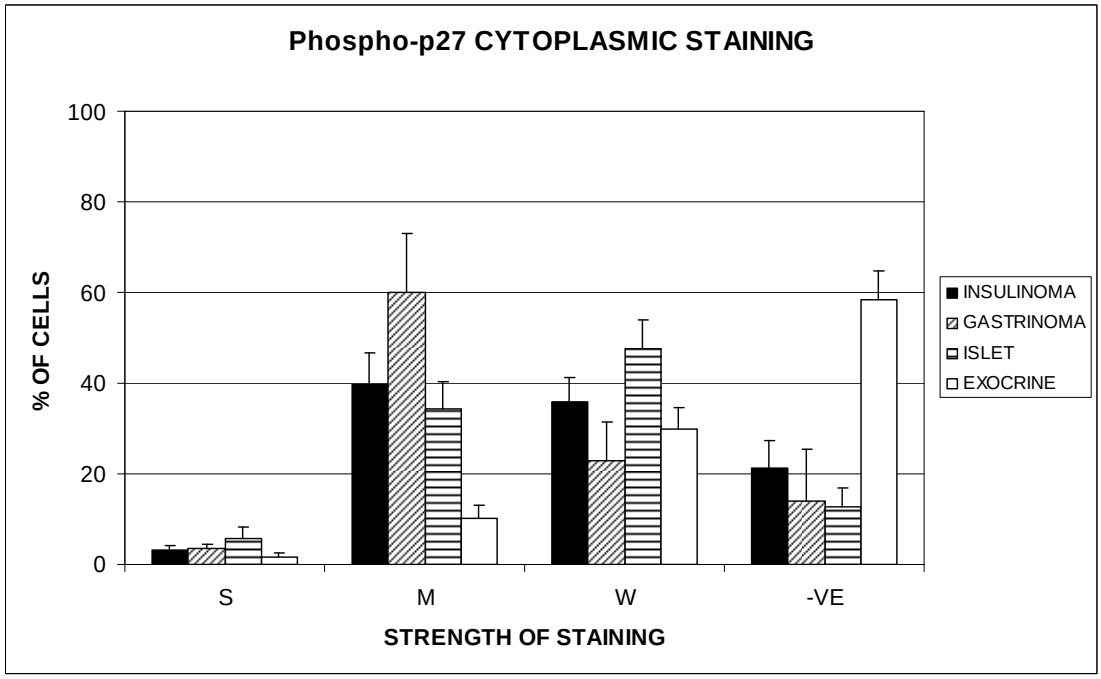

Figure 3.39 Graph comparing the relative strength of phospho-p27 cytoplasmic staining for all tissue types

On comparison of total counts (figure 3.40), cytoplasmic staining was seen in a high proportion of insulinoma (78.9 +/- 6.2%), gastrinoma (86.2 +/- 11.6%) and islets (87.4 +/- 4.2%). Exocrine pancreas samples, in comparison, had the lowest positive cytoplasmic count at 41.5 +/- 6.2%, predominantly due to the reduction in moderate staining compared to the other tissues. It is clear that there is no statistical difference in the cytoplasmic staining of insulinoma and islets or that of gastrinoma. All three endocrine tissues are, however, significantly different from the exocrine pancreas.

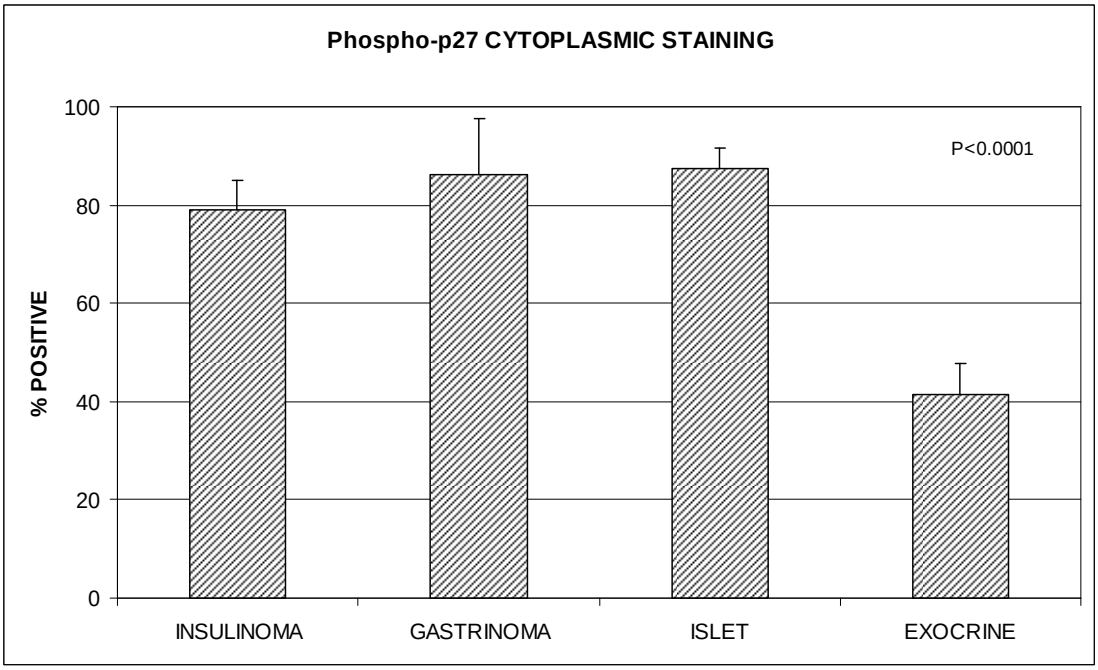

Figure 3.40 Graph comparing total positive phospho-p27 cytoplasmic staining for all tissue types

Kruskal-Wallis test P < 0.0001

Kruskal-Wallis: all pairwise comparisons (Conover-Inman)

INSULINOMA and EXOCRINE P < 0.0001

GASTRINOMA and EXOCRINE P = 0.0028

ISLET and EXOCRINE P < 0.0001

3.2.12 JAB1 (Jun activation domain-binding protein 1) immunohistochemistry

p27 degradation is related to its export from the nucleus and the protein that appears to be responsible is JAB1, which is a coactivator of the c-jun transcription factor. JAB1 binds to the C-terminal part of p27 in the nucleus and over-expression causes translocation of p27 into the cytoplasm. This decreases the amount of p27 in the cell by up-regulating its degradation.

Slides were treated with an anti-JAB1 IgG monoclonal antibody purified from mouse ascites and supplied from Zymed laboratories. It reacts with a peptide from the N-terminal region of JAB1. Optimisation was achieved with an antibody dilution of 1:250. Tonsil sections were used as positive controls, an example of which is shown below.

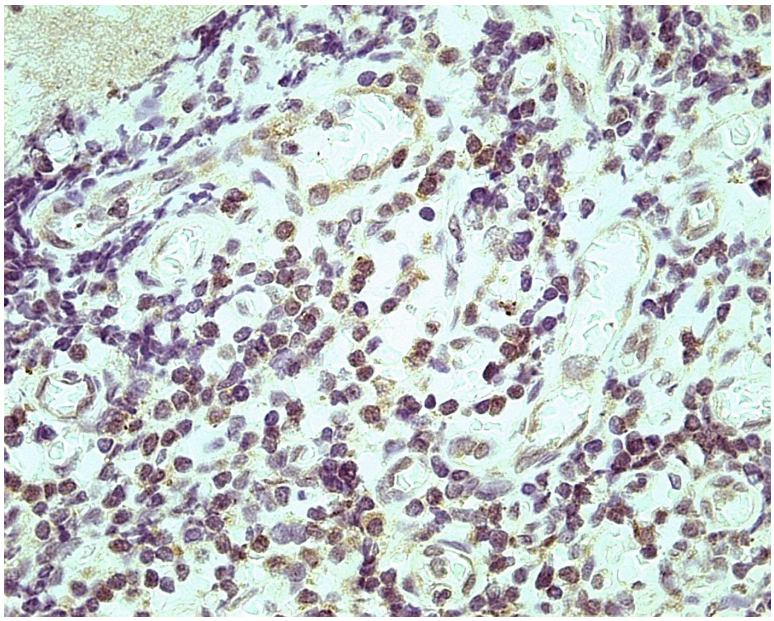

Figure 3.41 Slide showing a positive control slide (tonsil) for JAB1 with predominantly nuclear staining seen.

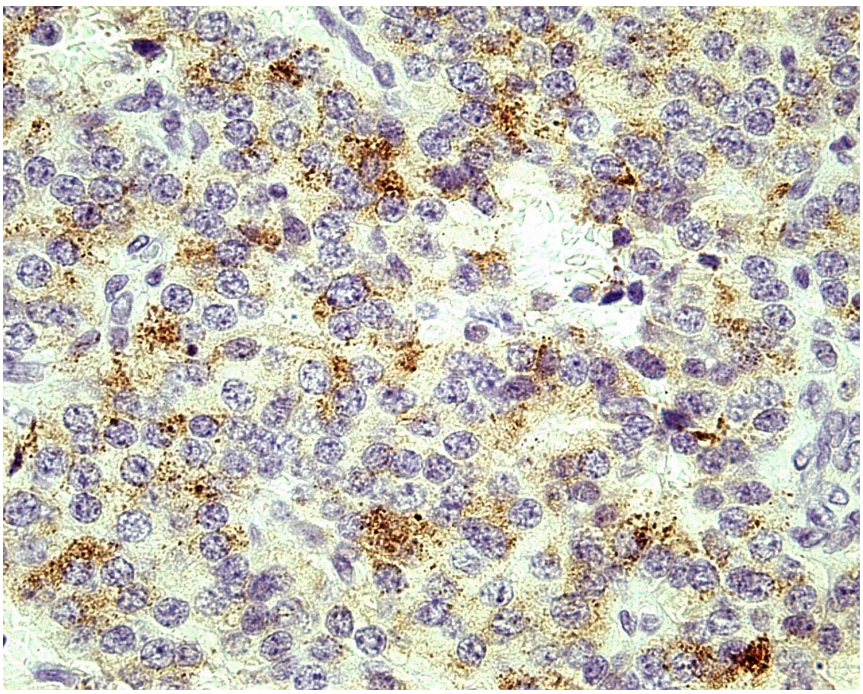

Figure 3.42 Slide showing predominantly cytoplasmic JAB1 staining in tumour sample 8

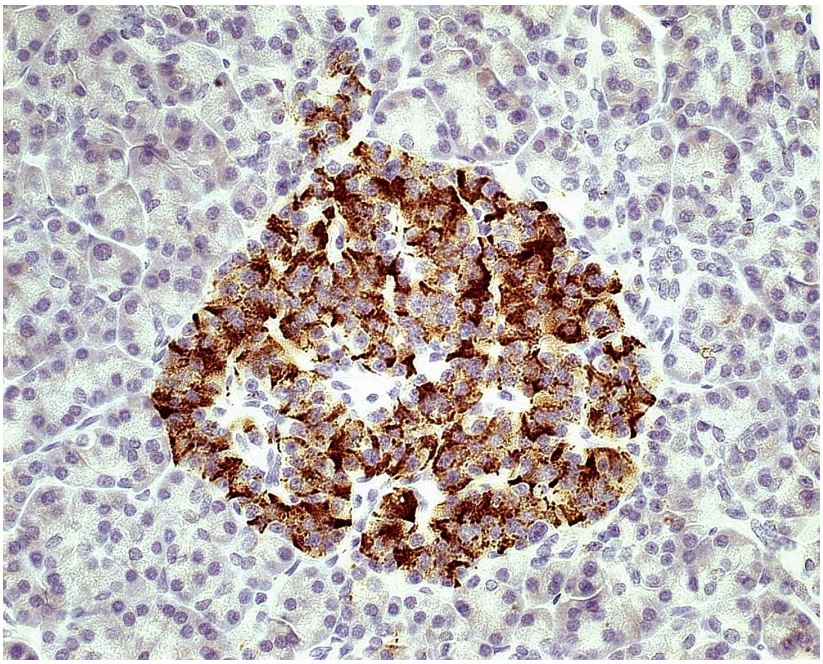

Figure 3.43 Slide showing typical strong cytoplasmic staining for JAB1 in islet sample 8

3.2.13 JAB1 staining in insulinoma, gastrinoma, islet and exocrine pancreas

In our series the pattern of JAB1 staining in all tissues is overwhelmingly cytoplasmic, with either no or negligible nuclear staining seen (figures 3.44 – 3.47).

Insulinoma, gastrinoma and islet series had essentially no nuclear staining identified, but significant cytoplasmic staining levels at 75.3 +/- 7.6% ($p<0.0001$), 41.4 +/- 28.3% ($p<0.05$) and 98.4 +/- 0.8% ($p<0.0001$) respectively (figures 3.48 – 3.50). In the exocrine series (figure 3.51), there was 2.1 +/- 0.9% nuclear staining compared to 27.3 +/- 6.95% cytoplasmic staining ($p<0.001$).

The pattern of cytoplasmic staining is varied between the tissues with insulinoma showing a broadly equal distribution in strength of staining whereas islets show increasingly strong staining. In contrast, gastrinoma and exocrine pancreas samples show a pattern of decreasing strength of staining.

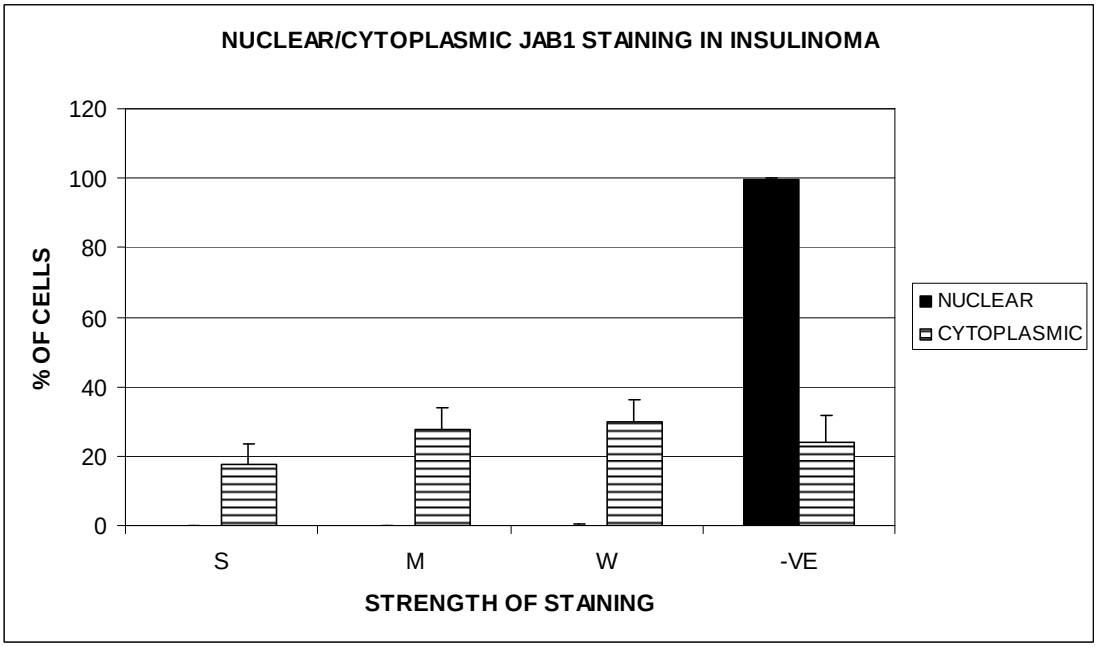

Figure 3.44 Graph showing the location and strength of JAB1 staining in insulinoma samples (S=strong, M=moderate, W=weak, -VE=negative)

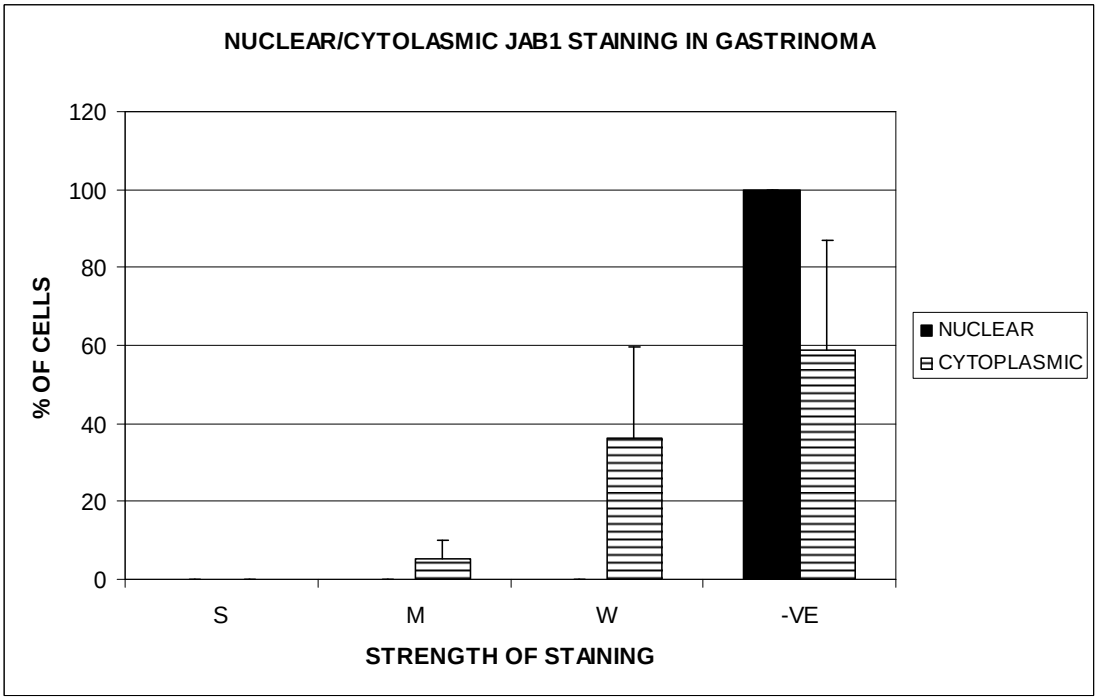

Figure 3.45 Graph showing the location and strength of JAB1 staining in gastrinoma samples (S=strong, M=moderate, W=weak, -VE=negative)

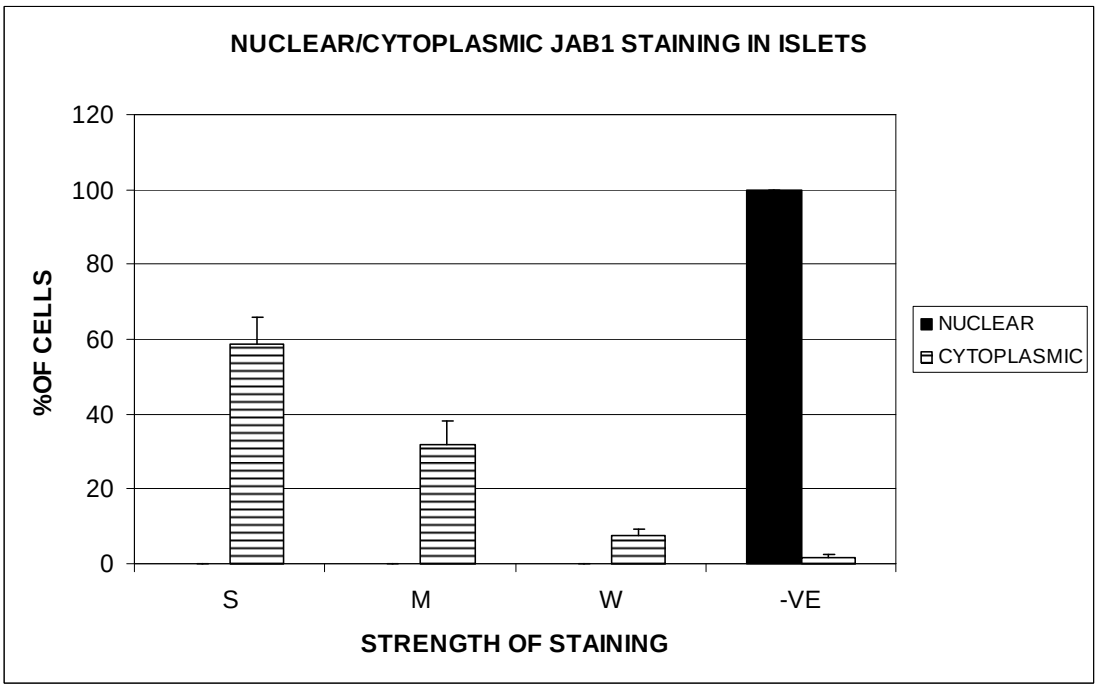

Figure 3.46 Graph showing the location and strength of JAB1 staining in islet samples (S=strong, M=moderate, W=weak, -VE=negative)

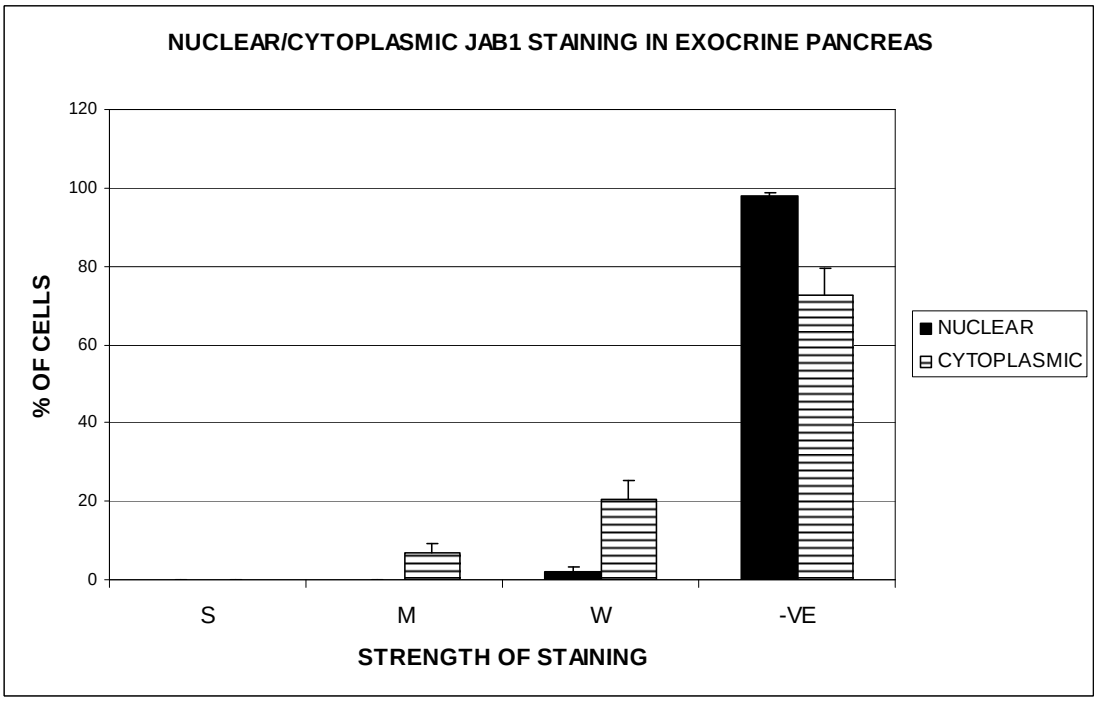

Figure 3.47 Graph showing the location and strength of JAB1 staining in exocrine samples (S=strong, M=moderate, W=weak, -VE=negative)

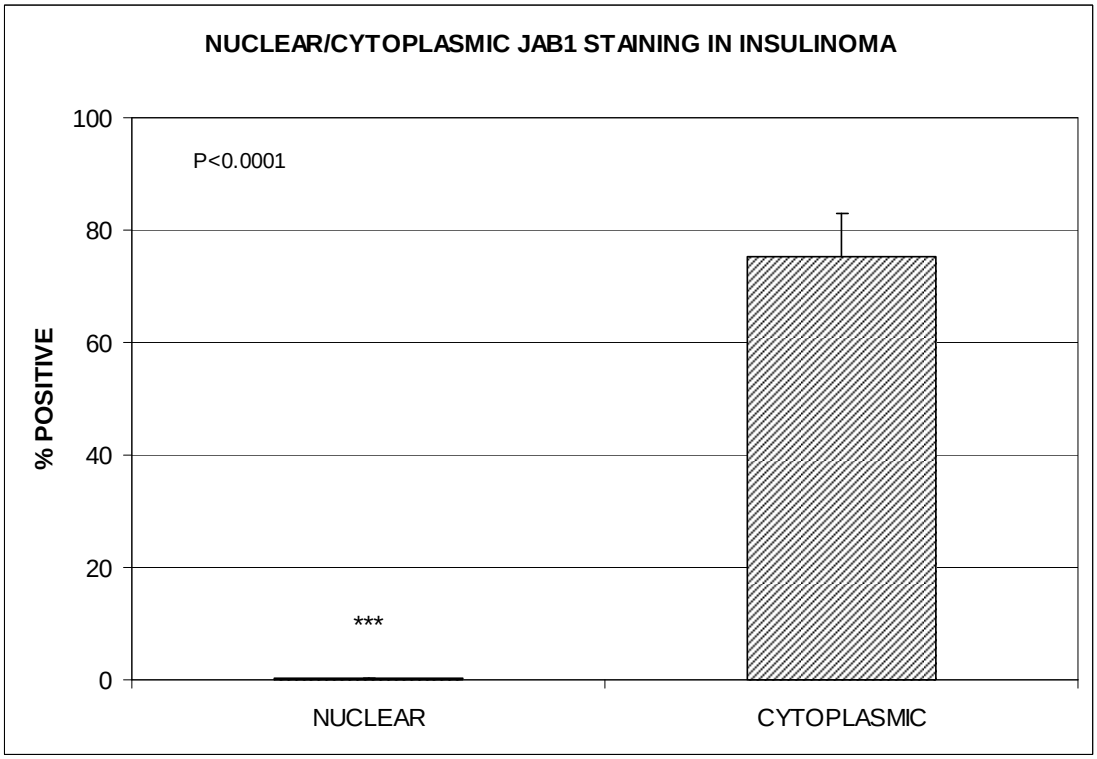

Figure 3.48 Graph showing the total positive (S+M+W) JAB 1 nuclear and cytoplasmic staining in insulinoma samples.

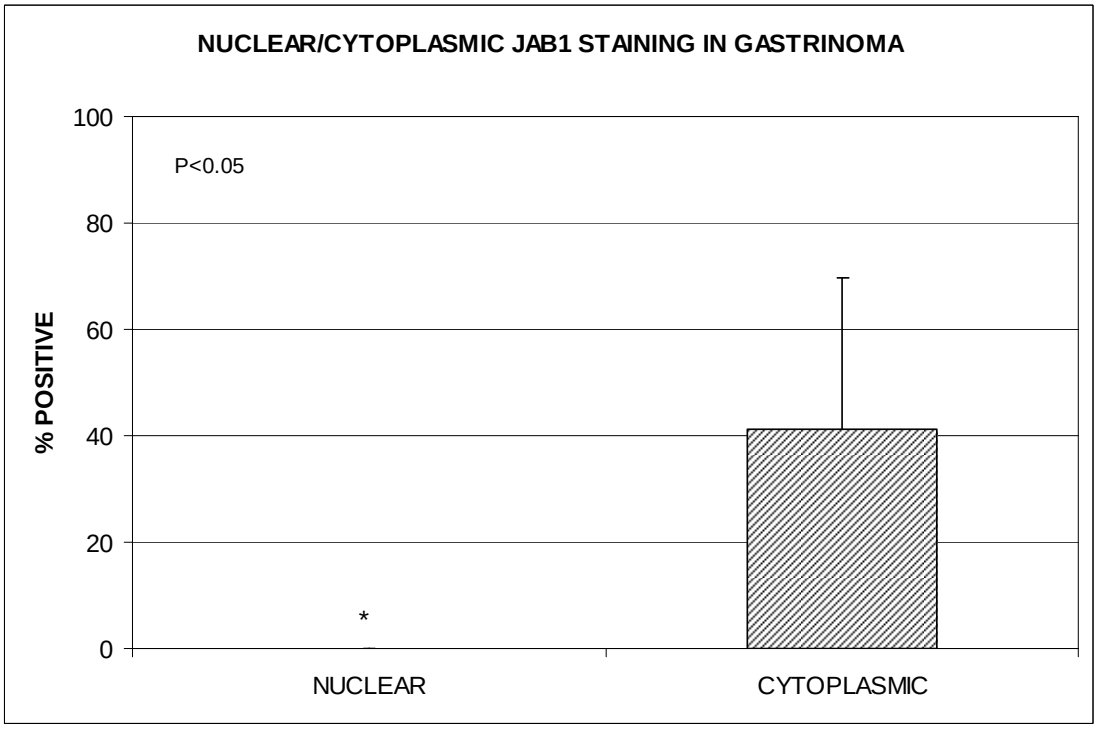

Figure 3.49 Graph showing the total positive (S+M+W) JAB1 nuclear and cytoplasmic staining in gastrinoma samples.

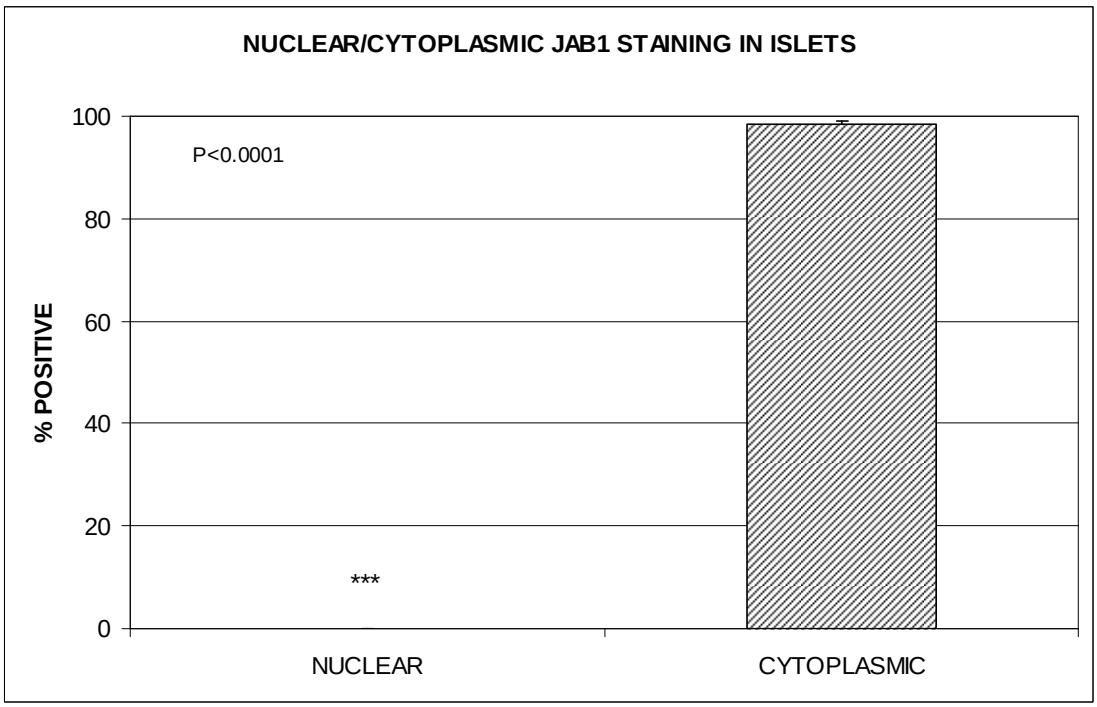

Figure 3.50 Graph showing the total positive (S+M+W) JAB1 nuclear and cytoplasmic staining in islet samples.

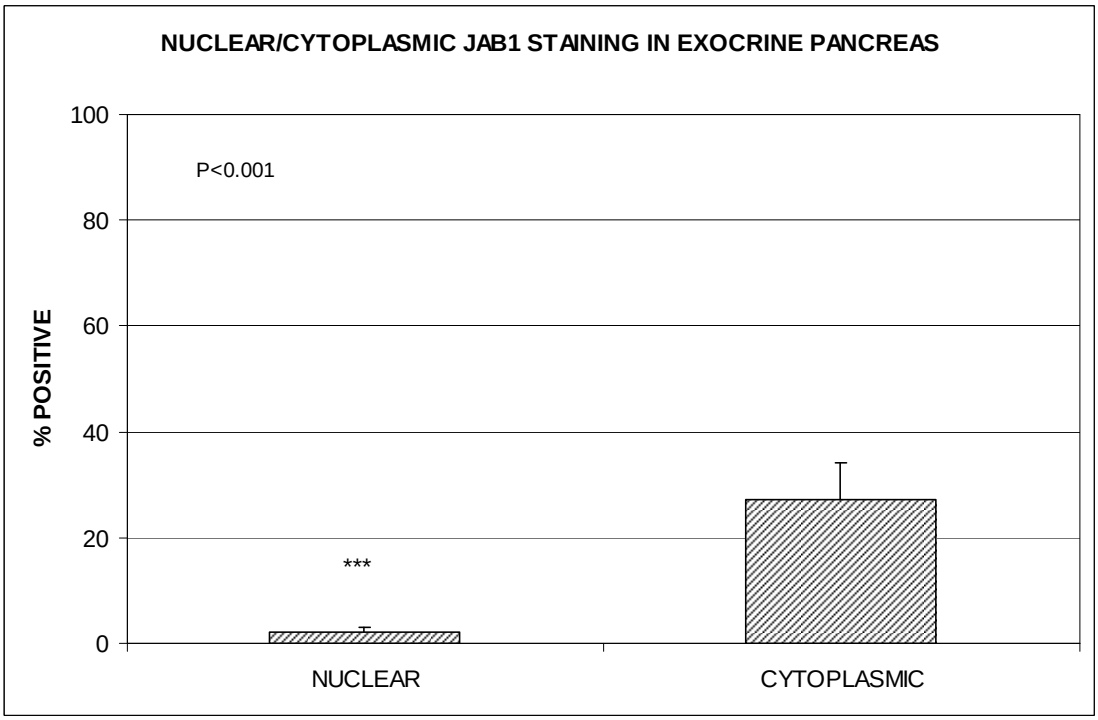

Figure 3.51 Graph showing the total positive (S+M+W) JAB1 nuclear and cytoplasmic staining in exocrine samples.

3.2.14 Cytoplasmic JAB1 Staining

Looking at all tissues together, reveals the varied patterns of JAB1 cytoplasmic staining (figure 3.52).

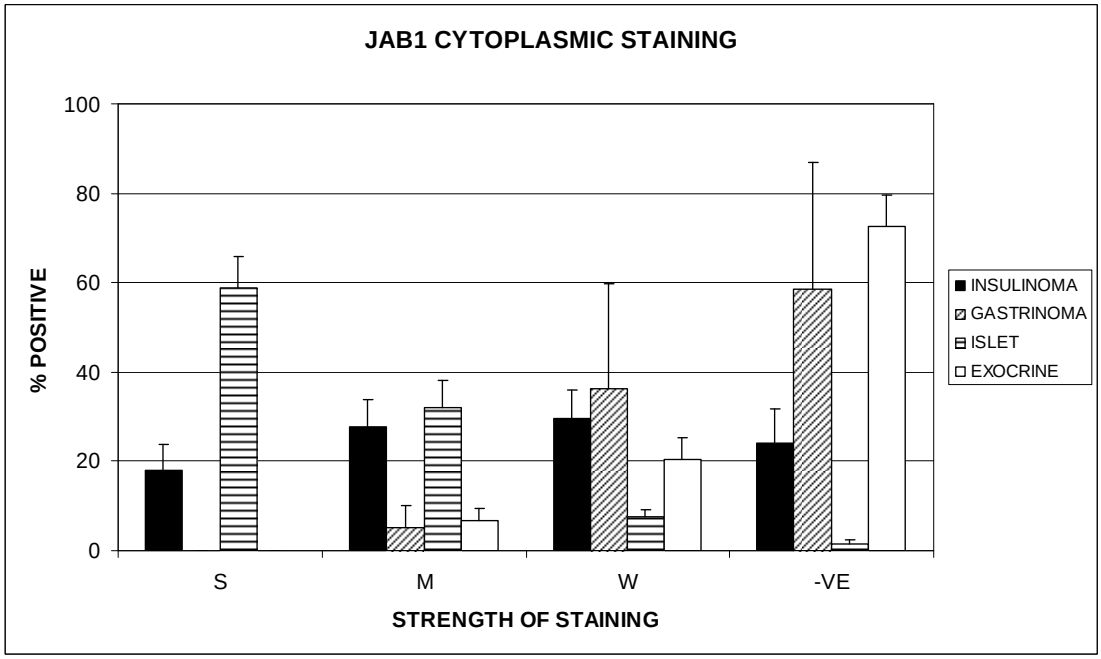

Figure 3.52 Graph comparing the relative strength of JAB1 cytoplasmic staining for all tissue types

Comparing the total positive counts for each tissue simplifies the picture considerably. It is seen that there is significantly less cytoplasmic expression of JAB1 in insulinoma compared to islets. Also, despite the large SEM in the gastrinoma group, there is still a significant difference between it and the islet group. Exocrine tissue is shown to have the least cytoplasmic expression of JAB1, and this is significantly lower than that of islets or insulinoma.

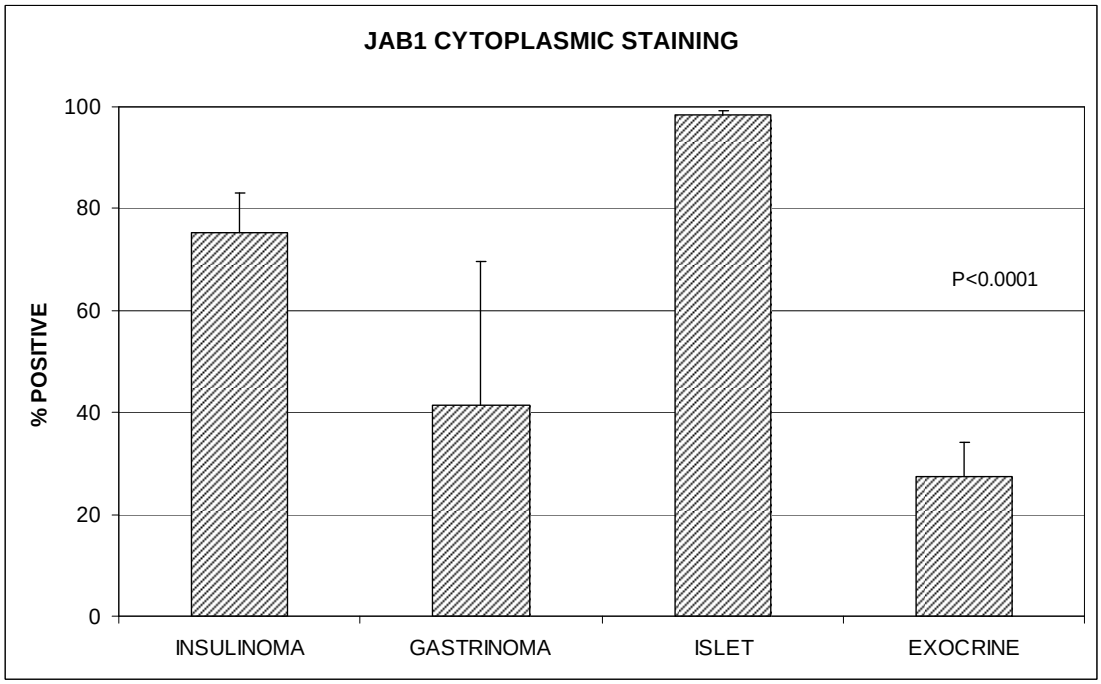

Figure 3.53 Graph comparing total positive JAB1 cytoplasmic staining for all tissue types

Kruskal-Wallis test	P < 0.0001
Kruskal-Wallis: all pairwise comparisons (Conover-Inman)	
INSULINOMA and ISLET	P < 0.0001
INSULINOMA and EXOCRINE	P < 0.0001
GASTRINOMA and ISLET	P = 0.0002
ISLET and EXOCRINE	P < 0.0001

As the pattern of staining is varied between groups, the differences are highlighted further when weak staining is excluded from total positive counts.

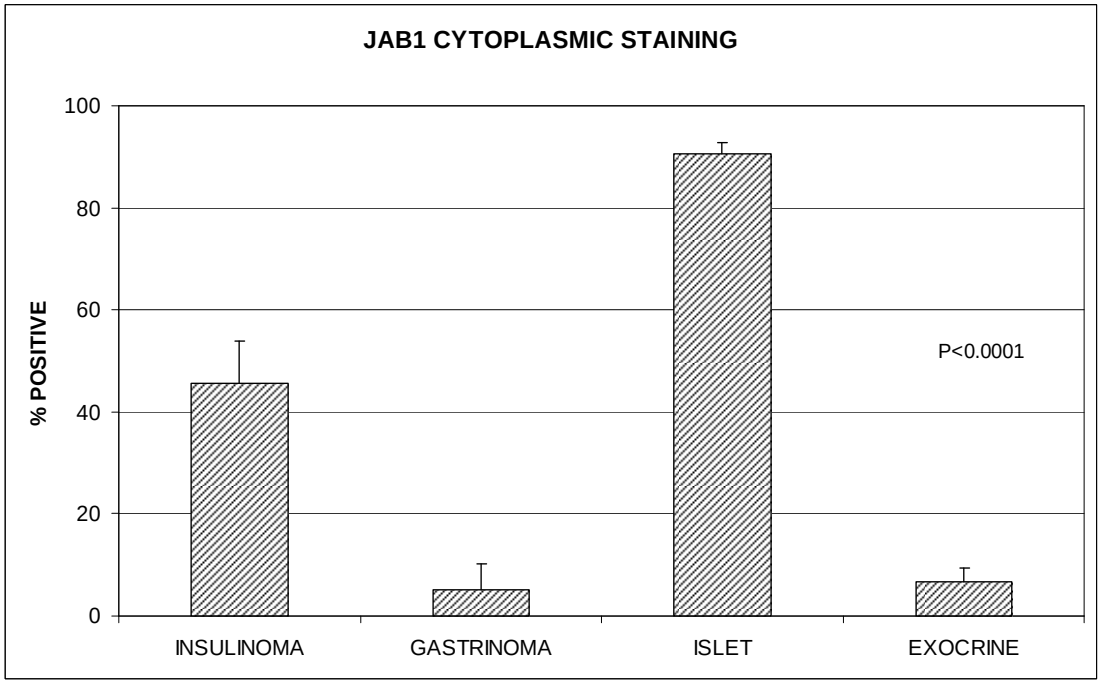

Figure 3.54 Graph comparing JAB1 positive staining (where positive = strong +moderate staining) for all tissue types.

Kruskal-Wallis test P < 0.0001

Kruskal-Wallis: all pairwise comparisons (Conover-Inman)

INSULINOMA and GASTRINOMA P = 0.0165

INSULINOMA and ISLET P < 0.0001

INSULINOMA and EXOCRINE P < 0.0001

GASTRINOMA and ISLET P < 0.0001

ISLET and EXOCRINE P < 0.0001

3.2.15 Phospho-Akt (p-Akt) Immunohistochemistry

Cells were treated with phospho-Akt (Ser473) antibody from cell Signaling Technology. It is a polyclonal antibody isolated from rabbits following immunisation with mouse phospho-Akt. It detects Akt1 only when phosphorylated at serine 473. It also detects Akt2 and Akt3 when phosphorylated at equivalent sites. Tonsil was used as a positive control and optimal staining was achieved with an antibody dilution of 1:100.

Immunohistochemistry with p-Akt proved the most problematic to optimise and interpret. Overnight incubation with primary antibody at $4^{o}C$ gave the best results but interpretation could be difficult as cytoplasmic staining may be confused with background staining. Extra care and optimisation was required to give the results obtained.

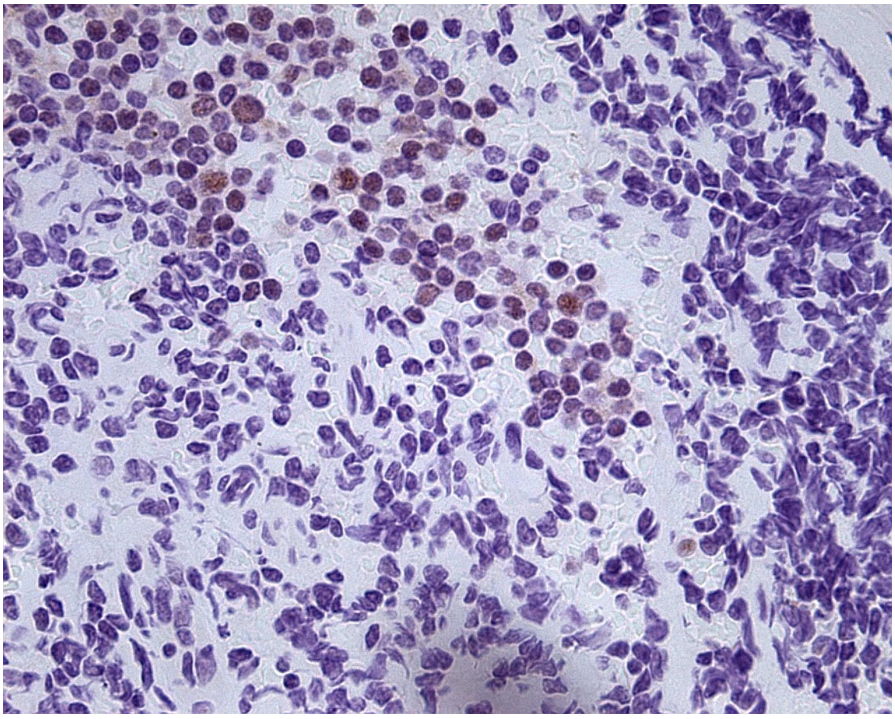

Figure 3.55 Slide showing p-AKT positive control (tonsil) with nuclear staining

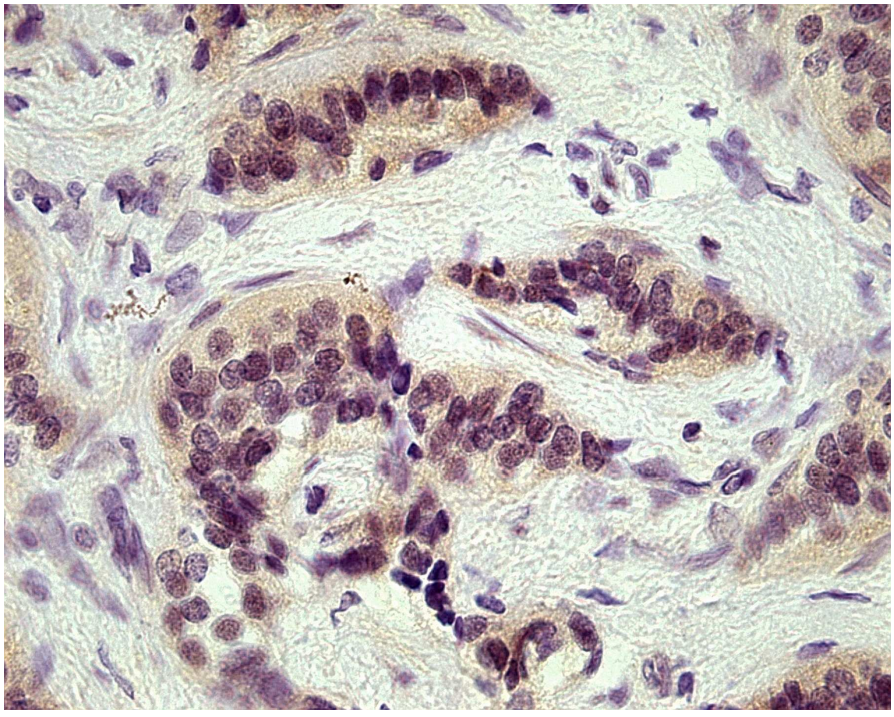

Figure 3.56 Slide showing diffuse cytoplasmic staining and minimal background staining for p-AKT in tumour sample 5

3.2.16 p-AKT staining in insulinoma, gastrinoma, islet and exocrine pancreas

Widespread nuclear and cytoplasmic staining for p-Akt was seen in all four tissue types with cytoplasmic staining being predominant (figures 3.57 – 3.60).

Insulinoma (figure 3.61) showed positive nuclear staining in 58.2 +/- 8.6% compared to a substantially higher cytoplasmic staining of 90.3 +/- 3.9% ($p<0.001$).

Gastrinoma (figure 3.62) nuclear staining was lower at 37.3 +/- 22.2% compared to cytoplasmic staining of 92.2 +/- 1.7% ($p<0.05$).

Islets (figure 3.63) had a higher level of p-Akt nuclear staining than any other tissue at 82.3 +/- 5.2% but cytoplasmic staining was higher still at 98.1 +/- 0.7% ($p<0.001$).

Exocrine pancreas (figure 3.64) shows both the lowest nuclear staining and cytoplasmic staining but the pattern is still the same with nuclear staining at 35.6 +/- 7.5% and cytoplasmic staining at 83.9 +/- 6% ($p<0.0001$)

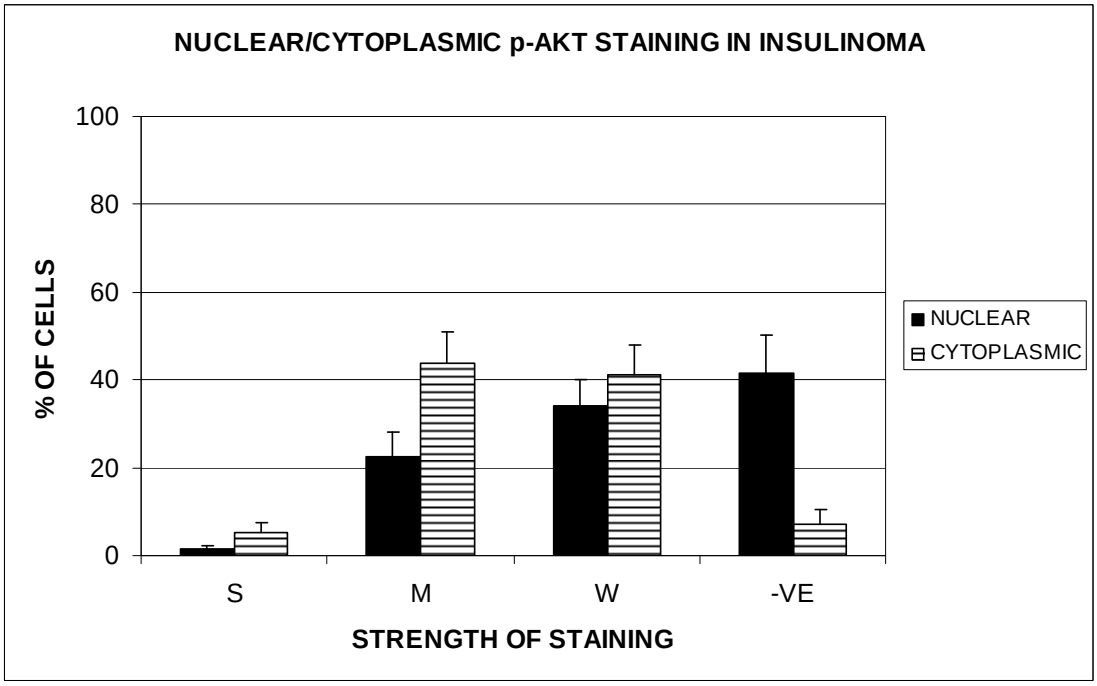

Figure 3.57 Graph showing the location and strength of p-Akt staining in insulinoma samples (S=strong, M=moderate, W=weak, -VE=negative)

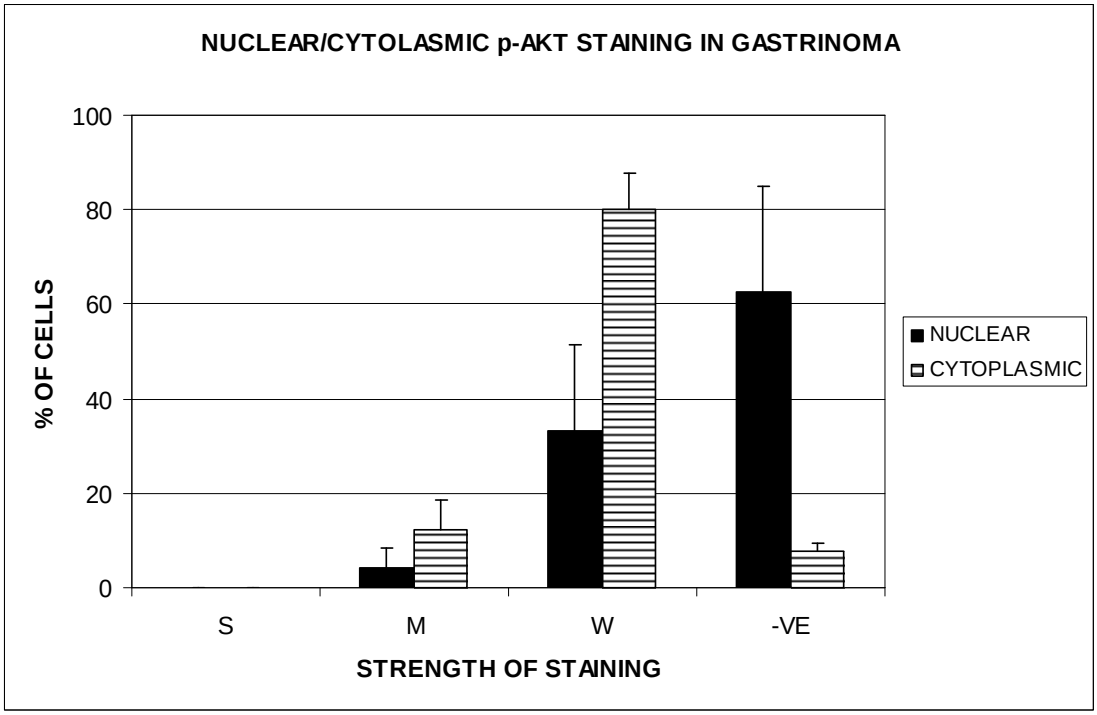

Figure 3.58 Graph showing the location and strength of p-Akt staining in gastrinoma samples (S=strong, M=moderate, W=weak, -VE=negative)

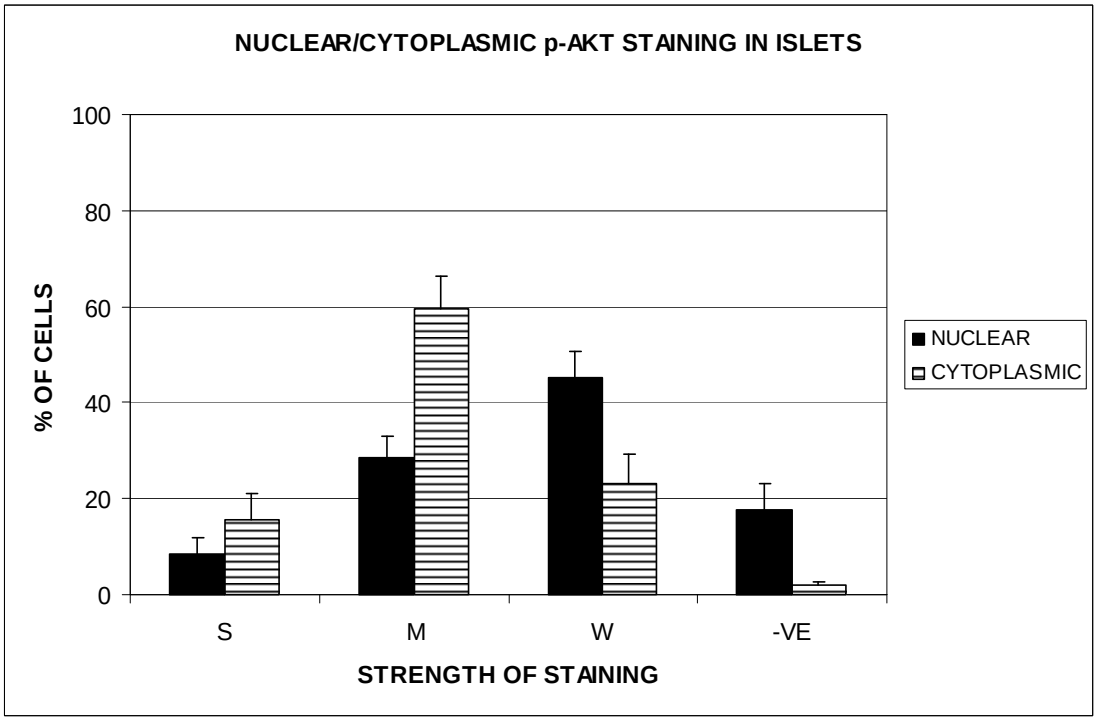

Figure 3.59 Graph showing the location and strength of p-Akt staining in islet samples (S=strong, M=moderate, W=weak, -VE=negative)

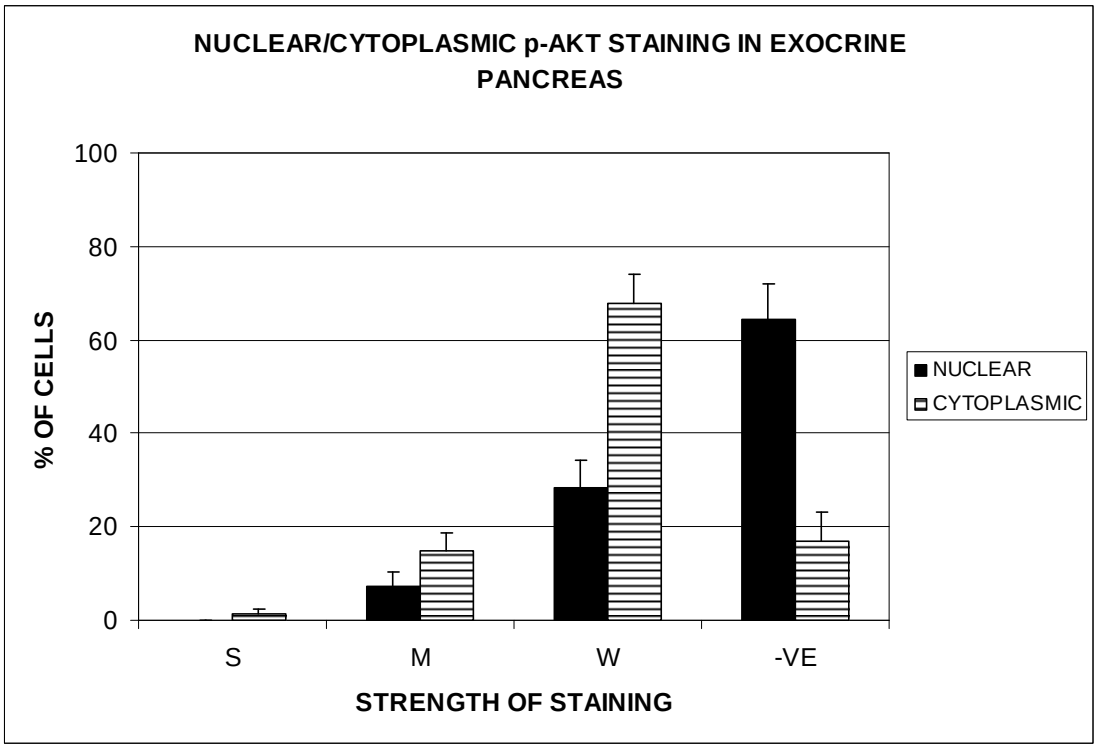

Figure 3.60 Graph showing the location and strength of p-Akt staining in exocrine samples (S=strong, M=moderate, W=weak, -VE=negative)

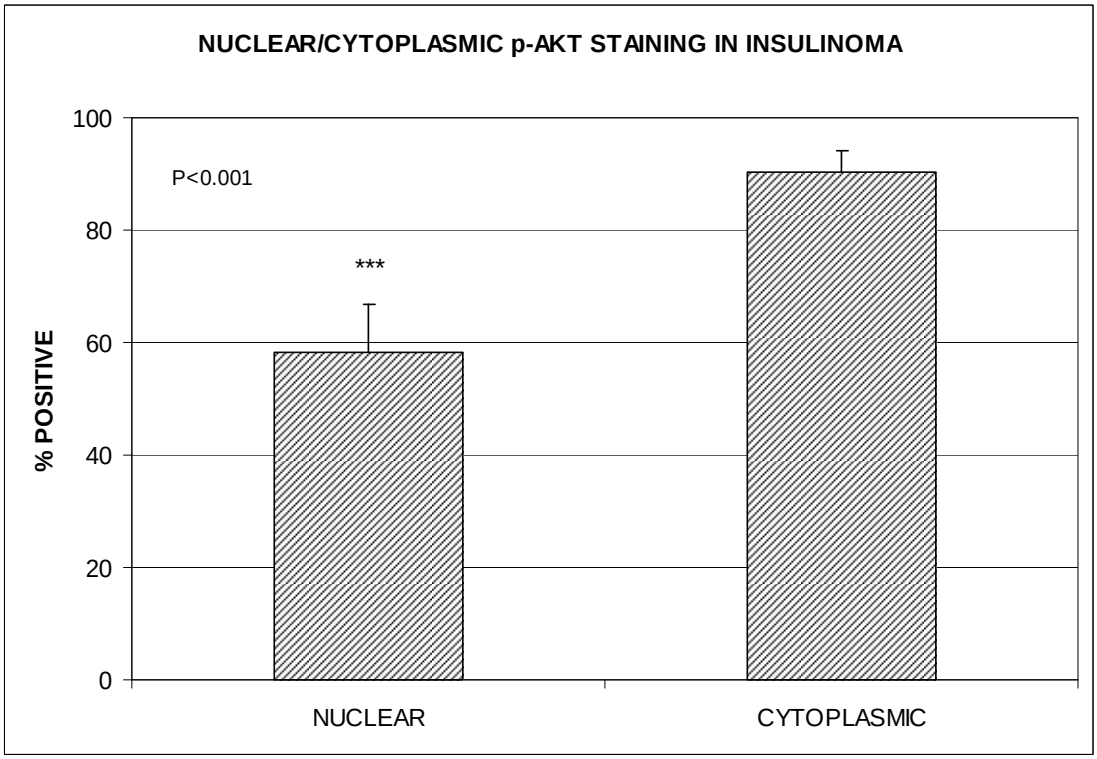

Figure 3.61 Graph showing the total positive (S+M+W) p-Akt nuclear and cytoplasmic staining in insulinoma samples.

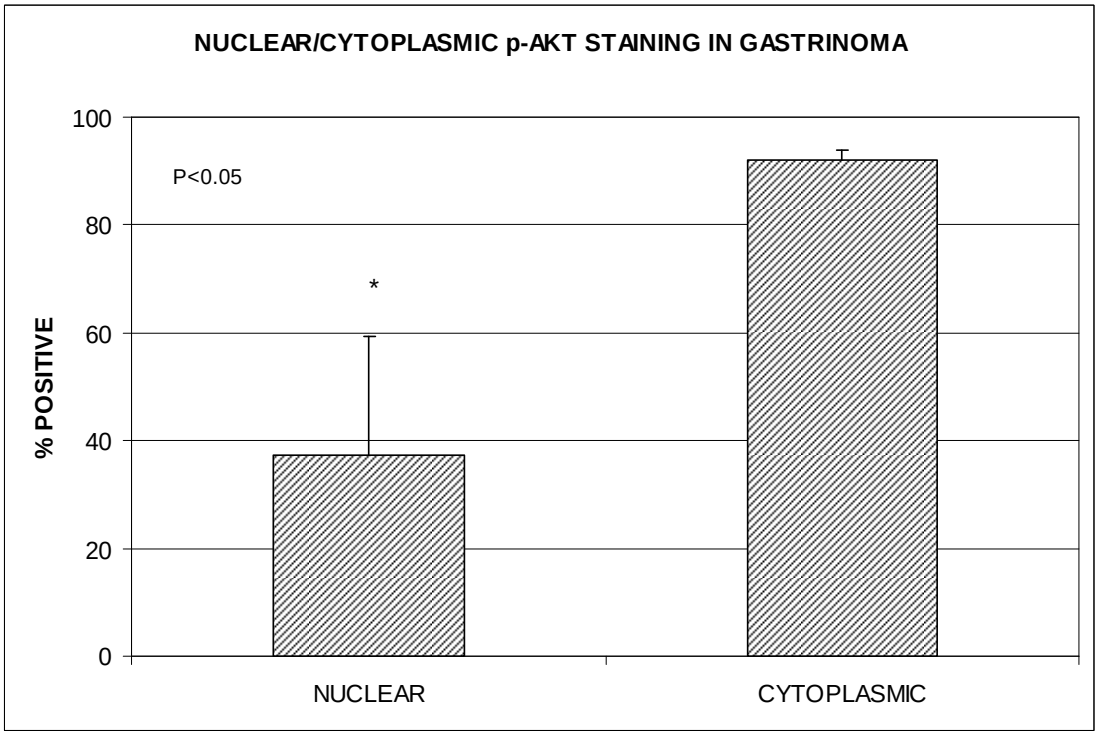

Figure 3.62 Graph showing the total positive (S+M+W) p-Akt nuclear and cytoplasmic staining in gastrinoma samples.

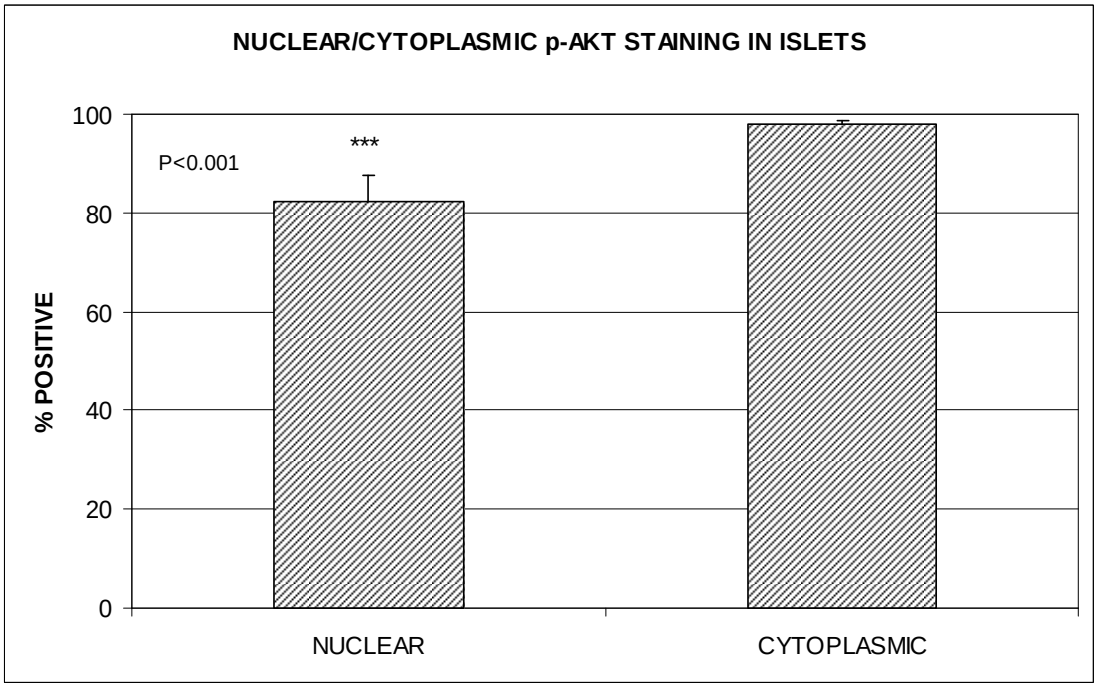

Figure 3.63 Graph showing the total positive (S+M+W) p-Akt nuclear and cytoplasmic staining in islet samples.

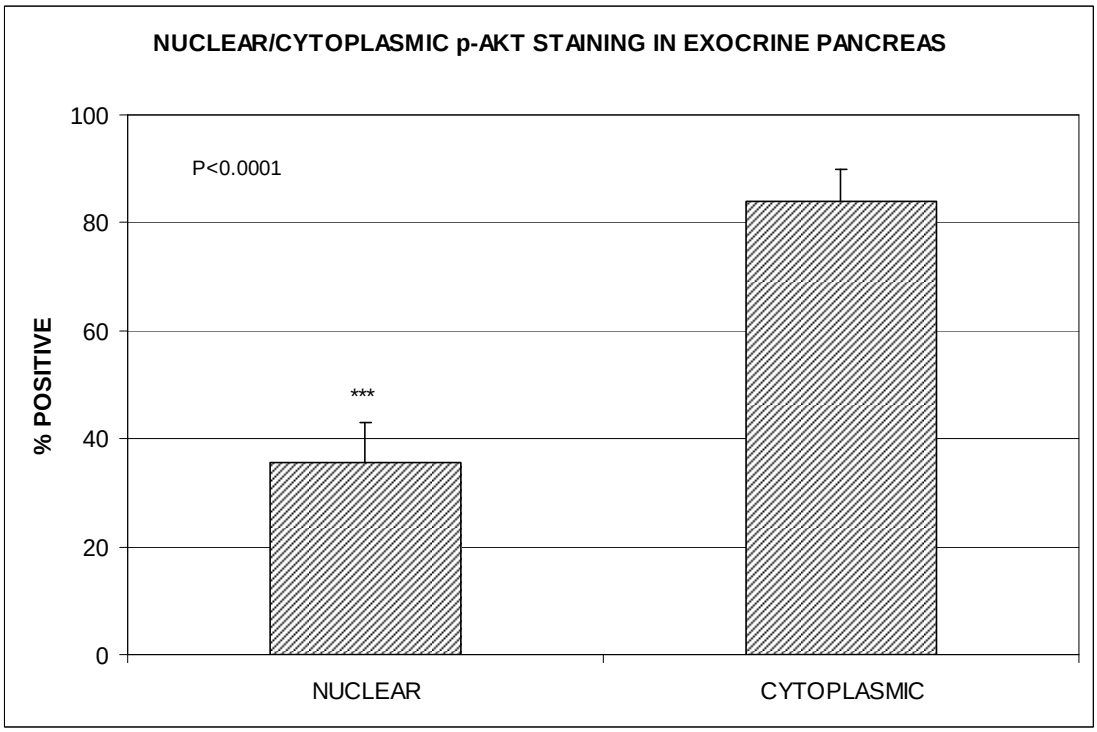

Figure 3.64 Graph showing the total positive (S+M+W) p-Akt nuclear and cytoplasmic staining in exocrine samples.

3.2.17 Comparing nuclear p-Akt staining

Comparing positive nuclear staining (figures 3.65 and 3.66), reveals that there is significantly lower expression of p-Akt within the nuclei of insulinomas compared to islets. A similar finding is seen with gastrinomas. Furthermore, exocrine pancreas shows significantly lower expression than either insulinomas or islets.

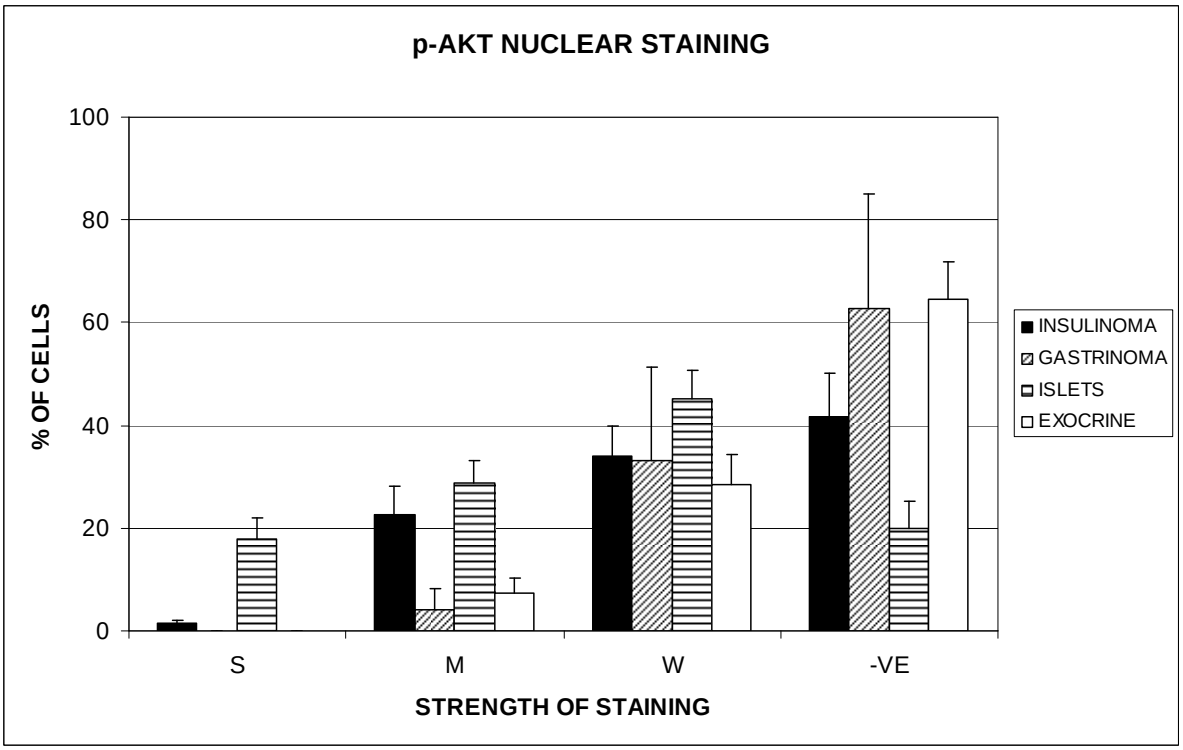

Figure 3.65 Graph comparing the relative strength of p-Akt nuclear staining for all tissue types

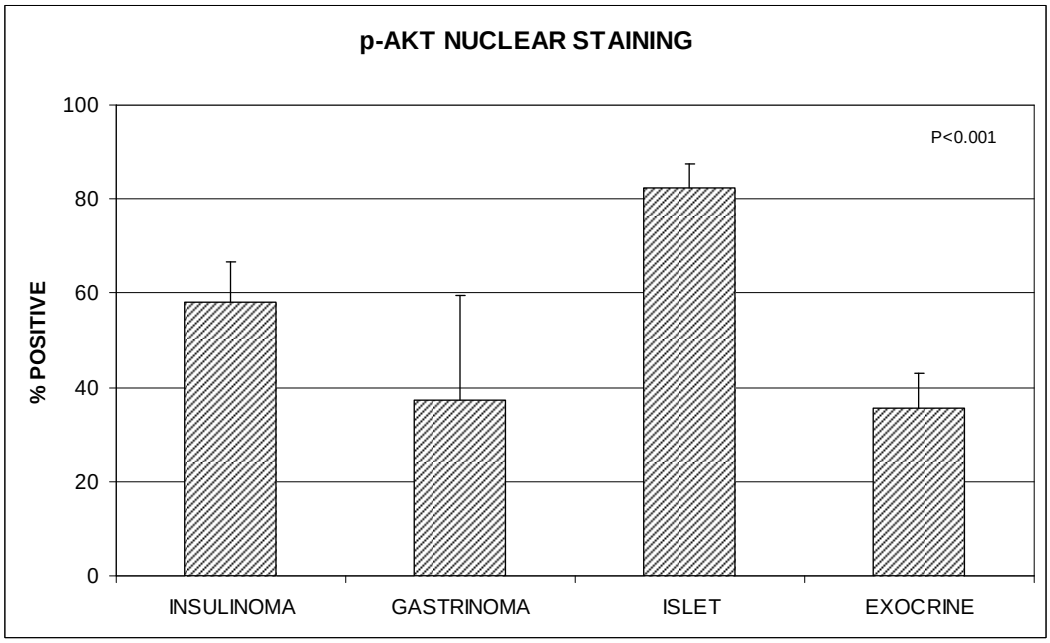

Figure 3.66 Graph comparing total positive p-Akt nuclear staining for all tissue types

Kruskal-Wallis test	P = 0.0003
Kruskal-Wallis: all pairwise comparisons (Conover-Inman)	
INSULINOMA and ISLET	P = 0.0216
INSULINOMA and EXOCRINE	P = 0.0106
GASTRINOMA and ISLET	P = 0.0335
ISLET and EXOCRINE	P < 0.0001

3.2.18 Comparing cytoplasmic p-Akt staining

There was widespread cytoplasmic staining in all tissues. Staining was predominantly weak to moderate with islets showing the strongest levels of staining.

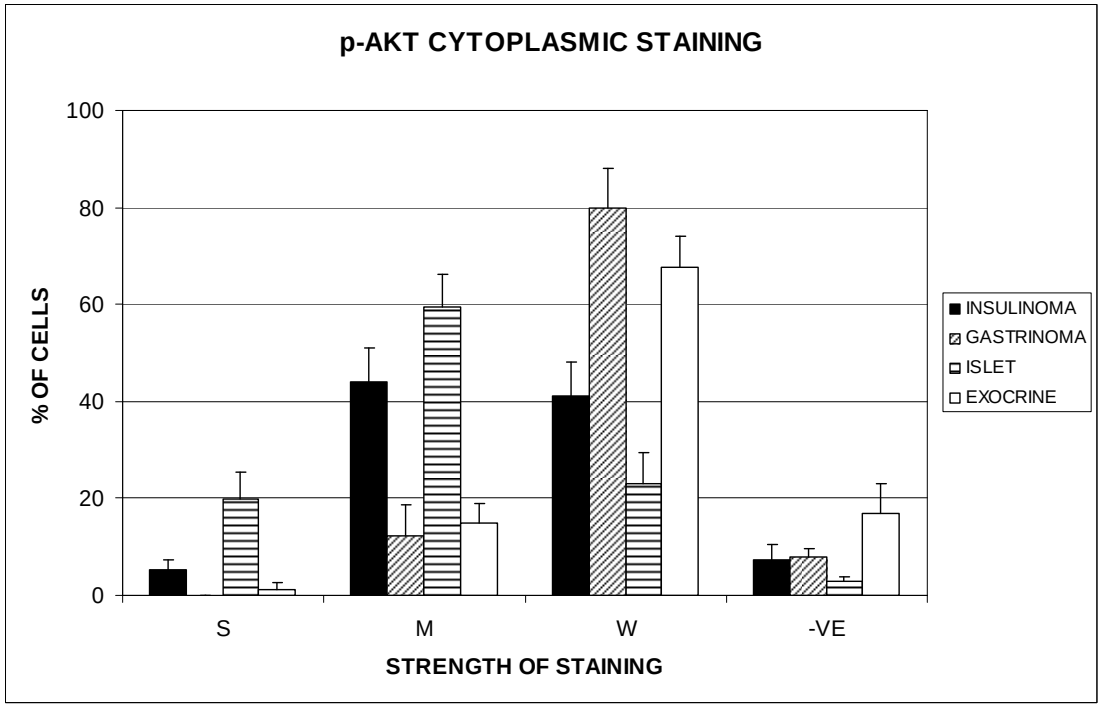

Figure 3.67 Graph comparing the relative strength of p-Akt cytoplasmic staining for all tissue types

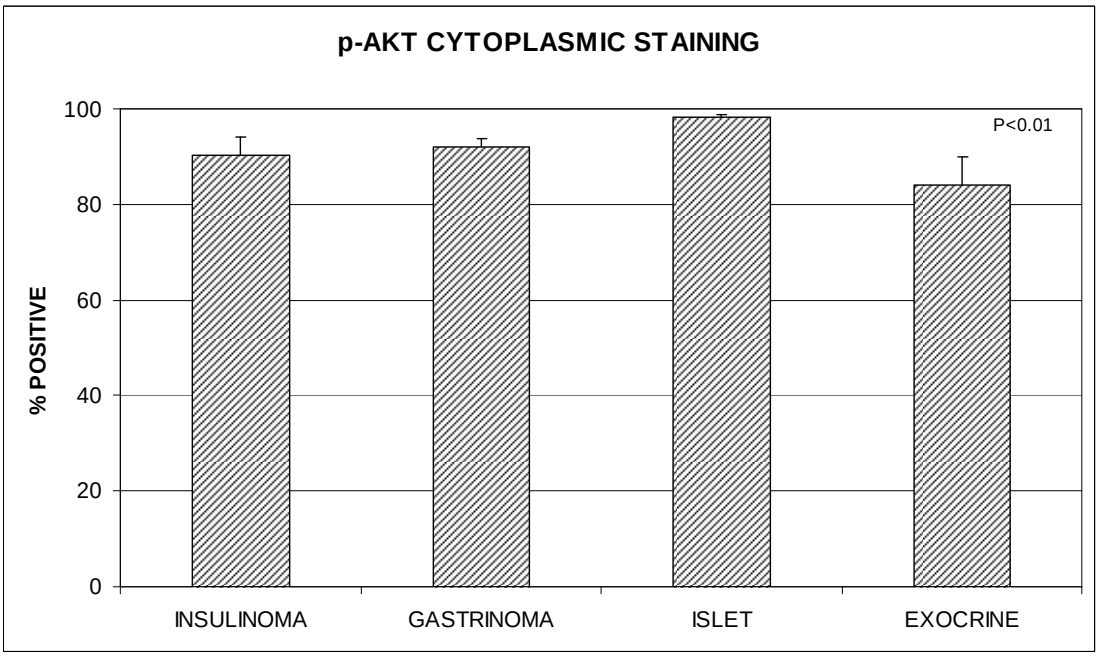

Figure 3.68 Graph comparing total positive p-Akt cytoplasmic staining for all tissue types

Kruskal-Wallis test	P = 0.0017
Kruskal-Wallis: all pairwise comparisons (Conover-Inman)	
INSULINOMA and ISLET	P = 0.0175
GASTRINOMA and ISLET	P = 0.0092
ISLET and EXOCRINE	P = 0.0002

All tissues have stained highly positive. We noted however, that a pattern becomes apparent when positive staining is considered as strong and moderate only.

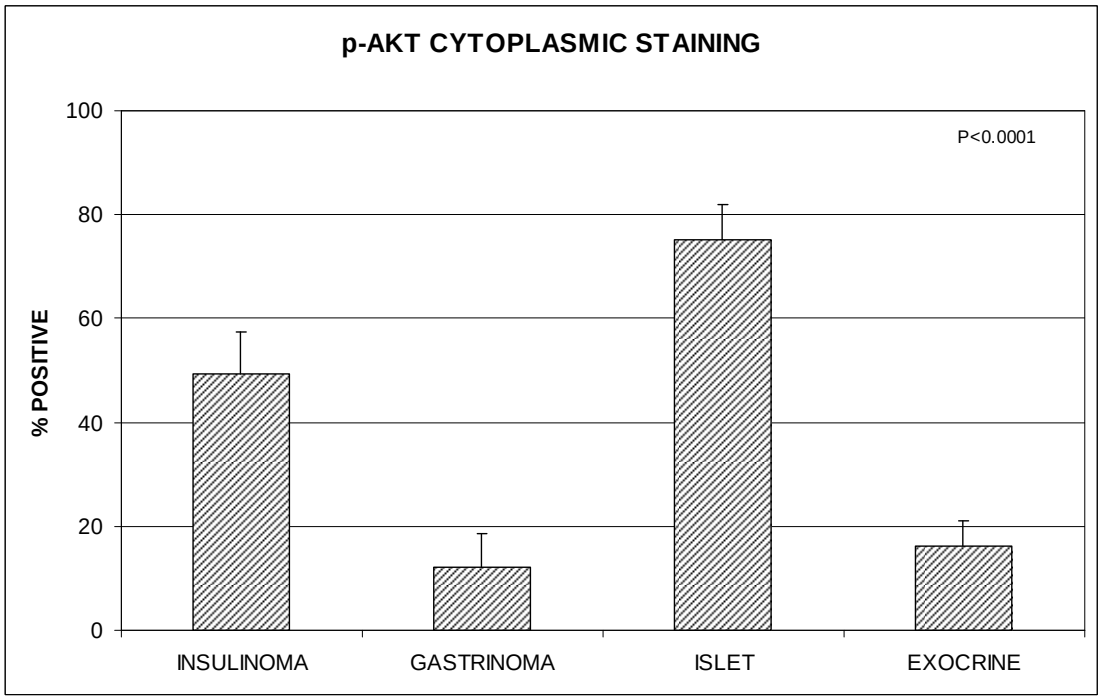

Figure 3.69 Graph comparing cytoplasmic p-Akt positive staining (where positive = strong +moderate staining) for all tissue types.

Kruskal-Wallis test	P < 0.0001
Kruskal-Wallis: all pairwise comparisons (Conover-Inman)	
INSULINOMA and ISLET	P = 0.0263
INSULINOMA and EXOCRINE	P = 0.0005
GASTRINOMA and ISLET	P = 0.0026
ISLET and EXOCRINE	P< 0.0001

3.2.19 PTEN immunohistochemistry

PTEN was stained for using a mouse monoclonal IgG antibody which reacts with a protein corresponding to a 200 amino-acid C-terminal region of the PTEN molecule. Tonsil sections were used as a control and an antibody dilution of 1:100 was found to give best optimisation.

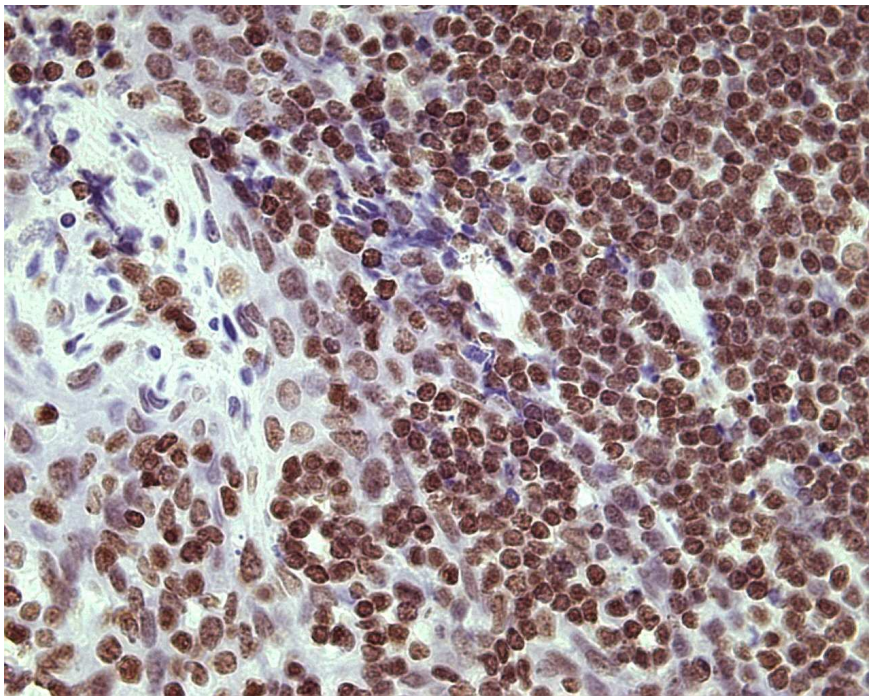

Figure 3.70 Slide showing strong nuclear staining for PTEN in the tonsil positive control

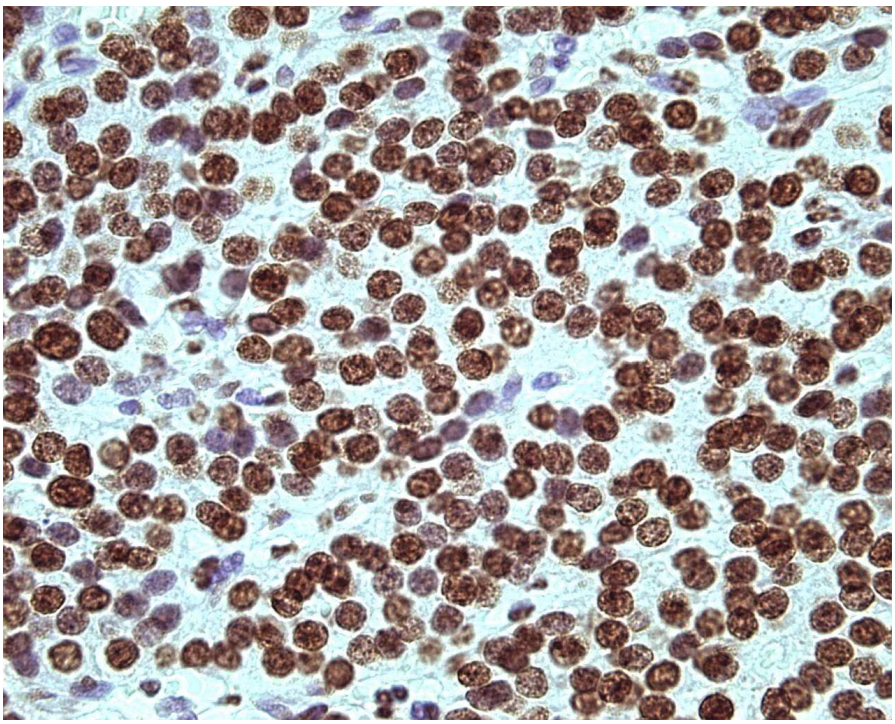

Figure 3.71 Slide showing good nuclear PTEN staining in tumour sample 8

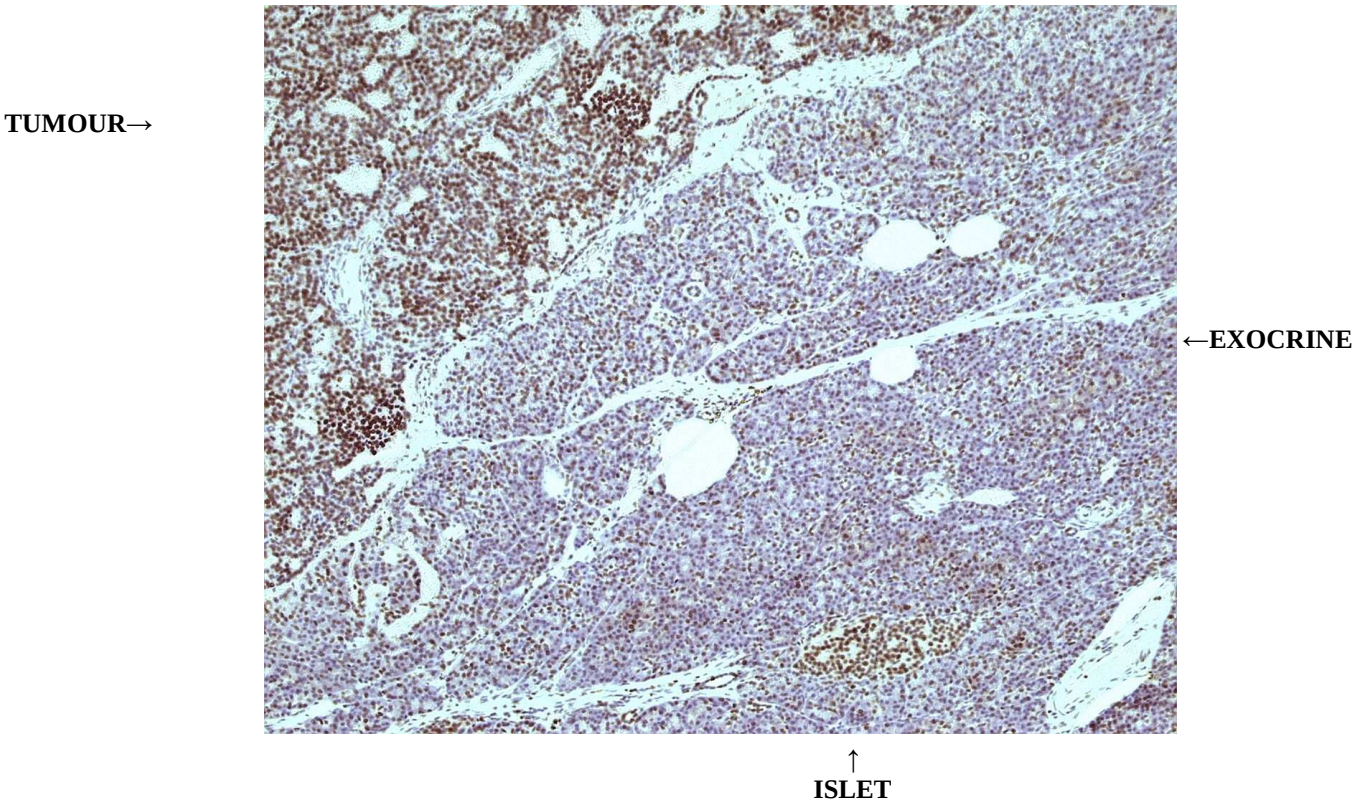

Figure 3.72 Lower powered slide showing the difference in PTEN staining between the different tissue types in sample 8

3.2.20 PTEN staining in insulinoma, gastrinoma, islet and exocrine pancreas

The pattern of PTEN staining seen is clearly seen in all tissues (figures 3.73 – 3.76). There is very high degree of positive nuclear staining and very little cytoplasmic staining.

Insulinoma show positive nuclear staining in 95.6 +/- 2.1% of cells compared to cytoplasmic staining of 5.6 +/- 2.9%. Gastrinoma are even more black and white with 99.6 +/-0.4% positive staining and 0% cytoplasmic staining seen. Islets show 97.8 +/- 0.7% positive nuclear staining compared to10 +/- 6.9% cytoplasmic staining. Exocrine showed the lowest nuclear staining at 73.2 +/- 3.2% but clearly showed no cytoplasmic staining at all.

There is no significant difference between insulinoma and islets nor gastrinoma. All three endocrine tissues show significantly more nuclear PTEN expression than exocrine pancreas.

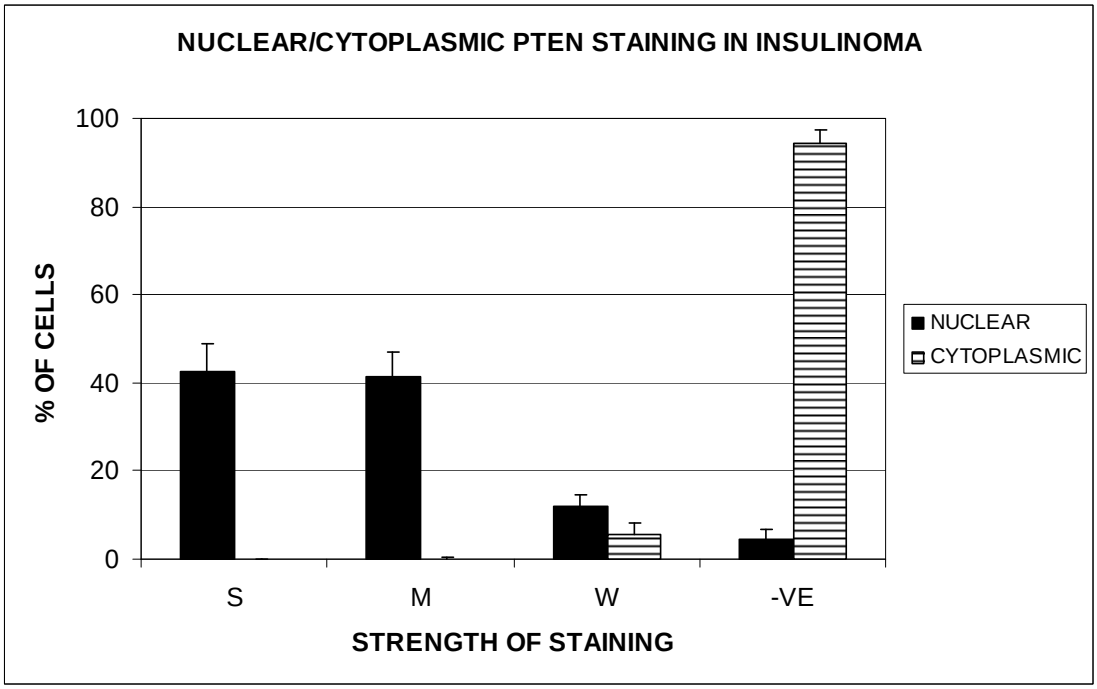

Figure 3.73 Graph showing the location and strength of PTEN staining in insulinoma samples (S=strong, M=moderate, W=weak, -VE=negative)

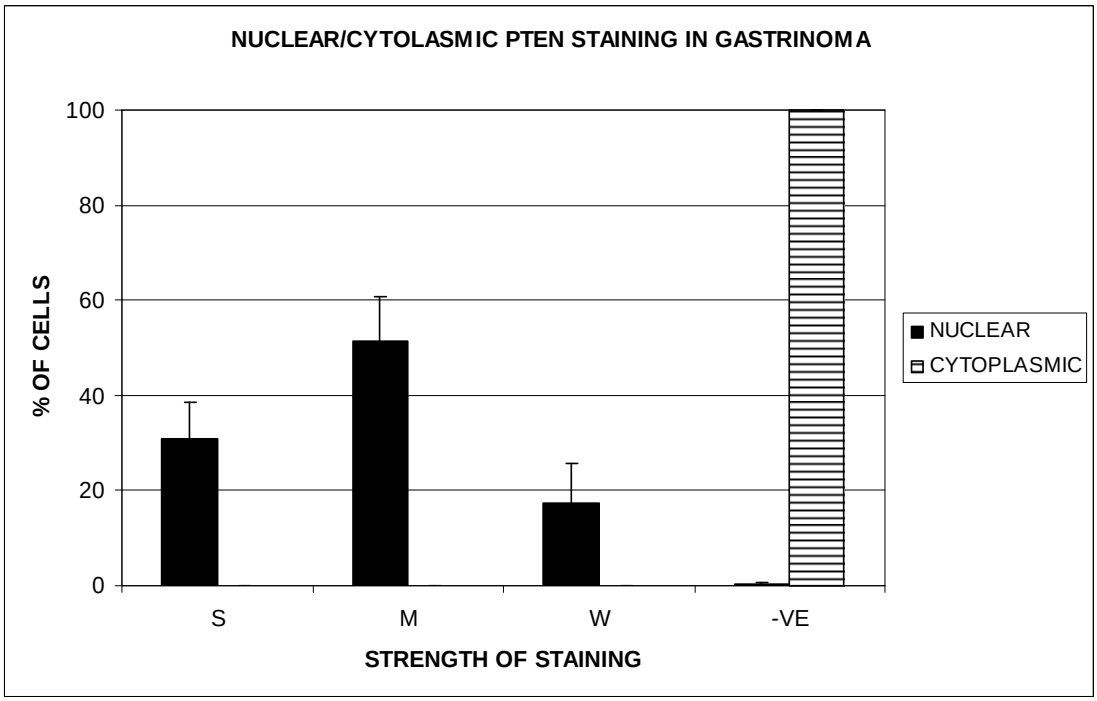

Figure 3.74 Graph showing the location and strength of PTEN staining in gastrinoma samples (S=strong, M=moderate, W=weak, -VE=negative)

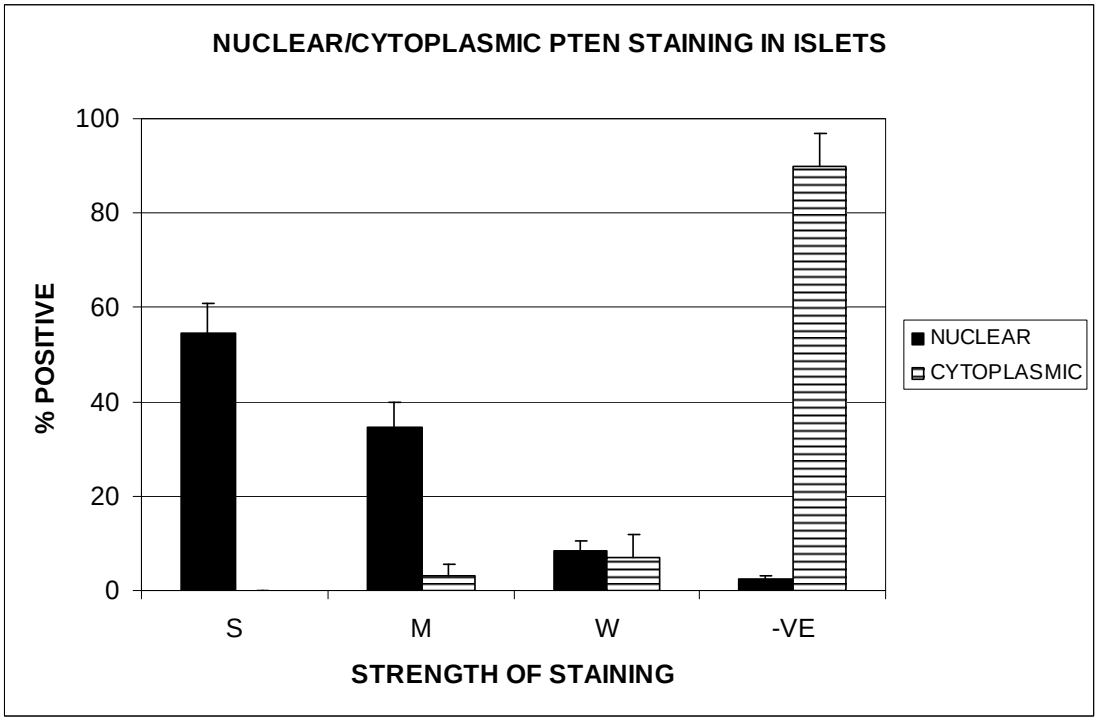

Figure 3.75 Graph showing the location and strength of PTEN staining in islet samples (S=strong, M=moderate, W=weak, -VE=negative)

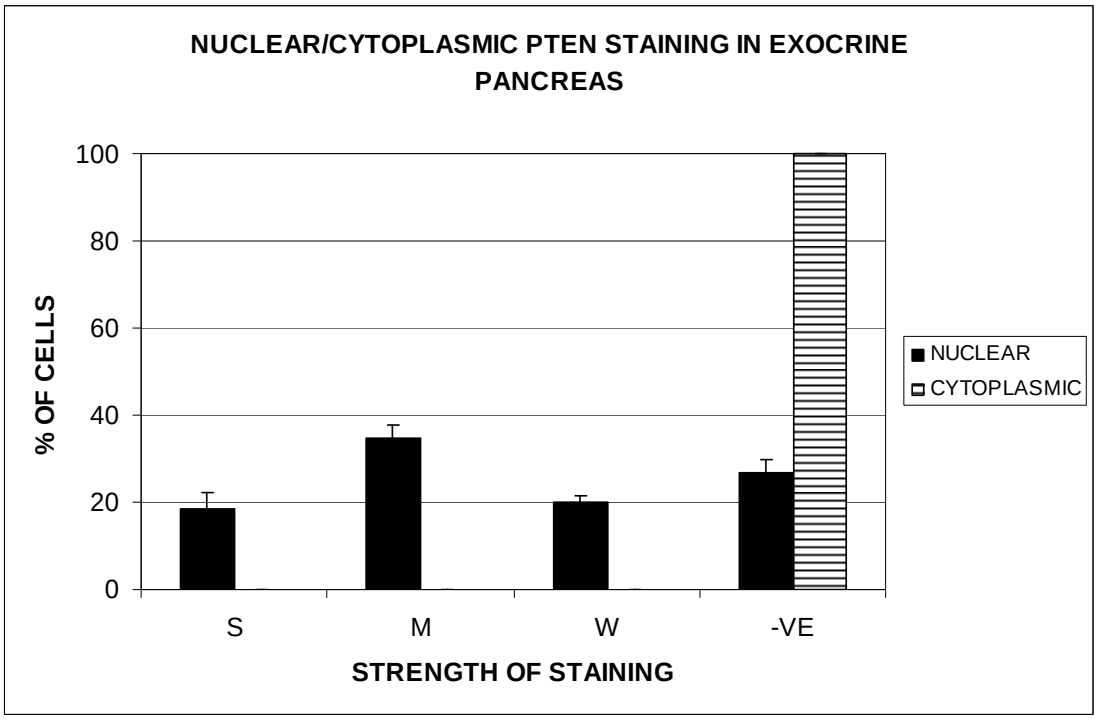

Figure 3.76 Graph showing the location and strength of PTEN staining in exocrine samples (S=strong, M=moderate, W=weak, -VE=negative)

3.2.21 Comparing nuclear PTEN staining

When comparing the nuclear staining of PTEN across the different tissues it is clear that there is a similar staining pattern with heavy strong and moderate staining seen.

Looking at total positive counts for the tissues there is no difference between insulinoma, gastrinoma or islets. All three, however, show significantly more staining than exocrine tissue.

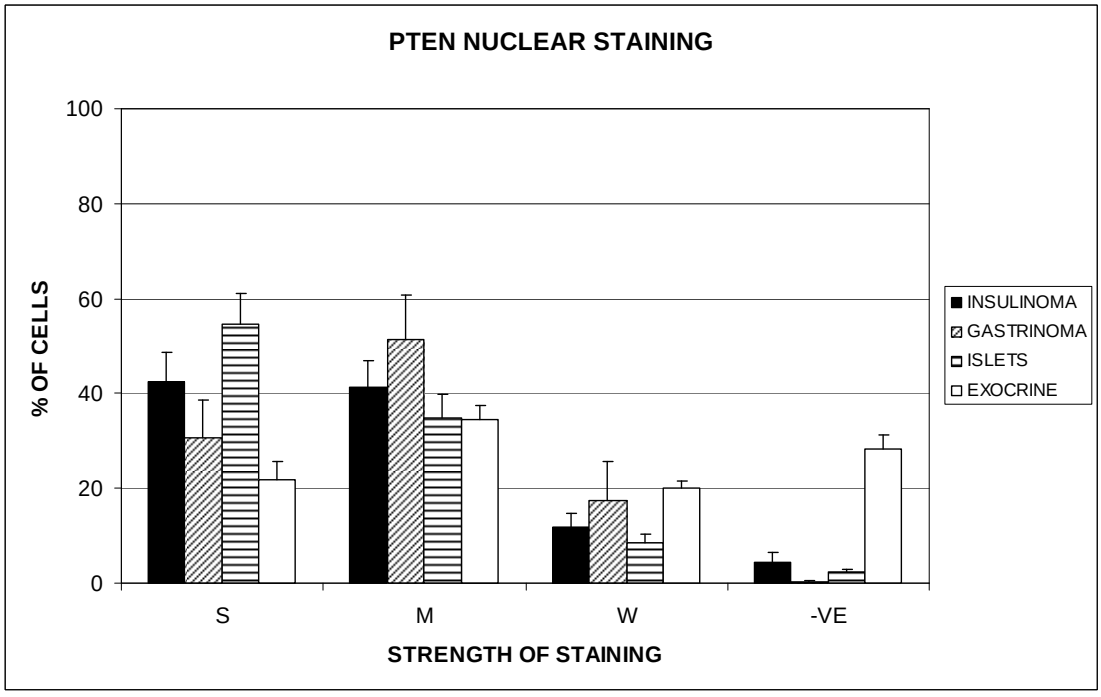

Figure 3.77 Graph comparing the relative strength of PTEN nuclear staining for all tissue types

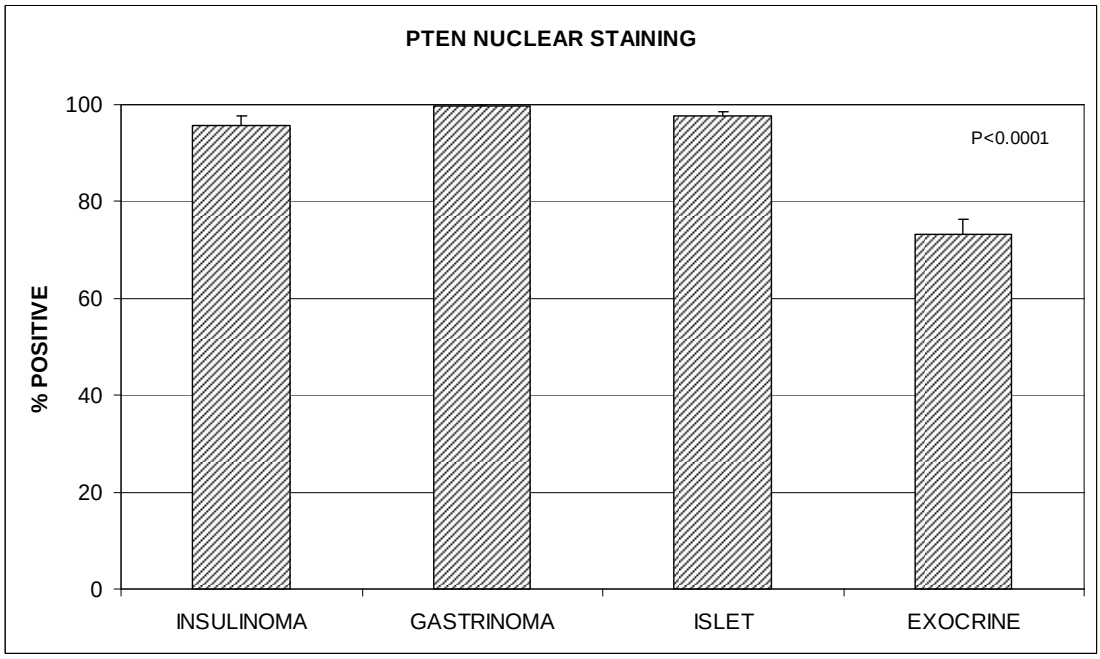

Figure 3.78 Graph comparing total positive PTEN nuclear staining for all tissue types

Kruskal-Wallis test	P < 0.0001
Kruskal-Wallis: all pairwise comparisons (Conover-Inman)	
INSULINOMA and EXOCRINE	P < 0.0001
GASTRINOMA and EXOCRINE	P = 0.0007
ISLET and EXOCRINE	P < 0.0001

When positive staining is considered as strong plus moderate staining, there is no change in the pattern seen.

3.2.22 Comparing cytoplasmic PTEN staining

No differences are seen when comparing the cytoplasmic staining of any of the tissues.

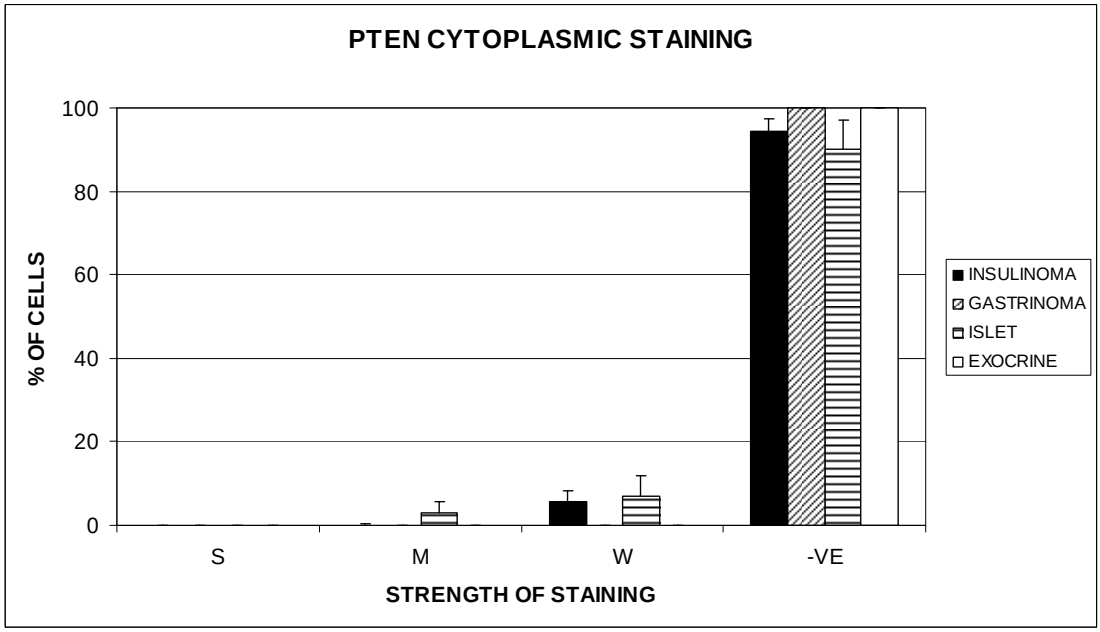

Figure 3.79 Graph comparing the relative strength of PTEN cytoplasmic staining for all tissue types

3.2.23 Ki-67 immunohistochemistry

A rabbit anti-human polyclonal antibody to Ki-67 protein was used (AO47, Dako, Cambridgeshire, UK). This antibody had been previously optimised in the laboratory and good staining was seen with standard dilutions of 1:200.

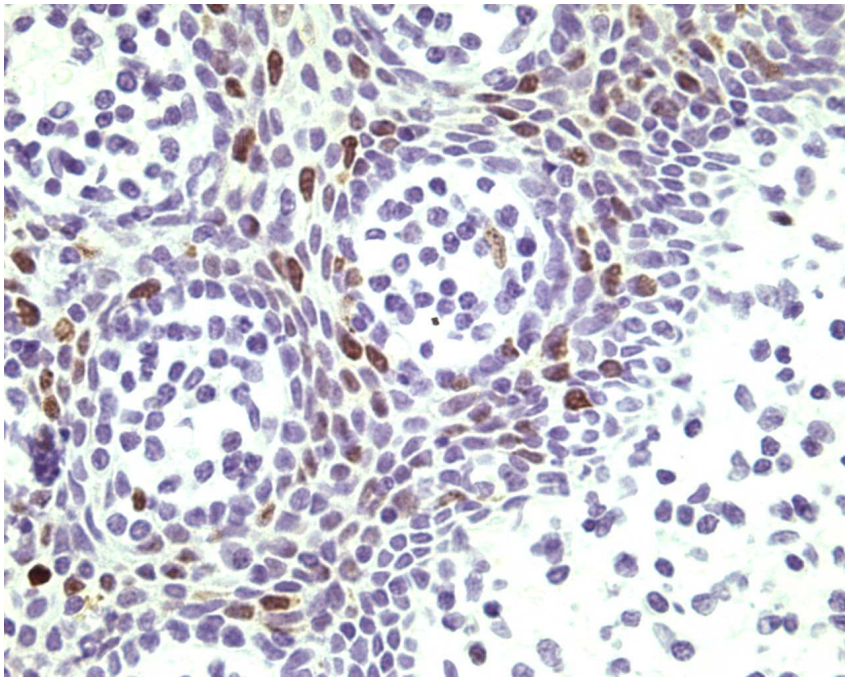

Figure 3.80 Slide showing good nuclear Ki-67 staining in tonsil positive control

An estimation of the percentage of positive Ki-67 staining for insulinomas and gastrinomas was performed in the laboratory by a consultant histopathologist (Dr E Carlsen).

Table 5 Ki-67 staining for insulinoma samples

	Ki-67 STAINING (% POSITIVE)		
ID	**TUMOUR**	**ISLET**	**EXOCRINE**
1	<1	<1	<1
2	<1	<1	<1
3	<1	<1	<1
5	<1	<1	<1
6	<1	<1	<1
7	<1	<1	<1
8	<1	<1	<1
9	<1	<1	<1
10	<5	<1	<1
11	<5	<1	<1
12	<1	<1	<1
13	<5	<1	<1
14	<1	<1	<1
15	<5	<1	<1
17	<1	<1	<1
18	<1	<1	<1
19	<1	<1	<1
20	<1	<1	<1
23	<1	<1	<1
25	<1	<1	<1

Table 6 Ki-67 staining for gastrinoma samples

	Ki-67 STAINING (% POSITIVE)		
ID	**TUMOUR**	**ISLET**	**EXOCRINE**
4	<1	<1	<1
22	<5	<1	<1
24	<1	<1	<1

3.2.24 Insulinoma proliferation sub group analysis

Within the insulinoma group there were 4 tumours that may have been proliferating at a higher rate as shown by the Ki-67 Index (ID 10, 11, 13 and 15). To identify whether these are acting differently to less proliferative tumours, they were separated out for comparison.

Although not statistically significant, probably due to the small sample size, there was a trend for the less proliferative tumours to express less nuclear PPARγ (% positive staining, 2.6 +/- 1.9% vs 31.1 +/- 20.1%).

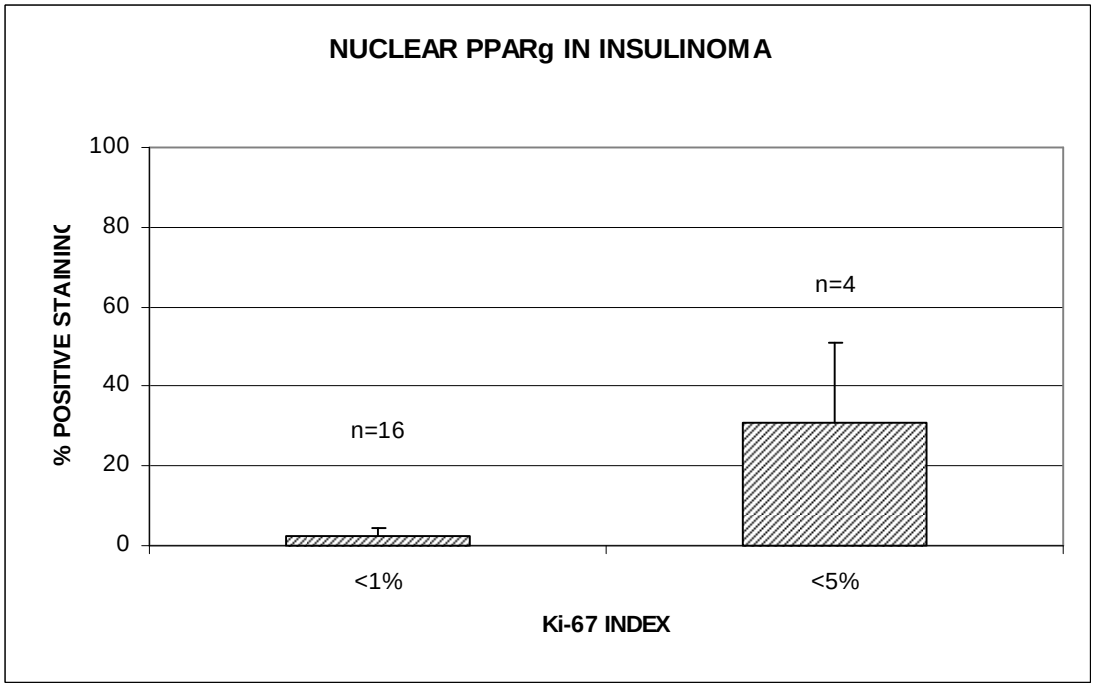

Figure 3.81 Graph showing total positive nuclear PPARγ in insulinomas split into two groups based on their Ki-67 index.

With p27 staining it was noted that there was a trend for reduced nuclear and cytoplasmic p27 expression. On testing this reached statistical significant in the cytoplasmic group.

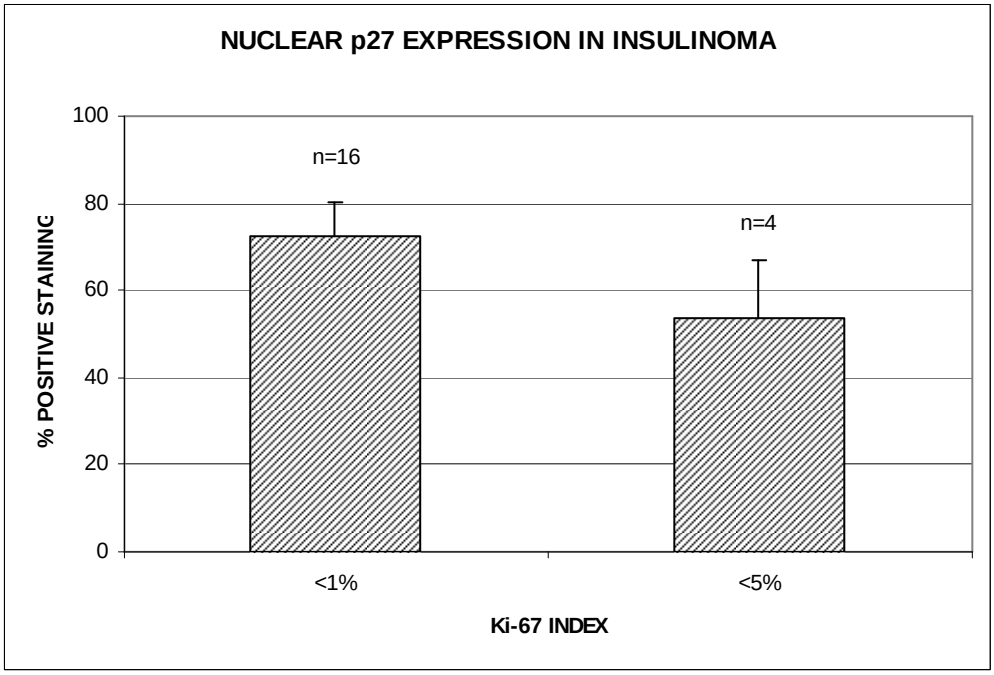

Figure 3.82 Graph showing total positive nuclear p27 in insulinomas split into two groups based on their Ki-67 index. (% positive = 72.4 +/- 7.7% (for insulinomas <1%) vs 53.8 +/- 13.4% (for insulinomas <5%))

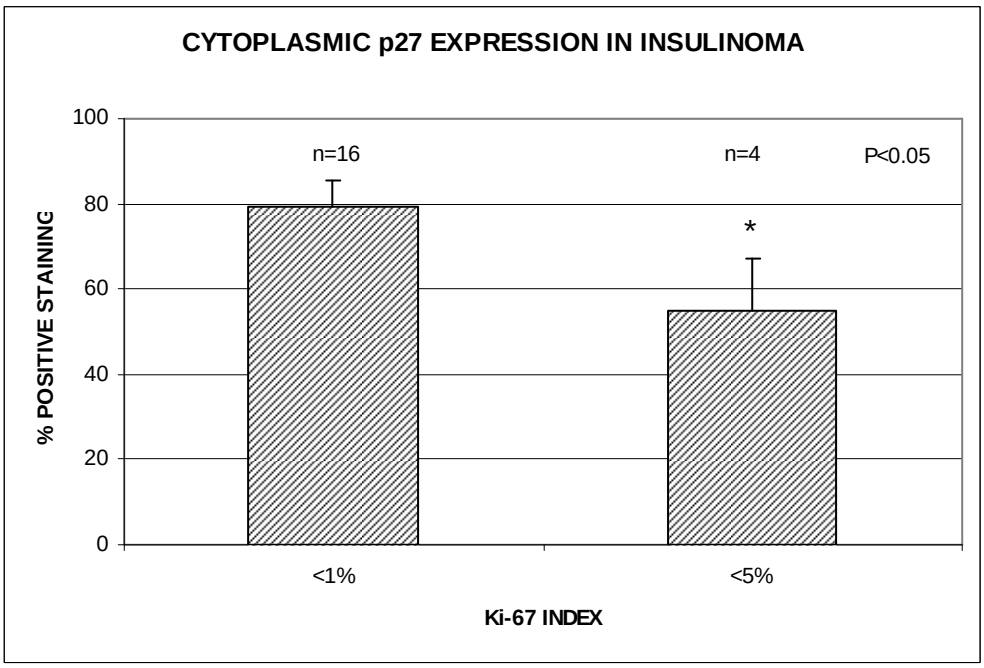

Figure 3.83 Graph showing total positive cytoplasmic p27 in insulinomas split into two groups based on their Ki-67 index. (% positive = 79.5 +/- 5.9% (for insulinomas <1%) vs 54.9 +/- 12.5% (for insulinomas <5%))

Mann-Whitney test P = 0.0499

With phospho-p27, there was little difference between the nuclear staining but there was lower cytoplasmic staining in those tumours with a higher Ki-67 index, (86.9 +/- 5% vs 46.5 +/- 16.7%). This did not reach statistical significance.

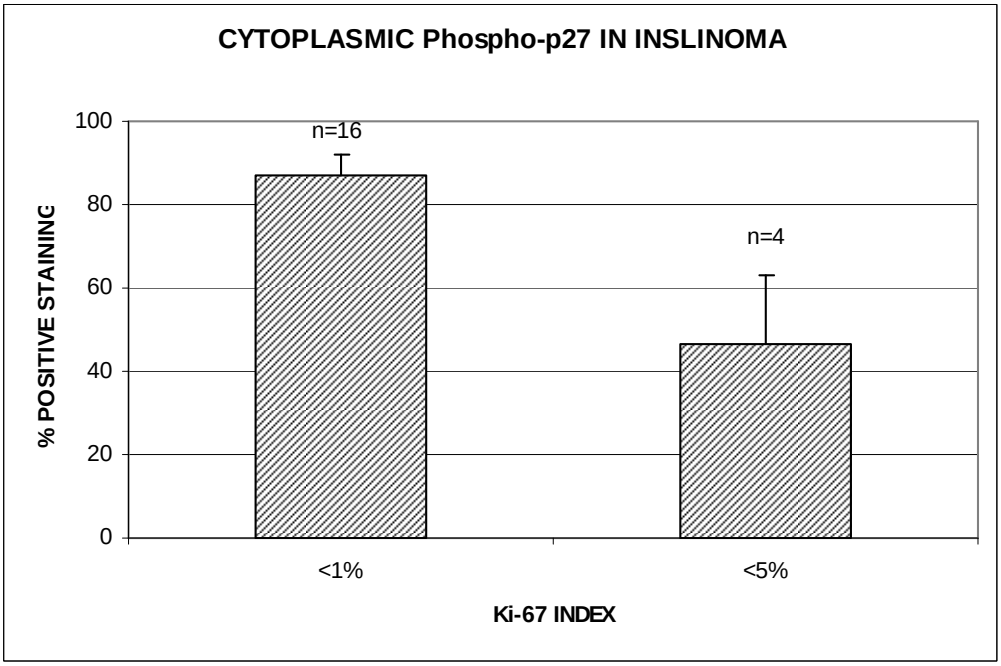

Figure 3.84 Graph showing total positive cytoplasmic phospho-p27 in insulinomas split into two groups based on their Ki-67 index.

Assessing JAB1 staining revealed a significant difference in the cytoplasmic staining. It was found that tumours with the higher Ki-67 index showed lower JAB1 expression in the cytoplasm, (85.9 +/- 5.8% vs 33.2 +/- 20.6%).

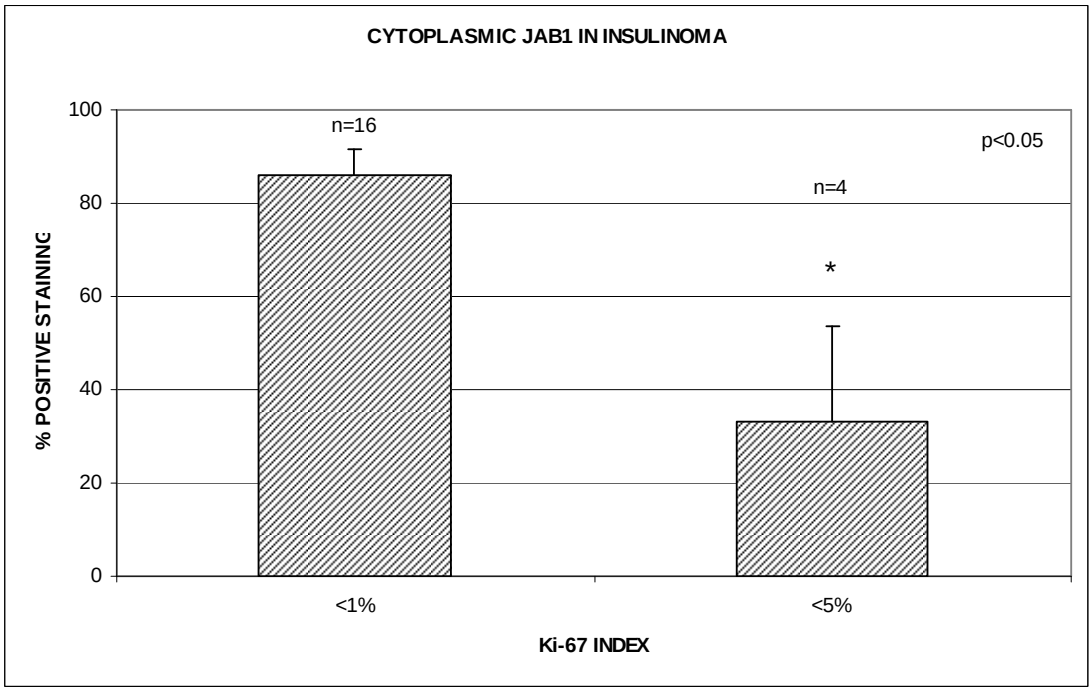

Figure 3.85 Graph showing total positive cytoplasmic JAB1 in insulinomas split into two groups based on their Ki-67 index.

Mann-Whitney test P = 0.0293

No obvious differences were noted in the staining patterns with phospho-Akt or PTEN series.

3.2.25 Summary of immunohistochemistry

Immunohistochemistry was performed using seven different antibodies: PPARγ, p27, phospho-p27, JAB1, phospho-Akt, PTEN and Ki-67. With the exception of Ki-67 (see below), we wanted to identify the location of these proteins (nuclear or cytoplasmic) and to identify any pattern of differences between the tissue types.

Regarding PPARγ expression in the whole series, we were unable to demonstrate any significant nuclear or cytoplasmic expression, despite good staining of positive controls.

In the p27 series, good staining was seen in both the nucleus and cytoplasm. In fact, there was significantly more cytoplasmic than nuclear staining seen with gastrinoma and islet cells. On comparing the tissues, no difference was found in the nuclear expression of p27 between insulinoma, gastrinoma or islets, but there was significantly lower expression of p27 in the cytoplasm of insulinomas compared to islets. Nuclear and cytoplasmic staining in insulinomas, gastrinomas and islets was significantly higher than that seen in exocrine tissue.

In the phospho-p27 series, the expression is overwhelmingly within the cytoplasm of all tissue types. Very little nuclear staining was identified and there were no differences between tissue types. Despite the high levels of cytoplasmic staining there was no difference in expression between insulinomas, gastrinomas or islets. All three tissues showed significantly higher cytoplasmic expression compared to exocrine tissue.

In the series of JAB1 staining, all tissues overwhelmingly showed cytoplasmic expression, with either no or negligible nuclear staining seen. Although there is a

variation in the pattern of staining, overall there was a significantly lower cytoplasmic expression of JAB1 in insulinomas and gastrinomas compared to islets. Both insulinomas and islets showed significantly higher expression compared to exocrine tissue.

In the phospho-Akt series, widespread nuclear and cytoplasmic staining was seen in all four tissue types, with cytoplasmic expression being significantly higher than nuclear in all tissues. There was significantly lower nuclear expression of p-Akt in insulinomas and gastrinomas compared to islets. Exocrine pancreas shows significantly lower nuclear expression than either insulinoma or islets. Despite very high levels of cytoplasmic staining there was significantly less expression in insulinomas and gastrinomas compared to islets. Again, exocrine expression was lower than either insulinoma or islets.

PTEN staining was similar in all tissues. There was very high degree of positive nuclear staining and very little cytoplasmic staining. No significant differences were identified between insulinoma, gastrinoma and islets. All three show significantly more nuclear PTEN expression than exocrine pancreas.

Regarding the Ki-67 subgroup analysis, tumours with a higher Ki-67 index had significantly less cytoplasmic p27 and JAB1. Trends were noted towards higher nuclear expression of PPARγ, lower nuclear expression of p27 and lower cytoplasmic phospho-p27.

RESULTS III

Cell Cultures

3.3.1 Cell Culture Work

Three cell lines were obtained by kind permission of Professor N Lemoine (Institute of Cancer, Barts and The London, Queen Mary's School of Medicine and Dentistry). The cell lines denoted as CM, BON and QGP1 represent human insulinoma, carcinoid and somatostatinoma cell lines respectively.

The three cells lines were successfully transferred and cultured in our laboratory under the conditions explained in the methods section.

Work with these cells can be divided into three main sections, RNA/DNA, protein expression and proliferation studies

3.3.1.1 RNA Extraction

Cells were harvested, washed in PBS and separated by centrifuging. RNA was then extracted using standard Promega extraction protocol as described. RNA was then subjected to spectrophotometry and RNA gel electrophoresis with good results.

Example of RNA 1% agarose gel

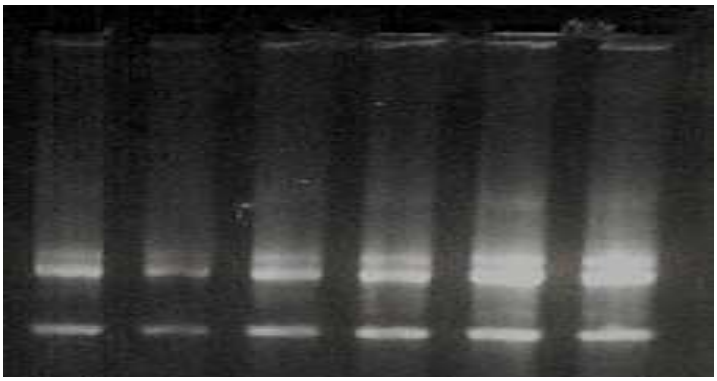

CM CM BON BON QGP QGP

Samples were subject to reverse transcription using ABI standard protocols as described. To check quality, cDNA were subjected to PCR using standard Promega protocols to check for short GAPDH.

SHORT GAPDH

SM H2O +VE CM CM BON BON QGP QGP

←GAPDH

Size marker = phix 174 Hinf 1 +VE = positive control

Samples were considered to be of a reasonable quality to proceed with further investigation.

3.3.1.2 Expression of PPARγ

To check for the expression of PPARγ mRNA in our cell lines, cDNA samples were subjected to PCR for PPARγ using Qiagen standard PCR protocols

PPARγ primers were obtained from Sigma-Genosys as described in the methods section.

SM H2O +VE CM CM BON BON QGP QGP QGP

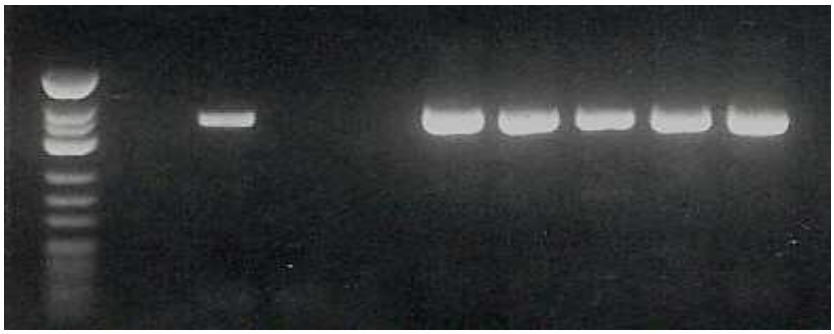

←**PPARγ**

Size marker phix 174 Hinf 1 +VE = positive control

Figure 3.86 Gel showing the products of PCR for PPARγ on mRNA extracted from cell lines CM, BON and QGP1

The duplicate samples had been extracted on separate days and therefore the negative PPARγ results with CM cell line were thought to be a true finding.

3.3.1.3 Repeat PPARγ PCR

In view of the unusual finding that the cell line CM did not express PPARγ mRNA but PPARγ protein was apparently being detected in my Westerns blots, it was felt that the cell lines should be subjected to further RNA extraction, RT and repeated PPARγ PCR.

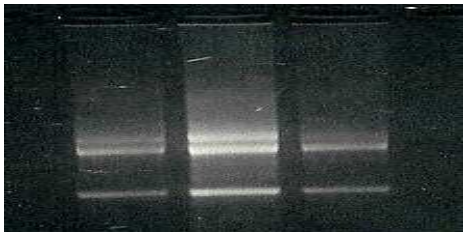

CM BON QGP1

RNA 1% agarose gel of repeated extractions of cell lines CM BON and QGP1

REPEATED PPARγ PCR

SM H2O +VE A B C D E F G

Size marker phix 174 Hinf 1 +VE = POSITIVE CONTROL

Figure 3.87 Gel showing the products of repeat PCR for PPARγ on mRNA extracted from cell lines CM, BON and QGP1

SAMPLES	A	BON	(previous sample with positive result)
	B	QGP1	(previous sample with positive result)
	C	CM	(1st previous sample with negative result)
	D	CM	(2nd previous sample with negative result)
	E	CM	(Newly prepared sample as above on RNA gel)
	F	BON	(Newly prepared sample as above on RNA gel)
	G	QGP1	(Newly prepared sample as above on RNA gel)

From the gel it can be confirmed that the previous samples give the same results with this new PCR i.e. both previous CM samples do not express PPARγ mRNA whereas both BON and QGP1 do. This has been confirmed again with the newly extracted samples represented by E, F and G.

3.3.2 Somatostatin Receptor PCR

It is widely accepted that a large proportion of neuroendocrine tumours express somatostatin receptors and clinical therapy often utilises somatostatin analogues. It was felt worthwhile to identify whether these cell line expressed these somatostatin receptors (SSTR's). Somatostatin is thought to act through five membrane receptors which are expressed variably in tissues and tumours. The somatostatin analogue octreotide for example activates SSTR receptor subtype 2 (SSTR2), and to a lesser extent receptor subtype 5 (SSTR5). The inhibition of cellular proliferation attributed to somatostatin analogues may involve several signal transduction pathways including the MAP Kinase pathway and stimulation of the cyclin dependent kinase inhibitor p27

Previously extracted RNA from all 3 cell lines was subjected to PCR for receptors 1-5 using Promega PCR standard protocols, previously optimised in our laboratory.

3.3.2.1 PCR FOR SSTR 1

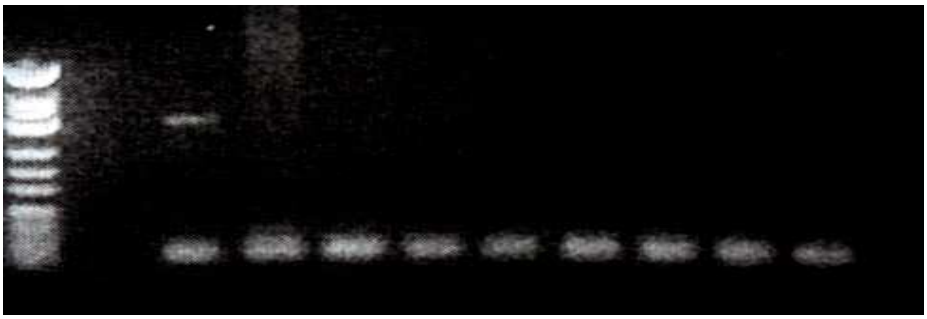

Figure 3.88 Gel showing the products of PCR for SSTR1 on mRNA extracted from cell lines CM, BON and QGP1

SM = phix 174 Hinf 1 SSTR 1 product 401 bp

X = pituitary tumour tested to see if it could be used in the future as a positive control

Repeat labels represent samples extracted on different days

3.3.2.2 PCR FOR SSTR 2 AND 3

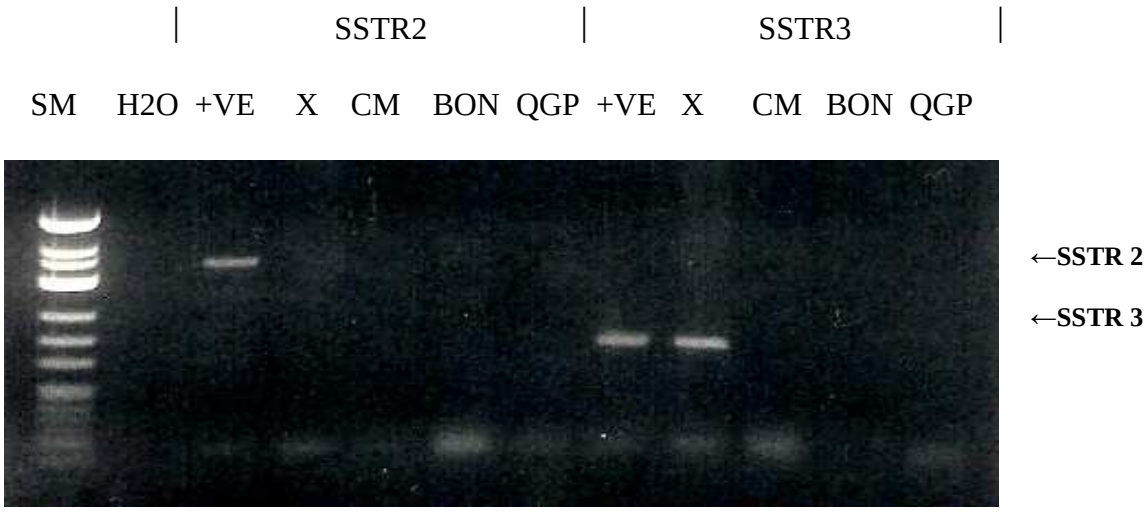

SM = phix 174 Hinf 1 SSTR 2 product 459 bp SSTR 3 product 225bp

Figure 3.89 Gel showing the products of PCR for SSTR2 and 3 on mRNA extracted from cell lines CM, BON and QGP1

3.3.2.3 PCR FOR SSTR 4 AND 5

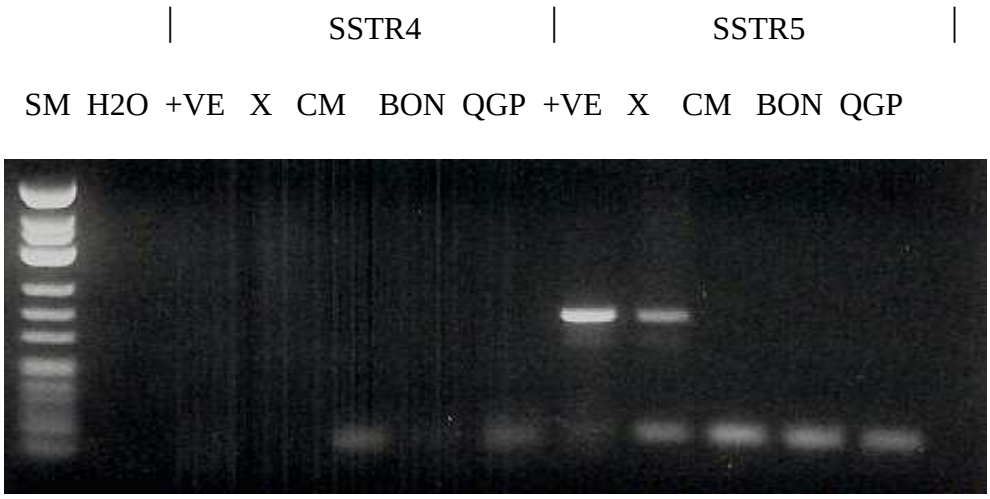

SM= phix 174 Hinf 1 SSTR 4 product 451 bp SSTR 5 product 233 bp

Figure 3.90 Gel showing the products of PCR for SSTR4 and 5 on mRNA extracted from cell lines CM, BON and QGP1

Despite repeated experimentation, we concluded that cell lines CM, BON and QGP1 do not express any of the somatostatin receptors 1-5 mRNA.

Regarding the PCR for SSTR4, it is acknowledged that the +ve control sample was negative and therefore interpretation of our findings for this receptor could be in doubt. Given that the experiment was repeated with the same results and given the lack of other SSTR's within our cell lines. It is probable that these cell lines do not express SSTR4 either. It is likely that our positive control actually is inappropriate and does not express SSTR4 itself. As a side note, sample X, a pituitary tumour (growth hormone secreting) added to see if it could be used as a positive control in the future, was positive for receptors 3 and 5

3.3.3 PPARγ Protein Expression

Proliferating cells from all three cell lines were harvested using cytobuster protein extraction reagent (Novagen) as described in methods and subjected to protein assay to determine concentration. Samples were held -80^{0}C awaiting experimentation.

3.3.3.1 Western Blotting To Assess PPARγ Protein Presence

Following protein denaturing, 20µg protein samples were loaded into a 10% Tris-HCL gel and subject to electrophoresis. Electroblotting onto a PVDF membrane (Hybond-P, Amersham) was then performed and the resultant membrane washed and treated with 5% non fat milk to prevent non specific binding of the antibody.

A PPARγ mouse monoclonal IgG antibody from Santa Cruz (sc-7273) was obtained and optimised in the laboratory. A 1:50 dilution of this 1st antibody diluted in non fat milk was applied to the membrane and left on motion rollers overnight at 4^{0}C.

Following washing a 1:10000 dilution of a goat antimouse 2nd antibody was applied for 90 minutes.

The resultant washed membrane was treated with LumiGLO reagent and peroxidise (Cell Signalling Technology) – a chemiluminescent detection system – and light emission was recorded by optimising exposure to X-Ray film.

3.3.3.2 PPARγ Western Result

1st	PPARγ (Santa Cruz)	1:50	4^0C overnight
2nd	Goat anti-mouse	1:10000	90 mins
Lumiglow	5 mins		Exposure 8 mins

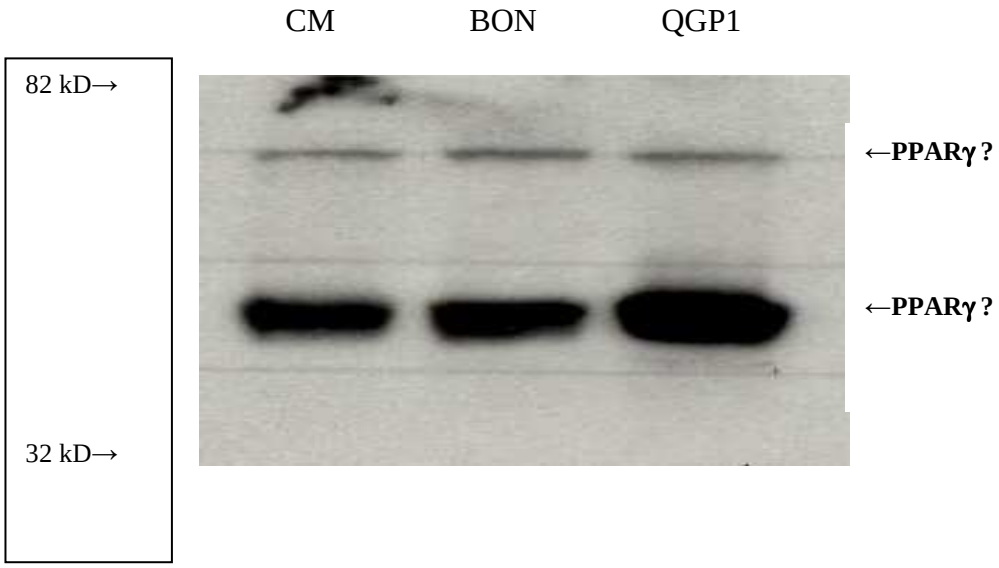

Kaleidoscope pre stained standards (Bio-Rad) – shown to scale.

Figure 3.91 Western blot result for PPARγ in the cell lines CM, BON and QGP1

The PPARγ protein is 67 kD in weight. Double bands were unexpected and although the top line of bands would most likely be the correct weight, the strength of the lower bands made us question which was correct.

To help answer the question, the membrane was stripped and re-probed with a different PPARγ antibody (Calbiochem-Novabiochem Corp., La Jolla, CA, USA).

1^0	PPARγ (Calbiochem)	1:2000	room temp 90 mins
2^0	Goat anti-rabbit	1:10000	90 mins
Lumiglow	5 mins		Exposure 2 mins

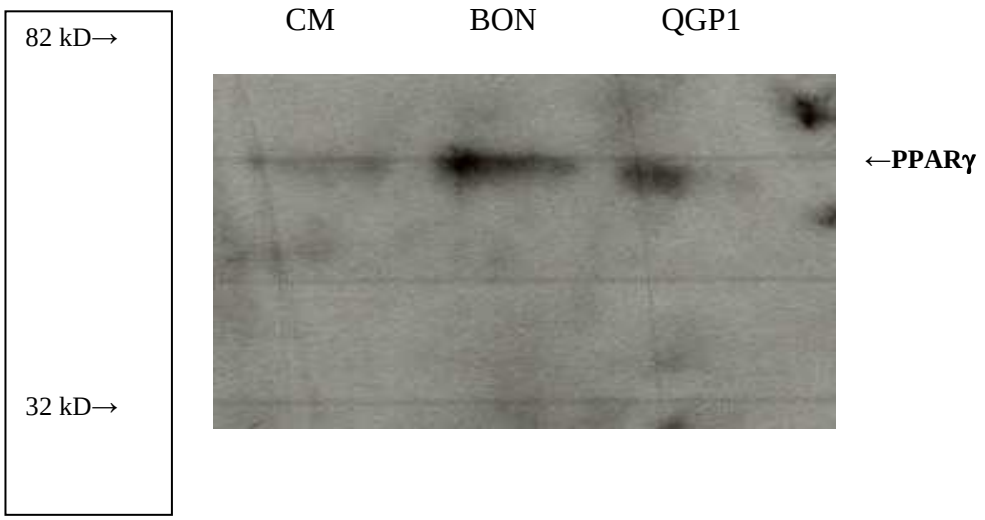

Figure 3.92 Repeat western blot result for PPARγ in the cell lines CM, BON and QGP1 following administration of a different PPARγ antibody.

The figures are both to the same scale. Clearly, the lower line has disappeared with the second antibody confirming that with the Santa Cruz antibody the upper band was the correct band for PPARγ.

The same membrane was probed for β-actin (43 kD)

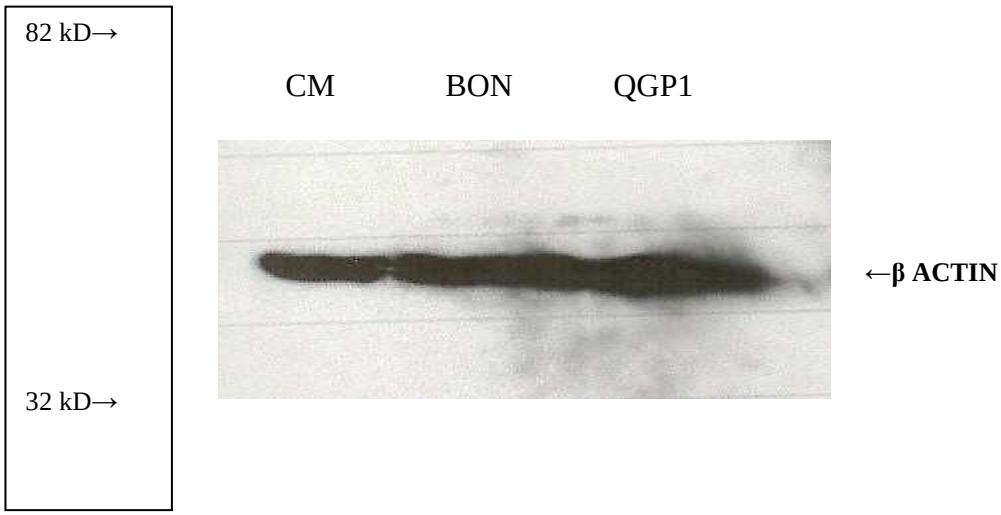

Figure 3.93 Western blot result for β-actin on the same membrane as above

The expression of PPARγ protein in the CM cell line was unexpected, as repeated PCR for PPARγ cDNA was negative. I thought it best to repeat the Western experiments again using the protein samples from the above experiment (OLD), and newly extracted protein from all three cell lines (NEW).

3.3.3.3 Repeat Western for PPARγ

Conditions as above for Santa Cruz PPARγ antibody

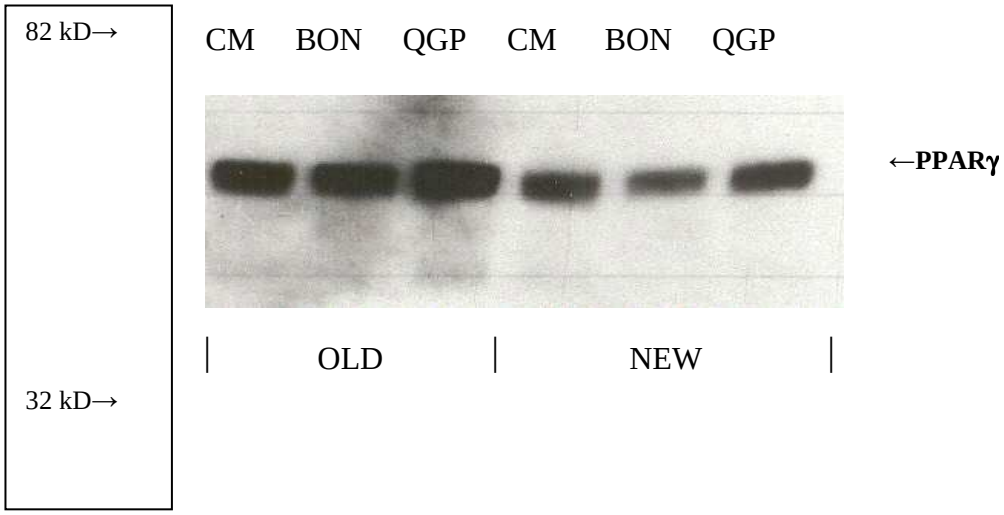

Figure 3.94 Repeat western blot for PPARγ in the cell lines CM, BON and QGP1 following re extraction of proteins

The membrane was stripped and re-probed for β-actin using the same conditions as above

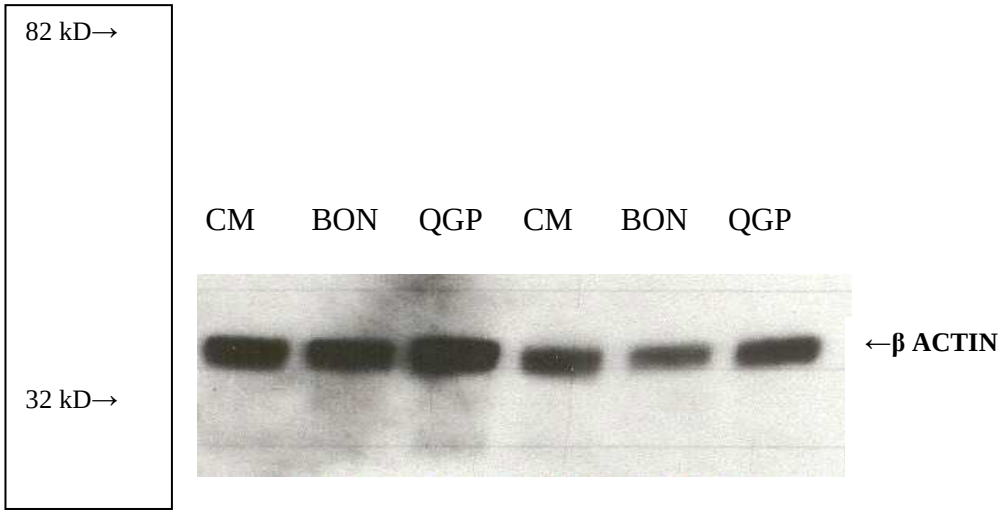

Figure 3.95 Western blot result for β-actin on the same membrane as above

3.3.4 Proliferation Studies

Cells were harvested and counted as described to calculate concentration of cells per ml of media. The correct volume of cell suspension was then pipetted into plate wells to give 50 000 cells per well. Cells were left for 8 hours to allow for cell adhesion prior to experimentation

3.3.4.1 Rosiglitazone (PPARγ agonist) studies

Optimising the duration of treatments

Experimental plates were set up as described in methods. Tritiated thymidine was added to the wells 8 hours prior to the completion of the experimental period. Scintillation counting on completion of the time period allowed for assessment of the proliferation or inhibition of cell lines. Preliminary experiments were set up to assess the most suitable time period for treatments.

Rosiglitazone treated QGP1 cells at 24, 48, 72 and 96 hours

Example of results generated and tabulated in Excel.

QGP1 ROSI 24HOURS						
Molar Conc	ROW 1	ROW 2	ROW 3	ROW 4	AVERAGE	SD
CONTROL	20822.40	62214.40	49836.50	103434.70	59077.00	17142.175
x10--4	1734.90	8867.80	6561.50	11723.70	7221.98	2111.8414
x10--5	58615.50	54805.50	42751.00	50589.80	51690.45	3400.7971
x10--6	58266.50	90781.00	47548.80	46016.20	60653.13	10405.719
x10--7	53239.20	72567.20	68966.90	68694.40	65866.93	4300.7517
x10--9	73149.30	77005.50	60652.60	56186.80	66748.55	4957.1984

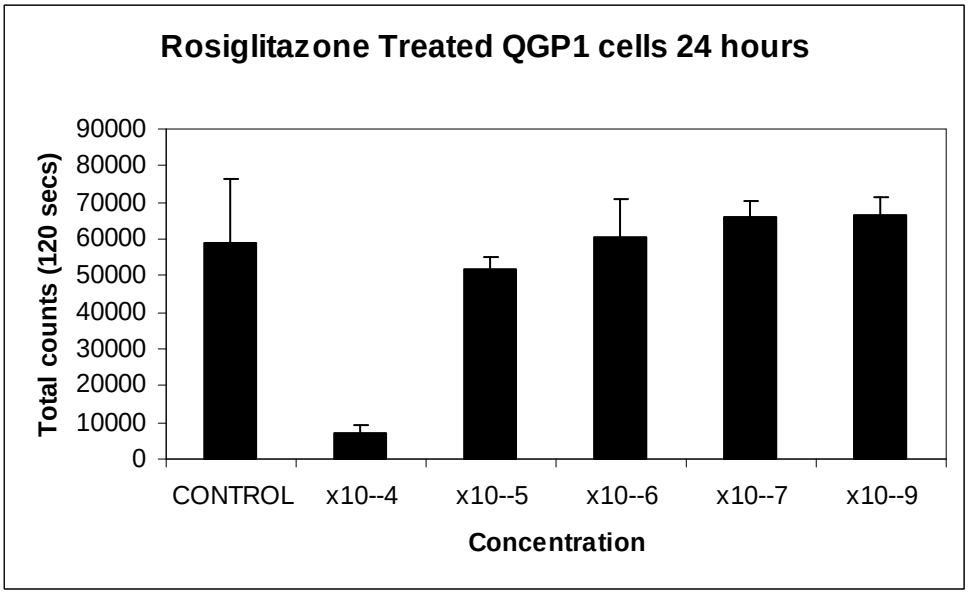
Rosiglitazone Treated QGP1 cells 24 hours
Total counts (120 secs)
90000
80000
70000
60000
50000
40000
30000
20000
10000
0
CONTROL
x10--4
x10--5
x10--6
x10--7
x10--9
Concentration

A

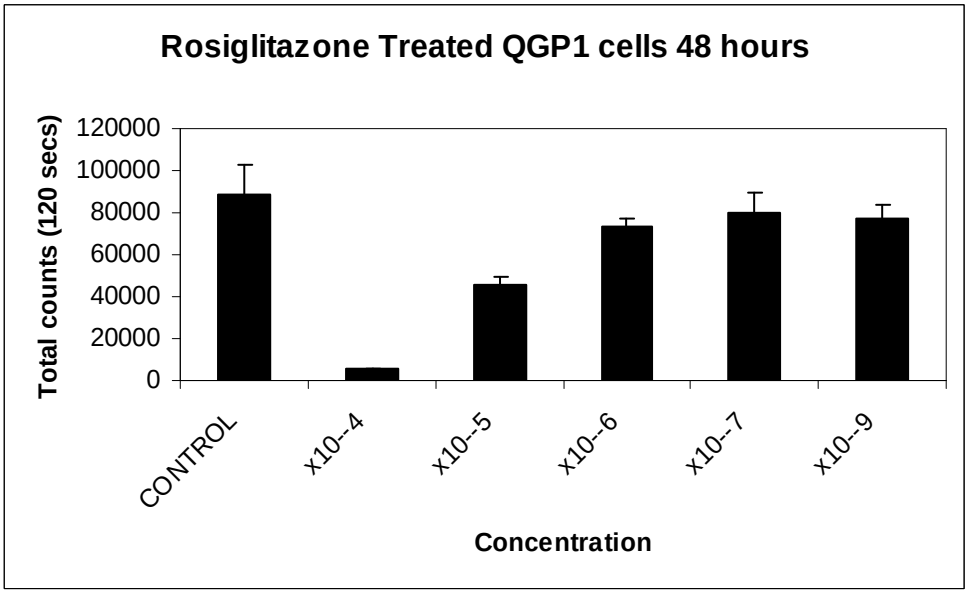
Rosiglitazone Treated QGP1 cells 48 hours
Total counts (120 secs)
120000
100000
80000
60000
40000
20000
0
CONTROL
x10--4
x10--5
x10--6
x10--7
x10--9
Concentration

B

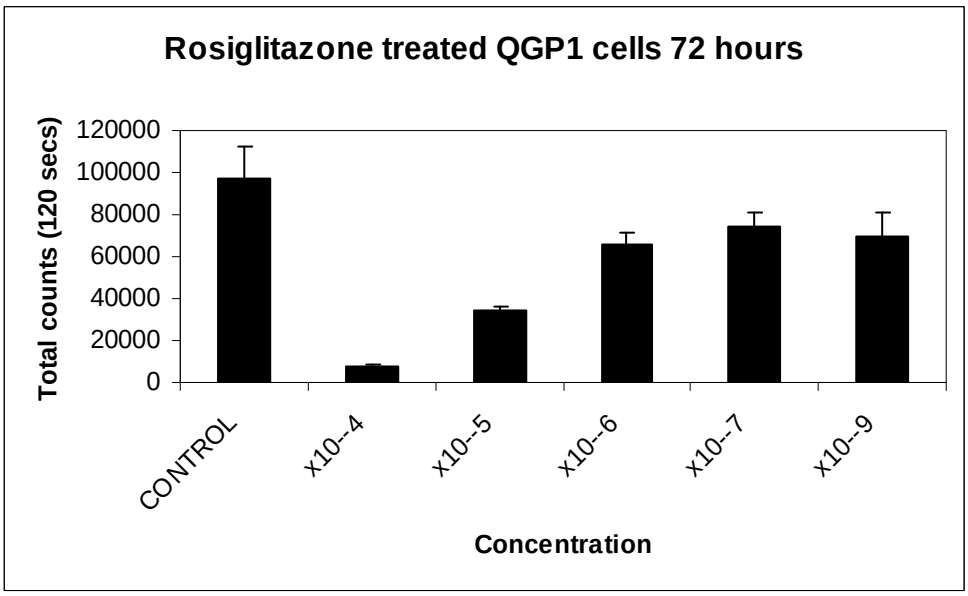

C

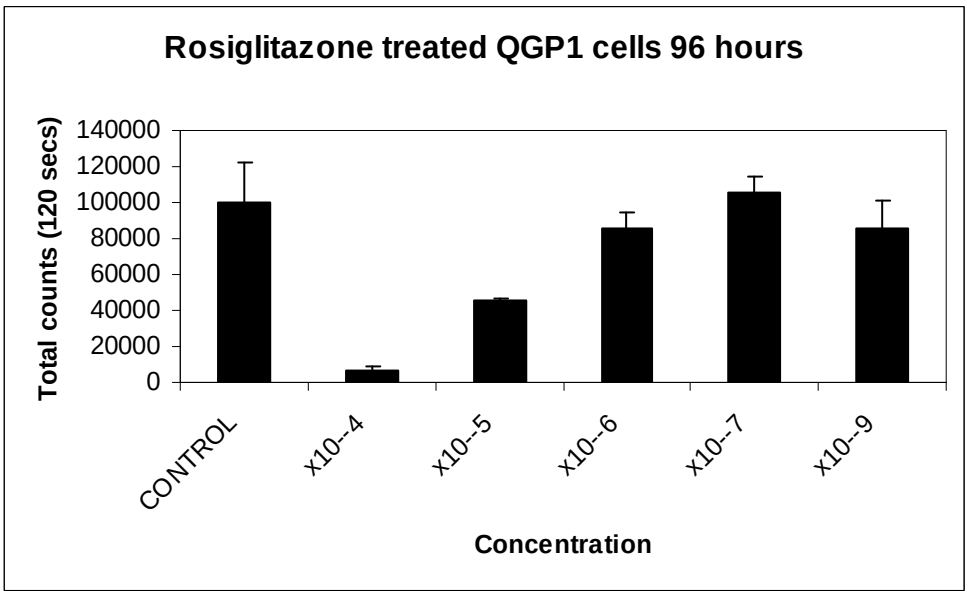

D

Figure 3.96 Graphs A-D showing thymidine scintillation counts as a marker of cellular proliferation versus molar concentration in QGP1 cells following treatment of rosiglitazone for, 24, 48, 72 and 96 hours.

Preliminary treatment series were performed for all cell lines and it was felt that 48 hours was the best time frame for treatments. It appeared that at 72 and 96 hours some of the cells were becoming detached or dying.

Example of length of treatment leading to variability of counts

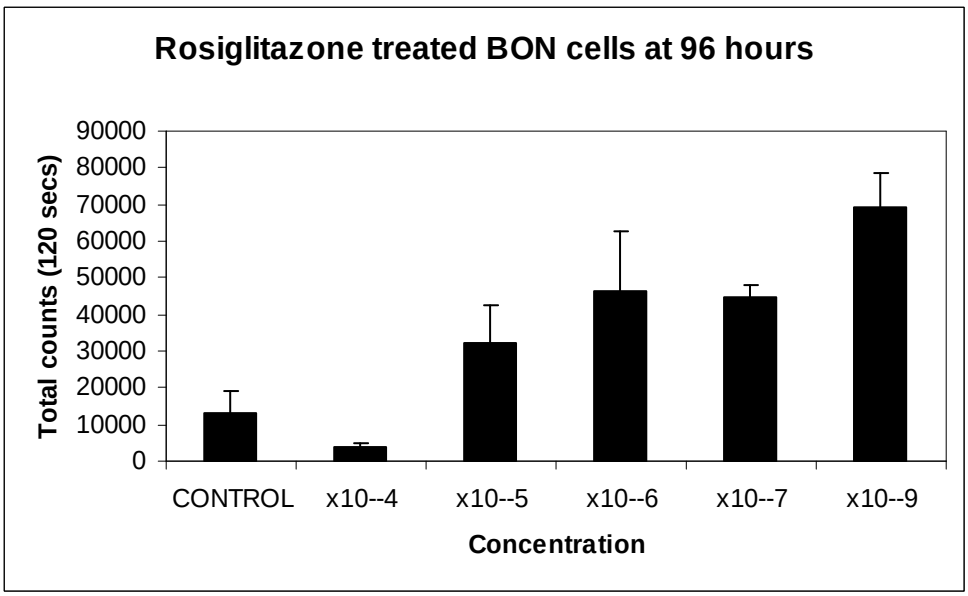

Figure 3.97 Graph showing variability in thymidine scintillation counts in BON cells following treatment of rosiglitazone for 96 hours probably due to cell death.

3.3.4.2 Combined results of proliferation studies with Rosiglitazone treated QGP1 cells

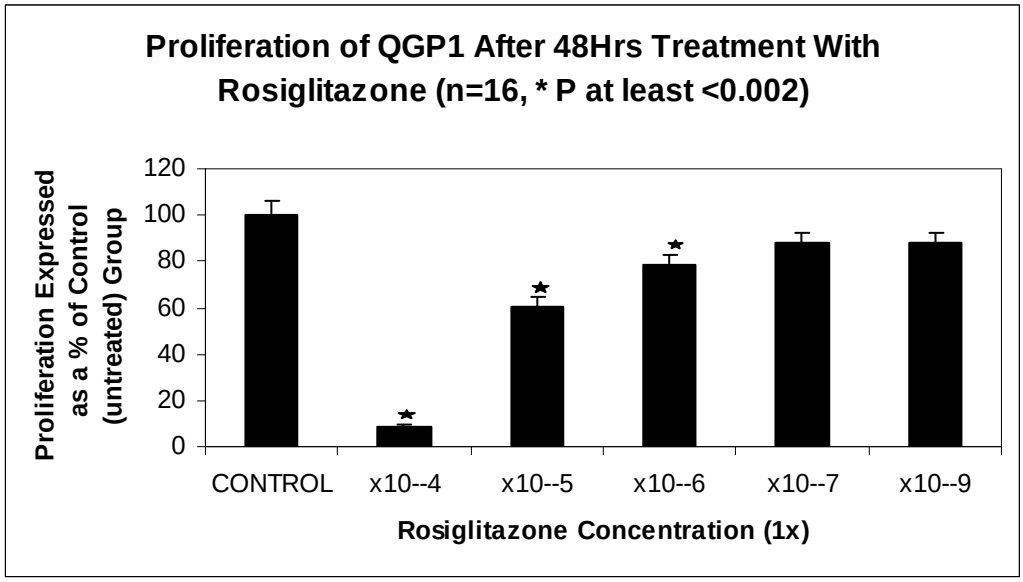

Figure 3.98 Graph showing a reduction in proliferation of QGP1 cells after 48 hours at higher concentrations of rosiglitazone

3.3.4.3 Combined results of proliferation studies with Rosiglitazone treated BON cells

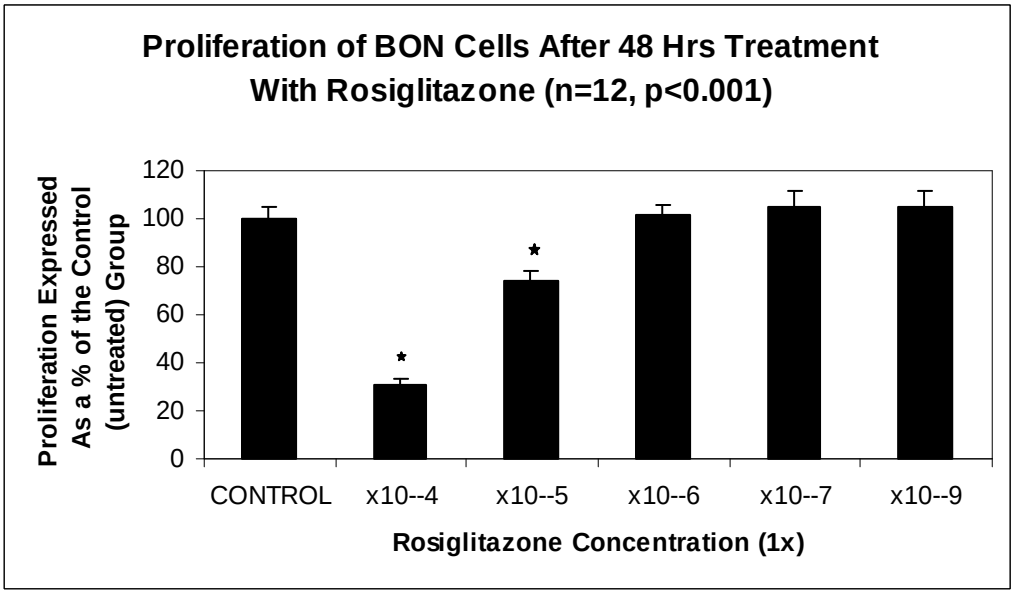

Figure 3.99 Graph showing a reduction in proliferation of BON cells after 48 hours at higher concentrations of rosiglitazone

3.3.4.4 Combined results of proliferation studies with Rosiglitazone treated CM cells

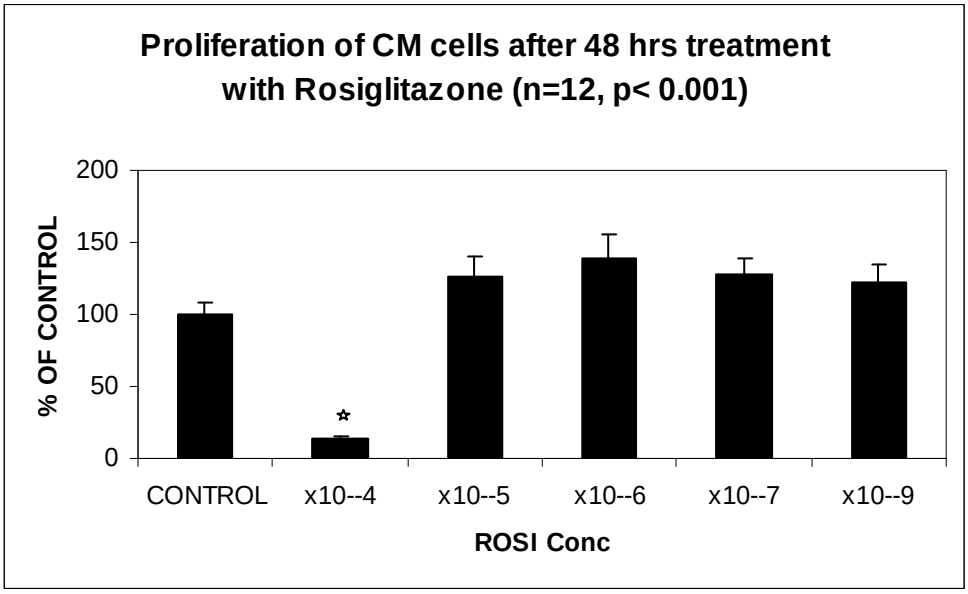

Figure 3.100 Graph showing a reduction in proliferation of CM cells after 48 hours of treatment at only the highest concentration of rosiglitazone

3.3.4.5 Proliferation studies with Dimethyl Sulfoxide (DMSO)

Dimethyl sulfoxide (DMSO) is a colourless liquid that is an important solvent dissolving both polar and non-polar compounds. Use of DMSO in medicine increased when it was discovered it could penetrate the skin and other membranes without damaging them carrying other compounds into a biological system. It is often used in PCR reactions and has been used as a cryoprotectant. It is thought to have a low toxicity.

Rosiglitazone was supplied in concentrated form and dissolved in DMSO. Subsequent dilutions to treatment dose levels in H_2O reduced the effective concentration of DMSO in the wells during the treatment periods, but we felt that an effect of the DMSO on the cells should be excluded.

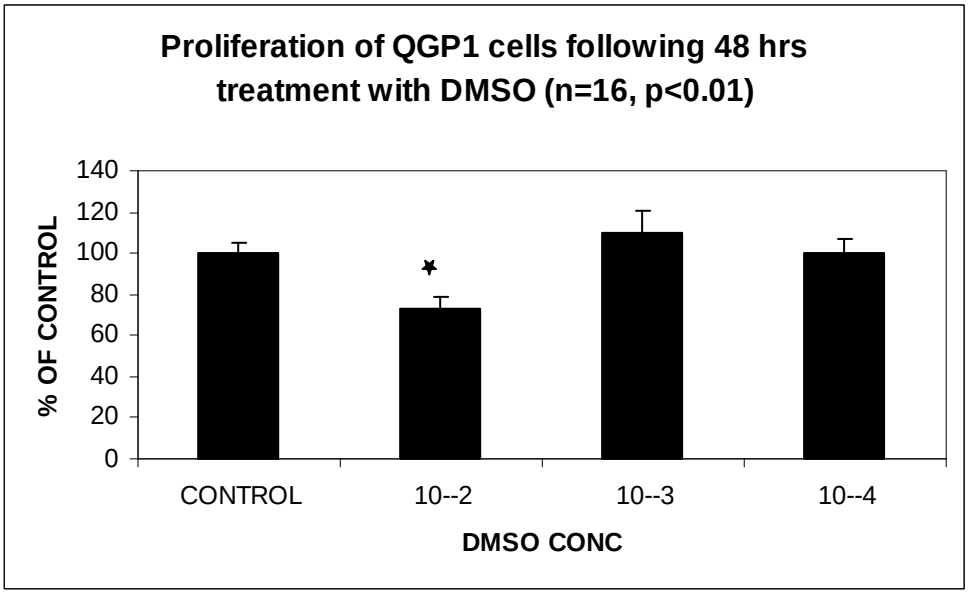

Figure 3.101 Graph showing the proliferation versus increasing DMSO dilutions of QGP1 cells after 48 hours of treatment. It can be seen that there is a significant reduction in proliferation at the highest concentration.

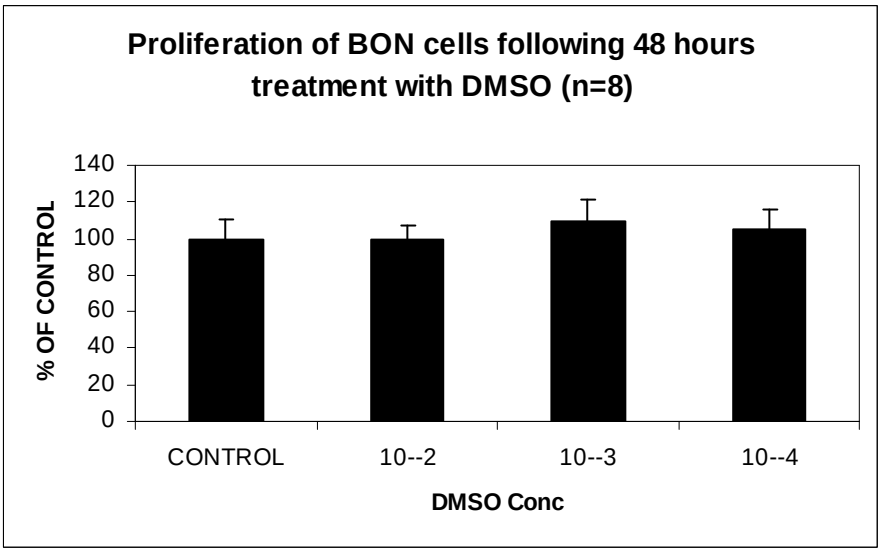

Figure 3.102 Graph showing the proliferation of BON cells after 48 hours of treatment with DMSO dilutions.

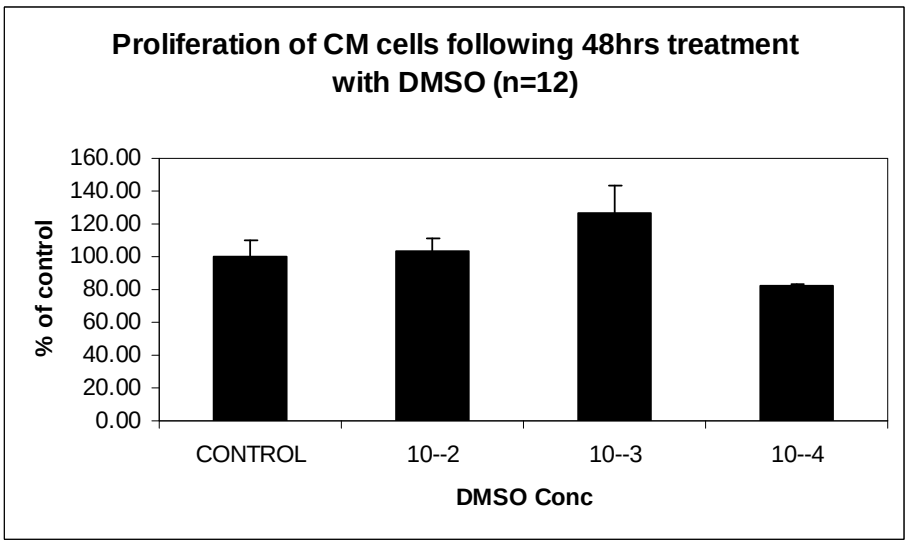

Figure 3.103 Graph showing the proliferation of CM cells after 48 hours of treatment with DMSO dilutions.

3.3.4.6 Rosiglitazone versus DMSO treatments on QGP1 cells

As it appeared that there might be an effect by DMSO on the QGP1 cells at the highest concentration, I was concerned that the effect seen could be solely due to the DMSO rather than the rosiglitazone. An experiment was set up where a comparison could be made. From the same harvest of cells two plates of QGP1 cells were set up. To one, treatment doses of rosiglitazone were added, to the other, comparative concentrations of DMSO. The cells were treated in exactly the same way and subjected to tritiated thymidine incorporation prior to the end of the experiment.

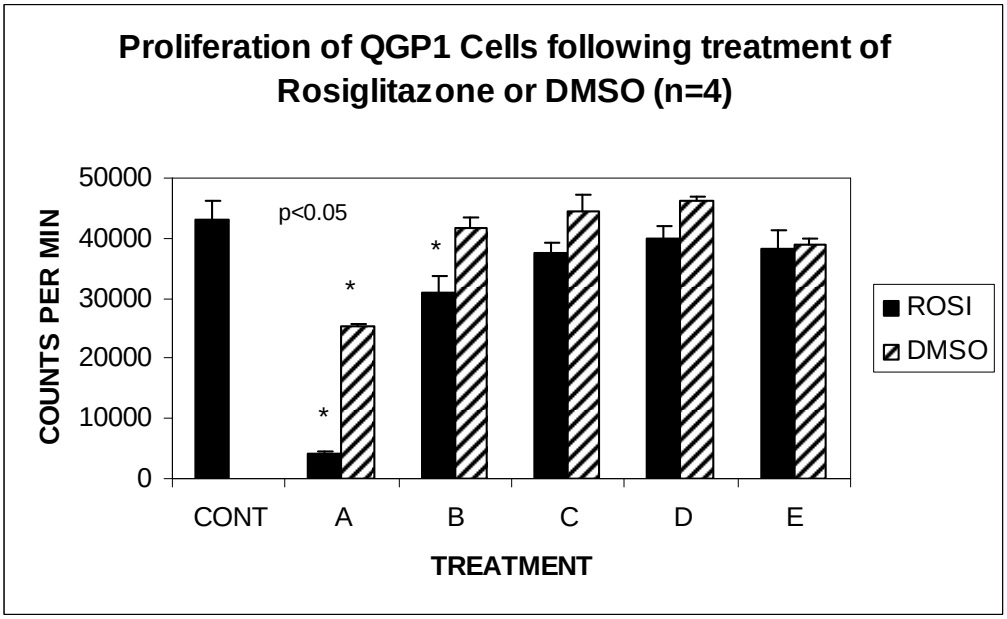

Figure 3.104 Graph showing direct comparison of the effects of DMSO compared to Rosiglitazone treatment

		Rosiglitazone	DMSO
Concentrations (M):	A	$1x10^{-4}$	$1x10^{-2}$
	B	$1x10^{-5}$	$1x10^{-3}$
	C	$1x10^{-6}$	$1x10^{-4}$
	D	$1x10^{-7}$	$1x10^{-5}$
	E	$1x10^{-9}$	$1x10^{-7}$

Kruskal-Wallis test	P =0.0075
Kruskal-Wallis: all pairwise comparisons (Conover-Inman)	
CONTROL and x10^{-4}M Rosi	P < 0.0001
CONTROL and x10^{-4}M DMSO	P = 0.0011
CONTROL and x10^{-5}M Rosi	P = 0.0035

In this experiment the expected pattern of inhibition of proliferation by the addition of rosiglitazone is seen in the 10^{-4}M and 10^{-5}M groups, with the 10^{-6}M group just missing statistical significance. With the DMSO group it is seen that there is no significant effect of DMSO in any of the treatment groups B to E. DMSO, therefore, maybe contributing partially to the anti-proliferative effects seen with rosiglitazone at 10^{-4}M concentrations in the QGP1 cell line.

3.3.5 Recovery studies

To ensure that the effects seen by rosiglitazone were reversible and not toxic to the cells, I decided to show recovery of cellular proliferation following removal of rosiglitazone.

Initial experiments were performed on the CM cell line. CM cells were treated with 10^{-4}M and 10^{-5}M concentration of rosiglitazone and treated for 48hrs as per usual protocols. Treatments were then washed off and the cells left in normal media for a further 48 hrs. As can be seen in figure 3.105, CM cells at 10^{-4}M concentration did not recover.

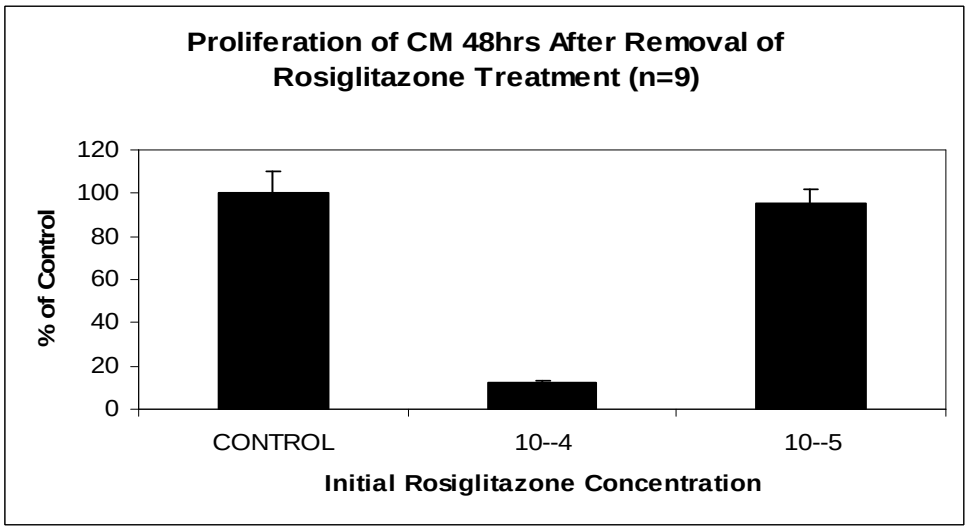

Figure 3.105 showing no recovery of CM cells following treatment and subsequent removal of 10^{-4} M rosiglitazone

The non recovery of the CM cell line, at the only concentration at which reduction in proliferation was seen with rosiglitazone treatment, led to significant concern that the anti-proliferative effects being seen were due to toxicity. I therefore set up more robust

experiments for BON and QGP1 cell lines to see whether the effects seen in these cell lines was due to toxicity of rosiglitazone.

The experiments were set up at the same time and date and from the same harvest of cell cultures to minimise error between groups.

First set was treated with rosiglitazone for 48 hrs and harvested

Second set was treated with rosiglitazone for 48 hrs then washed and left in normal media for a further 48 hours prior to harvesting.

Third set was treated with rosiglitazone for 96 hrs and harvested at the same time as set 2.

The first set is essentially a control to make sure that we see the expected effects of rosiglitazone treatment. The second set is the experimental group. The third set is another control group to identify that there is a continued effect of rosiglitazone treatment and that the cells do not spontaneously recover or escape from treatment effects.

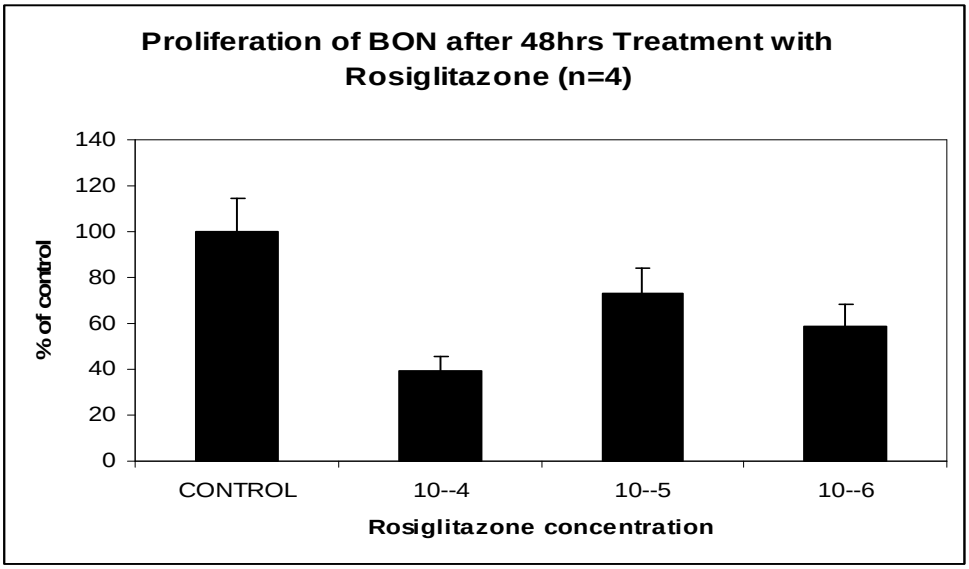
Proliferation of BON after 48hrs Treatment with Rosiglitazone (n=4)
% of control
140
120
100
80
60
40
20
0
CONTROL
10--4
10--5
10--6
Rosiglitazone concentration

A

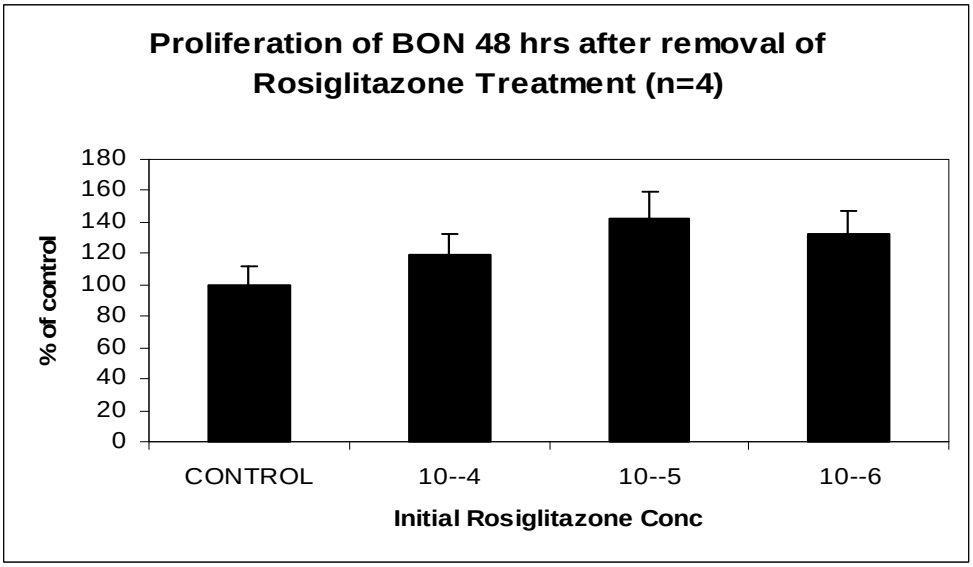
Proliferation of BON 48 hrs after removal of Rosiglitazone Treatment (n=4)
% of control
180
160
140
120
100
80
60
40
20
0
CONTROL
10--4
10--5
10--6
Initial Rosiglitazone Conc

B

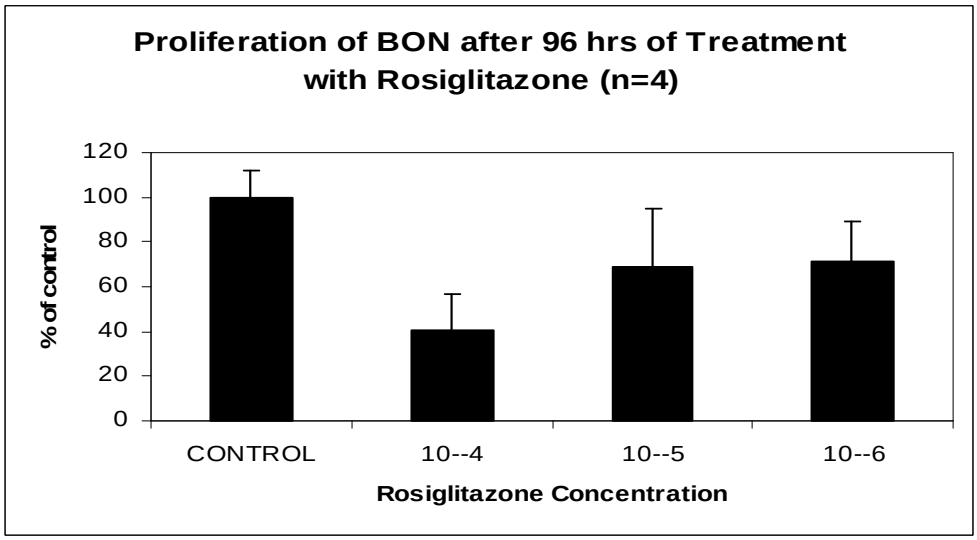

C

Figure 3.106 Graph A-C showing the expected pattern of proliferation in BON cells after 48 hours of rosiglitazone treatment (A) followed by full recovery following removal (B) and the continued reduction in proliferation if the treatment is left on for 96 hours (C)

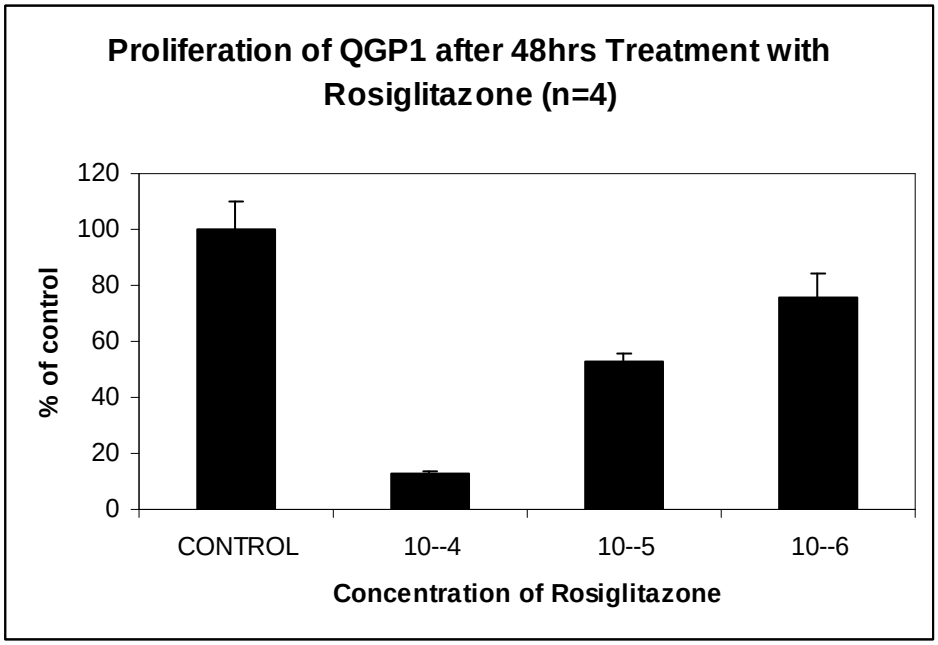
Proliferation of QGP1 after 48hrs Treatment with Rosiglitazone (n=4)
% of control
120
100
80
60
40
20
0
CONTROL
10--4
10--5
10--6
Concentration of Rosiglitazone

A

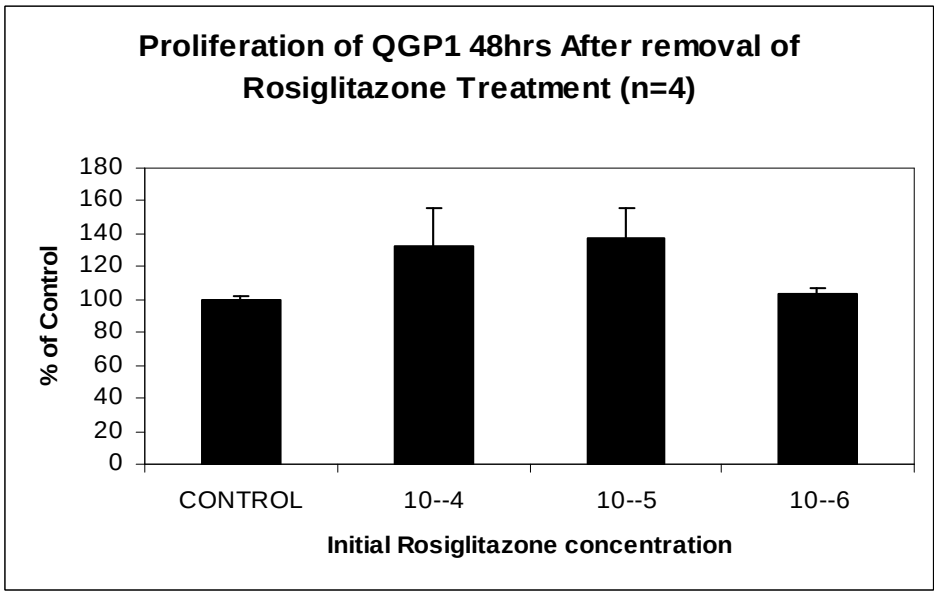
Proliferation of QGP1 48hrs After removal of Rosiglitazone Treatment (n=4)
% of Control
180
160
140
120
100
80
60
40
20
0
CONTROL
10--4
10--5
10--6
Initial Rosiglitazone concentration

B

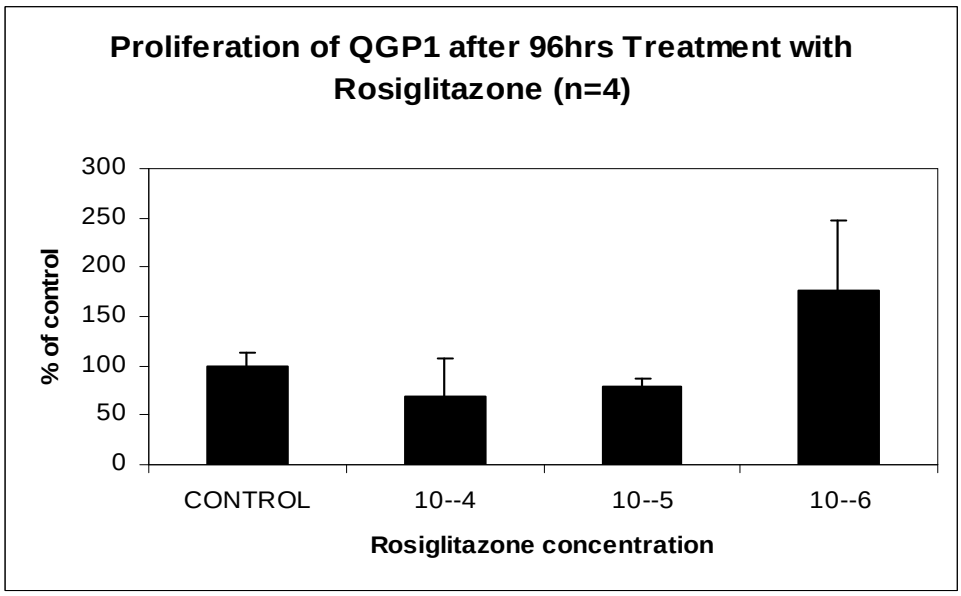

C

Figure 3.107 Graph A-C showing the expected pattern of proliferation in QGP1 cells after 48 hours of rosiglitazone treatment (A) followed by full recovery following removal (B) and the continued reduction in proliferation if the treatment is left on for 96 hours (C)

From the recovery studies it is seen that there is good recovery of both BON and QGP1 cells following removal of treatments. However, it appears that a toxic effect of rosiglitazone on CM cells cannot be ruled out. CM cells were therefore excluded from anatgonist experiments.

3.3.6 Antagonist Studies

We have shown that by adding rosiglitazone to cell lines BON and QGP1 at various concentrations, the proliferation of these cells can be reduced. We have also established that at the highest concentration of these treatments, the solvent in which the rosiglitazone is dissolved may also be having an additive effect. We have shown that by removing the treatments, washing and adding normal media to the treated cell lines normal cellular proliferation returns after 48 hours. To complete the PPARγ cell proliferation experiments I decided to try and prevent the effect of rosiglitazone by blocking the PPARγ receptors irreversibly, thereby confirming that the effects seen are mediated by PPARγ.

3.3.6.1 Results for QGP1 and BON with Antagonist T0070907

T0070907 antagonist (2-Chloro-5-nitro-N-(4-pyridyl)benzamide)
(Calbiochem-Novabiochem Corp., La Jolla, CA, USA).

T0070907 is a potent, specific, irreversible, and high-affinity antagonist of PPARγ with a K_i of 1 $x10^{-9}$M. It also displays >800-fold greater selectivity for PPARγ over PPARα and PPARδ (K_i = 0.85 $x10^{-6}$M and 1.8 $x10^{-6}$M, respectively).

A 1 $x10^{-6}$ M concentration of antagonist was used. Following standard plating and preparation, cells were pre-treated with the antagonist for 90 minutes prior to the addition of rosiglitazone. Incorporation of thymidine, harvesting and assessment of proliferation were performed as for previous experiments.

With antagonist treatment, there was still a significant effect on proliferation of QGP1 by the higher concentration of rosiglitazone. Effects of rosiglitazone at concentrations of 10^{-5}M and 10^{-6}M did however appear to be reduced.

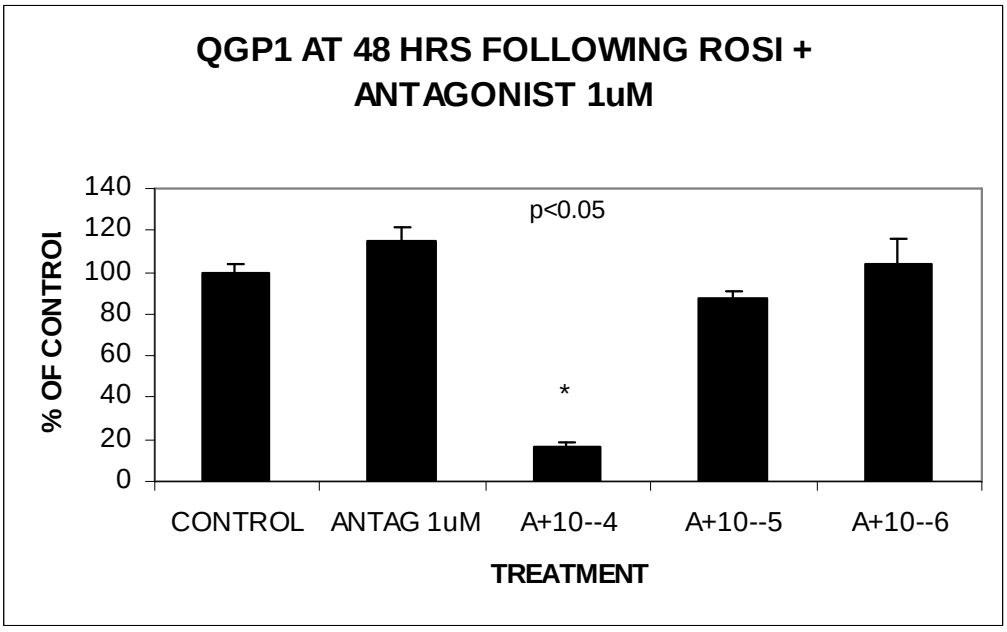

Figure 3.108 Graph showing the effects on proliferation of QGP1 cells following treatment with T0070907 antagonist and combinations of antagonist and rosiglitazone (n=4 for all groups)

Kruskal-Wallis test P=0.0104

Kruskal-Wallis: all pairwise comparisons (Conover-Inman)

CONTROL and ANTAG P = 0.1454

CONTROL and A+10^{-4}M P = 0.002

CONTROL and A+10^{-5}M P = 0.1235

CONTROL and A+10^{-6}M P = 0.6382

Similar findings were seen when BON cells were treated in the same manner with possible inhibition at lesser concentrations. A strong anti-proliferative effect was however still seen at the higher concentration of rosiglitazone.

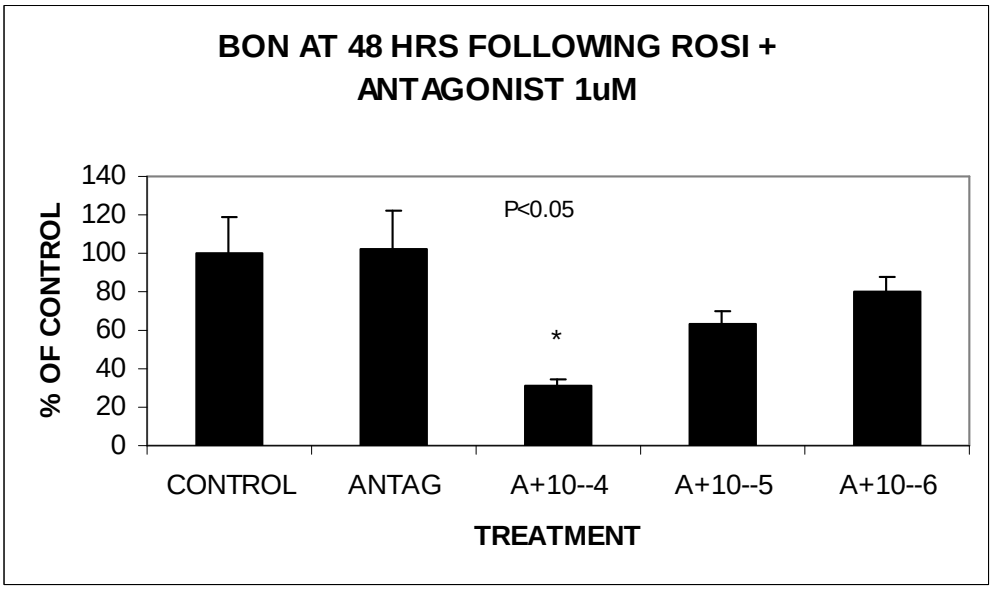

Figure 3.109 Graph showing the effects on proliferation of BON cells following treatment with T0070907 antagonist and combinations of antagonist and rosiglitazone (n=4 for all groups)

Kruskal-Wallis test	P=0.0176
Kruskal-Wallis: all pairwise comparisons (Conover-Inman)	
CONTROL and ANTAG	P > 0.999
CONTROL and A+10^{-4}M	P = 0.0007
CONTROL and A+10^{-5}M	P = 0.0535
CONTROL and A+10^{-6}M	P = 0.3114

It was felt that antagonism by T0070907 had not been fully successful. Further investigation was deemed necessary and a different antagonist was sought.

3.3.6.2 Results for QGP1 and BON with Antagonist GW9662

GW9662 antagonist (2-Chloro-5-nitro-N-phenyl-benzamide)

(Sigma, St Louis, Missouri, USA).

GW9662 is an irreversible PPARγ antagonist. GW9662 binds PPARγ with IC50 in nanomolar range, and is 10- and 600-fold less potent in binding PPARα and PPARδ, respectively.

Exactly the same methods were used as for previous treatments with antagonist T0070907. Following pre-treatment of QGP1 cells with GW9662, rosiglitazone was added at the concentrations shown. Cells were harvested at 48 hours and proliferation assessed by tritiated thymidine uptake.

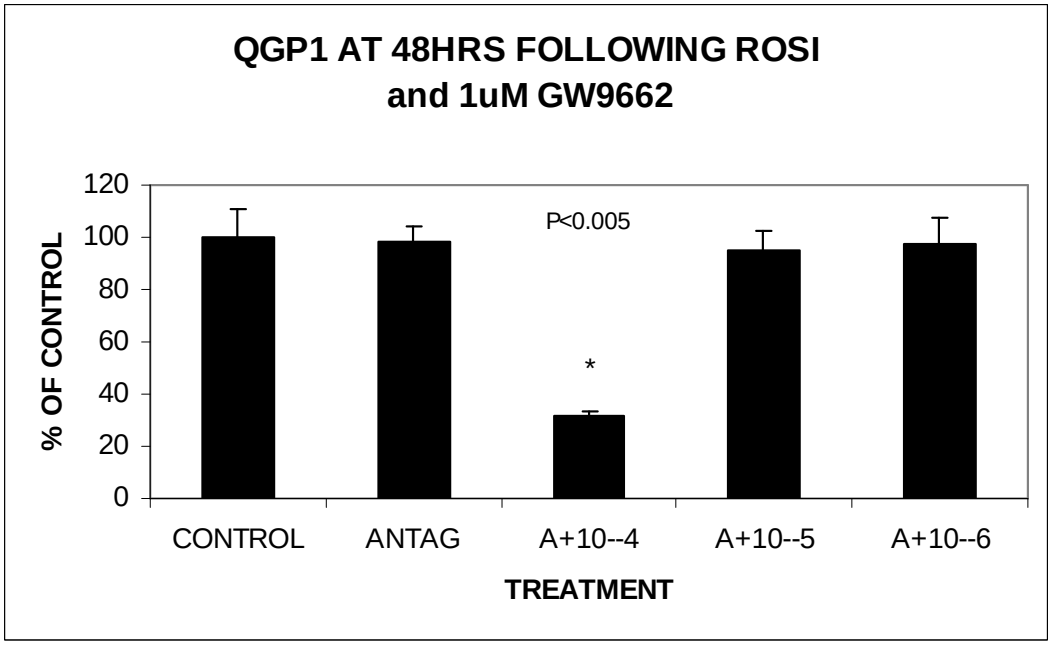

Figure 3.110 Graph showing the effects on proliferation of QGP1 cells following treatment with GW9662 antagonist and combinations of antagonist and rosiglitazone (n=8 for all groups)

Kruskal-Wallis test	P=0.0018
Kruskal-Wallis: all pairwise comparisons (Conover-Inman)	
CONTROL and ANTAG	P = 0.5474
CONTROL and A+10^{-4}M	P < 0.0001
CONTROL and A+10^{-5}M	P = 0.2114
CONTROL and A+10^{-6}M	P = 0.4359

Again only partial antagonism was seen with the anti-proliferative effect of the highest dose of rosiglitazone not being abolished. Experiments were repeated for BON and again only partial antagonism was seen.

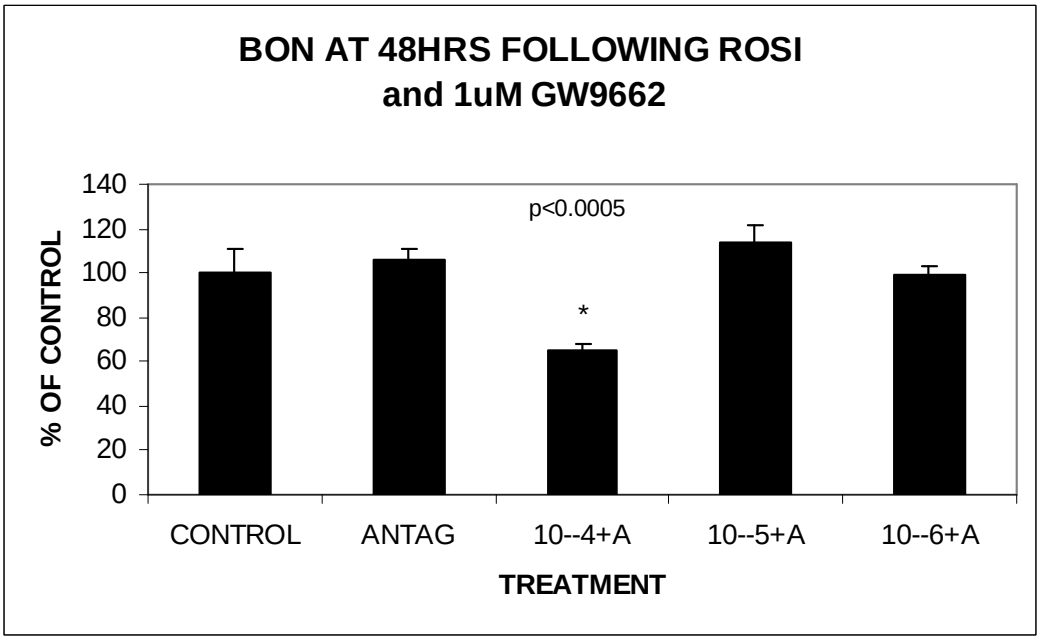

Figure 3.111 Graph showing the effects on proliferation of BON cells following treatment with GW9662 antagonist and combinations of antagonist and rosiglitazone (n=8 for all groups)

Kruskal-Wallis test P=0.0005

Kruskal-Wallis: all pairwise comparisons (Conover-Inman)

CONTROL and ANTAG P = 0.0799

CONTROL and A+10^{-4}M P = 0.0019

CONTROL and A+10^{-5}M P = 0.0521

CONTROL and A+10^{-6}M P = 0.6757

3.3.6.3 Direct comparison studies

So far all antagonist experiments had been run without a comparative treated group at the same concentration of rosiglitazone. It was felt that if the antagonist was having a true effect then there should be significant difference seen when cells treated with rosiglitazone are compared directly with cells treated with antagonist and rosiglitazone. Thus direct comparison studies were performed at rosiglitazone concentrations of 10^{-4}M, 10^{-5}M and 10^{-6}M.

For QGP1, there was no significant effect seen when the antagonist was added to the treatment group. At concentrations of 10^{-5}M and 10^{-6}M there was a possible trend seen towards antagonism with increased proliferation. Proliferation as a percentage of the non antagonised group was 109.7 +/- 12.6% in the 10^{-5}M group and 117.7 +/- 9% for the 10^{-6}M group. Neither was statistically significant from the treatment only group.

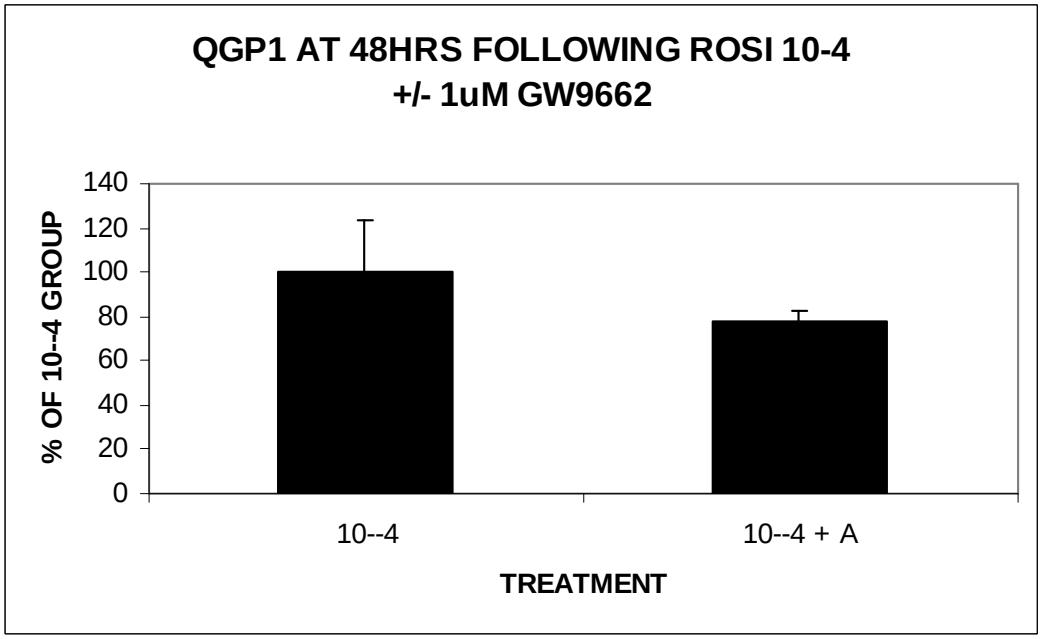
QGP1 AT 48HRS FOLLOWING ROSI 10-4
+/- 1uM GW9662
% OF 10--4 GROUP
140
120
100
80
60
40
20
0
10--4
10--4 + A
TREATMENT

A

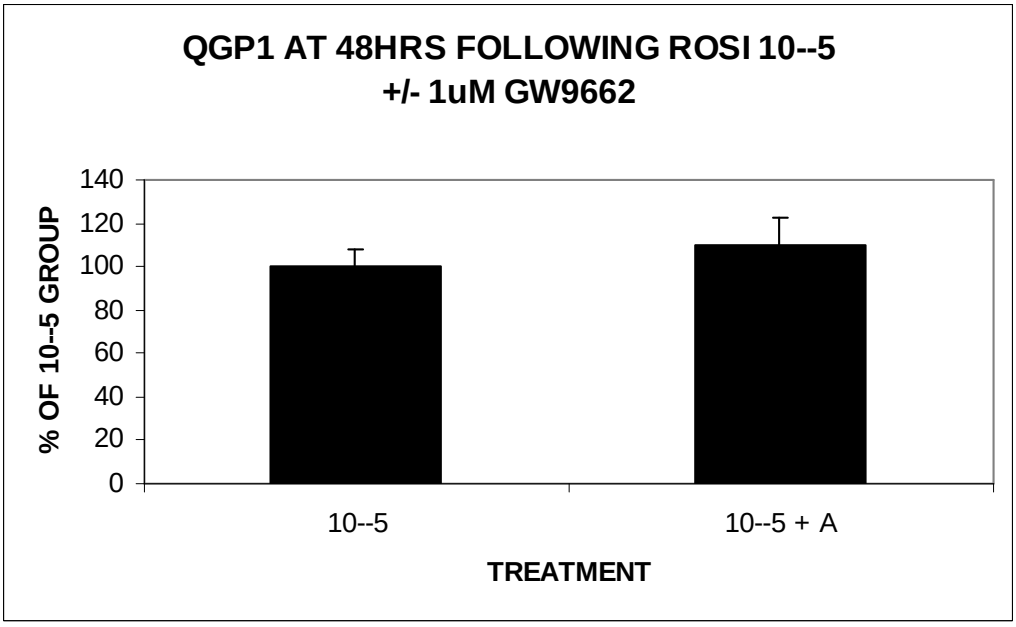
QGP1 AT 48HRS FOLLOWING ROSI 10--5
+/- 1uM GW9662
% OF 10--5 GROUP
140
120
100
80
60
40
20
0
10--5
10--5 + A
TREATMENT

B

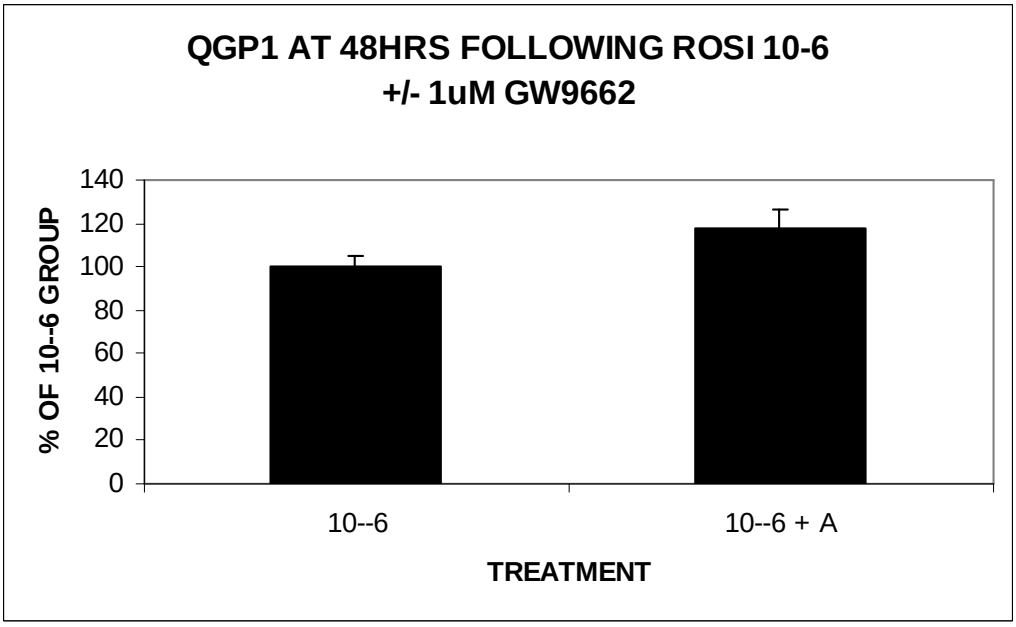

C

Figure 3.112 Graph A-C showing a direct comparison of proliferation of QGP1 cells treated with rosiglitazone at 10^{-4}M (A), 10^{-5}M (B) and 10^{-6}M (C) when one group is pre treated with the antagonist GW9662 (n=8, all groups)

A similar picture is seen with BON cells treated in the same way. There is a trend for increased proliferation on addition of the antagonist but the difference is not statistically significant. In the 10^{-4} M group, proliferation as a percentage of the non antagonised group was 127.3 +/- 11.8%. In the 10^{-5} M group, proliferation was 120.5 +/- 12.7%.

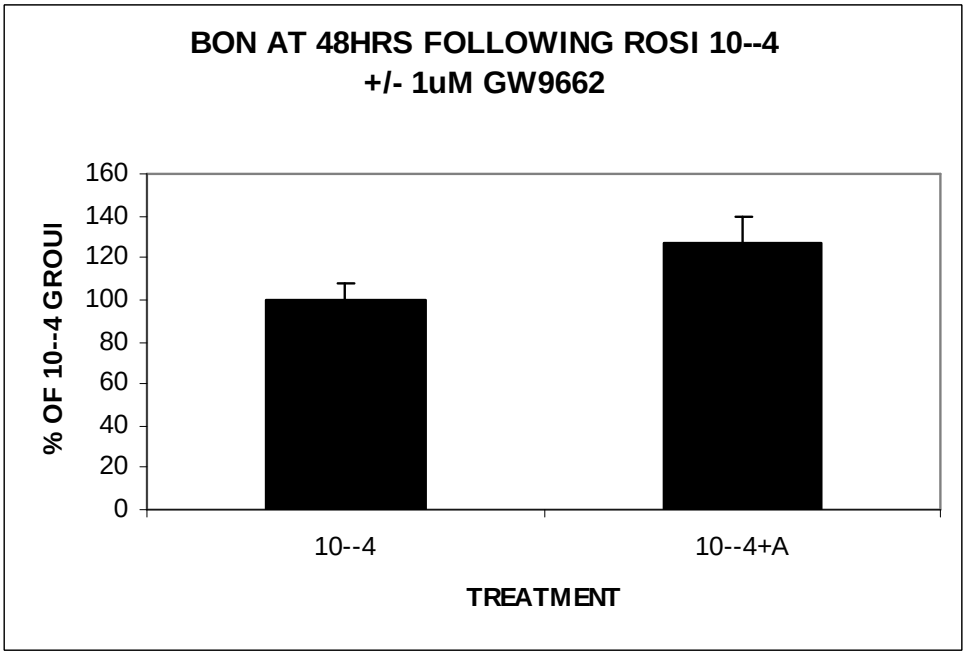

A

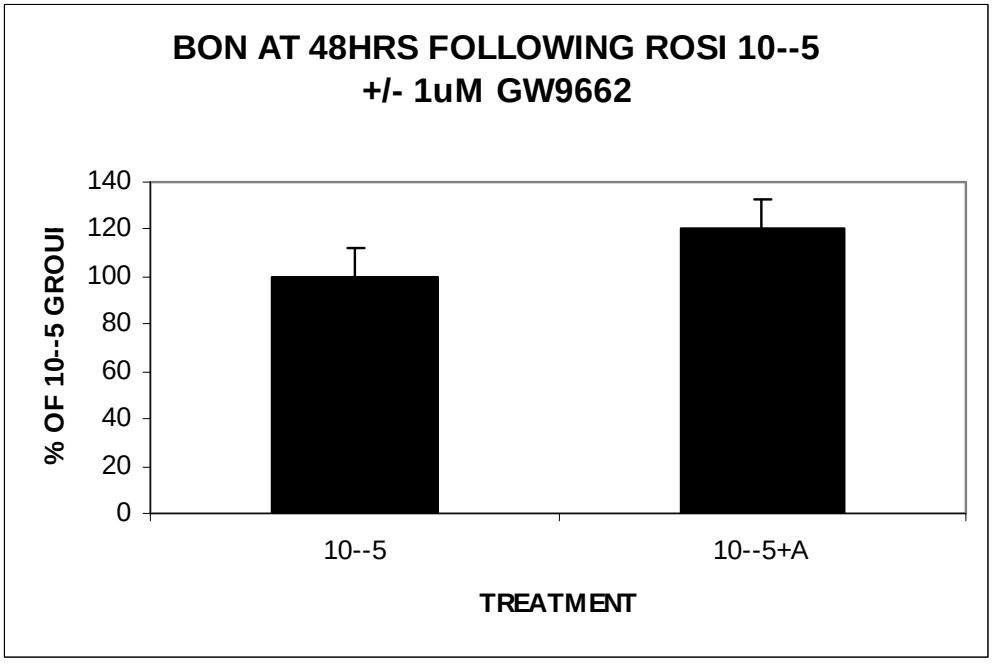

B

Figure 3.113 Graph A-B showing a direct comparison of proliferation of BON cells treated with rosiglitazone at 10^{-4}M (A) and 10^{-5}M (B) when one group is pre treated with the antagonist GW9662 (n=8, all groups)

At 1μM ($1x10^{-6}$M) concentration of GW9662 full antagonism of PPARγ receptors should be occurring. To remove any doubts regarding inadequate antagonist concentration the direct comparison experiments were repeated again for both QGP1 and BON with a concentration of 10μM GW9662 (results not shown). Again, proliferation was not significantly increased with addition of the antagonist.

CHAPTER 4

DISCUSSION

4.1 Human Pancreatic Tumours

At the outset of the project, there was a selection of pancreatic neuroendocrine tumours held in the 'tumour bank' within the Academic Department of Endocrinology at St Bartholomew's Hospital. My initial aim was to use these tumour samples for extraction of RNA and subsequent PCR work to look at PPARγ expression. Further studies planned involved PCR (conventional ± real time) to identify any variations in other cell cycle markers. Unfortunately, it was found that there were too few samples that gave good quality reliable RNA for any substantial results to be gained. Attempts at gaining further fresh tissues samples led to the submission for ethical approval for collection and work on fresh tissue samples from two sites, including The Hammersmith Hospital (with the help of Professor A Grossman and Mr John Lynn respectively). Although agreement was gained in principle the incidence of resection was too low, even across two sites, for this to become viable given the time constraints of the project. Further work on human tissue samples was therefore halted.

All human tissue samples available to us were subjected to RNA extraction, reverse transcription and PCR for GAPDH and PPARγ. Of the eight subjects (5 insulinomas and 3 gastrinomas) PPARγ expression was identified variably in the majority. The simple interpretation of this finding is that PPARγ is expressed in the majority of insulinomas and gastrinomas. This suggests that the majority of insulinomas and gastrinomas may be susceptible to the effects of ligands of this receptor such as the thiazolidinediones. Ultimately, proliferation could be affected by interaction with this receptor. There is good evidence to suggest that the thiazolidinediones, such as rosiglitazone, can reduce the proliferation of certain types of cancers of adipose tissue (Tontonoz et al, 1997), colon (Sarraf et al, 1998), breast (Mueller et al, 1998), prostate

(Mueller et al, 2000), liver (Rumi et al, 2001), lung (Tsubouchi et al, 2000), and pancreatic acinar tissue (Elnemr et al, 2000). Most of these models are non-human but there is also evidence extending into human tumours such as liposarcoma (Demetri et al, 1999) and prostate cancer (Mueller et al, 2000).

A further aspect of the tissue collection also has to be considered: as samples were taken prior to the start of the project, there is no way that I can guarantee that samples were harvested correctly and only contain tumour, i.e. it is possible that samples could inadvertently contain normal pancreas along with tumour taken at the time of resection. This contamination would weaken the power of the study.

4.2 Immunohistochemistry

The aims of the immunohistochemistry work were multiple. Firstly, I wanted to confirm the presence of PPARγ within the chosen samples, then identify its cellular location, and quantify the strength of staining for each tissue type (insulinoma, gastrinoma, islet and exocrine pancreas). Subsequently, I wished to compare the different tissues types against each other, using total positive counts for both nuclear and cytoplasmic compartments. This procedure was then repeated using antibodies for p27, phospho-p27, JAB 1, phospho-Akt and PTEN, all previously implicated in the development of endocrine tumours (Lidhar et al 1999, Kouvaraki et al 2006, Stanger et al 2006, Schleiman et al 2003, Altomare et al 2002) and compare the expression of these proteins with PPARγ levels.

Regarding PPARγ expression in exocrine tissue and islets, I was unable to demonstrate any significant nuclear or cytoplasmic expression. This was confirmed with repeated

experiments. Good staining of positive controls suggested that the antibody was working correctly and staining had been optimised appropriately. That we could not show significant PPARγ expression in the islets is in contradiction to previous reports of high expression (Dubois et al 2000). Significant islet cell hyperplasia has been shown in mice models in which the expression of the PPARγ gene in β cells has been eliminated (Rosen et al 2003) suggesting both presence and a significant anti proliferative effect. PPARγ expression has also been shown in human pancreatic cancer cell lines Capan-1, AsPC-1, BxPC-3, PANC-1 and MIA PaCa-2. My results, therefore, were unexpected.

My expectation that PPARγ would be widely expressed in these tissues was not supported by my findings. In the absence of significant previously published data in this area, my preliminary conclusions are that PPARγ is only expressed at very low levels in these tissues.

Following Ki-67 analysis of the samples, it was clear that there were several tumours that were proliferating at a higher rate. I thought it was of interest to separate these tumours out from the lesser proliferating tumours to see if there was any difference in the expression of PPARγ. Although statistical significance was not achieved in the PPARγ group, due to the low numbers, there was certainly a trend showing that higher proliferating tumours express PPARγ in greater proportion.

The CDK inhibitor p27 is a tumour suppressor protein that acts in the nucleus to enforce cell cycle checkpoints. p27 inhibits and binds to many cyclin/CDK complexes, including cyclin D/CDK4, cyclin E/CDK2, and cyclin A/CDK2. This inhibition can block progression through different phases of the cell cycle. The known actions of p27 are thus predominantly nuclear with expectation that localisation is similar. It has been

documented, however, that translocation of p27 from the nucleus to the cytoplasm and loss of p27 through proteasomal degradation can occur in certain cancers, including breast, prostate, gastric, lung, ovarian, pancreatic, and hepatocellular carcinomas. The status of p27 may be a predictor of patient outcomes in these cancers (Viglietto et al, 2002 , Nikoleishvili et al, 2008, Claudio et al, 2002, Gamboa-Dominguez et al, 2007, Pateras et al, 2006, Qin et al, 2001).

In this p27 series, staining was seen in both the nucleus and cytoplasm. p27 staining was predominantly cytoplasmic in all three endocrine tissues (insulinoma, gastrinoma and islets - significantly so in gastrinoma and islets). Exocrine pancreas showed slightly higher nuclear than cytoplasmic expression, but both at much lower levels than that of the endocrine tissues. There are two main points of note with these results. Firstly, it appears that there is significantly higher expression of p27 within all three endocrine tissues compared to exocrine pancreas, suggesting a more significant role for p27 within these tissue types. Secondly, the expected p27 expression is, in general, nuclear and although my findings show that there is a high level of nuclear expression of p27 there is also a high level of cytoplasmic staining.

As mentioned above, re-localisation of p27 into the cytoplasm has been seen in various cancers, with the assumption that the inhibitory effects of p27 on cell cycle progression are reduced. Is it possible that we are seeing a re-localisation in our samples? This is unlikely for two reasons. Cytoplasmic staining does not appear to be high at the expense of nuclear staining – both show high levels. It may also be expected, that on direct comparison of the tissues, there would be lower nuclear and higher cytoplasmic expression in neoplastic tissues compared to benign tissues. This was not the case, with no difference found in the nuclear expression of p27 between insulinoma and islets, and

conversely, there was significantly lower expression of p27 in the cytoplasm of insulinoma.

It has previously been reported that p27 is inversely related to Ki-67 index in a number of endocrine tissues (Lloyd et al 1997). With separation of the insulinoma group by Ki-67 labelling, lower p27 expression was seen in both the nucleus and cytoplasm of samples with a higher Ki-67 index. This finding concurs with the idea that p27 is reduced in more highly proliferating tumours.

In a study by Canavese et al (2001), immunohistochemical p27 expression in 109 endocrine tumours of the pancreas and gastro-intestinal tract (pancreas tumours included 17 insulinoma, 10 gastrinoma and 5 glucagonoma) was compared with Ki-67. They too concluded that p27 expression was inversely related to Ki-67 labelling. Interestingly, however, they also found that the vast majority of pancreatic neuroendocrine tumours, both benign and malignant, were highly expressing p27 (usually between 70-100%) and no difference in p27 expression could be seen between normal (islets), hyperplastic and corresponding tumours. Similarly, in a study by Guo et al (2001), increased p27 expression was seen in both benign and malignant neuroendocrine tumours of the pancreas and four pancreatic islet tumour cell lines as assessed by Western analysis. No difference was seen between benign and malignant tumours.

Other investigators have reported anomalous over-expression of p27 in human tumour tissues. This includes Burkitt's lymphoma and diffuse large B-cell lymphoma (Sanchez-Beato et al, 1999), thyroid tumours (Baldassarre et al 1999), oesophageal squamous cell carcinoma (Anayama et al, 1998), and node-negative breast carcinoma (Reed et al

1999). Some of the possible mechanisms proposed by the authors include inactivation of p27 by cyclin D3, abnormal sequestration of p27 in the cytoplasm and dysregulation of cyclin D1 expression.

Phosphorylation is a key mechanism which p27 undergoes prior to transport out of the nucleus and degradation. If p27 deactivation was a significant feature of pancreatic neuroendocrine tumours, enhanced transport out of the cell and increased phospho-p27 levels in the cytoplasm may be expected. In this study, phospho-p27 expression has been shown to be overwhelmingly cytoplasmic in all tissue types. Very little nuclear staining was identified and there were no differences between the three endocrine tissues. In our JAB1 series, all tissues overwhelmingly showed cytoplasmic expression, with negligible nuclear staining seen. Interestingly, normal islets showed the strongest positive cytoplasmic staining for JAB1, significantly higher than either insulinoma or gastrinoma, quite the opposite to the idea that neoplastic tissues would have enhanced p27 transport into the cytoplasm. Interpretation of my results would therefore not support enhanced p27 phosphorylation and shuttling out of the nucleus in the aetiology of pancreatic neuroendocrine tumours.

The protein kinase Akt, also known as protein kinase B (PKB), plays a pivotal role in tumourigenesis (Testa et al, 2001). Akt is activated by phospholipid binding and phosphorylation at threonine 308 by PDK1 and phosphphorylation within the C-terminus at serine 473. Through the phosphorylation and relocalisation of key regulatory molecules such as Bad (Datta et al, 1997), caspase-9 (Cardone et al, 1998), forkhead transcription factors (Brunet et al, 1999), p21 (Zhou et al, 2001) and p27 (Shin et al, 2002), phospho-Akt (p-Akt) functions to promote cell survival by inhibiting apoptosis. Cytoplasmic relocalisation of p27 secondary to Akt mediated

phosphorylation at threonine 157 has been shown in human primary breast cancer (Viglietto et al, 2002, Shin et al 2002). In the pancreas, transgenic mice that express a constitutively active Akt/PKB have been shown to have a significant increase in islet cell mass, due largely to proliferation of insulin containing β cells (Bernal-Mizrachi et al, 2001).

In all four tissue types, both nuclear and cytoplasmic staining was seen for p-Akt. Cytoplasmic expression was significantly higher than nuclear expression in all tissues. On comparing the tissues, there is significantly lower nuclear and cytoplasmic expression of p-Akt in insulinoma and gastrinoma compared to islets. This is contrary to the expected finding that neoplastic tissues will have higher levels of the pro-survival p-Akt, and suggests that the phosphoinositide-3-kinase (PI3K)-Akt pathway is unlikely to play a major role in pancreatic neuroendocrine tumours

PTEN is a tumour suppressor gene and is thought to negatively control the PI3K-Akt pathway. Over-expression of PTEN with subsequent influence on the expression of p-Akt would identify this pathway as important in tumourigenesis of pancreatic neuroendocrine tumours. Although there is a high degree of nuclear expression seen, no significant difference was identified between the neoplastic cells of insulinoma and gastrinoma, and that of normal islets.

Regarding exocrine tissue, there appears to be a fundamental difference compared to the endocrine tissues. Although, the pattern of staining has been similar, there are significantly reduced levels of expression of nearly all the cell cycle markers tested. With the exclusion of PPARγ, where no tissue showed significant expression, exocrine tissue has consistently shown lower expression of p27, phospho-p27, JAB 1, Phospho-

Akt and PTEN compared to all three endocrine tissues whether benign or neoplastic. Higher levels of expression in the endocrine tissues suggest that these cell cycle participants are more important in the cell cycling of the endocrine tissues

Despite the potential of these cell cycle participants in dysregulation, the results have not been able to support a significant role for p27, its phosphorylation or mislocalisation in the tumourigenesis of these tumours. Cellular p27 effects can be modulated by cell cycle pathways involving PTEN and PI3K/Akt, which have been previously implicated in tumourigenesis. My evidence again, does not support direct involvement of these pathways in our series. The high levels of expression without evidence of direct involvement may suggest increased expression secondary to alternate pathways as yet unclarified.

During the course of the experimental work, insulinomas have been compared to the islets, being considered its control. This has been widely accepted as pancreatic islet cell tumours show marked cytological similarity to pancreatic islets and are therefore believed to originate from the endocrine pancreas. It is of interest therefore that Vortmeyer et al (2004) et al, have suggested that pancreatic islet cell tumours do not necessarily originate from islets. In MEN 1 patients with characteristic allelic deletions, microdissection of the tumour, surrounding acinar/ductal pancreas and islets revealed similar abnormalities present in the acinar/ductal samples but not in the islets, concluding therefore that the islets are not the origin. Use of islets as control could therefore be called into question. My immunohistochemical findings showed a high degree of similarity and behaviour between these two tissue types and comparison is still valid, in that, differences noted may be indicative of differences between neoplastic and benign behaviour. The importance of this potential embryological difference is,

however, noted. Methodological and theoretical difficulties in harvesting nearby acinar/ductal tissue and justifying its use as control material, maybe difficult to overcome and it is felt that this was beyond the time constraints of this project.

4.3 Cell Proliferation

Human neuroendocrine tumour cell lines CM (insulinoma), BON (carcinoid) and QGP1 (somatostatinoma) were made available to us due to the kindness of Professor N Lemoine. As for the resected tumour and immunohistochemistry series, I initially investigated the expression of PPARγ within the cell lines. All cell lines gave good quality RNA and underwent conventional PCR for PPARγ. I confirmed that both BON and QGP 1 expressed PPARγ mRNA but CM cell line did not. All cell lines were, however, subject to Western blotting to confirm protein expression. Interestingly, all cells lines showed evidence of PPARγ protein expression including the CM cell line. Repeated RNA extraction and PCR, with similarly repeated protein extraction and Western blotting failed to clarify this inconsistency. The possibility of the discrepancy being due to a splice variant was considered. Splice variants have been identified and characterised (Chen Y, Jimenez A, Medh J, 2006). Personal communication with Dr J Medh confirms that the discrepancy is unlikely to be due to a splice variant. The primers are in the region of exons 1-6 which is common in all splice variants. On balance, it is the opinion of the author that CM cell line does not express PPARγ mRNA and consequently should not express PPARγ protein.

It is also of interest that the validity of the CM cell line as a true insulinoma cell line has recently been called into question (Gragnoli, 2008), as various severe and consistent chromosomal aberrations were identified including chromosome 11 tetraploidy and

translocation abnormalities. Jonnakuty and Gragnoli (2007) karyotyped the CM celll line and confirmed its human origin but also identified 64 chromosomes with structural abnormalities. This information may have significant bearing on the reliability of this study as it has to be acknowledged that the cell lines are not truly immortalised and therefore are subject to potential phenotypic instability over time.

Somatostatin inhibits cell proliferation and growth hormone secretion through interaction with SSTRs. Five SSTRs have been cloned in the human, mouse, and rat; and many studies have investigated the tissue distribution, expression, binding affinity to somatostatin, and downstream signal transduction pathways of these five receptors (Benali et al 2000, Fisher et al, 1998). My cell lines were subjected to RNA extraction and PCR for all 5 SSTRs to identify expression patterns. The results failed to confirm expression of any of the SSTRs in any of the cell lines. Plans for cellular proliferation studies following treatment of somatostatin analogues was therefore excluded from the project. One possible explanation for lack of expression may be that the cell lines have undergone too many passages and they have lost normal expression patterns.

In fact, loss of SSTRs in pancreatic cancers is not unique. Although both in vitro and in vivo studies have shown that SSTRs mediate strong growth inhibition in many cancer types including pancreatic cancer, previous clinical trials of somatostatin analogues in the treatment of advanced pancreatic cancer have failed (Canobbio et al, 1992). A review of the current knowledge of somatostatin, its receptors and pancreatic cancer has been published by Li et al (2005). They suggested that further detailed studies are needed to determine the reason why functional SSTRs are not expressed or not sufficient in pancreatic cancer cells.

PPARγ agonists have been shown to have anticancer activity against a variety of neoplastic cells in vitro. Liposarcoma, colon, breast, prostate, thyroid, myeloid leukaemia, lymphoma, lung, oesophageal, gastric, glioblastoma and pancreatic cancer cells have all variably been shown to have reduced growth in the presence of PPARγ ligands. In vivo studies are much less common. Originally, the identification that ligands of PPARγ could induce terminal differentiation in normal preadipocytes lead to attempts to induce differentiation of human liposarcoma cells, both in vitro and in vivo. Demitri et al (1999) gave the TZD troglitazone to a series of patients with liposarcoma which resulted in a retardation of growth and induction of differentiation in these tumours. Additionally, treatment of patients with advanced prostate cancer with troglitazone has shown to cause a high incidence of stabilization of prostate- specific antigen (Mueller et al. 2000). Sarraf et al (1998) showed that trogligazone decreased the growth of colon cells in vitro as well as when growing as xenographs in nude mice.

In contrast to PPARα knockout mice, PPARγ ablation is lethal. Initial attempts to generate a PPARγ knockout mouse model showed that null embryos die at about day 10 from impaired placental development (Barak et al, 1999). Subsequently the heterozygous state and tissue specific models have been developed (Review by Gray et al 2005). Rosen et al. (2003) generated a tissue specific β-islet cell mouse model in which the expression of the PPARγ gene in β-cells was eliminated (βγKO mice). These mice were found to have significant islet cell hyperplasia compared to control. Interestingly, the islets did not proliferate indefinitely suggesting that other growth regulating factors eventually come into play. This may also explain why tumour formation in the islet tissue of βγKO mice was not observed.

Most research has, of course, been directed at the metabolic consequences of PPARγ knockout models but several studies have concentrated on the potential effects on tumour formation. Heterozygous germ line deletions of PPARγ ($PPAR\gamma^{+/-}$) have been shown to be more susceptible to the formation of colonic tumours. After the injection of the colon specific carcinogen azoxymethane, all of the PPARγ +/- mice but only 50% of the wild type were dead from colonic cancer by 36 weeks (Girnun et al. 2001). Heterozygous $PPAR\gamma^{+/-}$ mice have also been shown to have a greater susceptibility to develop both breast and ovarian cancers after exposure to the carcinogen 7,12 dimethylbenzanthracene suggesting a potential protective effect of PPARγ. Lu et al (2005), utilisised heterozygous $PPAR\gamma^{+/-}$ mice to show a significant increase in susceptibility to N-methyl-N-nitrosourea induced gastric cancer compared to the wild type at 10 weeks (89.5% vs 55.5%). In the same experiments, simultaneous administration of troglitazone showed a significant reduction in incidence of gastric cancer in the wild type (55.5% to 9%) with a reduced effect seen in the heterozygous $PPAR\gamma^{+/-}$ group (89.5 to 80%). They concluded that PPARγ suppresses gastric carcinogenesis, troglitazone is chemopreventative and dependent on the PPARγ receptor.

Methods of examining overexpression of PPARγ have been developed. Garcia-Bates et al. (2008) used a lentiviral vector for PPARγ gene delivery and transduced multiple myeloma cells. Overexpression decreased multiple myeloma cell proliferation and induced spontaneous apoptosis even in the absence of an external ligand. The cells were also much more sensitive to ligand induced apoptosis. Bren Mattison et al (2008) developed transgenic mice after construction and administration of SP-C/PPARγ transgene. Mice were then subjected to injection of a standard intraperitoneal dose of urethane, a lung carcinoma carcinogen. After 20 weeks there was a 75% reduction in the

number of tumours identified in the PPARγ over expressing mice. In contrast to the predominantly protective effects seen with PPARγ, a transgenic mouse model has shown breast cancer tumours with accelerated kinetics. Saez et al. (2003) generated a transgenic mouse model that expressed a constitutionally active form of PPARγ by fusing the activation domain of herpes simplex virus Vp16 protein to PPARγ1. The effect of mammary specific VpPPARγ expression was evaluated by generating transgenic mice expressing it under the control of mouse mammary tumour virus (MMTV) promoter. These MMTV-VpPPARγ mice were morphologically identical to the wild type. On breeding with a known breast cancer mouse (MMTV-PyV), PyV/VpPPARγ females developed tumours with greatly accelerated kinetics and reduced survival.

Currently, I am unaware of any reported cellular proliferation studies on human neuroendocrine tumour cell lines investigating the effects of PPARγ agonists. Following a period of optimisation all three cell lines were treated with varying doses of rosiglitazone. Effects on CM cell line were limited to the highest concentration (10^{-4}M) of rosiglitazone. Effects on BON were seen at the two highest concentrations (10^{-4}M and 10^{-5}M) whereas QGP1 cells are shown to be the most sensitive been affected upto concentrations of 10^{-6}M. The potential role of DMSO having a toxic effect on the cell lines that would explain the findings was excluded, except at the highest concentration of rosiglitazone treated QGP1 cells. BON and QGP1 cell lines (CM not being tested) recovered following a period of treatment with rosiglitazone confirming that the effects were mediated by the treatment and that treatment effects were not ultimately life threatening to the cells. There is no toxicity data published on the antagonists T0070907 and GW9662 by the manufactures and an internet search has not revealed any evidence that the antagonists have a direct toxic effect on cell cultures.

PPARγ antagonist studies were performed on BON and QGP1 to identify whether the effects of rosiglitazone on these cell lines could effectively be blocked, thus confirming that the effects seen are mediated by the PPARγ receptor. Unexpectedly, the effects could only be partially blocked. This was then confirmed by treatment with a second antagonist and subsequent direct comparison studies. These studies did not show any significant increased proliferation in the group pretreated with the PPARγ antagonist. I conclude therefore that the PPARγ agonist rosiglitazone has a significant anti-proliferative effect on both BON and QGP1 cell lines but it appears that this effect may not be mediated by the PPARγ receptor. Similar findings have been reported in pituitary cell lines treated with rosiglitazone (Emery et al, 2006) and pancreatic adenocarcinoma (Galli et al, 2004). Indeed, evidence that the anti-proliferative effects of TZDs are independent of PPARγ receptor has been published (Palakurthi et al 2001) where tumour bearing mice injected with either PPARγ $^{-/-}$ or PPARγ$^{+/+}$ embryonic stem cells were treated with troglitazone. Tumour suppression was seen similarly in both mouse models suggesting an anti-proliferative effect of troglitazone, but one that is independent of the PPARγ receptor.

Explanations for this independent action are speculative, Galli et al, identified significant inhibition of matrix metallopeptidase 2 (MMP 2) gene expression. Proteins of the MMP family are involved in the breakdown of extracellular matrix in normal physiological processes, such as embryonic development, reproduction, and tissue remodeling, as well as in disease processes such as arthritis and metastasis. The same group identified that TZD treatment inhibits fibrinolytic activity in both PPARγ expressing and non-expressing cells and that this effect was correlated with upregulation of plasminogen activator inhibitor (PAI-1), a major physiological inhibitor of fibrinolysis. Another finding of TZD treatment which is independent of the PPARγ

receptor is the activation of 5' adenosine monophosphate-activated protein kinase (AMPK) (Lebrasseur et al 2006, Boyle et al, 2006). AMPK is mainly involved in cellular metabolism and acts as a switch regulating several intracellular systems including the cellular uptake of glucose, the β-oxidation of fatty acids and the biogenesis of glucose transporter 4 (GLUT 4) and mitochondria. It also has some effects on pathways involved in cellular cycling through molecules such as PI3K, Akt and mTOR.

Interestingly, Han and Roman (2006) reported that rosiglitazone reduced the phosphorylation of Akt and increased PTEN protein expression in non–small cell lung carcinoma (NSCLC) cells and this was associated with inhibition of proliferation. These effects were blocked or diminished by GW9662 (PPARγ antagonist, as used in this thesis). When the cells underwent transfection with a CMX-PPARγ over-expression vector, the effects of rosiglitazone on Akt, PTEN, and cell growth were restored even in the presence of GW9662. They also noted that rosiglitazone increased the phosphorylation of AMP-activated protein kinase (AMPK), whereas it decreased phosphorylation of p70 ribosomal protein S6 kinase (p70S6K), a downstream target of mTOR. Of note, GW9662 did not affect the phosphorylation of AMPK and p70S6K protein and the inhibitory effect of rosiglitazone on NSCLC cell growth was enhanced by the mTOR inhibitor rapamycin. Their conclusion was that rosiglitazone can inhibit NSCLC growth through PPARγ-dependent signals that inhibit Akt and stimulate PTEN. Also, through PPARγ-independent signals, rosiglitazone up-regulates AMPK, thereby down-regulating the mTOR/p70S6K pathway, which further contributes to growth inhibition.

Taken together, it would appear that the PPARγ independent actions maybe modulated through AMPK and mTOR pathways. Investigation of these pathways using the cell lines pre and post treatment with rosiglitazone would be of considerable interest.

4.4 Summary

The main aim of the project was to identify the expression of PPARγ in various pancreatic neuroendocrine tumour tissue types. I conclude that PPARγ is expressed to variable degrees in pancreatic neuroendocrine tumours. This is based on the evidence presented from the human tissue samples expressing in the majority of samples, despite poor quality, and that there was good evidence PPARγ was being expressed in the human neuroendocrine tumour cell lines BON and QGP1. These findings unfortunately, cannot be substantiated by the immunohistochemical results which failed to show widespread PPARγ expression.

Further aspects of the project have identified that it is unlikely that cyclin dependent kinase p27 is directly responsible for proliferation of these tumours. Phosphorylation and transport by JAB1 do not appear to be playing a vital role. Also, modulators of the cell cycle that influence p27 including p-Akt and the PI3K/Akt pathway influenced by PTEN do not appear to playing a primary vital role.

The PPARγ agonist rosiglitazone does have an anti-proliferative effect on human neuroendocrine cell lines BON and QGP1 at higher concentrations, but the evidence suggests that this action may not be mediated by the PPARγ receptor.

4.5 Future Work Considerations

There are various aspects of this project that could be expanded upon to take the work done so far further. Firstly, regarding frozen tissue samples, I have found significant difficulties utilising previously harvested samples. This may have been due to the inherent difficulties in working with pancreatic tissue because of the digestive enzymes it produces, the harvesting technique or the conditions of storage. To optimise future work, samples must be resected by a surgeon understanding the tissue requirements and the samples would have to undergo either RNA extraction or be frozen and held at -80oC immediately. To obtain enough samples, a multicentre collection strategy would have to be employed with ethical consent gained over several areas. If a reasonable tumour series could be gained then I would firstly repeat the PPARγ expression studies and investigate p27 expression. Further studies would depend on the results but due to the clinical importance of somatostatin analogues in neuroendocrine tumours, I would also like to study the expression of the somatostatin receptor subtypes. Real time PCR would be employed rather than conventional and results would ideally be related to the clinical aspects of the tumour.

A surprising aspect of the immunohistochemical work was the low level of expression of PPARγ in either exocrine, endocrine or cancerous tissues, despite good positive control staining. It would be interesting to repeat this series with alternative PPARγ antibodies.

With the cell proliferation studies, there are multiple possibilities for further work as very little work has been published in this area. The first set of studies that I would perform would be to assess the effects on proliferation of different PPARγ agonists such

as pioglitazone. The relative efficacies could then be determined. Further studies would be aimed at determining which cell cycle markers are being affected by the reduction in proliferation. Given the emphasis of the MD on the expression of p27 and its regulatory proteins, we would investigate the effects on p27 following treatment of the cell lines with PPARγ agonists. If significant effects were found, further investigation into the effect on p27 modulators such as JAB1, p-Akt and PTEN would be performed.

As the findings of the immunohistochemistry, did not suggest a significant role for p27 involvement in pancreatic neuroendocrine tumour development, it would be of interest to investigate alternative cell cycle pathways such as p21 and its related regulatory proteins. As discussed earlier, the PPARγ-independent anti-proliferative effects of rosiglitazone maybe due to pathways involving AMPK and mTOR, both of which would be targets for future work.

4.6 Presentations and Publications

ORAL PRESENTATIONS

Pancreatic Society of Great Britain and Ireland. Nov 2004

Title: A Significant Anti-Proliferative Role For The PPAR-gamma Agonist Rosiglitazone In The Human Neuroendocrine Pancreatic Tumour Cell Lines BON and QGP1

Ipsen pharmaceuticals presentation. March 2003

Title: Pancreatic Neuroendocrine Tumours. An investigation of disruption of the cell cycle in sporadic islet cell tumours.

Prize awarded

POSTER PRESENTATIONS

UKNETwork 3rd National Neuroendocrine tumour conference Nov 2004

British Association of Sugical Oncology. Nov 2004

ABSTRACT

A significant anti-proliferative role for the PPAR-gamma agonist rosiglitazone in the human neuroendocrine pancreatic tumour cell lines BON and QGP1.

M.R.Hanson et al. EJSO. Nov 2004, Vol 30, 9, 1031.

CHAPTER 5

REFERENCES

1. Akerstrom G, Hellman P. Surgery on neuroendocrine tumours. Best.Pract.Res.Clin.Endocrinol.Metab 2007;21(1):87-109.

2. Ahlgren U, Pfaff SL, Jessell TM, Edlund T, Edlund H. Independent requireement for ISL1 in formation of pancreatic mesenchyme and islet cells. 1997. Nature 385;257-260.

3. Altomare DA, Tanno S, De Rienzo A, Klein-Szanto AJ, Tanno S, Skele KL et al. Frequent activation of AKT2 kinase in human pancreatic carcinomas. J.Cell Biochem. 2002;87(4):470-6.

4. Anayama T, Furihata M, Ishikawa T, Ohtsuki Y, Ogoshi S. Positive correlation between p27Kip1 expression and progression of human esophageal squamous cell carcinoma. Int.J.Cancer 1998;79(4):439-43.

5. Andrew A, Kramer B, Rawdon BB. The origin of gut and pancreatic neuroendocrine (APUD) cells--the last word? J.Pathol. 1998;186(2):117-8.

6. Baldassarre G, Belletti B, Bruni P, Boccia A, Trapasso F, Pentimalli F et al. Overexpressed cyclin D3 contributes to retaining the growth inhibitor p27 in the cytoplasm of thyroid tumor cells. J.Clin.Invest 1999;104(7):865-74.

7. Barakat MT, Meeran K, Bloom SR. Neuroendocrine tumours. Endocr.Relat Cancer 2004;11(1):1-18.

8. Baroni MG, Cavallo MG, Mark M, Monetini L, Stoehrer B, Pozzilli P. Beta-cell gene expression and functional characterisation of the human insulinoma cell line CM. J.Endocrinol. 1999;161(1):59-68.

9. Beamer BA, Negri C, Yen CJ, Gavrilova O, Rumberger JM, Durcan MJ et al. Chromosomal localization and partial genomic structure of the human peroxisome proliferator activated receptor-gamma (hPPAR gamma) gene. Biochem.Biophys.Res.Commun. 1997;233(3):756-9.

10. Belchetz PE, Brown CL, Makin HL, Trafford DJ, Mason AS, Bloom SR et al. ACTH, glucagon and gastrin production by a pancreatic islet cell carcinoma and its treatment. Clin.Endocrinol.(Oxf) 1973;2(4):307-16.

11. Benali N, Ferjoux G, Puente E, Buscail L, Susini C. Somatostatin receptors. Digestion 2000;62 Suppl 1:27-32.

12. Bernal-Mizrachi E, Wen W, Stahlhut S, Welling CM, Permutt MA. Islet beta cell expression of constitutively active Akt1/PKB alpha induces striking hypertrophy, hyperplasia, and hyperinsulinemia. J.Clin.Invest 2001;108(11):1631-8.

13. Bonner-Weir S, Stubbs M, Reitz P, Taneja M, Smith FE. Partial pancreatectomy as a model of pancreatic regeneration. 1997. Sarvetnick N(ed) Pancreatic Growth and regeneration. Karger Landes System, Basel 138-153

14. Bottinger EP, Jakubczak JL, Roberts IS, Mumy M, Hemmati P, Bagnall K, Merlino G, Wakefield LM. Expression of a dominant negative mutant TGF-beta

type II receptor in transgenic mice reveals essential roles for TGF-baeta in regulation of growth and differentiation in the exocrine pancreas. 1997. EMBO J 16;2621-2633.

15. Bos JL. ras oncogenes in human cancer: a review. Cancer Res. 1989;49(17):4682-9.

16. Bouwens L, Kloppel G. Islet cell neogenesis in the pancreas. 1996. Virchows Arch 427:553-560.

17. Boyle J.G, Salt IP, Cleland SJ, Connell JMC. The acute stimulation of nitric oxide synthesis by rosiglitazone in human aortic endothelial cells is independent of the PPAR gamma receptor but is dependent on the fuel sensing enzyme AMPK. Endocrine abstracts 2006:11:375

18. Bren-Mattison Y, Meyer AM, Van Putten V, Li H, Kuhn K, Stearman R, Weiser-Evans M, Winn RA, Heasley L, Nemenoff RA. Antitumourigenic effects of peroxisome proliferators-activated receptor-gamma in non-small-cell lung cancer cells are mediated by suppression of cyclooxygenase-2 via inhibition of nuclear factor-kappaB. Mol Pharmacol. 2008 Mar:73(3):709-717

19. Brunet A, Bonni A, Zigmond MJ, Lin MZ, Juo P, Hu LS et al. Akt promotes cell survival by phosphorylating and inhibiting a Forkhead transcription factor. Cell 1999;96(6):857-68.

20. Burns KA, Vanden Heuvel JP. Modulation of PPAR activity via phosphorylation. Biochim.Biophys.Acta 2007;1771(8):952-60.

21. Canavese G, Azzoni C, Pizzi S, Corleto VD, Pasquali C, Davoli C et al. p27: a potential main inhibitor of cell proliferation in digestive endocrine tumors but not a marker of benign behavior. Hum.Pathol. 2001;32(10):1094-101.

22. Cardone MH, Roy N, Stennicke HR, Salvesen GS, Franke TF, Stanbridge E et al. Regulation of cell death protease caspase-9 by phosphorylation. Science 1998;282(5392):1318-21.

23. Cavallo MG, Barone MG, Toto A, Gearing AJH, Forsey T.Pozzilli P. Viral infection induces cytokine release by beta islet cells. 1996. Immunology 75;664.

24. Cavallo MG, Monetini L, Valente L, Barone F, Beales P, Russo M, Pozzilli P. Glutathione protects a human insulinoma cell line from tumour necrosis factor alpha mediated cytotoxicity. 1997. Int J Clinn Lab Res 27;44-47.

25. Chen Y, Jimenez AR, Medh JD. Identification and regulation of novel PPAR-gamma splice variants in human THP-1 macrophages. Biochim.Biophys.Acta 2006;1759(1-2):32-43.

26. Chung DC, Smith AP, Louis DN, Graeme-Cook F, Warshaw AL, Arnold A. A novel pancreatic endocrine tumor suppressor gene locus on chromosome 3p with clinical prognostic implications. J.Clin.Invest 1997;100(2):404-10.

27. Chung DC, Smith AP, Louis DN, Graeme-Cook F, Warshaw AL, Arnold A. Analysis of the retinoblastoma tumour suppressor gene in pancreatic endocrine tumours. Clin.Endocrinol.(Oxf) 1997;47(5):523-8.

28. Chung DC, Brown SB, Graeme-Cook F, Seto M, Warshaw AL, Jensen RT et al. Overexpression of cyclin D1 occurs frequently in human pancreatic endocrine tumors. J.Clin.Endocrinol.Metab 2000;85(11):4373-8.

29. Claudio PP, Zamparelli A, Garcia FU, Claudio L, Ammirati G, Farina A et al. Expression of cell-cycle-regulated proteins pRb2/p130, p107, p27(kip1), p53, mdm-2, and Ki-67 (MIB-1) in prostatic gland adenocarcinoma. Clin.Cancer Res. 2002;8(6):1808-15.

30. Costa-Guda J, Rosen ED, Jensen RT, Chung DC, Arnold A. Mutational analysis of PPARG as a candidate tumour suppressor gene in enteropancreatic endocrine tumours. Clin.Endocrinol.(Oxf) 2005;62(5):603-6.

31. Date Y, Nakazato M, Hashguchi S, Dezaki K, Kangawa K, Arima T, Matsuo H, Yada T, Matsukura S. Ghrelin is present in pancreatic-alpha cells of humans and rats and stimulates insulin secretion. 2002. Diabetes. 51;124-129

32. Datta SR, Dudek H, Tao X, Masters S, Fu H, Gotoh Y et al. Akt phosphorylation of BAD couples survival signals to the cell-intrinsic death machinery. Cell 1997;91(2):231-41.

33. Demetri GD, Fletcher CD, Mueller E, Sarraf P, Naujoks R, Campbell N et al. Induction of solid tumor differentiation by the peroxisome proliferator-activated receptor-gamma ligand troglitazone in patients with liposarcoma. Proc.Natl.Acad.Sci.U.S.A 1999;96(7):3951-6.

34. Detjen KM, Welzel M, Farwig K, Brembeck FH, Kaiser A, Riecken EO et al. Molecular mechanism of interferon alfa-mediated growth inhibition in human neuroendocrine tumor cells. Gastroenterology 2000;118(4):735-48.

35. Di Florio A, Adesso L, Capurso G, Geremia R, Sette C, Della Fave G. Src family kinases regulate the mTOR pathway in pancreatic endocrine cells. 2008 Pancreas. 37(4) 467.

36. Doihara H, Nozawa K, Kojima R, Kawabata E, Yokoyama T, Ito, H. QGP1 cells release %-HT viaTRPA1 activation:a model of human enterochromaffin cells. 2009. Mol. Cell. Biol. 331;1-2:239-245

37. Dubois M, Pattou F, Kerr-Conte J, Gmyr V, Vandewalle B, Desreumaux P et al. Expression of peroxisome proliferator-activated receptor gamma (PPARgamma) in normal human pancreatic islet cells. Diabetologia 2000;43(9):1165-9.

38. Duerr EM, Chung DC. Molecular genetics of neuroendocrine tumors. Best.Pract.Res.Clin.Endocrinol.Metab 2007;21(1):1-14.

39. Ebrahimi SA, Wang EH, Wu A, Schreck RR, Passaro E Jr, Sawicki MP. Deletion of chromosome 1 predicts prognosis in pancreatic endocrine tumors. Cancer Res. 1999;59(2):311-5.

40. Elnemr A, Ohta T, Iwata K, Ninomia I, Fushida S, Nishimura G et al. PPARgamma ligand (thiazolidinedione) induces growth arrest and differentiation markers of human pancreatic cancer cells. Int.J.Oncol. 2000;17(6):1157-64.

41. Elnemr A, Ohta T, Iwata K, Ninomia I, Fushida S, Nishimura G et al. PPARgamma ligand (thiazolidinedione) induces growth arrest and differentiation markers of human pancreatic cancer cells. Int.J.Oncol. 2000;17(6):1157-64.

42. Emery MN, Leontiou C, Bonner SE, Merulli C, Nanzer AM, Musat M et al. PPAR-gamma expression in pituitary tumours and the functional activity of the glitazones: evidence that any anti-proliferative effect of the glitazones is independent of the PPAR-gamma receptor. Clin.Endocrinol.(Oxf) 2006;65(3):389-95.

43. Evers BM, Ishizuka J, Townsend C, Thompson JC. The human carcinoid cell line, BON. A model system for the study of carcinoid tumours. 1994 Annals New York Academy of Sciences 733;393-406

44. Evers BM, Townsend CM, Jr., Upp JR, Allen E, Hurlbut SC, Kim SW et al. Establishment and characterization of a human carcinoid in nude mice and effect of various agents on tumor growth. Gastroenterology 1991;101(2):303-11.

45. Farrow B, Evers BM. Activation of PPARgamma increases PTEN expression in pancreatic cancer cells. Biochem.Biophys.Res.Commun. 2003;301(1):50-3.

46. Fisher WE, Doran TA, Muscarella P, Boros LG, Ellison EC, Schirmer WJ. Expression of somatostatin receptor subtype 1-5 genes in human pancreatic cancer. J.Natl.Cancer Inst. 1998;90(4):322-4.

47. Forrer F, Valkema R, Kwekkeboom DJ, de Jong M, Krenning EP. Neuroendocrine tumors. Peptide receptor radionuclide therapy. Best.Pract.Res.Clin.Endocrinol.Metab 2007;21(1):111-29.

48. Fredersdorf S, Burns J, Milne AM, Packham G, Fallis L, Gillett CE et al. High level expression of p27(kip1) and cyclin D1 in some human breast cancer cells: inverse correlation between the expression of p27(kip1) and degree of malignancy in human breast and colorectal cancers. Proc.Natl.Acad.Sci.U.S.A 1997;94(12):6380-5.

49. Galli A, Ceni E, Crabb DW, Mello T, Salzano R, Grappone C et al. Antidiabetic thiazolidinediones inhibit invasiveness of pancreatic cancer cells via PPARgamma independent mechanisms. Gut 2004;53(11):1688-97.

50. Gamboa-Dominguez A, Seidl S, Reyes-Gutierrez E, Hermannstadter C, Quintanilla-Martinez L, Busch R et al. Prognostic significance of p21WAF1/CIP1, p27Kip1, p53 and E-cadherin expression in gastric cancer. J.Clin.Pathol. 2007;60(7):756-61.

51. Garcia-Bates, T, Berstein S, Phipps, R. Peroxisome proliferators-activateed recptorγ overexpression suppresses growth and in duces apoptosis in human multiple myeloma cells. Clin Cancer Res 2008:14(20). 6414

52. Gentil PA, Mosnier JF, Buono JP, Berthelot P, Chipponi J, Balique JG et al. The relationship between MIB-1 proliferation index and outcome in pancreatic neuroendocrine tumors. Am.J.Clin.Pathol. 1998;109(3):286-93.

53. Gerdes J, Schwab U, Lemke H, Stein H. Production of a mouse monoclonal antibody reactive with a human nuclear antigen associated with cell proliferation. Int.J.Cancer 1983;31(1):13-20.

54. Gerdes J, Lemke H, Baisch H, Wacker HH, Schwab U, Stein H. Cell cycle analysis of a cell proliferation-associated human nuclear antigen defined by the monoclonal antibody Ki-67. J.Immunol. 1984;133(4):1710-5.

55. Girnun G, Sarraf P, Mueller E, Drori S, GonzalesF, Speigelman B. The role of PPARγ as a tumour suppressor gene in colon carcinogenesis. Keystone Symposisa:The PPARs: a transcription odyssey (abst) 73, 2001

56. Gragnoli C. The CM cell line derived from liver metastasis of malignant human insulinoma is not a valid beta cell model for in vitro studies. J.Cell Physiol 2008;216(2):569-70.

57. Gray S, Dalla Nora E, Vidal-Puig AJ, Mouse models of PPARγ deficiency: dissecting PPARγ s role in metabolic homeostasis. Biochemical Society Transactions 2005;33(5) 1053-1057.

58. Groszer M, Erickson R, Scripture-Adams DD, Lesche R, Trumpp A, Zack JA et al. Negative regulation of neural stem/progenitor cell proliferation by the Pten tumor suppressor gene in vivo. Science 2001;294(5549):2186-9.

59. Gueli N, Toto A, Palamieri G, Carmenini G, Delpino A, Ferrini U. In vitro growth of a cell line originated from a human insulinoma. J Exp Clin Canc Res 1987:6:281-5.

60. Guo SS, Arora C, Shimoide AT, Sawicki MP. Frequent deletion of chromosome 3 in malignant sporadic pancreatic endocrine tumors. Mol.Cell Endocrinol. 2002;190(1-2):109-14.

61. Guo SS, Wu X, Shimoide AT, Wong J, Moatamed F, Sawicki MP. Frequent overexpression of cyclin D1 in sporadic pancreatic endocrine tumours. J.Endocrinol. 2003;179(1):73-9.

62. Gustafsson BI, Kidd M, Modlin IM. Neuroendocrine tumors of the diffuse neuroendocrine system. Curr.Opin.Oncol. 2008;20(1):1-12.

63. Han S, Roman J. Rosiglitazone suppresses human lung carcinoma cell growth through PPARgamma-dependent and PPARgamma-independent signal pathways. Mol.Cancer Ther. 2006;5(2):430-7.

64. Harvey M, Vogel H, Lee EY, Bradley A, Donehower LA. Mice deficient in both p53 and Rb develop tumors primarily of endocrine origin. Cancer Res. 1995;55(5):1146-51.

65. Hibberts NA, Simpson DJ, Bicknell JE, Broome JC, Hoban PR, Clayton RN et al. Analysis of cyclin D1 (CCND1) allelic imbalance and overexpression in sporadic human pituitary tumors. Clin.Cancer Res. 1999;5(8):2133-9.

66. Hogan BLM, Blessing < Winnier GE, Susuki N, Jones CM. Growth factors in development; the role of TGF-beta related polypeptide signalling molecules in embryogenesis. Development. 1994. suppl. 53-60.

67. Hogg J, Hill DJ, Han VK,. The ontogeny of in sulin like growth factor (IGF) and IGF-binding protein gene expression in the rat pancreas. 1994. J Mol Endocrinol 13;49-58.

68. Hopfner M, Sutter AP, Gerst B, Zeitz M, Scherubl H. A novel approach in the treatment of neuroendocrine gastrointestinal tumours. Targeting the epidermal growth factor receptor by gefitinib (ZD1839). Br.J.Cancer 2003;89(9):1766-75.

69. Iguchi H, Hayashi I, Kono A. A somatostatin secreting cell line established from ahuman pancreatic islet cell carcinoma (somatostatinoma): release experiment and immunohistochemical study. 1990; Cancer Res. 50;3691-93.

70. Ikezoe T, Miller CW, Kawano S, Heaney A, Williamson EA, Hisatake J et al. Mutational analysis of the peroxisome proliferator-activated receptor gamma gene in human malignancies. Cancer Res. 2001;61(13):5307-10.

71. Ito Y, Yoshida H, Nakamura Y, Tomoda C, Uruno T, Takamura Y et al. Expression of Jun activation domain-binding protein 1 and p27 (Kip1) in thyroid medullary carcinoma. Pathology 2005;37(3):216-9.

72. Jonnakuty C, Gragnoli C. Kayotype of the human insulinoma CM cell line-β cell model in vitro? Journal of Cellullar Physiology. 2007;213:661-662.

73. Jonsson J, Carlsson L, Edlund T, Edlund H. Insulin promoter factor1 is required for pancreas development in mice. 1994. Nature 371;606-609.

74. Kaku M, Nishiyama T, Yagawa K, Abe M. Establishment of a carcinoembryonic antigen-producing cell line from human pancreatic carcinoma. Gann 1980;71(5):596-601.

75. Kaltsas GA, Besser GM, Grossman AB. The diagnosis and medical management of advanced neuroendocrine tumors. Endocr.Rev. 2004;25(3):458-511.

76. Kanaka-Gantenbein C, Dicou E, Czernichow P, Scharfman R. Presence of nerve growth factor and its receptors in an in vitro model of islet cell development; implication in normal islet morphogenesis. 1995. Endocrinology 136;3154-3162.

77. Katona TM, Jones TD, Wang M, Abdul-Karim FW, Cummings OW, Cheng L. Molecular evidence for independent origin of multifocal neuroendocrine tumors of the enteropancreatic axis. Cancer Res. 2006;66(9):4936-42.

78. Kawa S, Nikaido T, Unno H, Usuda N, Nakayama K, Kiyosawa K. Growth inhibition and differentiation of pancreatic cancer cell lines by PPAR gamma ligand troglitazone. Pancreas 2002;24(1):1-7.

79. Kim KY, Kim SS, Cheon HG. Differential anti-proliferative actions of peroxisome proliferator-activated receptor-gamma agonists in MCF-7 breast cancer cells. Biochem.Pharmacol. 2006;72(5):530-40.

80. Kim SK, Hebrok M, Melton DA. Notochrd to endoderm signalling is required for pancreas development. 1997. Development 124;4243-4252.

81. Kliewer SA, Forman BM, Blumberg B, Ong ES, Borgmeyer U, Mangelsdorf DJ et al. Differential expression and activation of a family of murine peroxisome proliferator-activated receptors. Proc.Natl.Acad.Sci.U.S.A 1994;91(15):7355-9.

82. Kloppel G, Perren A, Heitz PU. The gastroenteropancreatic neuroendocrine cell system and its tumors: the WHO classification. Ann.N.Y.Acad.Sci. 2004;1014:13-27.

83. Kloppel G, Rindi G, Anlauf M, Perren A, Komminoth P. Site-specific biology and pathology of gastroenteropancreatic neuroendocrine tumors. Virchows Arch. 2007;451 Suppl 1:S9-27.

84. Kloppel G. Tumour biology and histopathology of neuroendocrine tumours. Best.Pract.Res.Clin.Endocrinol.Metab 2007;21(1):15-31.

85. Knouff C, Auwerx J. Peroxisome proliferator-activated receptor-gamma calls for activation in moderation: lessons from genetics and pharmacology. Endocr.Rev. 2004;25(6):899-918.

86. Korbonits M, Chahal HS, Kaltsas G, Jordan S, Urmanova Y, Khalimova Z et al. Expression of phosphorylated p27(Kip1) protein and Jun activation domain-binding protein 1 in human pituitary tumors. J.Clin.Endocrinol.Metab 2002;87(6):2635-43.

87. Kouvaraki MA, Rassidakis GZ, Tian L, Kumar R, Kittas C, Claret FX. Jun activation domain-binding protein 1 expression in breast cancer inversely correlates with the cell cycle inhibitor p27(Kip1). Cancer Res. 2003;63(11):2977-81.

88. Kouvaraki MA, Rassidakis GZ, Tian L, Kumar R, Kittas C, Claret FX. Jun activation domain-binding protein 1 expression in breast cancer inversely correlates with the cell cycle inhibitor p27(Kip1). Cancer Res. 2003;63(11):2977-81.

89. Kouvaraki MA, Korapati AL, Rassidakis GZ, Tian L, Zhang Q, Chiao P et al. Potential role of Jun activation domain-binding protein 1 as a negative regulator of p27kip1 in pancreatic adenocarcinoma. Cancer Res. 2006;66(17):8581-9.

90. Kristiansen G, Jacob J, Buckendahl AC, Grutzmann R, Alldinger I, Sipos B et al. Peroxisome proliferator-activated receptor gamma is highly expressed in pancreatic cancer and is associated with shorter overall survival times. Clin.Cancer Res. 2006;12(21):6444-51.

91. LeBrasseur NK, Kelly M, Tsao TS, Farmer SR, Saha AK, Ruderman NB et al. Thiazolidinediones can rapidly activate AMP-activated protein kinase in mammalian tissues. Am.J.Physiol Endocrinol.Metab 2006;291(1):E175-E181.

92. Leotlela PD, Jauch A, Holtgreve-Grez H, Thakker RV. Genetics of neuroendocrine and carcinoid tumours. Endocr.Relat Cancer 2003;10(4):437-50.

93. Li J, Yen C, Liaw D, Podsypanina K, Bose S, Wang SI et al. PTEN, a putative protein tyrosine phosphatase gene mutated in human brain, breast, and prostate cancer. Science 1997;275(5308):1943-7.

94. Li M, Fisher WE, Kim HJ, Wang X, Brunicardi CF, Chen C et al. Somatostatin, somatostatin receptors, and pancreatic cancer. World J.Surg. 2005;29(3):293-6.

95. Lidhar K, Korbonits M, Jordan S, Khalimova Z, Kaltsas G, Lu X et al. Low expression of the cell cycle inhibitor p27Kip1 in normal corticotroph cells, corticotroph tumors, and malignant pituitary tumors. J.Clin.Endocrinol.Metab 1999;84(10):3823-30.

96. Lloyd RV, Jin L, Qian X, Kulig E. Aberrant p27kip1 expression in endocrine and other tumors. Am.J.Pathol. 1997;150(2):401-7.

97. Lott ST, Chandler DS, Curley SA, Foster CJ, El Naggar A, Frazier M et al. High frequency loss of heterozygosity in von Hippel-Lindau (VHL)-associated and sporadic pancreatic islet cell tumors: evidence for a stepwise mechanism for malignant conversion in VHL tumorigenesis. Cancer Res. 2002;62(7):1952-5.

98. Lu CD, Morita S, Ishibashi T, Hara H, Isozaki H, Tanigawa N. Loss of p27Kip1 expression independently predicts poor prognosis for patients with resectable pancreatic adenocarcinoma. Cancer 1999;85(6):1250-60.

99. Lu J, Imamura K, Nomura S, <mafune K, Nakajima A, Kadowaki T, Kubota N, Kaminishi M. Chemopreventative Effect of peroxisome proliferators activated receptorγ on gastric carcinogenesis in mice. Cancer Res 2005;65(11) 4769-4774

100. Mashima H, Ohnishi H, Wakabayashi K, Seno MYamada H, Kojima I. Betacellulin and activin A co-ordinately convert amylase secreting pancreatic AR42J cells into insulin secreting cells. 1996. J Clin Invest. 97;1647-1654.

101. Modlin IM, Lye KD, Kidd M. A 5-decade analysis of 13,715 carcinoid tumors. Cancer 2003;97(4):934-59.

102. Modlin IM, Kidd M, Latich I, Zikusoka MN, Shapiro MD. Current status of gastrointestinal carcinoids. Gastroenterology 2005;128(6):1717-51.

103. Modlin IM, Oberg K, Chung DC, Jensen RT, de Herder WW, Thakker RV et al. Gastroenteropancreatic neuroendocrine tumours. Lancet Oncol. 2008;9(1):61-72.

104. Montagnoli A, Fiore F, Eytan E, Carrano AC, Draetta GF, Hershko A et al. Ubiquitination of p27 is regulated by Cdk-dependent phosphorylation and trimeric complex formation. Genes Dev. 1999;13(9):1181-9.

105. Motomura W, Okumura T, Takahashi N, Obara T, Kohgo Y. Activation of peroxisome proliferator-activated receptor gamma by troglitazone inhibits cell growth through the increase of p27KiP1 in human. Pancreatic carcinoma cells. Cancer Res. 2000;60(19):5558-64.

106. Mueller E, Sarraf P, Tontonoz P, Evans RM, Martin KJ, Zhang M et al. Terminal differentiation of human breast cancer through PPAR gamma. Mol.Cell 1998;1(3):465-70.

107. Mueller E, Smith M, Sarraf P, Kroll T, Aiyer A, Kaufman DS et al. Effects of ligand activation of peroxisome proliferator-activated receptor gamma in human prostate cancer. Proc.Natl.Acad.Sci.U.S.A 2000;97(20):10990-5.

108. Mutter GL, Lin MC, Fitzgerald JT, Kum JB, Baak JP, Lees JA et al. Altered PTEN expression as a diagnostic marker for the earliest endometrial precancers. J.Natl.Cancer Inst. 2000;92(11):924-30.

109. Nakayama K, Ishida N, Shirane M, Inomata A, Inoue T, Shishido N et al. Mice lacking p27(Kip1) display increased body size, multiple organ hyperplasia, retinal dysplasia, and pituitary tumors. Cell 1996;85(5):707-20.

110. Nikoleishvili D, Pertia A, Trsintsadze O, Gogokhia N, Managadze L, Chkhotua A. Expression of p27((Kip1)), cyclin D3 and Ki67 in BPH, prostate cancer and hormone-treated prostate cancer cells. Int.Urol.Nephrol. 2008;40(4):953-9.

111. Oliver G, Sosa-Pineda B, Geisendorf S, Spana EP, Doe CQ, Gruss P. Prox-1, a prospero-related homeobox gene expressed during mouse development. 1993. Mech Dev 44;3-16.

112. Palakurthi SS, Aktas H, Grubissich LM, Mortensen RM, Halperin JA. Anticancer effects of thiazolidinediones are independent of peroxisome proliferator-activated receptor gamma and mediated by inhibition of translation initiation. Cancer Res. 2001;61(16):6213-8.

113. Pang K, Mukonoweshuro C, Wong GC. Beta cells arise from glucose transporter type 2 (GLUT2) expressing epithelial cells of the developing rat pancreas. 1994. Proc Natl Acad Sci USA 91;9559-9563.

114. Paramio JM, Navarro M, Segrelles C, Gomez-Casero E, Jorcano JL. PTEN tumour suppressor is linked to the cell cycle control through the retinoblastoma protein. Oncogene 1999;18(52):7462-8.

115. Parekh D, Ishizuka J, Townsend CM, Jr., Haber B, Beauchamp RD, Karp G et al. Characterization of a human pancreatic carcinoid in vitro: morphology, amine and peptide storage, and secretion. Pancreas 1994;9(1):83-90.

116. Patel L, Pass I, Coxon P, Downes CP, Smith SA, Macphee CH. Tumor suppressor and anti-inflammatory actions of PPARgamma agonists are mediated via upregulation of PTEN. Curr.Biol. 2001;11(10):764-8.

117. Pateras IS, Apostolopoulou K, Koutsami M, Evangelou K, Tsantoulis P, Liloglou T et al. Downregulation of the KIP family members p27(KIP1) and p57(KIP2) by SKP2 and the role of methylation in p57(KIP2) inactivation in nonsmall cell lung cancer. Int.J.Cancer 2006;119(11):2546-56.

118. Pelosi G, Bresaola E, Bogina G, Pasini F, Rodella S, Castelli P et al. Endocrine tumors of the pancreas: Ki-67 immunoreactivity on paraffin sections is an independent predictor for malignancy: a comparative study with proliferating-cell nuclear antigen and progesterone receptor protein immunostaining, mitotic index, and other clinicopathologic variables. Hum.Pathol. 1996;27(11):1124-34.

119. Perren A, Weng LP, Boag AH, Ziebold U, Thakore K, Dahia PL et al. Immunohistochemical evidence of loss of PTEN expression in primary ductal adenocarcinomas of the breast. Am.J.Pathol. 1999;155(4):1253-60.

120. Peters J, Jurgensen A, Kloppel G. Ontogeny, differentiation and growth of the endocrine pancreas. Virchows Arch. 2000;436(6):527-38.

121. Pictet R, Rutter WJ. Development of the embryonic endocrine pancreas. 1972. Geiger SR (Ed) Handbook of Physiology, Sect 7 25-66

122. Pittinger GL, Vinik AI, Rosenberg L. The partial isolation and characterisation of ilotropin. A novel islet specific growth factor. 1992. Adv Exp Med Biol 321;123-130.

123. Plockinger U, Wiedenmann B. Neuroendocrine tumors. Biotherapy. Best.Pract.Res.Clin.Endocrinol.Metab 2007;21(1):145-62.

124. Prado CL, Pugh-Bernard AE, Elghazi L, Sosa-Pineda B, Sussel L. Ghrelin cells replace insulin-producing β cells in two mouse models of pancreas development. 2004. PNAS 101:9:2924-2929

125. Qin LF, Ng IO. Expression of p27(KIP1) and p21(WAF1/CIP1) in primary hepatocellular carcinoma: clinicopathologic correlation and survival analysis. Hum.Pathol. 2001;32(8):778-84.

126. Ragu K, Tang S, Dube ID, Kamel-Reid S, Bryce DM, Breitman ML. Characterisation and developmental expression ofTlx-1, the murine homolog of HOX11. 1993. Mech Dev. 44;51-64.

127. Reed W, Florems VA, Holm R, Hannisdal E, Nesland JM. Elevated levels of p27, p21 and cyclin D1 correlate with positive oestrogen and progesterone receptor status in node-negative breast carcinoma patients. Virchows Arch. 1999;435(2):116-24.

128. Rigaud G, Missiaglia E, Moore PS, Zamboni G, Falconi M, Talamini G et al. High resolution allelotype of nonfunctional pancreatic endocrine tumors: identification of two molecular subgroups with clinical implications. Cancer Res. 2001;61(1):285-92.

129. Rindi G, Capella C, Solcia E. Cell biology, clinicopathological profile, and classification of gastro-enteropancreatic endocrine tumors. J.Mol.Med. 1998;76(6):413-20.

130. Rockall AG, Reznek RH. Imaging of neuroendocrine tumours (CT/MR/US). Best.Pract.Res.Clin.Endocrinol.Metab 2007;21(1):43-68.

131. Rooman I, Schuit F, Bouwens L. Effect of vascular endothelial growth factor on growth and differentiation of pancreatic ductal epithelium. 1997. Lab Invest 76;225-232

132. Rosen ED, Kulkarni RN, Sarraf P, Ozcan U, Okada T, Hsu CH et al. Targeted elimination of peroxisome proliferator-activated receptor gamma in beta cells leads to abnormalities in islet mass without compromising glucose homeostasis. Mol.Cell Biol. 2003;23(20):7222-9.

133. Rumi MA, Sato H, Ishihara S, Kawashima K, Hamamoto S, Kazumori H et al. Peroxisome proliferator-activated receptor gamma ligand-induced growth inhibition of human hepatocellular carcinoma. Br.J.Cancer 2001;84(12):1640-7.

134. Sabatino L, Casamassimi A, Peluso G, Barone MV, Capaccio D, Migliore C et al. A novel peroxisome proliferator-activated receptor gamma isoform with

dominant negative activity generated by alternative splicing. J.Biol.Chem. 2005;280(28):26517-25.

135. Saez E, Rosenfeld J, Livolsi A, Olsen P, Lombardo E, Nelson M, Banayo E, Cardiff R, Izpisua-Belmonte JC, Evans RM. PPARγ signaling exacerbates mammary gland tumour development. Genes and Development 18:528-540.

136. Sanchez-Beato M, Camacho FI, Martinez-Montero JC, Saez AI, Villuendas R, Sanchez-Verde L et al. Anomalous high p27/KIP1 expression in a subset of aggressive B-cell lymphomas is associated with cyclin D3 overexpression. p27/KIP1-cyclin D3 colocalization in tumor cells. Blood 1999;94(2):765-72.

137. Sanvito F Herrera PL, Huarte J, Nichols A, Montesano R, Orci L, Vassalli JD. TGF-beta1 influences the relative development of the exocrine and endocrine pancreas in vitro. 1994. Development 120:3451-3462.

138. Sarraf P, Mueller E, Jones D, King FJ, DeAngelo DJ, Partridge JB et al. Differentiation and reversal of malignant changes in colon cancer through PPARgamma. Nat.Med. 1998;4(9):1046-52.

139. Sarraf P, Mueller E, Smith WM, Wright HM, Kum JB, Aaltonen LA et al. Loss-of-function mutations in PPAR gamma associated with human colon cancer. Mol.Cell 1999;3(6):799-804.

140. Sawai H, Liu J, Reber HA, Hines OJ, Eibl G. Activation of peroxisome proliferator-activated receptor-gamma decreases pancreatic cancer cell invasion through modulation of the plasminogen activator system. Mol.Cancer Res. 2006;4(3):159-67.

141. Schlieman MG, Fahy BN, Ramsamooj R, Beckett L, Bold RJ. Incidence, mechanism and prognostic value of activated AKT in pancreas cancer. Br.J.Cancer 2003;89(11):2110-5.

142. Sheaff RJ, Groudine M, Gordon M, Roberts JM, Clurman BE. Cyclin E-CDK2 is a regulator of p27Kip1. Genes Dev. 1997;11(11):1464-78.

143. Shin I, Yakes FM, Rojo F, Shin NY, Bakin AV, Baselga J et al. PKB/Akt mediates cell-cycle progression by phosphorylation of p27(Kip1) at threonine 157 and modulation of its cellular localization. Nat.Med. 2002;8(10):1145-52.

144. Stanger A. Nucleus-independent chemical shifts (NICS): distance dependence and revised criteria for aromaticity and antiaromaticity. J.Org.Chem. 2006;71(3):883-93.

145. Sui L, Dong Y, Ohno M, Watanabe Y, Sugimoto K, Tai Y et al. Jab1 expression is associated with inverse expression of p27(kip1) and poor prognosis in epithelial ovarian tumors. Clin.Cancer Res. 2001;7(12):4130-5.

146. Sundin A, Garske U, Orlefors H. Nuclear imaging of neuroendocrine tumours. Best.Pract.Res.Clin.Endocrinol.Metab 2007;21(1):69-85.

147. Teitelman G, Alpert S, Polak JM, Martinez A, Hanahan D. Precursor cells of mouse endocrine pancreas coexpressess insulin, glucagons and the neuronal

proteins tyrosine hydroxylase and neuropeptide Y, but not pancreatic polypeptide. 1993. Development 118:1031-1039.

148. Teitelman G, Lee JK. Cell lineage analysis of pancreatic islet cell development: glucagons and insulin cells arise from chatecholaminergic precursors present in pancreatic ducts. 1987. Dev Biol. 121;454-466

149. Testa JR, Bellacosa A. AKT plays a central role in tumorigenesis. Proc.Natl.Acad.Sci.U.S.A 2001;98(20):10983-5.

150. Theocharis S, Margeli A, Vielh P, Kouraklis G. Peroxisome proliferator-activated receptor-gamma ligands as cell-cycle modulators. Cancer Treat.Rev. 2004;30(6):545-54.

151. Thompson EA. PPARgamma physiology and pathology in gastrointestinal epithelial cells. Mol.Cells 2007;24(2):167-76.

152. Tomoda K, Kubota Y, Kato J. Degradation of the cyclin-dependent-kinase inhibitor p27Kip1 is instigated by Jab1. Nature 1999;398(6723):160-5.

153. Tontonoz P, Singer S, Forman BM, Sarraf P, Fletcher JA, Fletcher CD et al. Terminal differentiation of human liposarcoma cells induced by ligands for peroxisome proliferator-activated receptor gamma and the retinoid X receptor. Proc.Natl.Acad.Sci.U.S.A 1997;94(1):237-41.

154. Toumpanakis C, Meyer T, Caplin ME. Cytotoxic treatment including embolization/chemoembolization for neuroendocrine tumours. Best.Pract.Res.Clin.Endocrinol.Metab 2007;21(1):131-44.

155. Toyota M, Miyazaki Y, Kitamura S, Nagasawa Y, Kiyohara T, Shinomura Y et al. Peroxisome proliferator-activated receptor gamma reduces the growth rate of pancreatic cancer cells through the reduction of cyclin D1. Life Sci. 2002;70(13):1565-75.

156. Tsubouchi Y, Sano H, Kawahito Y, Mukai S, Yamada R, Kohno M et al. Inhibition of human lung cancer cell growth by the peroxisome proliferator-activated receptor-gamma agonists through induction of apoptosis. Biochem.Biophys.Res.Commun. 2000;270(2):400-5.

157. Turque N, Plaza S, Radvanyi F, Carriere C, Saule SS. Pax-QNR/Pax-6 a paired box- and homeobox-containing gene expressed in neurons, is also expressed in pancreatic endocrine cells. 1994. Mol Endocrinol 8;929-938

158. Ullrich A Schlessinger J. Signal transduction by receptors with tyrosine kinase activity. 1990. Cell 61;203-212.

159. Upchurch BHH, Aponte GW, Leiter AB. Expression of peptide YY in all 4 islet cell types in developing mouse pancreas suggests a common peptide YY producing progenitor. 1994. Development 120;2245-252.

160. Viglietto G, Motti ML, Bruni P, Melillo RM, D'Alessio A, Califano D et al. Cytoplasmic relocalization and inhibition of the cyclin-dependent kinase inhibitor p27(Kip1) by PKB/Akt-mediated phosphorylation in breast cancer. Nat.Med. 2002;8(10):1136-44.

161. Viglietto G, Motti ML, Bruni P, Melillo RM, D'Alessio A, Califano D et al. Cytoplasmic relocalization and inhibition of the cyclin-dependent kinase inhibitor p27(Kip1) by PKB/Akt-mediated phosphorylation in breast cancer. Nat.Med. 2002;8(10):1136-44.

162. Vlach J, Hennecke S, Amati B. Phosphorylation-dependent degradation of the cyclin-dependent kinase inhibitor p27. EMBO J. 1997;16(17):5334-44.

163. Volante M, Allia E, Gugliotta P, Funaro A, Broglio F, Deghenghi R, Mucciolo G, Ghigo E, Papotti M. Expression of ghrelin and of the GH secretagogue receptor by the pancreatic islet cells and related endocrine tumours. 2002. J Clin Endocrinol Metab. 87;1300-1308.

164. Vortmeyer AO, Huang S, Lubensky I, Zhuang Z. Non-islet origin of pancreatic islet cell tumors. J.Clin.Endocrinol.Metab 2004;89(4):1934-8.

165. WangRN, Rehfeld JF, Neilson FC, Kloppel G. Expression of gastrin and transforming growth factor-alpha during duct to islet cell differentiation in the pancreas of duct ligatedd adult rats. 1997. Diabetologia. 40;887-893.

166. Wang T, Xu J, Yu X, Yang R, Han ZC. Peroxisome proliferator-activated receptor gamma in malignant diseases. Crit Rev.Oncol.Hematol. 2006;58(1):1-14.

167. Wierup N, Svensson H, Mulder H, Sundler F. The ghrelin cell: a novel developmentally regulated islet cell in the human pancreas. 2002. Regulatory Peptides. 107;63-69.

168. Yang K, Fan KH, Lamprecht SA, Edelmann W, Kopelovich L, Kucherlapati R et al. Peroxisome proliferator-activated receptor gamma agonist troglitazone induces colon tumors in normal C57BL/6J mice and enhances colonic carcinogenesis in Apc1638 N/+ Mlh1+/- double mutant mice. Int.J.Cancer 2005;116(4):495-9.

169. Zhou BP, Liao Y, Xia W, Spohn B, Lee MH, Hung MC. Cytoplasmic localization of p21Cip1/WAF1 by Akt-induced phosphorylation in HER-2/neu-overexpressing cells. Nat.Cell Biol. 2001;3(3):245-52.

170. Zikusoka MN, Kidd M, Eick G, Latich I, Modlin IM. The molecular genetics of gastroenteropancreatic neuroendocrine tumors. Cancer 2005;104(11):2292-309.

CHAPTER 6

APPENDIX

Immunohistochemistry counting sheet

Immuno grid explanation:

The grid is split into 5 large squares each representing one high powered field as seen on the computer screen.

Each large square is split into columns representing:

nuclear staining

cytoplasmic staining

There are 5 rows to each large square. The first four represent strength of staining:

strong

moderate

weak

negative

The fifth row contains the total number of cells that has been counted in each field. This will be a number out of approximately one hundred

	Nuclear	Cytoplasmic
strong		
moderate		
weak		
negative		
No. of cells counted		

Working sheet

ANTIBODY: DATE:

SLIDE NUMBER: TUMOUR/NORM/ISLET:

Total cells counted =

	NEGATIVE	WEAK	MEDIUM	STRONG
NUCLEAR				
CYTOPLASMIC				

Comments:

Immunohistochemistry data tables

PPARγ - TUMOUR SAMPLES - INSULINOMA

	NUCLEAR						CYTOPLASMIC					
ID	**S**	**M**	**W**	**-VE**	**+VE**	**S+M**	**S**	**M**	**W**	**-VE**	**+VE**	**S+M**
1	0	0	0	100	0	0	0	0	0	100	0	0
2	0	0	30	70	30	0	0	0	0	100	0	0
3	0	0	0	100	0	0	0	0	0	100	0	0
5	0	0	0	100	0	0	0	0	0	100	0	0
6	0	0	0	100	0	0	0	0	0	100	0	0
7	0	0	0	100	0	0	0	0	0	100	0	0
8	0	0	0	100	0	0	0	0	0	100	0	0
9	0	0	0	100	0	0	0	0	0	100	0	0
10	0	0	0	100	0	0	0	0	0	100	0	0
11	0	0	0	100	0	0	0	0	0	100	0	0
12	0	0	0	100	0	0	0	0	0	100	0	0
13	0	0	39.7	60.3	39.7	0	0	0	0	100	0	0
14	0	0	0	100	0	0	0	0	0	100	0	0
15	12.3	38.6	33.6	15.5	84.5	50.9	0	0	0	100	0	0
17	0	0	0	100	0	0	0	0	0	100	0	0
18	0	0	0	100	0	0	0	0	0	100	0	0
19	0	0	1	99	1	0	0	0	0	100	0	0
20	0	0	2.4	97.6	2.4	0	0	0	0	100	0	0
23	0	0	0	100	0	0	0	0	0	100	0	0
25	0	0	8.3	91.7	8.3	0	0	0	9	94	9	0
AV	0.62	1.93	5.75	91.71	8.30	2.55	0.00	0.00	0.45	99.70	0.45	0.00
SEM	0.62	1.93	2.82	4.68	4.68	2.55	0.00	0.00	0.45	0.30	0.45	0.00

GASTRINOMA

	NUCLEAR						CYTOPLASMIC					
ID	**S**	**M**	**W**	**-VE**	**+VE**	**S+M**	**S**	**M**	**W**	**-VE**	**+VE**	**S+M**
4	0	0	0	100	0	0	0	0	0	100	0	0
22	0	0	5.6	94.4	5.6	0	0	0	0	100	0	0
24	0	0	0	100	0	0	0	0	0	100	0	0
AV	0	0	1.87	98.13	1.87	0	0	0	0	100	0	0
SEM	0	0	0.72	0.72	0.72	0	0	0	0	0	0	0

PPARγ - ISLET SAMPLES

	NUCLEAR						CYTOPLASMIC					
ID	**S**	**M**	**W**	**-VE**	**+VE**	**S+M**	**S**	**M**	**W**	**-VE**	**+VE**	**S+M**
1	0	0	0	100	0	0	0	0	0	100	0	0
2	0	0	6.3	93.7	6.3	0	0	0	0	100	0	0
4	0	0	0	100	0	0	0	0	0	100	0	0
5	0	0	0	100	0	0	0	0	0	100	0	0
6	0	0	0	100	0	0	0	0	0	100	0	0
7	0	0	0	100	0	0	0	0	0	100	0	0
8	0	0	0	100	0	0	0	0	0	100	0	0
9	0	0	0	100	0	0	0	0	0	100	0	0
10	0	0	0	100	0	0	0	0	0	100	0	0
11	0	0	0	100	0	0	0	0	0	100	0	0
12	0	0	0	100	0	0	0	0	0	100	0	0
13	0	0	0	100	0	0	0	0	0	100	0	0
14	0	0	0	100	0	0	0	0	0	100	0	0
15	0	0	8.5	91.5	8.5	0	0	0	0	100	0	0
17	0	0	0	100	0	0	0	0	0	100	0	0
18	0	0	0	100	0	0	0	0	0	100	0	0
20	0	0	7.8	92.2	7.8	0	0	0	0	100	0	0
23	0	0	0	100	0	0	0	0	0	100	0	0
25	0	0	7	93	7	0	0	0	0	100	0	0
AV	0	0	1.56	98.44	1.56	0	0	0	0	100	0	0
SEM	0	0	0.70	0.70	0.70	0	0	0	0	0	0	0

PPARγ - EXOCRINE PANCREAS SAMPLES

	NUCLEAR						CYTOPLASMIC					
ID	**S**	**M**	**W**	**-VE**	**+VE**	**S+M**	**S**	**M**	**W**	**-VE**	**+VE**	**S+M**
1	0	0	0	100	0	0	0	0	0	100	0	0
2	0	0	3.5	96.5	3.5	0	0	0	0	100	0	0
3	0	0	0	100	0	0	0	0	0	100	0	0
5	0	0	0	100	0	0	0	0	0	100	0	0
6	0	0	0	100	0	0	0	0	0	100	0	0
7	0	0	0	100	0	0	0	0	0	100	0	0
8	0	0	0	100	0	0	0	0	0	100	0	0
9	0	0	0	100	0	0	0	0	0	100	0	0
10	0	0	0	100	0	0	0	0	0	100	0	0
11	0	0	0	100	0	0	0	0	0	100	0	0
12	0	0	0	100	0	0	0	0	0	100	0	0
13	0	0	0	100	0	0	0	0	0	100	0	0
14	0	0	0	100	0	0	0	0	0	100	0	0
15	0	0	7	93	7	0	0	0	0	100	0	0
17	0	0	0	100	0	0	0	0	0	100	0	0
18	0	0	0	100	0	0	0	0	0	100	0	0
19	0	0	3.2	96.8	3.2	0	0	0	0	100	0	0
20	0	0	0	100	0	0	0	0	0	100	0	0
23	0	0	0	100	0	0	0	0	0	100	0	0
25	0	0	0	100	0	0	0	0	0	100	0	0
AV	0	0	0.69	99.32	0.69	0	0	0	0	100	0	0
SEM	0	0	0.40	0.40	0.40	0	0	0	0	0	0	0

p27 - TUMOUR SAMPLES

INSULINOMA

	NUCLEAR						CYTOPLASMIC					
ID	**S**	**M**	**W**	**-VE**	**+VE**	**S+M**	**S**	**M**	**W**	**-VE**	**+VE**	**S+M**
1	0	0	2.8	97.2	2.8	0	0	34.9	46.6	18.5	81.5	34.9
2	0	1	33.2	65.8	34.2	1	0.2	3	78.7	18.1	81.9	3.2
3	0	0	10.3	89.7	10.3	0	15.3	65.5	9.3	9.9	90.1	80.8
5	10.5	39.5	15.3	34.7	65.3	50	8.2	67.8	7.7	16.3	83.7	76
6	4.6	20.2	51.1	24.1	75.9	24.8	2.5	22.4	64.6	10.5	89.5	24.9
7	2.5	14.3	39.7	43.5	56.5	16.8	0.8	6	49.8	43.4	56.6	6.8
8	7.1	32.2	46.4	14.3	85.7	39.3	0	7.5	61	31.4	68.5	7.5
9	56.5	30	7.7	5.8	94.2	86.5	0	0	0	100	0	0
10	2.1	10.3	56.9	30.7	69.3	12.4	0	0.9	53.6	48.6	54.5	0.9
11	2.9	9.1	19.5	68.5	31.5	12	1.7	6.5	18.9	72.9	27.1	8.2
12	11.4	35.4	39.5	13.7	86.3	46.8	0.6	8.9	72.3	18.2	81.8	9.5
13	2.6	9	19.2	69.2	30.8	11.6	2.4	19.8	28.2	49.6	50.4	22.2
14	16	73.7	7.3	3	97	89.7	0.9	6.6	82.7	9.8	90.2	7.5
15	16	37	30.4	6.6	83.4	53	4.2	16.6	66.8	12.4	87.6	20.8
17	44.1	36.6	14.6	4.7	95.3	80.7	6.3	73.7	15.3	4.7	95.3	80
18	17.4	75.8	4.6	2.2	97.8	93.2	2.8	76.2	16.6	4.4	95.6	79
19	30.1	41	16.9	12	88	71.1	4.3	39.8	46.7	9.2	90.8	44.1
20	23.7	42.1	28.1	16.1	93.9	65.8	1.2	27.5	64.9	6.4	93.6	28.7
23	18.9	22.2	41.1	17.8	82.2	41.1	1.1	9.4	72.8	16.7	83.3	10.5
25	31.6	42.5	20.2	5.7	94.3	74.1	2.6	46.1	40.4	10.9	89.1	48.7
AV	14.90	28.60	25.24	31.27	68.74	43.50	2.76	26.96	44.85	25.60	74.56	29.71
SEM	3.51	4.84	3.64	6.81	6.81	7.22	0.83	5.80	5.86	5.66	5.63	6.41

GASTRINOMA

	NUCLEAR						CYTOPLASMIC					
ID	**S**	**M**	**W**	**-VE**	**+VE**	**S+M**	**S**	**M**	**W**	**-VE**	**+VE**	**S+M**
4	16.8	39.6	31.1	12.5	87.5	56.4	0	1.1	92.7	6.2	93.8	1.1
22	9.8	40.2	43.3	6.7	93.3	50	0	73.2	20.3	6.5	93.5	73.2
24	3.1	10.2	37.8	49	51.1	13.3	0	2	92.9	5.1	94.9	2
AV	9.90	30.00	37.40	22.73	77.30	39.90	0.00	25.43	68.63	5.93	94.07	25.43
SEM	3.96	9.90	3.53	13.24	13.21	13.43	0.00	23.88	24.17	0.43	0.43	23.88

p27 - ISLET SAMPLES

	NUCLEAR						CYTOPLASMIC					
ID	**S**	**M**	**W**	**-VE**	**+VE**	**S+M**	**S**	**M**	**W**	**-VE**	**+VE**	**S+M**
1	0	6.7	34.4	58.9	41.1	6.7	9.1	23.4	32	35.5	64.5	32.5
2	0	0	10.7	89.3	10.7	0	48	38.7	10.7	2.6	97.4	86.7
4	0	0	4.4	95.6	4.4	0	56.9	24.4	12.1	6.6	93.4	81.3
5	0	0	5	95	5	0	12.2	82.3	5	0	99.5	94.5
6	0	0	3.4	96.6	3.4	0	50.7	33.8	13.2	2.3	97.7	84.5
7	2.5	9.9	15.5	82.1	27.9	12.4	37.7	47	14.4	0.9	99.1	84.7
8	7.3	25.1	49.8	17.8	82.2	32.4	21.1	51.8	21.6	5.5	94.5	72.9
9	5.5	16.5	57.7	20.3	79.7	22	20.2	60.3	17.2	2.3	97.7	80.5
10	7.3	13	60.1	19.6	80.4	20.3	10.3	13	60.1	16.6	83.4	23.3
11	5.8	33.9	44.5	15.8	84.2	39.7	30.6	45.8	14.5	9.1	90.9	76.4
12	4.9	28	51.1	16	84	32.9	12.4	37.1	41.4	9.1	90.9	49.5
13	23.6	40.2	24.7	11.5	88.5	63.8	2.7	32.6	56.2	8.7	91.5	35.3
14	53.6	24.3	14.5	7.6	92.4	77.9	41.7	35.1	14.9	8.3	91.7	76.8
15	63.5	25.3	7	4.2	95.8	88.8	17.9	60.7	14.2	7.2	92.8	78.6
17	27.6	36.2	29.1	7.1	92.9	63.8	15.1	58.1	22.2	4.6	95.4	73.2
18	33.1	41.2	22.1	3.6	96.4	74.3	17.8	60.2	18.9	3.1	96.9	78
20	44.7	42.4	8.3	4.6	95.4	87.1	9.4	64.3	20.7	5.6	94.4	73.7
23	29.8	37.6	22.9	9.7	90.3	67.4	9.4	59.6	24.5	6.5	93.5	69
25	12.2	20.4	57.6	9.8	90.2	32.6	17.6	51	25	6.4	93.6	68.6
AV	16.92	21.09	27.52	35.01	65.52	38.01	23.20	46.27	23.09	7.42	92.57	69.47
SEM	4.56	3.50	4.63	8.46	8.32	7.29	3.70	3.94	3.40	1.79	1.78	4.53

p27 - EXOCRINE PANCREAS SAMPLES

	NUCLEAR						CYTOPLASMIC					
ID	**S**	**M**	**W**	**-VE**	**+VE**	**S+M**	**S**	**M**	**W**	**-VE**	**+VE**	**S+M**
1	0	8	16.8	75.2	24.8	8	0	0	0	100	0	0
2	0	5.6	18.4	76	24	5.6	0	3.3	11.9	84.8	15.2	3.3
3	0	1	6	93	7	1	0	0	4.8	95.2	4.8	0
5	0	0	11.3	88.7	11.3	0	0	0	5.6	94.4	5.6	0
6	0	5.8	17.2	77	23	5.8	0	1.3	6	92.7	7.3	1.3
7	6.6	10.5	13.5	69.4	30.6	17.1	0	0	0	100	0	0
8	2.4	6.4	19.8	71.4	28.6	8.8	0	0	0	100	0	0
9	6.8	14.3	19.3	59.6	40.4	21.1	0	0	0	100	0	0
10	0.3	7.4	20.3	72	28	7.7	0	0	0	100	0	0
11	1.5	10.6	31.5	56.4	43.6	12.1	0	0.2	29	70.8	29.2	0.2
12	0.8	4.2	20.2	74.8	25.2	5	0.6	4	31.4	64	36	4.6
13	3	4	19	74	26	7	0.4	4	64.1	31.5	68.5	4.4
14	4.1	8.6	13.1	74.2	25.8	12.7	0	2.5	33.8	63.7	36.3	2.5
15	1.9	3.9	8.2	86	14	5.8	0.2	4.5	23.3	72	28	4.7
17	2.4	5.7	23.6	68.3	31.7	8.1	0.4	3.9	41.9	53.8	46.2	4.3
18	4.4	9.4	21.2	65	35	13.8	1.4	4.4	32.4	61.8	38.2	5.8
19	5.2	8.2	14.7	71.9	28.1	13.4	1	4	21.9	73.1	26.9	5
20	0	3.6	15	81.4	18.6	3.6	0	0	8.4	91.6	8.4	0
23	4.4	14.4	18.4	59.2	37.2	18.8	0	1.6	14.8	83.6	16.4	1.6
25	3.7	12.1	18.7	65.5	34.5	15.8	0	0	6.5	93.5	6.5	0
AV	2.38	7.19	17.31	72.95	26.87	9.56	0.20	1.69	16.79	81.33	18.68	1.89
SEM	0.51	0.89	1.24	2.13	2.08	1.30	0.09	0.42	3.92	4.29	4.29	0.49

Phospho-p27 - TUMOUR SAMPLES

INSULINOMA

	NUCLEAR						CYTOPLASMIC					
ID	**S**	**M**	**W**	**-VE**	**+VE**	**S+M**	**S**	**M**	**W**	**-VE**	**+VE**	**S+M**
1	0	0	6.7	93.3	6.7	0	0	27.7	60.7	11.6	88.4	27.7
2	0	0	0	100	0	0	4.1	69.6	25.6	0.7	99.3	73.7
3	0	0	0	100	0	0	6.1	57.9	26.3	9.7	90.3	64
5	0	0	6.7	93.3	6.7	0	1.1	28.9	63.2	6.8	93.2	30
6	0	0	0	100	0	0	4.3	24.8	58.9	12	88	29.1
7	0	0	0	100	0	0	0	56.4	29.4	14.2	85.8	56.4
8	0	0	0	100	0	0	5.6	54.1	39.1	1.2	98.8	59.7
9	0	0	0	100	0	0	5	84.6	4.6	5.8	94.2	89.6
10	0	0	0	100	0	0	1.2	4.8	33.4	60.6	39.4	6
11	0	0	0	100	0	0	6.7	37.9	50.3	5.1	94.9	44.6
12	0	0	0	100	0	0	18.4	76.4	5.2	0	100	94.8
13	0	0.1	5	94.9	5.1	0.1	0	3.2	16.1	80.7	19.3	3.2
14	0	0	0	100	0	0	3.4	82.4	13.4	0.8	99.2	85.8
15	0	0	12	88	12	0	0	2.3	30	67.7	32.3	2.3
17	0	0	0	100	0	0	0	11.4	76.4	12.2	87.8	11.4
18	0	0	0	100	0	0	1.5	12.5	61.9	24.1	75.9	14
19	0	0	0	100	0	0	0	2.4	14.2	83.4	16.6	2.4
20	0	0	0	100	0	0	0	8.9	75.2	15.9	84.1	8.9
23	0	0	0	100	0	0	1.2	75.2	15.2	8.4	91.6	76.4
25	0	0	0	100	0	0	2.3	74.2	21.4	2.1	97.9	76.5
AV	0	0.01	1.52	98.48	1.53	0.01	3.05	39.78	36.03	21.15	78.85	42.83
SEM	0	0.01	0.75	0.75	0.75	0.01	0.96	6.82	5.18	6.18	6.18	7.37

GASTRINOMA

	NUCLEAR						CYTOPLASMIC					
ID	**S**	**M**	**W**	**-VE**	**+VE**	**S+M**	**S**	**M**	**W**	**-VE**	**+VE**	**S+M**
4	0	0	0	100	0	0	5.1	85.4	9.5	0	100	90.5
22	0	2.3	12	85.7	14.3	2.3	2.1	42	19.1	36.8	63.2	44.1
24	0	0	6.1	93.9	6.1	0	3.4	52.4	39.5	4.7	95.3	55.8
AV	0	0.77	6.03	93.20	6.80	0.77	3.53	59.93	22.70	13.83	86.17	63.47
SEM	0	0.77	3.46	4.14	4.14	0.77	0.87	13.08	8.85	11.56	11.56	13.93

Phospho-p27 - ISLET SAMPLES

	NUCLEAR						CYTOPLASMIC					
ID	**S**	**M**	**W**	**-VE**	**+VE**	**S+M**	**S**	**M**	**W**	**-VE**	**+VE**	**S+M**
1	0	0	6.7	93.3	6.7	0	0	31.4	45.7	22.9	77.1	31.4
2	0	0	5.3	94.7	5.3	0	0	4.2	71.2	24.6	75.4	4.2
4	0	0	0	100	0	0	44.9	35.2	14.2	5.7	94.3	80.1
5	0	0	0	100	0	0	0	28.7	61.2	10.9	89.9	28.7
6	0	0	0	100	0	0	0	17.5	72.3	11.2	89.8	17.5
7	0	0	0	100	0	0	0	8.4	80.4	11.2	88.8	8.4
8	0	0	0	100	0	0	0	7.1	84.3	8.6	91.4	7.1
9	0	0	0	100	0	0	0.4	11.2	83.5	4.9	95.1	11.6
10	0	0	0	100	0	0	27.2	51.4	15.2	6.2	93.8	78.6
11	0	0	5.4	94.6	5.4	0	3.8	56.4	35.4	4.4	95.6	60.2
12	0	0	0	100	0	0	11.5	40.5	37.4	10.1	89.4	52
13	0	9.7	30.1	60.2	39.8	9.7	4.4	76.4	14.1	5.1	94.9	80.8
14	0	0	0	100	0	0	4.5	73.4	16.4	5.7	94.3	77.9
15	0	0	6.4	93.6	6.4	0	0	28.4	61.4	10.2	89.8	28.4
17	0	0	0	100	0	0	0	0	15.5	84.5	15.5	0
18	0	0	0	100	0	0	2.8	70.8	24.8	1.6	98.4	73.6
20	0	0	0	100	0	0	2.3	18.4	72.5	6.8	93.2	20.7
23	0	0	4.3	95.7	4.3	0	0	11.4	85.1	3.5	96.5	11.4
25	0	0	0	100	0	0	5.3	80.1	12.3	2.3	97.7	85.4
AV	0	0.51	3.06	96.43	3.57	0.51	5.64	34.26	47.52	12.65	87.42	39.89
SEM	0	0.51	1.61	2.10	2.10	0.51	2.64	6.10	6.53	4.23	4.23	7.20

Phospho-p27 - EXOCRINE PANCREAS SAMPLES

	NUCLEAR						CYTOPLASMIC					
ID	**S**	**M**	**W**	**-VE**	**+VE**	**S+M**	**S**	**M**	**W**	**-VE**	**+VE**	**S+M**
1	0	34.1	44.6	21.3	78.7	34.1	0	15.7	35.1	49.2	50.8	15.7
2	0	0	5.2	94.8	5.2	0	0	4.6	35.2	60.2	39.8	4.6
3	0	0	0	100	0	0	0	17.4	25.7	56.9	43.1	17.4
5	0	0	0	100	0	0	0	15.2	75.2	9.6	90.4	15.2
6	0	0	0	100	0	0	24.5	55.4	15.4	4.7	95.3	79.9
7	0	0	0	100	0	0	0	0	10.2	89.8	10.2	0
8	0	0	0	100	0	0	0	2.3	14.3	83.4	16.6	2.3
9	0	0	0	100	0	0	0	1.2	33.4	65.4	34.6	1.2
10	0	0	0	100	0	0	1.2	16.4	17.4	65	35	17.6
11	0	0	9.4	90.6	9.4	0	0	10.4	33.4	56.2	43.8	10.4
12	0	0	0	100	0	0	0	0.5	21.5	78	22	0.5
13	0	24.2	26.7	49.1	50.9	24.2	0	0	11.5	88.5	11.5	0
14	0	0	0	100	0	0	0	1.3	16.7	82	18	1.3
15	0	0	9.4	90.6	9.4	0	1.2	19.7	32.4	46.7	53.3	20.9
17	0	0	0	100	0	0	0	0	11.2	88.8	11.2	0
18	0	0	0	100	0	0	0	20.2	42.6	37.2	62.8	20.2
19	0	0	0	100	0	0	0.4	5.3	81.2	13.1	86.9	5.7
20	0	0	0	100	0	0	0	0	2.5	97.5	2.5	0
23	0	0	4.2	95.8	4.2	0	0	6.4	61.4	32.2	67.8	6.4
25	0	0	0	100	0	0	2.1	11.3	20.1	66.5	33.5	13.4
AV	0	2.92	4.98	92.11	7.89	2.92	1.47	10.17	29.82	58.55	41.46	11.64
SEM	0	2.04	2.53	4.52	4.52	2.04	1.22	2.89	4.79	6.23	6.23	3.97

JAB1 - TUMOUR SAMPLES

INSULINOMA

	NUCLEAR						CYTOPLASMIC					
ID	**S**	**M**	**W**	**-VE**	**+VE**	**S+M**	**S**	**M**	**W**	**-VE**	**+VE**	**S+M**
1	0	0	0	100	0	0	0	8.4	61.3	30.3	69.7	8.4
2	0	0	3.7	96.3	3.7	0	4.1	21.4	32.8	41.7	58.3	25.5
3	0	0	0	100	0	0	17.85	73.45	7.9	0.8	99.2	91.3
5	0	0	0	100	0	0	78.2	8.5	7.4	5.9	94.1	86.7
6	0	0	0	100	0	0	53.2	30.6	11.1	5.1	94.9	83.8
7	0	0	0	100	0	0	13.5	24.6	39.7	22.2	77.8	38.1
8	0	0	0	100	0	0	0	14.7	81.2	4.1	95.9	14.7
9	0	0	0	100	0	0	10.4	11.5	69.9	8.2	91.8	21.9
10	0	0	0	100	0	0	0	0	15.4	84.6	15.4	0
11	0	0	0	100	0	0	7.3	6.2	3.1	83.4	16.6	13.5
12	0	0	0	100	0	0	84.3	14.2	1.5	0	100	98.5
13	0	0	0	100	0	0	0	0	6.2	93.9	6.2	0
14	0	0	0	100	0	0	1.2	19.7	76.4	2.7	97.3	20.9
15	0	0	0	100	0	0	42.3	34.9	17.3	5.6	94.5	77.2
17	0	0	0	100	0	0	5.6	82.9	10.2	1.3	98.7	88.5
18	0	0	0	100	0	0	12.9	61.8	22.2	3.3	96.8	74.7
19	0	0	0	100	0	0	19.3	42.3	25.7	2.7	87.3	61.6
20	0	0	0	100	0	0	0	14.8	85.2	0	100	14.8
23	0	0	0	100	0	0	7.1	86.4	6.5	0	100	93.5
25	0	0	0	100	0	0	0	0	12.4	87.6	12.4	0
AV	0	0	0.19	99.82	0.19	0	17.86	27.81	29.67	24.17	75.34	45.68
SEM	0	0	0.19	0.18	0.19	0	5.79	6.16	6.42	7.66	7.60	8.34

GASTRINOMA

	NUCLEAR						CYTOPLASMIC					
ID	**S**	**M**	**W**	**-VE**	**+VE**	**S+M**	**S**	**M**	**W**	**-VE**	**+VE**	**S+M**
4	0	0	0	100	0	0	0	15.2	81.2	3.6	96.4	15.2
22	0	0	0	100	0	0	0	0	25.3	74.7	25.3	0
24	0	0	0	100	0	0	0	0	2.4	97.6	2.4	0
AV	0	0	0	100	0	0	0	5.07	36.30	58.63	41.37	5.07
SEM	0	0	0	0	0	0	0	5.07	23.40	28.30	28.30	5.07

JAB1 - ISLET SAMPLES

	NUCLEAR						CYTOPLASMIC					
ID	**S**	**M**	**W**	**-VE**	**+VE**	**S+M**	**S**	**M**	**W**	**-VE**	**+VE**	**S+M**
1	0	0	0	100	0	0	87.3	9.4	3.3	0	100	96.7
2	0	0	0	100	0	0	77.55	15.55	6.9	0	100	93.1
4	0	0	0	100	0	0	85.4	11.3	3.3	0	100	96.7
5	0	0	0	100	0	0	86.4	6.4	3.2	4	96	92.8
6	0	0	0	100	0	0	65	20.4	11.7	2.9	97.1	85.4
7	0	0	0	100	0	0	71.4	24.6	4	0	100	96
8	0	0	0	100	0	0	81.2	8.4	6.5	3.9	96.1	89.6
9	0	0	0	100	0	0	76.4	15.4	7.4	0.8	99.2	91.8
10	0	0	0	100	0	0	63.7	29.5	4.7	2.1	97.9	93.2
11	0	0	0	100	0	0	83.8	12.3	3.9	0	100	96.1
12	0	0	0	100	0	0	91.4	8.4	0.2	0	100	99.8
13	0	0	0	100	0	0	53.9	46.1	0	0	100	100
14	0	0	0	100	0	0	42.6	24.4	18.1	14.9	85.1	67
15	0	0	0	100	0	0	15	81.3	3.7	0	100	96.3
17	0	0	0	100	0	0	10.5	73.4	16.1	0	100	83.9
18	0	0	0	100	0	0	34.3	50.8	13.1	1.9	98.2	85.1
20	0	0	0	100	0	0	81.1	13.5	5.4	0	100	94.6
23	0	0	0	100	0	0	11.2	82.4	6.4	0	100	93.6
25	0	0	0	100	0	0	0	72.4	26.7	0.9	99.1	72.4
AV	0	0	0	100	0	0	58.85	31.89	7.61	1.65	98.35	90.74
SEM	0	0	0	0	0	0	6.99	6.19	1.55	0.80	0.80	2.00

JAB1 - EXOCRINE PANCREAS SAMPLES

	NUCLEAR						CYTOPLASMIC					
ID	**S**	**M**	**W**	**-VE**	**+VE**	**S+M**	**S**	**M**	**W**	**-VE**	**+VE**	**S+M**
1	0	0	0	100	0	0	0	0	12.9	87.1	12.9	0
2	0	0	5.3	94.7	5.3	0	0	11.7	44.4	43.9	56.1	11.7
3	0	0	0	100	0	0	0	0	5.6	94.4	5.6	0
5	0	0	0	100	0	0	0	0	2.3	97.7	2.3	0
6	0	0	0	100	0	0	0	0	6.7	93.3	6.7	0
7	0	0	0	100	0	0	0	0	2.4	97.6	2.4	0
8	0	0	0	100	0	0	0	0	0	100	0	0
9	0	0	0	100	0	0	0	32.1	35.4	32.5	67.5	32.1
10	0	0	0	100	0	0	0	0	0	100	0	0
11	0	0	0	100	0	0	0	0	53.4	46.6	53.4	0
12	0	0	0	100	0	0	0	0	2.3	97.7	2.3	0
13	0	0	13.6	86.4	13.6	0	0	0	17.6	82.4	17.6	0
14	0	0	0	100	0	0	0	0	0	100	0	0
15	0	0	0	100	0	0	0	7.2	30.0	62.9	37.1	7.2
17	0	0	0	100	0	0	0	36.4	51.1	12.5	87.5	36.4
18	0	0	0	100	0	0	0	23.0	69.1	8.0	92.0	23.0
19	0	0	0	100	0	0	0	0	30.7	69.3	30.7	0
20	0	0	12.4	87.6	12.4	0	0	0	8.1	91.9	8.1	0
23	0	0	4.2	95.8	4.2	0	0	24.3	35.7	40	60	24.3
25	0	0	6.4	93.6	6.4	0	0	0	3.6	96.4	3.6	0
AV	0	0	2.10	97.91	2.10	0	0	6.73	20.56	72.71	27.29	6.73
SEM	0	0	0.94	0.94	0.94	0	0	2.69	4.80	6.95	6.95	2.69

p-AKT - TUMOUR SAMPLES

INSULINOMA

	NUCLEAR						CYTOPLASMIC					
ID	**S**	**M**	**W**	**-VE**	**+VE**	**S+M**	**S**	**M**	**W**	**-VE**	**+VE**	**S+M**
1	0	0	0	100	0	0	3.1	78.2	18.7	0	100	81.3
2	0	6.75	66.55	26.7	73.3	6.75	0	20.75	72.9	6.35	93.65	20.75
3	0	6.0	80.9	13.2	86.9	6.0	0.0	44.5	47.4	8.2	91.9	44.5
5	0	20.3	74.8	4.9	95.1	20.3	8.4	81.2	7.5	2.9	97.1	89.6
6	5.3	39.6	46.2	8.9	91.1	44.9	8.9	76.4	12.8	1.9	98.1	85.3
7	0.8	58.2	35.6	5.4	94.6	59	0	44.3	52.1	3.6	96.4	44.3
8	0	0	21.5	78.5	21.5	0	0	16.2	75.4	8.4	91.6	16.2
9	0	9.7	86.4	3.9	96.1	9.7	2.3	86.2	11.5	0	100	88.5
10	3.2	47.2	24.4	21.2	74.8	50.4	4.3	83.7	10.2	1.8	98.2	88
11	0	0	19.7	80.3	19.7	0	13.2	78.5	8.3	0	100	91.7
12	0	46.4	50.1	3.5	96.5	46.4	5.4	86.4	8.2	0	100	91.8
13	0	26.1	23.5	50.5	49.5	26.1	0.0	2.1	31.7	66.3	33.8	2.1
14	0	0	6.8	93.2	6.8	0	0	9.2	86.1	4.7	95.3	9.2
15	7.4	73.5	12.7	6.4	93.6	80.9	24.3	63.4	11.2	1.1	98.9	87.7
17	0	0	3.2	96.8	3.2	0	0	4.2	92.5	3.3	96.7	4.2
18	0	0	14	86	14	0	0	13.9	77.9	8.3	91.7	13.9
19	9.6	18.3	31.2	41	59	27.8	0	10.7	37.7	1.7	48.4	10.7
20	0	0	7.6	92.4	7.6	0	0	5.4	85.4	9.2	90.8	5.4
23	0	35.3	45.8	18.9	81.1	35.3	2.4	36.3	45.2	16.1	83.9	38.7
25	3.1	64.7	31.7	0.5	99.5	67.8	34.2	36.2	29.6	0	100	70.4
AV	1.47	22.60	34.13	41.61	58.19	24.06	5.33	43.88	41.11	7.19	90.32	49.21
SEM	0.63	5.52	5.89	8.60	8.58	5.86	2.04	7.22	6.86	3.25	3.92	8.13

GASTRINOMA

	NUCLEAR						CYTOPLASMIC					
ID	**S**	**M**	**W**	**-VE**	**+VE**	**S+M**	**S**	**M**	**W**	**-VE**	**+VE**	**S+M**
4	0	12.4	68.9	18.7	81.3	12.4	0	24.9	64.2	10.9	89.1	24.9
22	0	0	10.15	89.85	10.15	0	0	6.55	88.3	5.15	94.85	6.55
24	0	0	20.3	79.7	20.3	0	0	5	87.5	7.5	92.5	5
AV	0	4.13	33.12	62.75	37.25	4.13	0	12.15	80	7.85	92.15	12.15
SEM	0	4.13	18.13	22.22	22.22	4.13	0	6.39	7.90	1.67	1.67	6.39

p-AKT - ISLET SAMPLES

	NUCLEAR						CYTOPLASMIC					
ID	**S**	**M**	**W**	**-VE**	**+VE**	**S+M**	**S**	**M**	**W**	**-VE**	**+VE**	**S+M**
1	0	20.4	53.4	26.2	73.8	20.4	12.6	73.4	13.1	0.9	99.1	86
2	0	6.8	52.4	40.9	59.2	6.8	0.0	8.5	81.6	10.0	90.1	8.5
4	6.1	31.7	38.4	23.8	76.2	37.8	10.4	73.8	13.7	2.1	97.9	84.2
5	0	38.3	53.2	8.5	91.5	38.3	0	85.2	10.6	4.2	95.8	85.2
6	25.4	50.4	16.2	8	92	75.8	43.6	36.2	19.3	1.9	99.1	79.8
7	45.3	45.2	9.5	0	100	90.5	82.8	12.7	4.5	0	100	95.5
8	0	29.4	69.4	1.2	98.8	29.4	6.1	86.2	7.7	0	100	92.3
9	0	8.9	83.4	7.7	92.3	8.9	42.7	54.1	3.2	0	100	96.8
10	0	3.2	15.4	81.4	18.6	3.2	0	9.1	82.3	8.6	91.4	9.1
11	46.8	40.7	12.5	0	100	87.5	51.2	46.7	2.1	0	100	97.9
12	0	9.9	21.3	68.8	31.2	9.9	8.6	75.1	16.3	0	100	83.7
13	0	10	75.4	14.6	85.4	10	2.1	89.4	8.5	0	100	91.5
14	4.6	64.5	24.1	6.8	93.2	69.1	4.8	83.7	11.1	0.4	99.6	88.5
15	19.4	38.9	41.2	0.5	99.5	58.3	11	68.4	18.4	2.2	97.8	79.4
17	0	11.3	75.2	13.5	86.5	11.3	13.2	82.3	4.5	0	100	95.5
18	0	17.4	67.7	14.9	85.1	17.4	3.7	83.9	9.4	3	97	87.6
20	8.6	45.3	40	6.1	93.9	53.9	0	11.2	87.6	1.2	98.8	11.2
23	4.3	59.3	35	1.4	98.6	63.6	0	78.3	20.4	1.3	98.7	78.3
25	0	13.7	74.8	14.5	88.5	13.7	6.3	70.7	22.5	0.5	99.5	77
AV	8.45	28.70	45.18	17.83	82.33	37.14	15.74	59.41	22.99	1.91	98.14	75.16
SEM	3.45	4.37	5.59	5.23	5.24	6.76	5.20	6.75	6.36	0.66	0.66	6.85

p-AKT - EXOCRINE PANCREAS SAMPLES

	NUCLEAR						CYTOPLASMIC					
ID	**S**	**M**	**W**	**-VE**	**+VE**	**S+M**	**S**	**M**	**W**	**-VE**	**+VE**	**S+M**
1	0	61.2	24.3	14.5	85.5	61.2	0	9.9	85.1	5	95	9.9
2	0	0	0	100	0	0	0	3.7	28.7	67.6	32.4	3.7
3	0	7.2	24.7	68.1	31.9	7.2	0	7.5	85.4	7.1	92.9	7.5
5	0	0	6.3	93.7	6.3	0	0	3.2	93.2	3.6	96.4	3.2
6	0	19.4	53.1	27.5	72.5	19.4	0	28.1	69.3	2.6	97.4	28.1
7	0	19.2	51.2	29.6	70.4	19.2	24.1	54.3	20.2	1.4	98.6	78.4
8	0	0	5.6	94.4	5.6	0	0	4.2	87.9	7.9	92.1	4.2
9	0	0	13.2	86.8	13.2	0	1.9	68.5	29.6	0	100	70.4
10	0	0	3.2	96.8	3.2	0	0	0	5.7	94.3	5.7	0
11	0	5.3	32.5	62.2	37.8	5.3	0	0	31	69	31	0
12	0	0	4.3	95.7	4.3	0	0	6.4	91.2	2.4	97.6	6.4
13	0	4.4	74.2	21.4	78.6	4.4	0	10.2	82.1	7.7	92.3	10.2
14	0	11.4	59.7	28.9	71.1	11.4	0	14.2	82.4	3.4	96.6	14.2
15	0	6.7	23.7	69.6	30.4	6.7	0	26.8	66.1	7.1	92.9	26.8
17	0	0	7.4	92.6	7.4	0	0	12.8	83.2	4	96	12.8
18	0	5.2	67.3	27.5	72.5	5.2	0	16.1	76.7	7.2	92.8	16.1
19	0	0	6.7	93.3	6.7	0	0	8.1	83.4	8.5	91.5	8.1
20	0	0	5	95	5	0	0	8.7	78.4	12.9	87.1	8.7
23	0	5.1	87.4	7.5	92.5	5.1	0	4.9	91.5	3.6	96.4	4.9
25	0	0	16.3	83.7	16.3	0	0	10.3	83.7	6	94	10.3
AV	0	7.26	28.31	64.44	35.56	7.26	1.30	14.90	67.74	16.91	83.94	16.20
SEM	0	3.15	6.10	7.49	7.49	3.15	1.20	3.96	6.19	6.11	6.01	4.76

PTEN - TUMOUR SAMPLES

INSULINOMA

	NUCLEAR						CYTOPLASMIC					
ID	**S**	**M**	**W**	**-VE**	**+VE**	**S+M**	**S**	**M**	**W**	**-VE**	**+VE**	**S+M**
1	17.3	21.2	24.2	37.8	62.7	38.5	0	2.1	11.4	86.5	13.5	2.1
2	9.4	65.8	24.1	0.7	99.3	75.2	0	0	15.7	84.3	15.7	0
3	33.6	54.3	12.2	0.0	100.0	87.9	0.0	0.0	8.5	91.6	8.5	0
5	48.6	20.9	9.9	20.6	79.4	69.5	0	0	14.3	85.7	14.3	0
6	73.4	16.5	10.1	0	100	89.9	0	0	0	100	0	0
7	69.4	11.3	6.2	13.1	86.9	80.7	0	0	3.4	96.6	3.4	0
8	83.2	6.4	4.9	5.5	94.5	89.6	0	0	0	100	0	0
9	21.6	53.8	16.4	8.2	91.8	75.4	0	0	0	100	0	0
10	13.4	79.6	7	0	100	93	0	0	0	100	0	0
11	23.1	67.5	9.4	0	100	90.6	0	0	0	100	0	0
12	76.8	18.6	4.6	0	100	95.4	0	0	0	100	0	0
13	0	40.0	58.5	1.6	98.4	40.0	0	0	0	100	0	0
14	61.3	35.4	3.3	0	100	96.7	0	0	0	100	0	0
15	38.3	51.4	10.3	0	100	89.7	0	0	56.2	43.8	56.2	0
17	93.4	6.6	0	0	100	100	0	0	0	100	0	0
18	29.4	63.1	7.5	0	100	92.5	0	0	0	100	0	0
19	16.4	72.4	10.8	0.4	99.6	88.8	0	0	0	100	0	0
20	15.4	81.4	3.2	0	100	96.8	0	0	0	100	0	0
23	72.7	15.6	11.7	0	100	88.3	0	0	0	100	0	0
25	51.2	45.6	3.2	0	100	96.8	0	0	0	100	0	0
AV	42.40	41.37	11.87	4.40	95.63	83.76	0	0.11	5.47	94.42	5.58	0.11
SEM	6.36	5.67	2.83	2.14	2.12	3.84	0	0.11	2.91	2.93	2.93	0.11

GASTRINOMA

	NUCLEAR						CYTOPLASMIC					
ID	**S**	**M**	**W**	**-VE**	**+VE**	**S+M**	**S**	**M**	**W**	**-VE**	**+VE**	**S+M**
4	46.3	41.6	11	1.1	98.9	87.9	0	0	0	100	0	0
22	21.9	70.2	8.0	0.0	100.0	92.1	0	0	0	100	0	0
24	24.1	42.4	33.5	0	100	66.5	0	0	0	100	0	0
AV	30.77	51.38	17.48	0.37	99.63	82.15	0	0	0	100	0	0
SEM	7.79	9.39	8.06	0.37	0.37	7.92	0	0	0	0	0	0

PTEN - ISLET SAMPLES

	NUCLEAR						CYTOPLASMIC					
ID	**S**	**M**	**W**	**-VE**	**+VE**	**S+M**	**S**	**M**	**W**	**-VE**	**+VE**	**S+M**
1	18.7	64.8	16.5	0	100	83.5	0	0	0	100	0	0
2	6.4	84.7	9.9	0	101	91.1	0	0	0	100	0	0
4	65.6	21.7	10.7	2	98	87.3	0	47.4	50.2	2.4	97.6	47.4
5	75.5	14.3	5.7	4.5	95.5	89.8	0	10.7	81.6	7.7	92.3	10.7
6	79.9	9.6	6.1	4.4	95.6	89.5	0	0	0	100	0	0
7	12.3	70.2	8.7	9.8	91.2	82.5	0	0	0	100	0	0
8	55.3	32.5	4.8	7.4	92.6	87.8	0	0	0	100	0	0
9	24.9	53.8	16.5	4.8	95.2	78.7	0	0	0	100	0	0
10	19.8	61.7	13.2	5.3	94.7	81.5	0	0	0	100	0	0
11	71.8	26.4	1.8	0	100	98.2	0	0	0	100	0	0
12	81.6	16.9	1.5	0	100	98.5	0	0	0	100	0	0
13	79.2	20.8	0	0	100	100	0	0	0	100	0	0
14	31.5	39.2	28.6	0.7	99.3	70.7	0	0	0	100	0	0
15	75.3	14.3	10.4	0	100	89.6	0	0	0	100	0	0
17	78.4	20.4	1.2	0	100	98.8	0	0	0	100	0	0
18	42.2	29.8	23.4	4.6	95.4	72	0	0	0	100	0	0
20	51.4	46.1	2.5	0	100	97.5	0	0	0	100	0	0
23	85.4	14.6	0	0	100	100	0	0	0	100	0	0
25	82.1	17.4	0.5	0	100	99.5	0	0	0	100	0	0
AV	54.59	34.69	8.53	2.29	97.82	89.29	0.00	3.06	6.94	90.01	9.99	3.06
SEM	6.33	5.15	1.88	0.70	0.68	2.14	0.00	2.53	4.92	6.87	6.87	2.53

PTEN - EXOCRINE PANCREAS SAMPLES

	NUCLEAR						CYTOPLASMIC					
ID	**S**	**M**	**W**	**-VE**	**+VE**	**S+M**	**S**	**M**	**W**	**-VE**	**+VE**	**S+M**
1	3.3	35.1	31.2	30.4	69.6	38.4	0	0	0	100	0	0
2	7.7	38.7	24.3	29.3	70.7	46.4	0	0	0	100	0	0
3	18.3	48.6	12.4	20.4	79.3	66.9	0	0	0	100	0	0
5	45.7	5.9	8.3	40.1	59.9	51.6	0	0	0	100	0	0
6	11.7	24.6	28.3	35.4	64.6	36.3	0	0	0	100	0	0
7	0	32.4	16.4	51.2	48.8	32.4	0	0	0	100	0	0
8	9.6	39.1	11.7	39.6	60.4	48.7	0	0	0	100	0	0
9	26.7	21.5	10.7	41.1	58.9	48.2	0	0	0	100	0	0
10	0	50	21.4	28.6	71.4	50	0	0	0	100	0	0
11	0	35.5	24.5	40	60	35.5	0	0	0	100	0	0
12	10.8	30.1	25.7	33.4	66.6	40.9	0	0	0	100	0	0
13	9.7	50.9	15.4	24	76	60.6	0	0	0	100	0	0
14	15.4	25.3	26.4	32.9	67.1	40.7	0	0	0	100	0	0
15	34.5	36.1	25.7	3.7	96.3	70.6	0	0	0	100	0	0
17	65.3	17.4	14.1	3.2	96.8	82.7	0	0	0	100	0	0
18	37.6	34.2	21.4	6.8	93.2	71.8	0	0	0	100	0	0
19	18.6	64.7	16.7	0	100	83.3	0	0	0	100	0	0
20	7.4	43.2	27.4	22	78	50.6	0	0	0	100	0	0
23	21.3	29.4	18.4	30.9	69.1	50.7	0	0	0	100	0	0
25	28.7	29.7	18.4	23.2	76.8	58.4	0	0	0	100	0	0
AV	18.62	34.62	19.94	26.81	73.18	53.24	0	0	0	100	0	0
SEM	3.80	2.93	1.48	3.16	3.16	3.39	0	0	0	0	0	0